

AN EXPERIMENTAL STUDY OF GEOMETRICAL
EFFECTS ON THE DRAG AND FLOW FIELD
OF 3-D NONCIRCULAR CYLINDERS
SEPARATED BY A GAP

by

KHALID MUSLEH SOWOUD

TL
629.13234
So 94e

AE

1992

M

Sow

Exp

TH
AE/1992/M
So 94e



DEPARTMENT OF AEROSPACE ENGINEERING

INDIAN INSTITUTE OF TECHNOLOGY KANPUR

MAY, 1992

**AN EXPERIMENTAL STUDY OF GEOMETRICAL
EFFECTS ON THE DRAG AND FLOW FIELD
OF 3-D NONCIRCULAR CYLINDERS
SEPARATED BY A GAP**

A THESIS

**submitted in partial fulfillment of
the requirements for the award of the degree of
MASTER OF TECHNOLOGY
IN
AEROSPACE ENGINEERING**

**BY
KHALID MUSLEH SOWOUD**

**to the
DEPARTMENT OF AEROSPACE ENGINEERING
INDIAN INSTITUTE OF TECHNOLOGY
Kanpur-208016
May, 1992**

Dedicated To ...

MY PARENTS, WIFE, DAUGHTER

AND
SISTER

TO ALL MY TEACHERS AND LOVE

3 JUN 1992

TH

CENTRAL LIBRARY

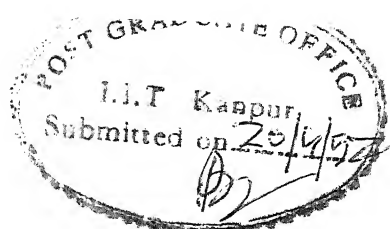
629.13234

Acc. No. A.113535

Se 94 e

AE-1992-M-SOW-EXP

CERTIFICATE



This is to certify that the thesis entitled "An Experimental Study of Geometrical Effects on the Drag and Flow Field of Three-Dimensional Non circular Cylinders Separated by a gap", is a record of the work carried out by Mr KHALID M. AL-MERSUMEY under my supervision and that it has not been submitted elsewhere for awarding a degree.

E. R. R.

(Dr. E. RATHAKRISHNAN)
Department of Aerospace Engineering
Indian Institute of Technology
KANPUR

Date : April 20, 1982

ACKNOWLEDGEMENTS

This Thesis was supervised by Dr. E. Rathakrishnan, to whom I express my deep gratitude and indebtedness for his encouragement, suggestions and direction at all stages of this work.

I am grateful to Shri K.S. Muddappa for his immense and prompt help during the various phases in experimental set up and in taking the readings.

I wish to express my thanks to Mr. H.C. Bhattacharya, in charge of Aerospace Engineering workshop for providing co-operation in the fabrication work. I would like to thank all the staff of Aerospace Engineering Workshop.

I am highly indebted to all my friends who have helped me directly or indirectly during my stay here.

Finally, I wish to express my thanks to the Aerospace Engineering Department, Indian Institute of Technology, Kanpur for the facilities which made the study for this thesis possible.

KHALID M. SOWOUD

AL-MERSUMEY

CONTENTS

<u>Chapter</u>	<u>Title</u>	<u>Page</u>
	Abstract	v
	Nomenclature	vii
	List of Figures	ix
	List of Photographs	xi
1	INTRODUCTION	
	1.1 General Introduction	1
	1.2 Review on Flow Pattern, Wake and Drag of Bluff Bodies	4
	1.3 Review of Literature	8
	1.4 Scope of Present Work	12
2	EXPERIMENTAL SET-UP AND MEASURING INSTRUMENTATION	
	2.1 Introduction	15
	2.2 Wind Tunnel	15
	2.3 Design of Experimental Models	16
	2.3.1 Design of Rear Body Model	16
	2.3.2 Design of Front Body Model	17
	2.3.3 Design of Threaded Shifts	17
	2.4 Measuring Instruments	18
	2.5 Experimental Procedure	20
	2.6 Measuring Accuracy	23
	2.7 Reading Corrections for Three-Component Balance	24

3	RESULTS AND DISCUSSIONS	
3.1	Drag Coefficient Results	27
3.1.1	Drag Coefficient for Rear Body alone	28
3.1.2	Drag Coefficient with D-shape Front Body	29
3.1.3	Drag Coefficient with Square-Plate Front Body	37
3.2	Comparison Between Drag Reduction for D-shape and Square-Plate Front Bodies.	43
3.3	Drag Regimes Classification for Optimum Flows.	46
3.4	Drag Coefficient and Reynolds Numbers Effects	48
4.	CONCLUSIONS AND RECOMMENDATION FOR FUTURE WORK	
4.1	Conclusions	50
4.2	Recommendation for Future Work	53
REFERENCES		55
FIGURES		58
PHOTOGRAPHS		82
APPENDICES		84
Appendix A	Three-component balance calibration (drag curve), drag coefficient measuring and percentage drag reduction with D-shape and square-plate front bodies.	84
Appendix B	Computer program for calculation pressure coefficients, tabulation of measured data and pressure coefficient results.	84

ABSTRACT

The present work describes an experimental investigation on the effects of various D-shapes and square-plates, placed coaxially as front body upstream of the square flat-faced, sharp-windward corners and rounded back rear body. Remarkable decrease in the drag of such a system was observed for certain combinations of the basic geometrical parameters, namely the width b_1/b_2 and gap g/b_2 ratios.

The experimental investigation was carried out for three-dimensional flow, with Reynolds number based on the width (b_2) in the range $1.0-1.8 \times 10^5$, the front body width b_1/b_2 and gap g/b_2 were varied between 0.25 to 1.0 and 0.25 to 2.25, respectively.

The results for rear body alone and rear body with two front bodies configurations are presented. The first configuration studied was the rear body alone with $b_2 = 100$ mm (square cross-section, sharp-windward corners and with rounded back). Its drag coefficient showed only a small variation with Reynolds numbers; $C_{D_o} = 1.42$ at $Re = 1.8 \times 10^5$, $C_{D_o} = 1.39$ at $Re = 1.4 \times 10^5$ and $C_{D_o} = 1.28$ at $Re = 1 \times 10^5$.

The second configuration studied was rear body with D-shape front body. The results show that, a D-shape front body of proper dimensions placed at a certain distance from the rear body can result in drastic reduction of drag of the combination. In the present investigation, the following geometry of the front body

and gap ratio was found to be optimum; $b_1^*/b_2 = 0.75, 0.37$ and 0.25 the corresponding optimum gap ratio are $g^*/b_2 = 0.25, 0.75$ and 0.50 , respectively. These combinations at subcritical Reynolds number 10^5 resulted in total drag reduction up to 42, 67 and 70 percent lower than that of rear body alone, respectively. For the same combination (b_1^*/b_2 and g^*/b_2), the drag reduction at $Re = 1.4 \times 10^5$ are 61, 55 and 58 percent and at $Re = 1.8 \times 10^5$ are 70, 67 and 66 percent, respectively.

The third configuration studied was rear body with square-plate front body. The results show that the optimum combination for rear body with square-plate shaped front body occurs at; $b_1^*/b_2 = 0.75, 0.625$ and 0.37 at an optimum gap ratio $g^*/b_2 = 0.50, 0.25$ and 0.50 respectively, whose total drag is up to 67, 48 and 61 percent lower than that of the near body alone, respectively, at subcritical Reynolds number $Re = 1 \times 10^5$. The drag for the same combination at $Re = 1.4 \times 10^5$ are 73, 58 and 57 and for $Re = 1.8 \times 10^5$ are 80, 72 and 70 percent lower than that of the rear body alone, respectively. The drag reduction for other tested geometries (rear body with D-shape or square-plate front bodies) are in the range of 10 to 30 percent.

Although pressure distribution for all the possible cases have been examined, the pressure distribution curves are presented only for the optimum combinations and compared with the pressure distribution for low and high gap ratios. Drag regimes based on optimum flows are classified onto low, medium and high-drag regimes for both D-shape and square-shape front bodies.

NOMENCLATURE

D Drag force; $D = \frac{1}{2} \rho v_{\infty}^2 S C_D$

C_D Drag Coefficient; $C_D = \frac{D}{1/2 \rho v_{\infty}^2 S}$

C_p Pressure coefficients; $C_p = \frac{p - p_{\infty}}{1/2 \rho v_{\infty}^2}$

q_{∞} Free stream dynamic pressure; $q_{\infty} = \frac{1}{2} \rho v_{\infty}^2$

v_{∞} Free stream velocity

S Rear body cross-sectional area; $S = b_2 \times b_2$

F_1, F_2 Upper and Lower rear body wind ward face; used for defining position on pressure distribution curves respectively

p Local static pressure on rear body

p_{∞} Static pressure in free stream

b_1, b_2 Width of front body and rear body, respectively

b_1^*/b_2 Optimum front body to rear body width ratio

g	Gap between front body and face of rear body
g^*/b_2	Optimum gap ratio for a given b_1^*/b_2
C_D^*	Optimum drag coefficient for a given b_1^*/b_2 and g^*/b_2
C_{D_0}	Drag coefficient of rear body alone
C_D	Drag coefficient of the combination of rear body + front body
Re	Reynolds number; $Re = \frac{V_\infty d_2}{(\rho_2) \nu}$
θ	Angle measured clockwise to a given point on the model surface from the stream direction
ν	Kinematic viscosity of air
ρ	Density of air

Subscript

- ∞ Free stream
- $*$ Optimum case

LIST OF FIGURES

<u>Fig. No.</u>	<u>Title</u>	<u>Page</u>
1	Drag coefficient of various shape bodies Re = 10^4 to 10^6 ; (a) for 3-dimensional; (b) for 2-dimensional bodies	58
2	Drag Coefficient of various shaped nose; Horner Ref. (2)	58
3	Schematic diagram of the experimental model, section AA (pressure test model number 1-39 refer to pressure tap location)	59
4	Schematic diagram of low speed wind tunnel	60
5	Schematic of experimental rear body parts	61
6	Schematic of experimental set-up showing the; (a) threaded rods, (b & c)Front body shapes	62
7	Schematic view of three-component balance with experimental model with square-pate front body	63
8	Pressure distribution for basic body (rear body alone)	64
9	Drag coefficient ratio C_D/C_{D_0} Vs. gap ratio for D-shape front body, $Re = (1 - 1.8) \times 10^5$	65

10	Percentage drag reduction for D-shape front body in optimum b_1^*/b_2 ratio	67
11	Pressure distribution on rear body surface with D-shaped front body.	69
12	Drag Coefficient ratio C_D/C_{D_0} Vs. gap ratio for square-shape front body, $Re = (1-1.8) \times 10^5$	72
13.	Percentage drag reduction for square-shape front body in optimum b_1^*/b_2 ratio	74
14	Pressure distribution on rear body surface with square-shape front body.	76
15	Maximum percentage drag reduction for each b_1/b_2 , the gap g^*/b_2 at which it occurs is shown beside each point; (a) D-shape, (b) square-shape front body.	79
16	Minimum drag coefficient for each D-shape and the gap at which it occurs; (I, II, III) refer to flow regimes.	80
17	Minimum drag coefficient for each square-shape and the gap at which it occurs; (I, II, III) refer to flow regimes.	81
18	Percentage drag reduction for optimum b_1/b_2 ratio variation with Reynolds number; (a) D-shape, (b) square-shape front body.	82

LIST OF PHOTOGRAPHS

<u>Photograph No.</u>	<u>Title</u>	<u>Page</u>
1	A view of the model in the tunnel showing test-section and pitot-static tube	83
2	Experimental model with three-component balance	83
3	Experimental models, multimanometer	84
4	Experimental three-component digital display	84

CHAPTER - 1

INTRODUCTION

1.1 Introduction

The subject of drag reduction is an interesting practical problem with wide range of application, and has always attracted the attention of aerodynamicist. This problem has assumed greater importance in recent years on account of escalating cost of the energy. For example, by reducing the total drag of the airplane, we may use smaller propulsion engine, and at the same time we can go farther for the same amount of fuel .

When any body is placed in a fluid stream, a force is exerted on the body which may be inclined to flow direction. This force owes its existence to viscosity of fluid and the pressure distribution over the body surface . The component of this force parallel to direction of flow is called 'Resistance or Drag force'.

Drag force can be divided into many types; pressure, friction, induced, wave, form and profile drag, each type contributing to the total drag force. Attention to pressure drag has been given in the present work.

The drag force in subsonic aerodynamics is generally recognized to be made up of contributions from the action of viscosity at the surface, termed " friction drag " and the stream wise component of the pressure distribution on the body, termed

the " pressure drag " . The drag of the slender bodies in the stream wise direction, such as airplane wing or fuselage, is mostly made up of friction drag . As bodies become thicker in the direction normal to the fluid stream, the contribution from pressure drag increases . At a certain thickness (relative to depth) the flow gets separated and such a body would generally be called a bluff body , the drag of which would be almost entirely due to pressure drag . Pressure drag is relatively very much greater than friction drag .

Pressure drag results from the distribution of forces normal to the body surface, this normal pressure drag may itself be considered as the sum of several distinct components, i.e:

- (a) Boundary layer normal-pressure drag, or boundary layer pressure drag (form drag).
- (b) Trailing vortex drag, or vortex drag (induced drag).
- (c) Wave drag (only for supersonic flow).

Pressure drag caused by boundary-layer separation is treated here in detail.

Most of the time we would like to have the drag as small as possible, but not always. Expenditure of power is required to overcome the drag of a body in one way or another.

There are many methods by which the pressure drag may be reduced, for the case of unstreamlined body shapes like rectangular and square cylinders; firstly, by rounding the edge of the front face of the body, as show in Fig. 2, secondly, by fixing a hemispherical fore body, thirdly, by fixing a strakes to the

front face and finally by shielding the front face by placing a front body coaxially up stream of it .

A simple example of interfering flow over two bluff-bodies is that in which one body is far downstream in the wake of another one. In this case, the drag of the downstream body is reduced owing to the reduced dynamic pressure in the wake in which it is immersed, while the drag of the first body is unaffected. This may be called a weak interaction. When downstream body is brought close to the base of the first one, the drag of the former may be significantly reduced. In addition, the drag of the first body may be strongly affected, this would be a strong interaction. There are many practical problems in which one bluff body is shielded by another one.

In present study, there is a particular technique of reducing the drag coefficient of sharp-edged, square cross-section with rounded back bluff body. Systematic drag force measurements have been carried out for two front body configurations (square cross-section plate and D-shape front bodies) at various width ratios b_1/b_2 , gap ratios g/b_2 , at three different speeds (low-speed, 3-D, closed-circuit wind-tunnel) . Remarkable decrease of the drag coefficient of such a system was observed for certain combinations of the basic geometrical parameters, namely b_1/b_2 and g/b_2 .

1.2 Review on Flow Pattern, Wake and Drag of Bluff Bodies

It is customary to decompose the total drag force into two parts; pressure drag and skin friction drag, represented by force coefficients C_D and C_F , respectively. The ratio of these two forces may be taken as a convenient criterion to decide whether a body is streamlined or bluff (Ref.5) :

when $\frac{C_D}{C_F} < 1.0$ 'the body is streamlined'

when $\frac{C_D}{C_F} \gg 1.0$ 'the body is bluff'

At high enough Reynolds numbers, many bodies of interest are (according to this definition) bluff bodies, i.e their pressure drag is much larger than the friction drag. Therefore, in present investigation we consider the skin friction forming only a small and insignificant part of the total drag . At subcritical Reynolds numbers, the flow over bluff bodies is characterized by a large wake and periodic, alternate vortex shedding. The separated shear layers feed vorticity to these alternating vortices that are continuously shed downstream. With this flow pattern, the pressure drag coefficient assumes very large values and often exceeds the flat plate drag coefficient of 2.0 (Ref.9). This fact is particularly true for non circular cross sections with sharp corners bluff bodies.

As Reynolds number increases beyond the critical value, transition occurs in the separated shear layer and the flow reattaches to the body as turbulent layer.

A two dimensional bluff body in a stream of low subsonic speed generates a wake in the from of Karman street, a regular array of vortices with circulation of alternate sign. This vortex wake is known to be associated with a large drag force on the body, and only device (such as a splitter plate placed in the near-wake) that causes the vortices to form further away from the body gives a reduction of drag.

Some three-dimensional bodies generate wakes in which there is noticeable periodicity, indicating some regular pattern of vortex shedding, but for axi-symmetric bodies any regular vortex shedding is only a minor feature of the flow. Correspondingly, the drag coefficient of axi-symmetric bluff bodies, based on their frontal areas, are usually considerably smaller than those of the related two-dimensional bodies as shown in the Fig 1. For example, at Reynolds number 10^6 the drag coefficient of a long circular cylinder with its axis normal to the stream is about 0.35, whereas that of a sphere is only about 0.1, Ref. (2).

The two major contributions toward a theoretical understanding of the flow past bluff bodies are the well-known ones of Kirchhoff and Karman. These attack two aspects of the problem that must be understood, namely, the potential flow in the vicinity of the cylinder and the wake further downstream.

In the free-stream line theory developed by Kirchhoff, the free shear layers which are known to separate from bluff bodies are idealized by surfaces (streamlines) of velocity discontinuity. These free streamlines divide the flow into a wake and an outer potential field. Kirchhoff's theory, however, considerably underestimates the drag, and the failure is easily traced to the assumption which is made about the velocity on the free streamline.

Karman, in his famous theory of the vortex street, attacked the problem by way of another characteristic feature of flow past bluff bodies, that is, the phenomenon of periodic vortex shedding. The theory is incomplete in that it cannot by itself relate the vortex-street dimensions and velocities to the cylinder dimension and free-stream velocity, (Ref.10).

The pressure distribution over a bluff bodies (disk, sphere, cylinder....etc) surface is not uniform and there always are regions of both high and low pressure . The high pressure regions are near stagnation point and on most concave surfaces, while the low-pressure regions are along and near convex surfaces and corners . The pressure distribution on the surfaces of several bluff bodies in a real flow exhibiting different pressure patterns . These pressure coefficient patterns all have one common feature-they may be divided in to two regions; a positive one and a negative one . These contributes to the overall bluff body pressure drag coefficient .

A flow approaching a bluff body is decelerated in the region of the stagnation point, accelerated in the boundary layer on the blunt surface, and separates near the sharp front edge of the body forming a separation bubble or an open separation region according to the length of the body in the main-stream direction. Since the separation bubble and the open separation region increase the total drag coefficient of a bluff body, it is necessary to control them.

There are many ways by which the pressure drag can be reduced, all of which have in common that the separation bubble or the wake zone due to open separation regime at the sharp-corners is reduced or even eliminated. Some of the commonly employ techniques are:

(1). A popular method, by simply rounding its edge, or corners, sufficiently as shown in Fig. 2 Horner, (Ref.2). The maximum reduction achieved by corner-rounding technique appear to be limited to 50% (Ref.2).

(2). By fixing strakes to the front face, the effect of strakes on the cross flow drag coefficient of a typical noncircular cylinder at subcritical Reynolds numbers, it is limited by strake height and, more particularly, its location on the windward face, has a strong influence on the flow pattern, base drag coefficient. Substantial drag reduction of the order of 80% are found to be possible by this technique (Ref.9).

(3). By shielding the body front face by placing a front body coaxially upstream . This shielding effect is brought about by the interaction of two bluff bodies . Koenig and Roshko (Ref.1) they study the shielding effect of two bluff bodies (disk placed coaxially upstream of circular cylinder) separated by a gap . They distinguish two cases ; 1) If one body is far downstream in the wake of another one, the drag of the downstream body is reduced owing to the reduced dynamic pressure in the wake in which it is immersed, while the drag of the first body is unaffected, this may called a wake interaction, and 2) When the downstream body is brought close to the base of the first one, the drag of the former may be significantly reduced .

(4). the drag is reduced by tandem arrangement, placing two or more bluff bodies in tandem for purpose of drag reduction is known to led . Morel and John (Ref.4) investigated the interaction of two disks placed normal to the flow direction . For the single disk (diameter d_2) the drag coefficient is 1.15 . If a second disk with a diameter $0.8d_2$ and gap ratio $g/d_2 = 0.54$ is placed ahead of the first disk, the drag coefficient reduces to a value 0.21 (81% drag reduction).

1.3 Review of Literature

Reviewing the previous studies on drag reduction may be of great benefit for the present study . There is large amount of information available in literature on this topic, they are restricted to two-dimensional and axi-symmetric shapes . But only

very little information is available for three-dimensional and non-axisymmetric bluff bodies, especially for square cross-section, this may be due to the fact that, the three-dimensional flow around a bluff-body is complicated, vorticity shed from the body has components in all three direction, and sometime causing a periodic structure to be set up .

The flow over two-dimensional bluff bodies was studied 81 years ago, by Eiffel (1910), his results show the effect of spacing on the drag of two disks arranged coaxially in a stream .

In 1985, Koenig and Roshko (Ref.1) studied experimentally the effects of geometry on the drag and flow field of two bluff bodies (disks placed coaxially upstream of circular cylinder) separated by a gap. For certain combinations of the basic geometric parameters, namely the diameter and gap ratios, they observed a remarkable decrease of the drag of such system, when the ratio of front-disk diameter d_1 , to the main-body diameter d_2 is about 0.75, the tandem bodies have a minimum drag coefficient of about 0.02. This occurs when the space between the bodies g is from 0.25 to 0.50 d_2 . But when the disk is placed too far in front of the main body, the wake does not attach smoothly but sets up an oscillation where the cavity flow becomes unsteady, the drag increases in this situation.

In 1987, Pamadi, Pereira and Gowda (Ref.9) studied experimentally the effect of strakes on the drag reduction of a typical non circular cross-section with sharp windward corners, and they

found that the strake height and, more particularly, its location on the windward face, has strong influence on the flow pattern, base pressure, and drag coefficient. By this technique they found that it is possible to get a reduction in drag of the order of 80% for an optimum condition of geometrical parameters.

In 1980, Morel and Bohn (Ref.4) studied experimentally the flow over two circular disks in tandem for the purpose of drag reduction. They showed that when two disks of unequal diameters, normal to the flow are placed in tandem, very significant drag reduction may be achieved by proper sizing of the disk diameter and the gap between them. Placing a properly sized disk at an optimum distance ahead of a single reference disk can result in a configuration whose total drag is up to 81 percent lower than that of the reference disk alone.

In 1978, Little and Whipkey (Ref.6) studied experimentally the aerodynamics of the drag and flow characteristics of locked vortex after body shapes formed by thin disks spaced along a central spindle. They found that in order to reduce drag, the disk or other device defining the downstream boundary of the locked vortex cavity must be large enough to separate the wake back flow from the cavity flow so that a locked vortex can exist in the cavity. Furthermore, the cavity thus formed must have dimensions such that the locked vortex effectively fills the cavity. This then appears to be the key for defining optimum locked vortex geometries-to define the cavity dimensions for a given flow which

will match the smooth stable vortex. They found the optimum combination, which gives that the minimum drag occurs at $D/D_o = 0.75$, $x/D_o = 0.6$, $d/D_o = 0.0938$ where D_o , D and d are fore body, disk and spindle diameter respectively and x is the axial distance from body base to disk.

1978, Nakaguchi (Ref.20) studied experimentally the aerodynamic characteristics of bars of square cross-section aligned with the flow, the results show the relationship between drag coefficient and angle of incidence for bars of various L/W ratio. For bars of L/W ratio less than 1.2 the drag coefficient remains fairly constant throughout the angle of incidence range ($\alpha = -3$ to 15 deg.). On bars of L/W ratio more than 1.6, however the drag coefficient increases parabolically as angle of incidence increases.

In 1977, Zdravkovic (Ref.3) studied experimentally the flow interference between two circular cylinders in various arrangements. He studied the flow pattern, drag coefficient and Reynolds Number effects.

In 1953, Roshko (Ref.10) made a semi empirical study on the drag and shedding frequency of two-dimensional bluff bodies. Dimensional analysis of a simple model of the region leads to a universal strouhal number which is then experimentally determined as a function of wake Reynolds number R^* . This result, together with free-streamline theory, allows the drag to be calculated from measurement of the shedding frequency and furnishes a useful correlation between different bluff cylinders.

However, very little work has been done to investigate the flow past two bluff bodies, like (square-cross sectional with sharp corners bodies) . Therefore, in the present study, flow past a square-cross sectional, sharp-corners and rounded back bluff body was investigated by measuring the drag and pressure distribution over it . Further, flow over the main body with a flat-plate and a D-shape placed in front of it was investigated to study the drag reduction mechanism . The configuration shown in Fig.3 was investigated in the present work . It consisted a square cross-section with rounded back and sharp-corner rear body with axis parallel to the wind-tunnel free stream, with $b_2 = 100$ mm and $R = 50$ mm.

1.4 Scope of the present work

Because of the complexity associated with the theoretical analysis of the problem, the study of drag-reducing techniques for bluff bodies has been almost entirely experimental. The bodies that have been studied have usually been two-dimensional, and sometimes axi-symmetric, and much less work has been done on three-dimensional bodies. Therefore, the objective of present work are:

1. To study experimentally the effects of geometries namely, width b_1/b_2 and gap g/b_2 ratios on the flow field and drag coefficient of three-dimensional, noncircular cylinders separated by a gap.

2. To achieve the optimum combinations (a certain combinations in width b_1^*/b_2 and gap g^*/b_2 ratios) at which the minimum drag coefficient C_D^* occurs for D-shape and square-plate front bodies .
3. To study the effect of Reynolds numbers variation on the drag coefficient and percentage drag reduction . The present experiments were carried out at three speeds, giving $Re = 1.0, 1.4$ and 1.8×10^5 based on the rear body width (b_2).
4. To investigate the behaviour of pressure coefficient (C_p) on the rear body midplane . Also, study this behaviour with D-shape and square-plate front bodies, by varying the width and gap ratios .
5. To classify the drag-regimes, which is based on the optimum flow for both D-shape and square-plate front bodies.

Measurement of drag and wall static pressures were made for the rear body alone and for rear body with square-plate and D-shape front bodies . The parametric variations considered in the present study are the following:

Model With D-shape Front Body

Reynolds number $Re_{b2} = 1, 1.4$ and 1.8×10^5

Width ratios $b_1/b_2 = 1.0, 0.75, 0.625, 0.50, 0.37$ and 0.25

Gap ratios $g/b_2 = 0.25, 0.50, 0.75, 1.0, 1.25, 1.50, 1.75, 2.0$
and 2.25

Curvature radius R (mm) = $50, 37.5, 31.25, 25, 18.5$ and 12.5

A total of 162 experiments were conducted for these combination .

Model With Square-plate Front Body

Reynolds number $Re_{b2} = 1, 1.4$ and 1.8×10^5

Width ratios $b_1/b_2 = 1.0, 0.75, 0.625, 0.50, 0.37$ and 0.25

Gap ratios $g/b_2 = 0.25, 0.50, 0.75, 1.0, 1.25, 1.50, 1.75, 2.0$
and 2.25

A total of 162 experiments were conducted for these combination .

EXPERIMENTAL SET-UP AND MEASURING INSTRUMENTATION

2.1 Introduction

There are many important aspects considered in the experimental set-up, wind tunnel, design and fabrication of experimental models (rear and front bodies), measuring instrument and devices which are used in present measurements for drag, lift and pitching moment.

The experimental testing procedure, reading data correlation and measuring accuracy are described in this chapter.

2.2 Wind Tunnel

The experiments were carried out in closed-circuit, low-speed, three-dimensional wind tunnel, having a velocity range up to 45 (m/s).

The main parts of the tunnel used are given in Fig.4, the layout consists of contraction cone (3), diffuser (4), return diffuser (5), turning vanes (7), screens (8) (the number beside each part is indicated the location of it in Fig.4).

Basically the wind tunnel used has two test-section , one is 2-dimensional, with dimension (5 . 6 x 1 x 4) and the second is 3-dimensional, with dimension (5 . 6 x 3 x 2), the tunnel is run by two 12-bladed fans which are rotated by a 15 H.P electric motor.

2.3 Design of Experimental Models

The experimental models shown in Fig.3, consist of three main parts:

- 1) Rear body (basic body) model
- 2) Front body
- 3) Threaded Rods

2.3.1 Design of Rear Body

The subcritical Reynolds number for the present model is around 1.1×10^5 (Ref.9). For Reynolds number more than 1.1×10^5 , the boundary layer separation from the front body corners is expected to be turbulent.

The rear body model is shown in Fig.3, having length 108 mm, height 100 mm and width 100 mm. It consists of three parts, as shown in Fig.5. First part is the square plate constructed out of perspex. It has (100 x 100) mm width and 15 mm thickness. At the center of this square plate 8 mm tapped hole is provided to fix a thread rod. At the other end of the rod, the front body will be fixed.

Second part of the model is square box made out of well-seasoned teak wood of 8 mm thickness. The sides are 100 mm long and 43 mm wide.

Third part is a half cylinder with outer radius 50 mm and inner radius 42 mm, constructed out of well-seasoned teak wood. Schematic diagram of all the three parts are shown in Fig.5.

All the parts are polished well by using sand paper to get a smooth surface finish. For pressure measurement, 39 wall pressure taps were provided on the rear body, at the midplane cross section (section AA) as shown in Fig.3. The pressure tubes from different tapes were taken out through two holes (10 mm radius) made at the bottom of third part, adjacent to the rear supports, and then were connected to the multimanometer.

2.3.2 Design of Front Body of the Model

Two shapes were used as front body, as shown in Fig.6 (b,c) are:

(1) Square cross-section flat plate with sharp-corners, as shown in Fig.6(b). Six such plate of 12 mm thickness were used. The length and width of the plate are varied from 25 to 100 mm. Each plate has a 6 mm tapped at the center to mount the threaded rod. All the six plates were made out of well-seasoned teak wood and polished to have a smooth surface finishing.

(2) D-shape front body, six models were constructed out of well-seasoned teak wood, with dimensions, as shown in Fig.6.c.

2.3.3. Design of Threaded Rods

Three shafts were made out of aluminum with 8 mm diameter, and lengths 55, 105 and 225 mm, as shown in Fig.6(a), to achieve all the desired gap ratio g/b_2 (0.25 to 2.25 in step of 0.25).

2.4 Measuring Instruments

In present experimental work, the following measurements were carried out:

(i) Free stream velocity (V_∞) was measured by using pitot-static tube, which is placed in the beginning, at the center line of the test-section. The pitot-static tube is fixed in roof of wind tunnel, as shown in photograph (1). It was connected by rubber tubes to multimanometer. The pitot-static tube measured the difference between freestream total pressure P_∞ and static pressure P_∞ , in term of water column. From the measured pressure, the freestream velocity V_∞ was calculated with the formula:

$$V_\infty = \sqrt{\frac{2(\Delta P) \rho_{H2O}}{\rho_{air}} g}$$

(ii) The pressure variation on the surface of rear body were measured with the wall pressure taps. The pressure tap locations at which pressure were measured are indicated, in Fig. 3. Altogether, there are 39 taps of 0.8 mm diameter and are located at the midplane cross-section of the rear body. The scale of θ is stretched between ($\theta = 0$ to 40 and 320 to 360 deg.) to bring out clearly the variation of pressure between the center line of the face and the outer corners. The pressure tubes from different tapes were taken out from the bottom and connected to multimanometer, which have about 60 tubes

and inclined at 30° to the horizontal, as shown in photograph (3).

(iii) Drag force of experimental model was measured directly using a three-component balance with electronic digital displays as shown in photograph (2 & 4). Installation details of a three-component balance device with experimental model are shown schematically (side view) in Fig. 7. The maximum rated load capacities for this balance are; ± 120 Newton for lift, ± 60 Newton for drag, and for pitching moment ± 2.5 Newton meter. Experience with this type of balance has shown it to be of sufficient accuracy to completely dispense with length calibration matrices and conversion co-efficient, interaction of one component to another have largely been eliminated and in any case are so small as to be negligible. The advantage of using this measuring device is that it does not disturb the flow, as it is kept outside the test-section. Since it does not require any pressure devices on the test-model, it is the most convenient way for measuring lift, drag and pitching moment directly. For mounting the model on the balance, a horizontal support was fabricated out of stainless-steel with length 240 mm, width 20 mm and 5 mm thickness. It is fixed by two screws with the two front vertical supports of the three-component balance. On this support, the rear body was firmly fixed.

2.5 Experimental Procedure

The present investigation consisted of drag force measurement and static pressure measurement in midplane of the rear body. These measurements have been carried out at three different speeds to cover the range of experiment Reynolds numbers from 1.0 to 1.8×10^5 . The steps followed for drag and wall static pressure measurements for rear body alone are:

(1). The three component-balance was placed under the wind tunnel test-section. It was not in any way connected to the tunnel structure. Otherwise, tunnel vibrations may be transmitted to the balance causing undesirable harmonics within the load sensing system.

(2). The balance was leveled in both longitudinal and lateral planes by using the sensitive liquid levels on the earth frame and adjusting the four corner screws until the bubbles are level in both planes.

(3). The digital display was kept in a suitable position as shown in photograph (4), near the wind tunnel test-section and connected the cables from the balance to it. For all former steps, the balance is locked by pitching pin.

(4). The basic body was mounted (rear body alone) on the horizontal strut 250 mm length, 20 mm width and 5 mm thickness fabricated out of stainless-steel. This struts was mounted on the main struts using 3 mm dowel pins.

(5). It was checked that the horizontal axes of the model are as required ($\alpha = 0.0$ deg.), the balance can be adjusted if necessary by adjusting the combined screw threads of the spherical bearings and their respective mounting studs.

(6). The power supply to the balance was switched on and allowed approximately ten minutes for the system to warm up. After that the pitch locking pin was removed.

(7). After the warming up period, all mechanical tare weights were adjusted to give approximate zero readings for drag, lift and pitching moment on the digital display.

(8). Finally, with the balance unlocked, pitch locking pin removed. I was ensured that all digital displays reading are zero. The three component-balance and model are now ready for testing.

(9). The pitot-static tubes and pressure tubes connection to the multimanometer was checked.

(10). Start the wind tunnel, adjusted the speed to 15.34 m/sec free stream velocity, allow five minutes for the wind tunnel to stabilizes. Record the drag, lift and pitching moment from the digital displays and static pressure reading from multimanometer. Increase the wind tunnel speed to give 20.38 m/sec and recorded the above readings for second speed. Repeat the same for third speed 26.84 m/sec. All the reading for rear body are tabulated in Appendix B.

Following testing procedure steps were done for rear body with front body:

(1). After completing all the planned measurements on the rear body, the threaded rod was mounted at the tapped hole at the center line of the rear body face, as shown in Fig.7. A 10 mm tube was placed on the threaded rod as sleeve. Different threaded rods and suitable sleeve were fabricated to result in gap ratio g/b_2 of 2.25, 2.0, 1.75, 1.50, 1.25, 1.0, 0.75, 0.50, and 0.25. The sleeve was used to ensure a smooth surface for the flow around the shaft. The D-shape front body was mounted at the other end of the threaded rod.

(2). The assembly was mounted by fixing the sleeve at the center of gravity, using a clamp. It was checked for zero angle of incidence.

(3). Repeated the experiments as earlier with a D-shape front body having $b_1/b_2 = 1.0$ at $g/b_2 = 2.25$.

(4). The second D-shape front body with $b_1/b_2 = 0.75$, and $g/b_2 = 2.26$ was the arrangement for the next set of measurements.

(5). For the other D-shapes having $b_1/b_2 = 0.625, 0.50, 0.37, 0.25$, repeated steps (3,4) for the same gap ratio $g/b_2 = 2.25$. The reading are tabulated in tables 1 to 6 ,in appendix B.

(6). Similar measurements were done with D-shape front body by running the gap ratio from 2.0 to 2.25, in steps of 0.25. All the experimental data are given in tables 6 to 54, in appendix B.

(7). For square-plate front body, repeated the steps (1,2,3,4,5 and 6). The reading are tabulated in table 1 to 54,in appendix B.

2.6. Measurements Accuracy

Measurements accuracy may be defined by the accuracy or sensitivity of the devices used, or the sensitivity, as minimum readable division, of each device used in measuring the different quantities.

In present work, the following consideration are taken into account.

1. Pitot-static tube errors

The location of the pitot-static tube, which was previously calibrated, must be adjusted so that its static hole is perpendicular to the flow, for error free reading.

2. Three-Component balance

After adjusting all mechanical tare weights for lift, drag and pitching moment arms of the wind tunnel balance, all the displays should read essentially zero. After the wind tunnel run stabilizes at a desired speed, digital display will still unstable in reading and we get the average reading for above variables. So, the maximum error in lift less than ($\pm 0.08\%$), less than ($\pm 0.08\%$) for pitching moment and less than ($\pm 0.03\%$) for drag. All this maximum error applied for full scale. And the maximum errors due to interactions are; lift into pitch are zero, lift into drag (0.08%), pitch into lift (0.03%), pitch into drag (0.03%), drag into lift (0.03%), drag into pitch (0.08%), all this maximum errors for full scale (3-component balance, operation report).

3. Multi manometer errors

Visual errors, which affect the values of reading, are usually within half of the smallest scale reading (± 0.5 mm).

2.7 Reading Corrections for three-component balance

In present work, the following corrections for drag reading were carried out:

(1). When the runs with all the models were over, the drag due to three-component balance supports (struts, clamp) was measured for three different speeds. These values were then subtracted from the total drag value for each b_1/b_2 ratio, the drag force for supports are $D = 1.42$ N at $V_\infty = 26.84$ m/sec, $D = 0.83$ N at $V_\infty = 20.38$ m/sec, $D = 0.44$ N at $V_\infty = 15.34$ m/sec.

(2). The different values obtained for drag were corrected using the calibration table of three-component balance as shown in Fig.19, in Appendix A. All the measured drag values were corrected by multiplying by (K_{drag}) , where (K_{drag}) is the correction factor.

(3). It is a well established fact that the measurements made in a wind tunnel whose test section is bounded by solid walls do not duplicate exactly a free-stream (unbounded) environment. This is a consequence of the constraining effect of the tunnel wall which made the wall streamlines follow the wall contours, rather than being shaped by the flow field around the tested model. This constraining effect is felt at the model itself and results in a modification of the local flow field around it. The larger the model frontal area, the stronger is the constraining effect the

tunnel walls exert by keeping the wall streamlines straight and, vice versa, the stronger is the influence of this effect back on the flow field around the body.

This effect and its magnitude have been the subject of many studies. Among them, one of the best known is the analysis performed by Maskell (Ref.22), who developed a theory for pressure-drag correction for the effects of model blockage. The correction has the following form :

$$\frac{C_D}{C_{D_c}} = 1.0 + \epsilon C_D b$$

where

C_{D_c} = Correct drag coefficient

ϵ = Blockage factor

b = Ratio of model front area to wind tunnel cross-sectional area (model blockage)

The above correction form (Maskells correction) is particularly suitable for the present configuration. But in present study, no blockage correction was applied to the data presented here. This is justified on the following basic : (1) configuration change were not large, and (2) all test were made at zero attack angle.

CHAPTER 3

RESULTS AND DISCUSSION

The recorded data consisting of the drag coefficient C_D for rear body with D-shape and square-plate front bodies at various width b_1/b_2 and gap g/b_2 ratios are presented in tables 1 and 2 of Appendix A, respectively.

The variation of the Drag coefficient with the gap ratio g/b_2 and with the width ratio b_1/b_2 is shown in Figs. 9 and 12, for three speeds. The optimum combination is indicated by an asterisk (*). It occurs at width b_1^*/b_2 and gap g^*/b_2 ratios, and the drag coefficient at the optimum case is marked by (C_D^*) . The percentage drag reduction are shown in Figs. 10 and 13, for D-shape and square-plate front bodies, respectively. Besides the above graphical representations, the calculated results for percentage drag reduction are presented in tables 3 and 4 of Appendix A. Maximum percentage drag reduction variation with b_1^*/b_2 ratio and with the gap ratio g^*/b_2 at which it occurs is shown in Fig. 15(a and b), respectively, for D-shape and square-plate bodies. Variation of the percentage drag reduction for optimum combination with the Reynolds number is shown in Fig. 18 (a and b) for D-shape and square-plate front bodies, respectively.

The measured pressure coefficient C_p for rear body alone (without front body), and with D-shape and square-plate front bodies at various width b_1/b_2 and gap g/b_2 ratios for three speeds, are presented in tables 1 to 55 of Appendix B. For comparison, the pressure distribution for optimum combination (b_1^*/b_2 and g^*/b_2) with large and small gap ratios for the same b_1/b_2 combination are represented by curves as shown in Figs. 11 and 14 for D-shape and square-plate front bodies at three speeds, respectively.

Comparison between the drag coefficient of D-shape and square-plate front bodies, and also the classification of drag coefficient into three regimes (low, medium and high-drag regimes), based on the optimum flow configuration as shown in Figs. 16 and 17, respectively, are discussed in this chapter.

3.1 Drag coefficient results

Many observation may be made on inspection of Figs. 9 and 12, showing the variation of drag coefficient C_D with width b_1/b_2 and gap g/b_2 ratios, for each front body was tested at three different speeds.

The effects of front body shape on the total drag coefficient of the rear body at different gap ratio g/b_2 and width ratio b_1/b_2 are discussed separately.

3.1.1. Drag coefficient for rear body alone

The first configuration studied was rear body alone with $b_2 = 100$ mm and $R = 50$ mm, where R are the radius of rounded back curvature. The value of drag coefficient C_{D_o} of the rear body was found to be; $C_{D_o} = 1.42$ at $Re = 1.8 \times 10^5$, $C_{D_o} = 1.39$ at $Re = 1.4 \times 10^5$ and $C_{D_o} = 1.28$ at $Re = 1 \times 10^5$.

The high drag coefficient for rear body C_{D_o} in range 1.28 to 1.42 refers to, first, part of it is resulting due to a deficit of pressure (suction pressure) on the downstream sides (top, bottom and rear faces), as shown in Fig.8 ($\theta = 40-320$ deg.), which occurs due to the flow separation at sharp corners of the front face and an excess (high positive) pressure due to the stagnation of the approach flow on the front face, as shown in Fig. 8 ($\theta = 0-40$ and 320-360 deg.). Secondly, due to boundary layers separated from the corners resulting in large wake zone behind the body, which is extensive wake, larger in size compared to the cross-sectional width of the body Fig.3. The wake is characterized by strong, alternate and periodic vortex shedding. The flow is oscillatory. The separated boundary layers at the sharp corners feed larger amounts of vorticity, which are shed continuously in downstream direction. This loss of energy appears in the form of a large, time-averaged base suction ($C_p \approx -1.0$) and a large drag force on the rear body. The pressure distribution on the rear body surface, is shown in Fig.8.

3.1.2. Drag coefficient for D-shape front body

This combination involved the rear body and D-shape front body with the curved portion of front body facing the flow direction. Combination drag coefficient C_D for different width ratios ($b_1/b_2 = 1.0, 0.75, 0.625, 0.50, 0.37$ and 0.25) are measured when the gap ratio g/b_2 changes from 0.25 to 2.25 , monotonically in increments of 0.25 .

Each combination of the front body and the rear body model was tested for three freestream speeds, and the corresponding Reynolds numbers based on the width (b_2) are $1.0, 1.4$ and 1.8×10^5 . The results are plotted in Fig. 9 and are discussed for each front body, separately:

For $b_1/b_2 = 1.0$, Fig.9a shows the combination drag coefficient C_D variation with the gap ratio g/b_2 and Reynolds number. For $Re = 1 \times 10^5$, the drag coefficient C_D was 1.61 at gap ratio 0.25 , and then decreased to 1.45 at gap ratio 0.50 and then increased reaching the maximum value 1.94 at gap ratio 0.75 and then the drag coefficient shows an oscillating nature reaching the optimum case for this combination, which has drag coefficient $C_D^* = 1.39$ at gap ratio $g^*/b_2 = 2.25$ as shown in Fig. 10. Still the drag coefficient is more than the C_D for rear body alone even in optimum case.

On the other hand, there was some evidence of Reynolds number effect on the results obtained with the same combination. For $Re = 1.4 \times 10^5$ and the gap ratio in range 0.25 to 0.75 , it was found that, drag coefficient reached a minimum at $g^*/b_2 = 0.50$

with value $C_D^* = 1.0$, which is 22 percent below the C_D for rear body alone. Beyond this minimum, the drag coefficient increased sharply, reaching a maximum value of $C_D = 1.83$ at $g/b_2 = 1.0$, and then it decreased slightly. For gap ratios in the range $g/b_2 = 1.25$ to 2.25 , the C_D values were limited between 1.4 to 1.6.

For $Re = 1.8 \times 10^5$, it is found that C_D attains a minimum value of $C_D^* = 0.75$ at gap ratio $g^*/b_2 = 0.25$, which is 47 percent below the C_D for rear body alone. Beyond this minimum, the drag coefficient increased reaching a maximum at $g/b_2 = 0.75$ with value 1.66, and then it decreased slightly. For gap ratio in the range 1.0 to 2.25, the C_D value is limited between 1.1 to 1.39.

For $b_1/b_2 = 0.75$, Fig. 9b shows the drag coefficient variation with the gap ratio g/b_2 and Reynolds number. For $Re = 1 \times 10^5$, the drag coefficient curve reaches the optimum value with $C_D^* = 0.74$ at gap ratio $g^*/b_2 = 0.25$, which is 42 percent below the C_D for rear body alone.

The optimum cases indicate that the separated boundary layers from the edges of front body, reattached at or near the corners of rear body. The corresponding pressure coefficient (C_p) distribution is shown in Fig. 11.

For gap ratio between 1.0 to 2.25, all the drag coefficients obtained are more than the C_D for rear body alone. This is because, the separated boundary layers from the edges of front body, reattached on the face of the rear body and again separated from its corners. In this case there are two wake zones, first one, behind the front body and second behind the rear body.

For $Re = 1.4$ and 1.8×10^5 , the two drag coefficient curves are similar in behaviour, both reached a minimum drag coefficient at $g^*/b_2 = 0.25$ with value $C_D^* = 0.54$ and 0.43 , which are 61 and 70 percent below the C_D for rear body alone, respectively.

The combination reached the optimum case at gap ratio $g^*/b_2 = 0.25$ at $Re = 1.8 \times 10^5$, which have drag coefficient $C_D^* = 0.43$ and the corresponding drag reduction is 70 percent below the C_D for rear body alone. According to the present results, the minimum drag coefficient for D-shape front body at $Re = 1.8 \times 10^5$, can be achieved only when $b_1/b_2 = 0.75$ and gap ratio $g^*/b_2 = 0.25$, as shown in Fig. 10.

For $b_1/b_2 = 0.625$, Fig.9c shows that all the three curves have similar behaviour for the Reynolds numbers 1.0 , 1.4 and 1.8×10^5 . They reached their minimum drag coefficient at $g/b_2 = 1.25$ with values 0.66 , 0.54 and 0.45 , which are 48, 61 and 68 percent below the C_D for rear body alone, for the corresponding Reynolds numbers. This refers to the flow pattern; on the front faces F1 and F2 shown in Fig.11(a-II). The face is completely subjected to zero pressure gradient for $g^*/b_2 = 1.25$. The high suction at the top ($\theta = 40-90$ deg.) and on the bottom surface ($\theta = 270-320$ deg.), due to reveals flow attachment on the top and bottom surfaces. Also, they reached the maximum at gap ratio 1.75 with values 0.97 , 1.27 and 1.74 , which are 31, 8 and -6 percent below the C_D for rear body alone, for the corresponding Reynolds numbers. This negative sign means the drag coefficient for combination is more than the drag coefficient for rear body

alone. As the gap ratio increased or decreased from the optimum gap 1.25 ratio, the C_p values as shown in Fig.11(a-I and III), in both cases the shear layers that separated from the D-shape front body attach to the front surface F1 and F2 of the rear body.

The optimum case for $b_1/b_2 = 0.625$, occurs at $g^*/b_2 = 1.25$. This drag coefficient C_D^* is very low and the corresponding drag reduction is high. This refers to the flow pattern; where the separated boundary layers from the edges of front body reattached to rear body shoulders at its face. It may be seen from the pressure distribution in Fig. 11(a-II), the pressure coefficient value on the rear body flat face are zero and in the rear side are very small ($C_p \approx 0.1$).

At gap ratio 0.25, the combination drag coefficient values are 0.84, 0.70 and 0.48, which was 34, 49 and 66 percent below the C_D for rear body alone, for the corresponding Reynolds numbers. The drag coefficient increased up to the gap ratio of 1.0, reaching the value 1.28, 1.02 and 0.73, which was zero, 26 and 48 percent below the C_D for rear body alone, respectively. The optimum case was at gap ratio 1.25, and then the drag coefficient increased reaching the maximum value at gap ratio 1.75.

For $b_1/b_2 = 0.50$, Fig.9d shows the drag coefficient results. For $Re = 1 \times 10^5$ and 1.4×10^5 the drag coefficient variation with gap ratio was similar in behaviour. The drag coefficient C_D at gap ratio 0.25 has values 0.96 and 0.82, which is 25 and 41 percent below the C_D for the rear body alone, respectively. At gap ratio 0.25 the drag coefficient reaches a

minimum value and we can consider the C_D and gap ratio 0.25 is the optimum case for width ratio 0.50. Referring to the flow pattern, it may be seen from the results of percentage drag reduction in table 3 in Appendix A.

The C_D jumped to values 1.30 and 1.07 at gap ratio 0.50, and then decreased to values 1.06 and 0.93, at gap ratio 0.75, respectively. For gap ratios in the range 1.0 to 1.25, the drag coefficient C_D is in range from 1.0 to 1.44 and from 1.08 to 1.23, respectively. The maximum value of C_D are 1.12 and 1.44, respectively at the gap ratio 2.25.

For $Re = 1.8 \times 10^5$, the drag coefficient has a minimum value of 0.55 at gap ratio 0.25, which is 61 percent below the C_D for rear body alone. The drag coefficient increases gradually with increasing gap ratios from 0.50 to 2.25 reaching the maximum value 0.97 at gap ratio 2.25, which was 25 percent below the C_D for rear body alone.

For $b_1/b_2 = 0.37$, the C_D results are shown in Fig.9e. All the three curves have reached a minimum drag coefficient at gap ratio 0.75 with values $C_D^* = 0.42$ at $Re = 1 \times 10^5$, $C_D^* = 0.62$ at $Re = 1.4 \times 10^5$ and $C_D^* = 0.46$ at $Re = 1.8 \times 10^5$, which are 67, 55 and 67 percent below the C_{D_0} for rear body alone, respectively. Low drag coefficient can be achieved for this combination only at gap ratio 0.75. At this gap ratio, the separated shear layers from the edges of front body reattached onto the rear body corners. The pressure coefficient C_p in the face of rear body is very close to zero, as shown in Fig. 11(b-II).

Beyond the optimum case, the drag coefficient increased slightly and was roughly constant between the gap ratios 1.0 to 2.25. For the small gap ratio 0.25 to 0.50, the drag coefficient C_D in larger magnitude compared with the optimum case ($b_1^*/b_2 = 0.37$ and $g^*/b_2 = 0.75$). As the gap increased or decreased (more or less) than the optimum gap Fig.11 (b-I and III) the C_P values become more positive than the optimum combination especially on the front face, and less negative in top, bottom and rear faces.

For $b_1/b_2 = 0.25$, Fig.9f, shows the similar variation of drag coefficient with the gap ratio for Reynolds numbers. For small gap ratio $g/b_2 = 0.25$, drag coefficient values are $C_D = 0.76$ at $Re = 1.0 \times 10^5$, $C_D = 0.88$ at $Re = 1.4 \times 10^5$ and $C_D = 0.75$ at $Re = 1.8 \times 10^5$, which is 40, 36, and 31 percent below the C_D for rear body alone, respectively. All the three curves reached the minimum values of $C_D^* = 0.39, 0.58$ and 0.48 , which are 70, 58 and 66 percent below the C_D for rear body alone, for corresponding the Reynolds numbers. The C_P values for the optimum combination is shown in Fig.11(c-II), on the front face F1 and F2. The C_P values are positive ($C_P = 0.4$) at the face, but on the top and bottom surfaces, there is high suction pressure due to flow attachment.

Beyond the minimum, the drag coefficient C_D increased sharply reaching the maximum values of 1.46, 1.39 and 0.98 at gap ratio 1.0, and then decreased again to second minimum values of 1.0, 0.72 and 0.72 at gap ratio 1.50, which are 17, 48 and 49 percent below the C_D for rear body alone, for the corresponding Reynolds numbers. For gap ratio in the range 1.75 to 2.25, the

drag coefficient is approximately constant, with value $C_D = 0.88$, 1.25, and 0.98 for the corresponding Reynolds numbers. As the gap increased or decreased (more or less) than the optimum gap, as shown in Fig.11 (c-I and III) the C_p values become more positive than the optimum combination especially on the front face, and less negative at the top, bottom and rear faces.

In summary, the combination of two bluff bodies in tandem often has lower drag than that of single bluff body. More precisely, if the width ratio for D-shape front body combination b_1/b_2 is in the range 0.25 to 0.75, then the combination drag coefficient, at a proper gap distance, will be lower than the drag coefficient of rear body alone. The combination (rear body with D-shape front body) which has a drag coefficient minimum are :

(i) $b_1^*/b_2 = 0.75$ (Figs. 9b and 15a), at gap ratio $g^*/b_2 = 0.25$, with values 0.74, 0.54 and 0.42, which are 42, 61 and 70 percent below the C_D for rear body alone, for corresponding the Reynolds number.

(ii) $b_1^*/b_2 = 0.625$ at gap ratio 1.25, which are 48, 61, and 68 percent below the C_D for the rear body alone, for corresponding the Reynolds number.

(iii) $b_1^*/b_2 = 0.37$ at gap ratio 0.75, which are 67, 55 and 67 percent below the C_D for rear body alone, for corresponding the Reynolds number.

(iv) $b_1^*/b_2 = 0.25$ at gap ratio 0.50, which are 70, 58 and 66 percent below the C_D for rear body alone, for the corresponding Reynolds numbers, as shown in Fig.10.

The drag coefficient of the optimum combination ($b_1^*/b_2 = 0.25$ and $g^*/b_2 = 0.50$) is as low as 0.39, which is 70 percent below the C_D for rear body alone.

From Fig.11 we note that there is a remarkable contrast in the variation of the pressure coefficient between the case for which $b_1/b_2 = 0.25$ and gap ratio 0.50, with the cases for which the gap ratios are small and large for the same b_1/b_2 ratio. For the optimum case, pressure coefficient value on the rear body flat face are small ($C_p = 0.3$) and on the rear side are very small ($C_p = -0.1$). This fact can be explained in terms of boundary layers, where it separated from the front body leading edges and are reattached onto or very close to the corners of front face of the rear body which is resulting a very small wake zone behind the rear body.

For the same width ratio $b_1/b_2 = 0.25$, but with gap ratio larger than the optimum ($g/b_2 = 1.50$), the boundary layers separated from the leading edges of front body and are reattached on the rear body flat face resulting in a larger pressure coefficient value on the rear body face ($C_p = 0.8$) compared with the optimum case ($C_p = 0.3$).

For the case with the gap ratio of 0.25, the separated boundary layers from the leading edges of front body reattach on the rear body flat face ($C_p \approx 0.8$), and again separated from the rear body face and reattachment out side the rear body corners,

that causes the pressure coefficient of ($C_p \approx -0.3$) at the rear surface. The pressure coefficient (C_p) for others optimum case are shown in Fig. 11.

3.1.3. Drag Coefficient for square-plate front body

In this combination, there is a square-plate shape placed upstream of the rear body. Combination drag coefficient C_D for different width ratios ($b_1/b_2 = 1.0, 0.75, 0.625, 0.50, 0.37$ and 0.25) are measured with the gap ratio g/b_2 varying from 0.25 to 2.25, in steps of 0.25.

Each combination of the front body and the rear body model was tested for three free stream speeds, and the corresponding Reynolds number based on the width (b_2) are; 1.0, 1.4 and 1.8×10^5 . The results are plotted in Fig.12, we will discuss the result for each front body separately:

For $b_1/b_2 = 1.0$, Fig.12a shows the drag coefficient variation with the gap ratio and Reynolds number. All the three curves are similar in behaviour. For Reynolds numbers 1.0, 1.4 and 1.8×10^5 , the drag coefficients with the gap ratio of 0.25 are 1.16, 0.98 and 0.85, which are 9, 22 and 40 percent below the C_D for rear body alone, for corresponding the Reynolds numbers. For gap ratio 0.50, all the three curves reach a minimum values C_D^* = 1.0, 0.86 and 0.69, which are 19, 38 and 51 percent below the C_D for the rear body alone, for corresponding the Reynolds numbers, and then the drag coefficient increased reaching the value 1.30, 1.25 and 0.86 at gap ratio 0.75, which are -2, 10 and 39 percent below the C_D for rear body alone. The negative sign in percentage

drag reduction, same as that explained in the previous section.

For large gap ratios 1.25 to 2.25 the drag coefficient increased reaching the maximum at gap ratio 2.25 with value 1.75, 1.6, and 1.53, which are -37, -22 and -8 percent below the C_D for the rear body alone, at the corresponding the Reynolds numbers.

For $b_1/b_2 = 0.75$, Fig.12b shows the variation of drag coefficient with gap ratio and Reynolds numbers. All the three curves are similar in behaviour. For the gap ratio of 0.25, the shear layers separates from the front body corners without reattachment, and the wake zone has open up, therefore, the drag coefficient is an order of magnitude more. The optimum case occurs at gap ratio $g^*/b_2 = 0.50$ with values C_D^* are 0.42, 0.37 and 0.28, which are 67, 73, and 80 percent below the C_D for rear body alone, respectively.

For the combination of square-plate front body and the rear body, the choice of $b_1/b_2 = 0.75$ and $g^*/b_2 = 0.5$ is the optimum case. This can be seen from Fig. 14 (a-II), where the pressure coefficient is completely negative over the enterice face of rear body and is quite uniform. Particularly it is interesting to observe that at gap ratio $g^*/b_2 = 0.50$, C_P values on the front face F1 and F2 are even more negative than those on the rear face ($\theta = 90-270$ deg.) as shown in Fig. 14 (a-II), therefore, the drag coefficient at this optimum combination has very small value, and the corresponding drag reduction is high (80%).

Beyond the optimum case, the drag coefficient increases reaching the value 1.16, 0.98 and 62 at gap ratio 0.75, which are

9, 29 and 56 percent below the C_D for rear body alone, for the corresponding Reynolds numbers. The drag coefficient reduced reaching the value 1.0, 0.82 and 0.62 at gap ratio 1.0, which are 18, 41 and 56 percent below the C_D for rear body alone. For gap ratio in range 1.25 to 2.25 and for $Re = 1 \times 10^5$, there is no drag reduction. More over placing the front body with $b_1/b_2 = 0.75$ at this gap ratio will add drag to that of rear body.

For $Re = 1.4$ and 1.8×10^5 , when the gap ratio (1.25 to 2.25) is increased, the percentage drag reduction decreased.

For $b_1/b_2 = 0.625$, Fig.12c shows the variation of drag coefficient C_D with the gap ratio and Reynolds numbers. All the three curves are similar in behaviour, reaching the minimum at gap ratio 0.25 with values $C_D^* = 0.66, 0.58$ and 0.3 , which are 48, 58 and 72 percent below the C_D for rear body alone, respectively. Hence the separated boundary layers reattach onto or very close to the rear body corners. The percentage drag reduction results are shown in Fig.13b. Maximum drag reduction for the optimum case (i.e. $b_1^*/b_2 = 0.625$ and $g^*/b_2 = 0.25$) is less than the former optimum case (i.e. $b_1^*/b_2 = 0.75$ and $g^*/b_2 = 0.50$), and this results is clearly seen from the C_P values as shown in Fig. 14b. Again the C_P values are completely negative for the optimum combination, as shown in Fig. 14 (b-II), but the C_P values on the front face F1 and F2 are roughly same to that on the rear face ($\theta = 90-270$ deg.) in negative values, therefore, the drag coefficient C_D is more than those on the optimum combination, as shown in Fig.14(a-II), and the corresponding drag reduction is small.

Beyond the optimum case, for the gap ratio in the range 0.50 to 2.25, the drag coefficient increases or percentage drag reduction decreases with increasing gap ratio, reaching the maximum value at gap ratio 2.25 with value 1.52, 1.34 and 1.0, which are -19, 3 ad 27 percent below the C_D for rear body alone, respectively.

For $b_1/b_2 = 0.50$, Fig.12d, shows that the drag coefficient C_D has very low values for low values of the gap ratio. For gap ratio 0.25 to 0.50, the drag coefficients C_D are roughly the same, and the minimum values $C_D^* = 0.66, 0.62$ and 0.44 , which are 48, 55 and 70 percent below the C_D for the rear body alone. Pressure coefficient for the optimum case is shown in Fig. 14.

Beyond the minimum case, the drag coefficient C_D increases with increase in gap ratio, reaching the values 1.21, 1.05 and 0.78 at gap ratio 1.25, which are 5, 24 and 45 percent below the C_D for rear body alone, for corresponding the Reynolds numbers. The drag coefficient decreased reaching the values 0.98, 0.84 and 0.72 at gap ratio 1.50, which are 23, 39 and 49 percent below the C_D for the rear body alone, and then increased reaching the maximum values 1.7, 1.3 and 0.88 at gap ratio 1.75, which was -33, 6, and 38 percent below the rear body alone, for corresponding the Reynolds numbers.

For $b_1/b_2 = 0.37$, Fig.12e shows the variation of drag coefficient with the gap ratio and Reynolds numbers. For gap ratio 0.25 the drag coefficient values are 0.93, 0.88 and 0.56, which are 27, 36 and 60 percent, when the gap ratio increased ($g^*/b_2 =$

0.50) the combination drag coefficient decreased reaching the optimum case with $C_D^* = 0.49, 0.50$ and 0.44 , which are 61, 57, and 70 percent below the C_D for rear body alone, for corresponding the Reynolds numbers.

Beyond the optimum case, the drag coefficient increased with increasing the gap ratio reaching the maximum values 1.36, 1.32 and 1.03 at gap ratio 2.0, which are -6, 5 and 27 percent below the C_D for rear body alone, for corresponding the Reynolds numbers. Further increase of gap ratio to 0.25, the drag decreased to 0.82, 0.97 and 0.88, which are 36, 30 and 38 percent below the C_D for rear body alone, respectively.

For $b_1/b_2 = 0.25$, Fig.12f shows that the drag coefficient for small gap ratio ($g/b_2 = 0.25$) attains the maximum values of 1.26, 1.16 and 0.852, which are 1, 16 and 40 percent below the C_D for rear body alone, for corresponding the Reynolds numbers. At the gap ratio 0.5, the drag coefficient reached the optimum case with $C_D^* = 0.89, 0.75$ and 0.56 , which are 30, 46 and 60 percent below the C_D for rear body alone, for corresponding the Reynolds numbers.

Beyond the optimum drag reduction at gap ratio 0.5, the drag coefficient increases slightly and is roughly constant between the gap ratios 0.75 to 2.25. This indicates that the flow pattern for this range of gap ratios are approximately similar.

From the above discussions it can be summarized that, the combination of the bluff bodies in tandem with the appropriate choice of width and gap ratios often has a drag below the C_D for

the rear body alone. The combination in square-plate front body which has a drag coefficient minimum are;

(i) $b_1^*/b_2 = 0.75$ at gap ratio 0.50, has 67, 73 and 80 percent drag reduction at the three sets of Re .

(ii) $b_1^*/b_2 = 0.625$ at gap ratio 0.25, has 48, 58 and 72 percent drag reduction.

(iii) $b_1^*/b_2 = 0.50$ at gap ratio 0.50, has 48, 55 and 70 percent drag reduction.

(iv) $b_1^*/b_2 = 0.37$ at gap ratio $g/b_2 = 0.50$, has 61, 57 and to percent below the C_D for rear body alone, for corresponding the Reynolds number as shown in Fig.13.

For the above combinations of square-plated body and rear body, the minimum absolute drag coefficient of 0.42, 0.37 and 0.28 achieved for the optimum combination with $b_1^*/b_2 = 0.75$. The contrast between the optimum cases where $b_1^*/b_2 = 0.75$ and $g^*/b_2 = 0.50$, with the same width ratio but for large and small gap ratio is shown in Fig.14. For large gap ratio $g/b_2 = 0.75$, the separated boundary layers reattached onto the rear body face, and again separated from the face, resulting in strong wake zone behind the rear body. But for optimum case, the flow separated from the edges of front body reattached onto or very close to rear body corners resulting in negative pressure coefficient at the enterice face. For small gap ratio $g/b_2 = 0.25$, as shown in Fig.14, the separated boundary layers go away from the rear body face.

For $b_1^*/b_2 = 0.625$ and 0.50 , the flow has approximately similar in behaviour as that at $b_1^*/b_2 = 0.75$, but for $b_1^*/b_2 = 0.37$ and at small gap ratio $g/b_2 = 0.25$, as shown in Fig.14, the separated boundary layers reattach on the rear body face and again separate from the face and then reattach downstream of the rear body face.

3.2. Comparison between drag coefficient for D-shape and square-shape front body.

From the measured surface pressure distribution on the basic model with D-shape and square-plate front bodies, the drag of the combination and their corresponding reduction compared to main body drag are calculated. The results are tabulated in tables 3 and 4 in Appendix A.

The drag coefficient C_D of a combination in two shapes of front bodies exhibits the characteristic behaviour seen in Figs. 9 and 12 for D-shape and square-plate front bodies, respectively. From the above tabulated results and figures, it appears that there are some differences in the combination drag coefficient C_D between D-shape and square-plate front bodies they are:

1. The drag coefficient C_D variation with gap ratio g/b_2 for D-shape were generally sharp, especially for $b_1/b_2 = 0.625$ and 0.25 , indicating a change in flow pattern, as shown in Fig.9 (c and f).

For $b_1/b_2 = 0.25$, Fig. 9f for example, show that the drag coefficient C_D = 0.76, 0.89 and 0.72 at gap ratio 0.25, which was 40, 36 and 31 percent below the C_D for the rear body alone, and then the C_D decreased sharply reaching the value $C_D = 0.39, 0.58$ and 0.48 at gap ratio 0.50, which was 70, 58 and 66 percent below the C_D for the rear body alone, respectively. The sharp downward jump in C_D between the gap ratio 0.25 and 0.50, indicates a change in flow pattern. At the first gap ratio $g/b_2 = 0.25$, the separated boundary layers from the front body edges reattach on to the rear body face, and then separate again at the corners making large wake zone. But for gap ratio $g/b_2 = 0.50$, the separated boundary layers reattach on to the rear body corners resulting in optimum case, as shown in Fig. 15a.

The drag coefficient variation with gap ratio g/b_2 for square-plate front body were generally smooth for all b_1/b_2 except for $b_1/b_2 = 0.75$. For gap ratios between 0.25 to 0.5, the drag coefficient increased with increasing gap ratio, as shown in Fig. 12.

2. Minimum drag coefficient C_D^* (optimum case), for the combination with D-shape front body was achieved with width ratios $b_1^*/b_2 = 0.25, 0.37$ and 0.75 at the gap ratio $g^*/b_2 = 0.50, 0.75$ and 0.25, respectively. The corresponding drag reduction for D-shape front body at optimum case are shown in Fig. 10 (a,b and c). But the minimum drag coefficient C_D^* with square-plate front body was achieved with width ratios $b_1^*/b_2 = 0.37, 0.50, 0.625$ and 0.75, at gap ratios $g^*/b_2 = 0.50, 0.50, 0.25$ and 0.50, respectively,

the corresponding drag reduction for square-plate front body combination are shown in Fig. 13 (a,b,c and d).

3. Maximum percentage drag reduction for D-shape combination is achieved for $b_1^*/b_2 = 0.25$ at $g^*/b_2 = 0.50$ as shown in Fig. 10. The minimum drag coefficient for this combination are $C_D^* = 0.39$, 0.58 and 0.48 as compared to $C_{D_o} = 1.28$, 1.39 and 1.42 of the rear body alone. The percentage drag reduction are 70, 66 and 58 percent below the C_D for the rear body alone, respectively. For the corresponding Reynolds numbers. The maximum percentage drag reduction for square-plate combination occurs at different b_1^*/b_2 and g^*/b_2 ($b_1^*/b_2 = 0.75$ and $g^*/b_2 = 0.50$ and 1.42) compared to D-shape combination.

4. For small width and gap ratios ($b_1/b_2 = 0.25$ to 0.37, $g/b_2 = 0.25$ to 0.50), the total drag reduction for the combination with D-shape front body is more than that with the square-plate front body as shown in Fig.15 (a and b), since, the D-shape front body is able to guide the separated boundary layers from its edges to the or very close to rear body corners.

Fig.15 (a and b) shows the maximum percentage drag reduction for each b_1/b_2 variation with the optimum width ratio b_1^*/b_2 , and the gap ratio g^*/b_2 at which it occurs for both D-shape and square-plate front body.

5. For small width and gap ratios, the D-shape front body has remarkable effects on drag reduction, significantly more than the square-plate front body. For width ratios 0.25 and at gap ratio 0.50, the percentage drag reduction for D-shape and square-plate at $Re = 1.0, 1.4$ and 1.8×10^5 are 70, 58 and 66 and 30, 46 and 60, respectively, as shown in Fig. 15 (a,b). For $b_1/b_2 \approx 0.40$ to 0.60, the percentage drag reduction decreases reaching a minimum at gap ratio 0.50, and then increases reaching a maximum at gap ratio 0.60 for D-shape front body, but there is a very little change in percentage drag reduction for square-plate front body as shown in Fig. 15 (a and b).

3.3. Drag regimes based on Optimum Flows

In Figs. 16 and 17 the C_D^* for each value of b_1^*/b_2 from Figs. 9 and 12 have been plotted against the corresponding optimum gap ratio g^*/b_2 . From Figs. 16 and 17 the gap and the width ratios are grouped and derived into three branches depending on C_D^* and Reynolds numbers, which is presented in table 1(a and b) below, for D-shape and square-plate front bodies, respectively.

For the combination with D-shape front body, the groups will be called the low, medium and high-drag regimes. Table 1 lists the corresponding minimum drag coefficient C_D^*/C_{D_0} , range of width ratio b_1^*/b_2 , gap ratio g^*/b_2 , and the Reynolds numbers at which it occurs.

Table 1. Optimum-drag regimes

(a) Optimum-drag regimes for the combination with D-shape front body

Regime	I	II	III
C_D^*/C_{D_0}	Low	Medium	High
For $Re = 100,000$	<0.58	$0.58 < C_D^*/C_{D_0} < 0.83$	$0.83 < C_D^*/C_{D_0} < 0.90$
$Re = 140,000$	<0.45	$0.45 < C_D^*/C_{D_0} < 0.52$	$0.52 < C_D^*/C_{D_0} < 0.77$
$Re = 180,000$	<0.34	$0.34 < C_D^*/C_{D_0} < 0.51$	$0.51 < C_D^*/C_{D_0} < 0.67$
b_1^*/b_2	$0.25-0.75$	$0.25-0.625$	$0.25-0.625$
g^*/b_2	$0.0-0.75$	$0.75-1.5$	$1.5-2.25$

(b) Optimum-drag regimes for the combination with square-plate front body

Regime	I	II	III
C_D^*/C_{D_0}	Low	Medium	High
For $Re = 100,000$	<0.64	$0.64 < C_D^*/C_{D_0} < 0.77$	$0.77 < C_D^*/C_{D_0} < 0.90$
$Re = 140,000$	<0.55	$0.55 < C_D^*/C_{D_0} < 0.61$	$0.61 < C_D^*/C_{D_0} < 0.70$
$Re = 180,000$	<0.37	$0.37 < C_D^*/C_{D_0} < 0.51$	$0.51 < C_D^*/C_{D_0} < 0.55$
b_1^*/b_2	$0.37-0.75$	$0.37-0.50$	$0.50-0.75$
g^*/b_2	$0.0-0.75$	$0.75-1.50$	$1.50-1.75$

The jump from regime I to III at $b_1^*/b_2 = 0.37$ for the combination with D-shape front body as shown in Fig.16, should be noted.

The classification of the optimum drag coefficient C_D^* corresponds to distinctively different flow types associated with each D-shape and square-plate front body. In the high drag regime (III), the front body (D-shape or square-plate) is too small to guide the separated flow onto the corners of the rear body; and also the high drag regime is obtained due to the small gap ratio. If the gap ratio is small or the front body is too close to the rear body, in this case, the separates flow reattaches on the rear body face and again separated from the rear body face, resulting in very strong wake.

In the low-drag regime(I) the front body, either D-shape or square-plate is in a range where the separated flow can reattach at or near the rear body corners, this regime is more stable than III and II, because the gap is too small.

3.4 Drag Coefficient and Reynolds Number Effects

The drag coefficient of each combination (rear body with D-shape and square-plate front body) variation with the gap ratio and Reynolds numbers (1, 1.4 and 1.8×10^5) are shown in Figs.9 & 12, respectively.

For the combination with D-shape front body, the drag coefficient decreased with increase in Reynolds number especially for large width ratios ($b_1/b_2 = 0.50 - 1.0$), as shown in Fig. 9 (a-d).

According to the present results, high drag coefficient for the D-shape combination occur at $Re = 1.4 \times 10^5$, especially for low width ratios as shown in Fig. 18 (a). This refers to flow pattern, for low width ratio ($b_1^*/b_2 = 0.25 - 0.37$) and the corresponding optimum gap ratio ($g^*/b_2 = 0.25 - 0.75$), where separated boundary layers from D-shape body reattach on the rear body front face, and again separate from it and then there is no reattachment on the rear body surfaces. In this case, the wake zone is much larger in size compared to the wake for at $Re = 1.0 \times 10^5$ and $Re = 1.8 \times 10^5$.

For the combination with square-plate front body, the drag coefficient generally decreased with increase in Reynolds number, as shown in Fig. 12 and Fig. 18 (b).

As Reynolds number increases beyond the critical value ($Re = 1.4 - 1.8 \times 10^5$), a transition occurs in the separated shear layer and the flow reattaches to the rear body as turbulent boundary layer. This reattached flow continues along the body to some extent but will eventually separates and forms a turbulent wake that is much smaller in size compared to the wake at critical Reynolds number, even at large gap ratio compared with the critical Reynolds number.

CHAPTER 4

CONCLUSIONS AND RECOMMENDATION FOR FUTURE WORK

4.1 Conclusions

The conclusions presented in this investigation are limited by the test condition and test procedures.

From the experimental data and analysis of results undertaken in this study on the effects of various D-shape and square-plate front bodies on the flow field and drag coefficient of the square cross-sectional, sharp-corners and rounded back rear body, it is possible to conclude the following:

1. Experiments with two bluff bodies (rear body with D-shape or square-plate front body of different width ratio b_1/b_2) placed in tandem and connected together as show in Fig. 7, showed that very significant drag reductions from that of a rear body alone can be achieved by proper sizing of the front body widths and of the gap between them.
2. Placing a D-shape front body of width b_1 ahead of rear body of interest with width b_2 , with $b_1/b_2 = 0.25$ and the distance between them of $0.50 b_2$, results in a combination with total drag coefficient $C_D = 0.39, 0.58$ and 0.48 as compared to rear body drag coefficient alone at the similar flow conditions of $C_{D_0} = 1.28, 1.39$, and 1.42 , respectively. This represents 70,

58 and 66 percent drag reduction, respectively at the corresponding to Reynolds number.

3. Total drag coefficient can also be reduced by placing a square-plate front body. A square-plate front body of width b_1 ahead of rear body of interest with width b_2 , with $b_1/b_2 = 0.75$ and the distance between them of $0.50 b_2$, results in a combination with total drag coefficient $C_D = 0.42, 0.37$ and 0.28 as compared to $C_{D_0} = 1.28, 1.39$ and 1.42 for rear body alone, at the similar flow conditions, respectively. This represents 67, 73 and 80 percent drag reduction, at the corresponding Reynolds number.
4. Although the above concluded values show impressive drag reduction for optimum condition of main and front bodies, there are situations with combination other than optimum where the drag of the combination is more than that of the main body alone, resulting in negative percentage drag reduction.
5. Detailed investigation of the D-shape front body with rear body combination led to identification of three operating regimes (low, medium and high-drag regimes), depending on the front body width ratio b_1/b_2 . Among them, the most important is regime I ($0.25 \leq b_1^*/b_2 \leq 0.75$), for D-shape front body as shown in Fig. 13, where the most significant drag reductions of the order up to 70% were observed (at gaps length around $0.50 b_2$).

6. The investigation results for square-plate front body with rear body combination also led to identification of three operating regimes (low medium and high-drag regimes), depending on the front body width and gap ratios. Among them, the most important is regime I ($0.625 \leq b_1^*/b_2 \leq 0.75$) for square-plate front body, as shown in Fig.14, where the most significant drag reductions of the order up to 80% were observed (at gap length around $0.50 b_2$).
7. The total drag on the two bluff bodies combination in present work (rear body with D-shape or square-plate front body) may be split into two parts:
 - (a) One acting on the front body plus the front surface of the rear body.
 - (b) The second being the base-pressure drag on the rear surface of the rear body.

For the case of D-shape front body, it is seen that practically all the drag reduction is caused by reduction of the base-pressure drag (increased base pressure), this also applies for the square shape front body. On the other hand, in the case of the minimum-drag combination (optimum case), decrease in both parts of the total drag contribute to the drag reduction.

From the above conclusions, we see that it is possible to reduce the drag up to 80 percent by properly choosing the geometry of the front body and gap ratios.

4.2 Recommendation for future work

An intriguing topic in bluff-body aerodynamics is the interaction of two bluff-bodies placed in tandem. The intriguing fact of this topic is that, the flow pattern and drag of a tandem combination (rear body and front body) cannot be easily predicted from the known flow characteristics of two individual bodies. From the present investigation of the shielding effects of various front bodies (D-shape and square-plate) placed upstream of flat-faced, sharp cornered, square cross-sectional, rounded back rear body for purpose of drag reduction. It is believed that the following aspects need further investigation:

1. More experimental work is required to investigate the influence of other types of front bodies (disk, hemispherical, etc) on the total drag force of the combination, since only two types (D-shape and square-plate) front bodies were used in this investigation.
2. The effect of angle of attack and Yaw on the flow characteristics, drag reduction and pressure coefficient is required to be investigated, since the present work was carried out with zero-angle of attack and yaw.
3. Effect of Reynolds numbers is required to be investigated in larger range, and also 2-dimensional bluff bodies need be studied, since the present work was carried out for 3-Dimensional bluff bodies and the Reynolds numbers in range $Re = 1$ to 1.8×10^5 .

4. The flow visualization experiment should be carried out , in a water or smoke tunnel. Identification of the flow regimes, separation and reattachment of shear layers and wake zone behind the rear body are based on the flow visualization photographs and the pressure distribution curves . In present study the results analysis is based on the pressure distribution data only .
5. The velocity field between the front body and rear body need be measured, to have further insight into drag regimes (low, medium and high-drag regimes), since there are fundamental differences in flow properties into these regimes.

REFERENCES

Koenig K. and Roshko A., "An Experimental Study of Geometrical Effects on the Drag and Flow Field of Two Bluff Bodies Separated by a Gap", Journal of Fluid Mechanics, Vol. 156, 1985, pp. 167-204.

Hoerner, S.F., "Fluid Dynamic Drag", Brick Town, New Jersey, 1965.

Zdravkorich M., "Review of Flow Interferences Between Two Circular Cylinders in Various Arrangements", Trans. ASME I: Journal Fluids Engg., Vol. 99, 1977, pp. 618-632.

Morel T., and Bohn. M., "Flow Over Two Circular Disks in Tandem ", Trans. ASME I: Journal Fluids Engg., Vol. 102, 1980, pp. 104-111.

Morel T., "Theoretical Lower Limits of Forebody Drag" Aeronautical Journal, 1979, Vol. 83, pp. 23-27.

Little B. H. and Whipkey R. R., "Locked Vortex Afterbodies", Journal Aircraft, Vol. 16, 1979, pp. 296-302.

Ronald L. Panton, "Incompressible Flow", New York, 1984, pp. 529-560.

Ota T., "An axisymmetric separated and Reattached Flow on Longitudinal Blunt Circular Cylinder" Trans. ASME E: Journal Applied Mechanics, Vol. 42, 1975, pp. 311-315.

Pamadi B.N., Pereira C. and Gowda B.H.L., "Drag Reduction by Strakes of Noncircular Cylinders", AIAA Journal, Vol. 26, No. 3, 1986, pp. 292-299.

Anatol Roshko, "On The Drag and Shedding Frequency of Two-Dimensional Bluff Bodies", NACA TN 3169, 1953, pp. 1-17.

Maskell E.C., "Some General Characteristics and Properties of Three-Dimensional Flow Fields", Proceedings, of the Symposium on the Aerodynamic Drag Mechanism of Bluff Bodies and Road Vehicles, New York, 1978, pp. 131-136.

Gerrard J.H., "The Mechanics of the Formation Region of Vortices Behind Bluff Bodies", Journal Fluid Mech., Vol. 25, Part 2, 1966, pp. 401-413.

Bostock B.R. and Mair W.A., "Pressure Distributions and Forces on Rectangular and D-shaped Cylinders", Aeronautical Quarterly, February 1972, pp. 1-8.

Leland H. and Brownson J., "Effects of Reynolds Number and Body Corner Radius on Aerodynamic Characteristics of A space Shuttle-Type Vehicle At Subsonic Mach Numbers", NACA TN, 94035, Sept. 24, 1971, pp. 1-30.

Anatol Roshko., "On The Wake and Drag of Bluff Bodies", Journal of the Aeronautical Sciences, Feb. 1955, pp. 124-132.

Bearman P.W. and Trueman D.M., "An Investigation of the Flow Around Rectangular cylinders", Aeronautical Quarterly, August 1972, pp. 229-237.

Schlichting H., "Boundary Layer Theory", London, 1955.

Hucho W.H. (Editor), "Aerodynamics of Road Vehicles", Butterworths, London, 1987.

Mair W.A. and Maull D.J., "Aerodynamic Behaviour of Bodies in the Wake of other Bodies", Transactions Royal Society, A, Vol. 269, 1971, pp. 425-437.

Nakagnchi H., "Recent Japanese Research on Three-Dimensional Bluff-Body Flows Relevant to Road-Vehicle Aerodynamics", Proceedings of the Symposium on the Aerodynamic Drag Mechanism of Bluff Bodies and Road Vehicles, New York, 1978, pp. 227-246.

Prandtl L. and Tietjens O., "Applied Hydro and Aeromechanics" Dover, 1934, pp.118-121.

Maskell E.C., "A Theory of the Blockage Effects of Bluff Bodies and Stalled Wings in a Closed Wind Tunnel", A.R.C. R & M 3400, Nov. 1963.

Castro I.P. and Robins A.G., "The Flow Around a Surface Mounted Cube in Uniform and Turbulent stream", J. of Fluid Mechanics , vol. 79, 1977, pp. 307-335.

Gowda B.H.L., Gerhardt H.J. and Kramer C., "Surface Flow Filed Around Three-Dimensional Bluff Bodies", J. of Wind Engg. and Ind. Aerody., vol. 11, 1983, pp. 405-420 .

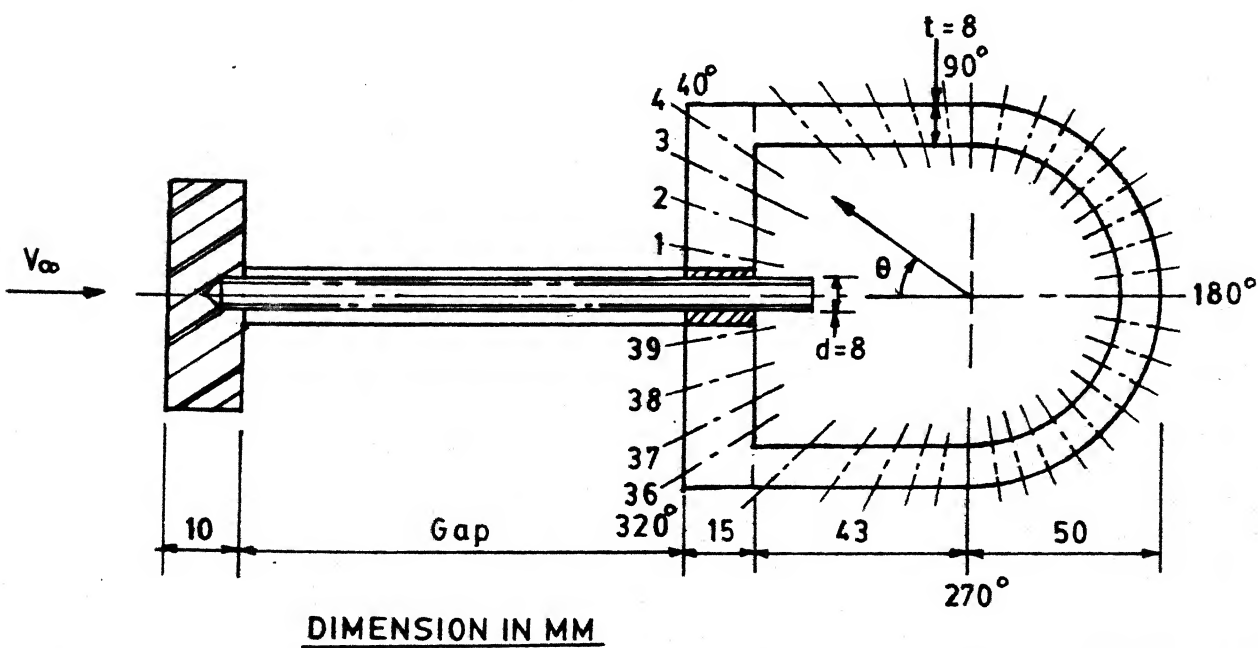
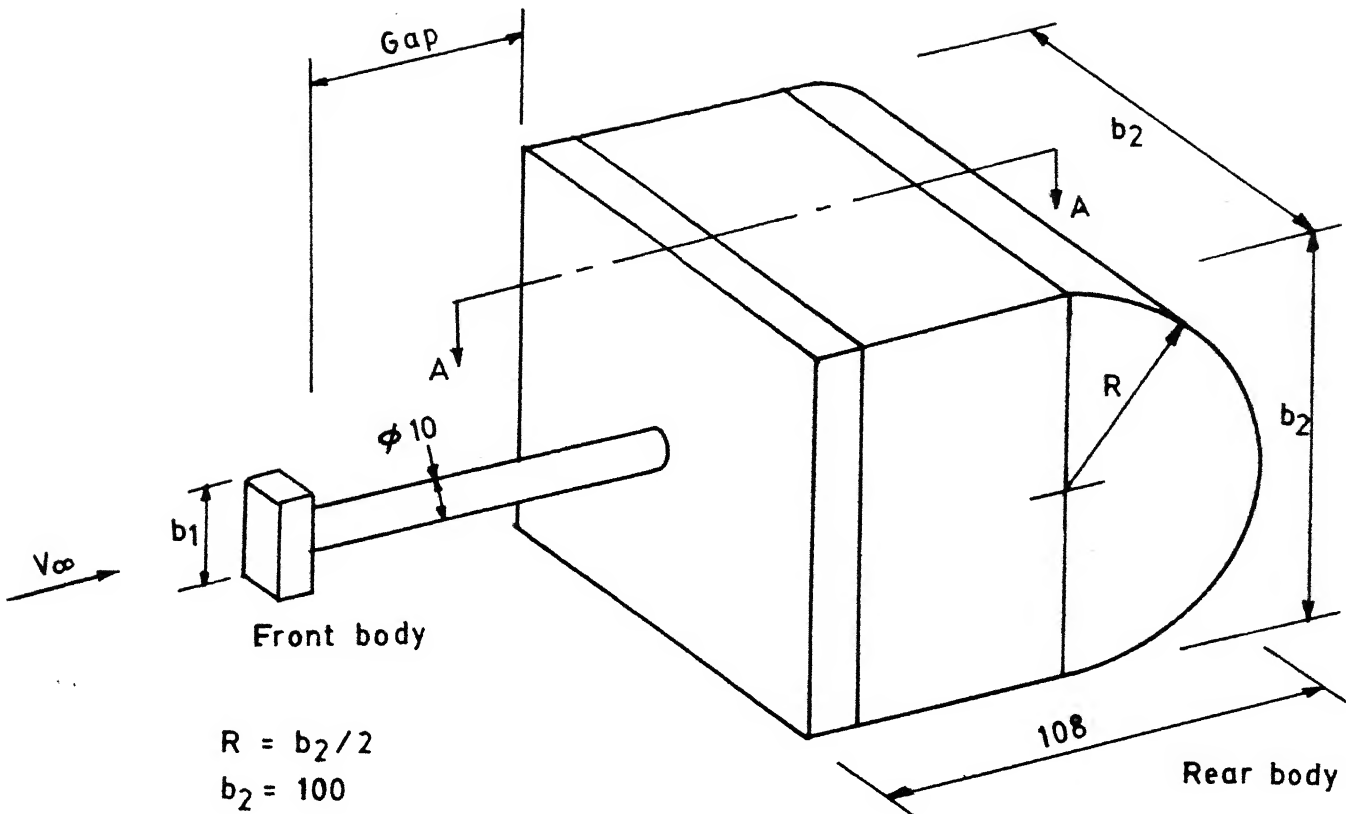
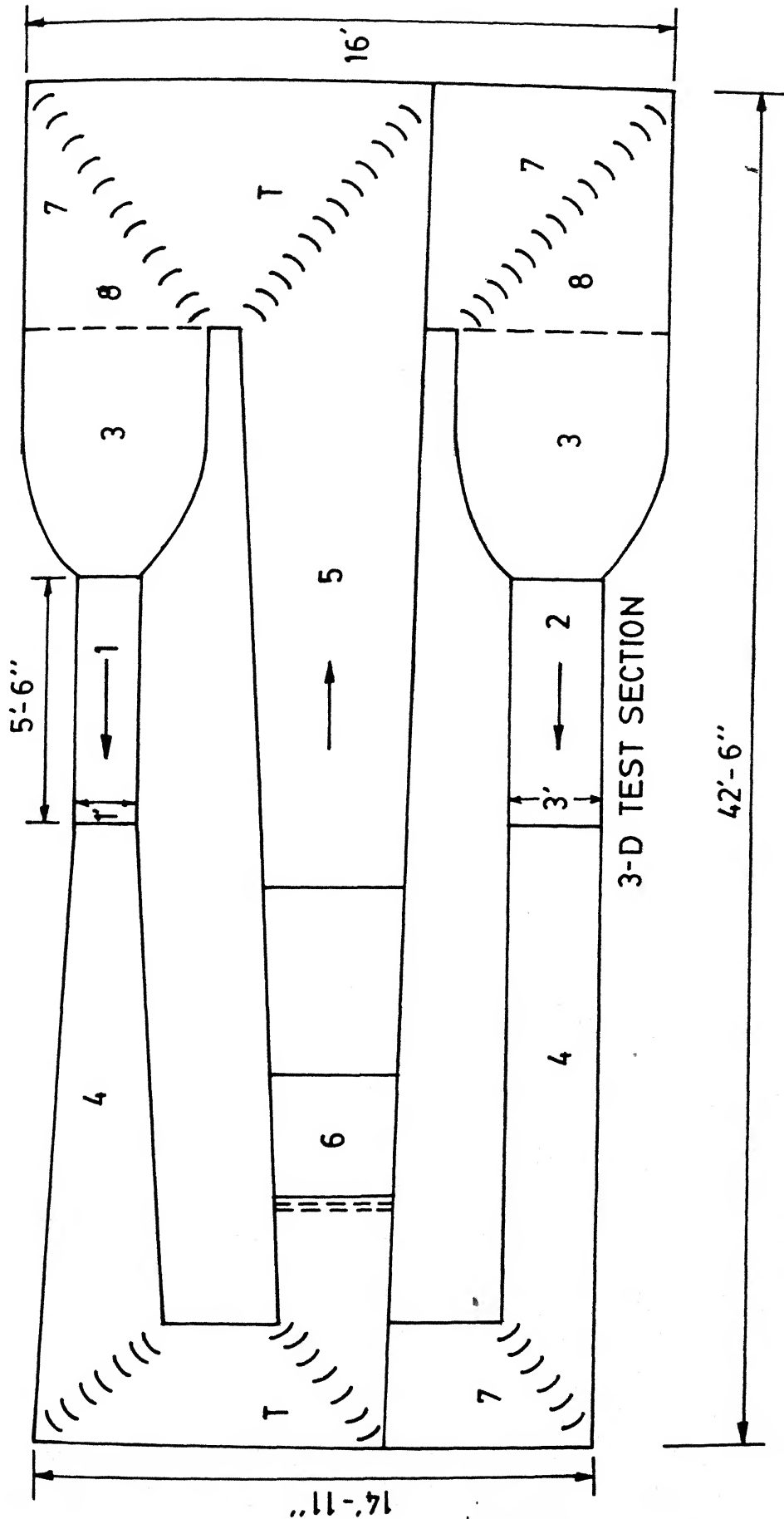


FIG. 3 SCHEMATIC DIAGRAM OF THE EXPERIMENTAL MODEL,
Section AA (Pressure test model number 1-39 refer to
pressure tap location)

Z-D TEST SECTION



1. 2 - D TEST SECTION (5'-6" x 1' x 4')
2. 3 - D TEST SECTION (5'-6" x 3' x 2')
3. CONTRACTION CONE
4. DIFFUSER
5. RETURN DIFFUSER
6. BLOWER SECTION (2-12 Blade-15 H.P. Fan)
7. TURNING VANES
8. SCREENS
- T. TURNING BOX

Fig. 4 Schematic diagram of low speed wind tunnel

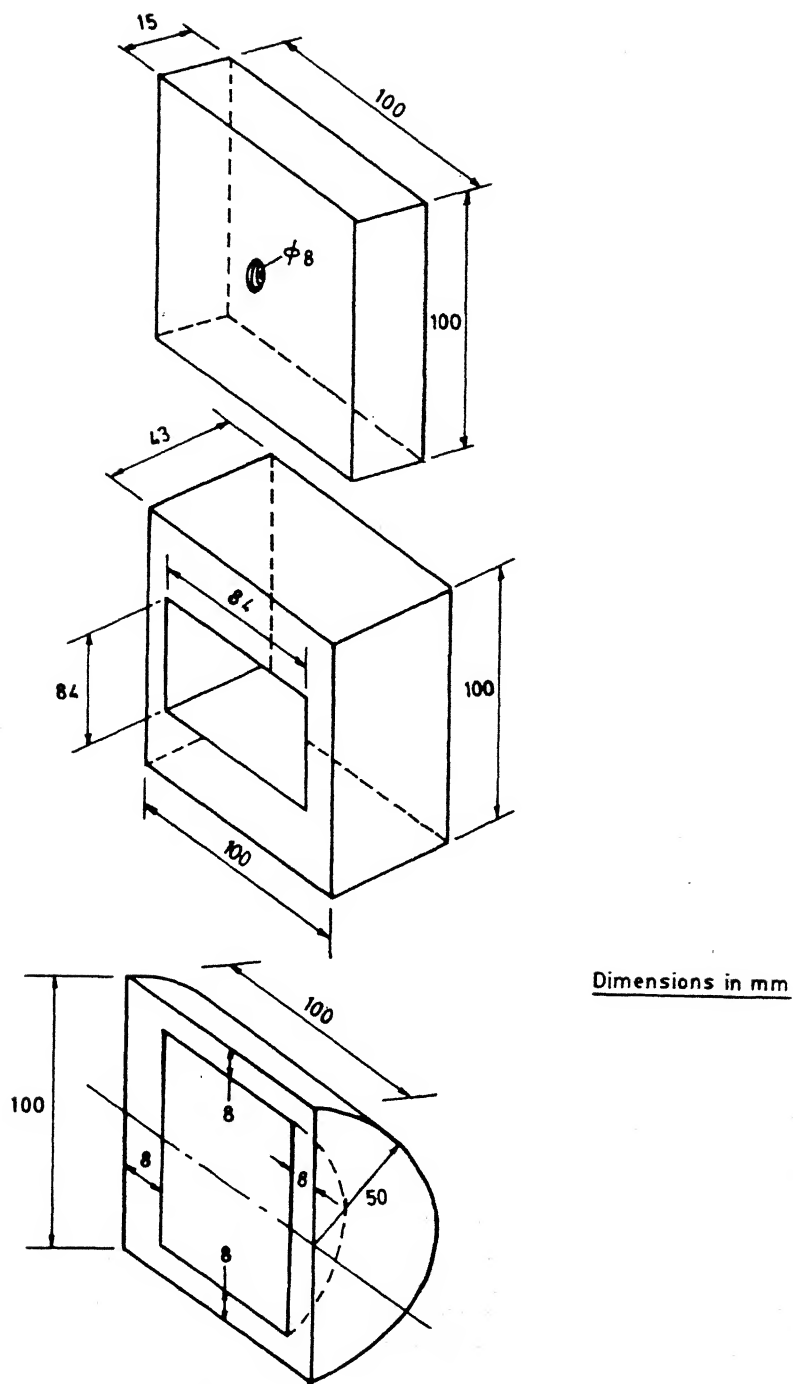
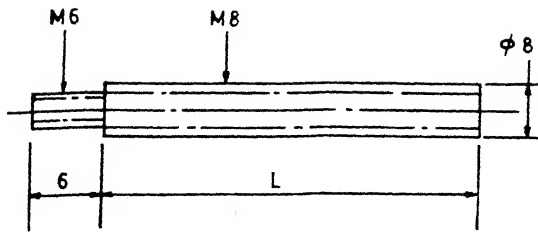
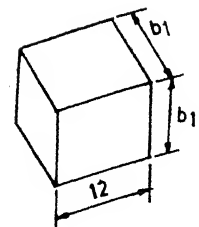


Fig.5 Schematic experimental rear body parts

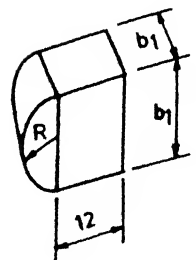


(a) Threaded Rods ($L=55, 105, 225$)



$b_1 = 25, 37, 50, 62.5, 75, 100$

(b) Front Body model (Sq. shaped)



$b_1 = 25, 37, 50, 62.5, 75, 100$
 $R = 12.5, 18.5, 25, 31.25, 37.5, 50$

Dimensions in mm

(c) Front Body model (D-Shaped)

Fig.6 Schematic experimental set-up showing the (a) Threaded rods , (b & c) Front body shapes

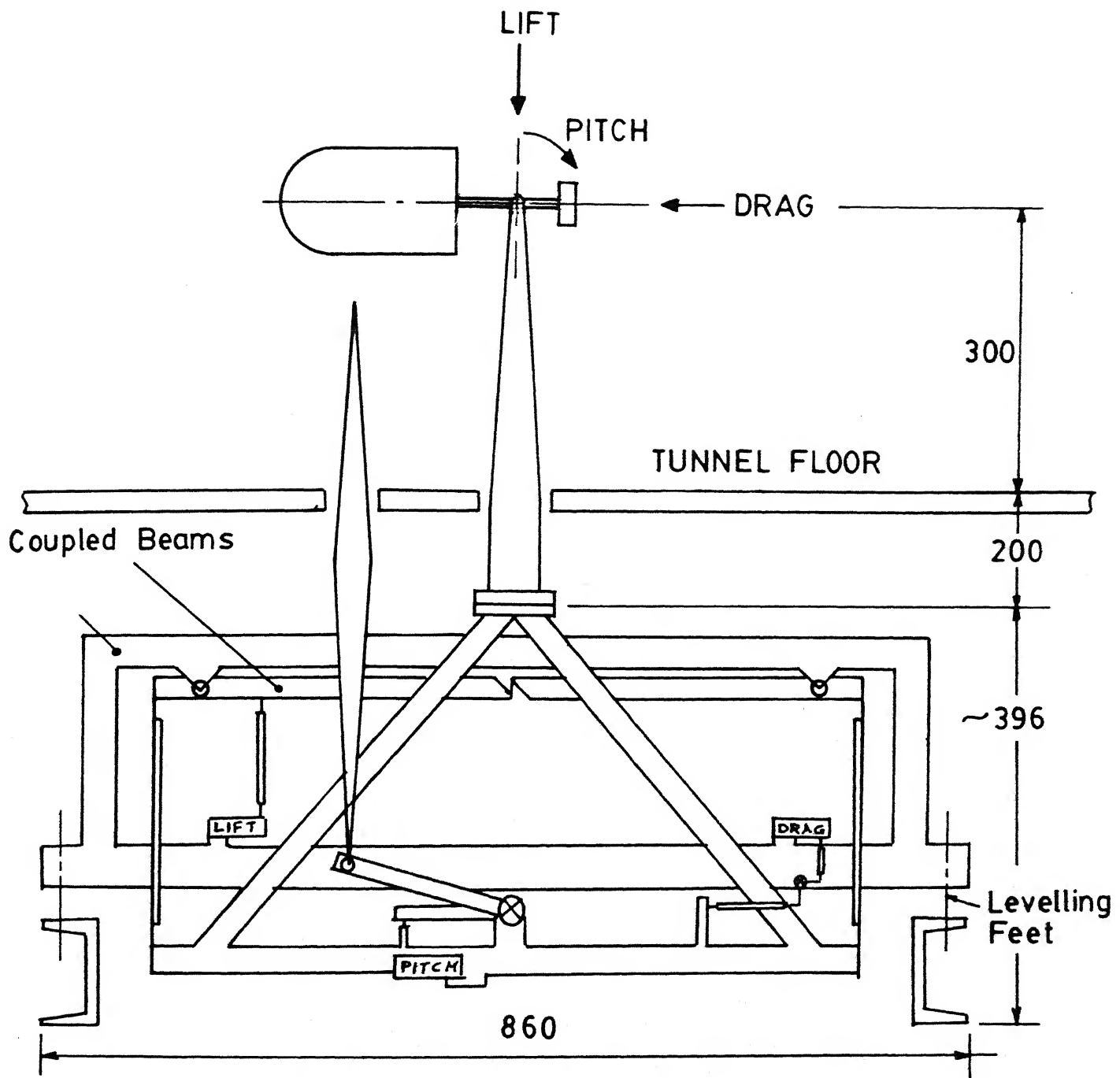


Fig. 7 Schematic view of three-component balance with experimental model with square-plate front body.

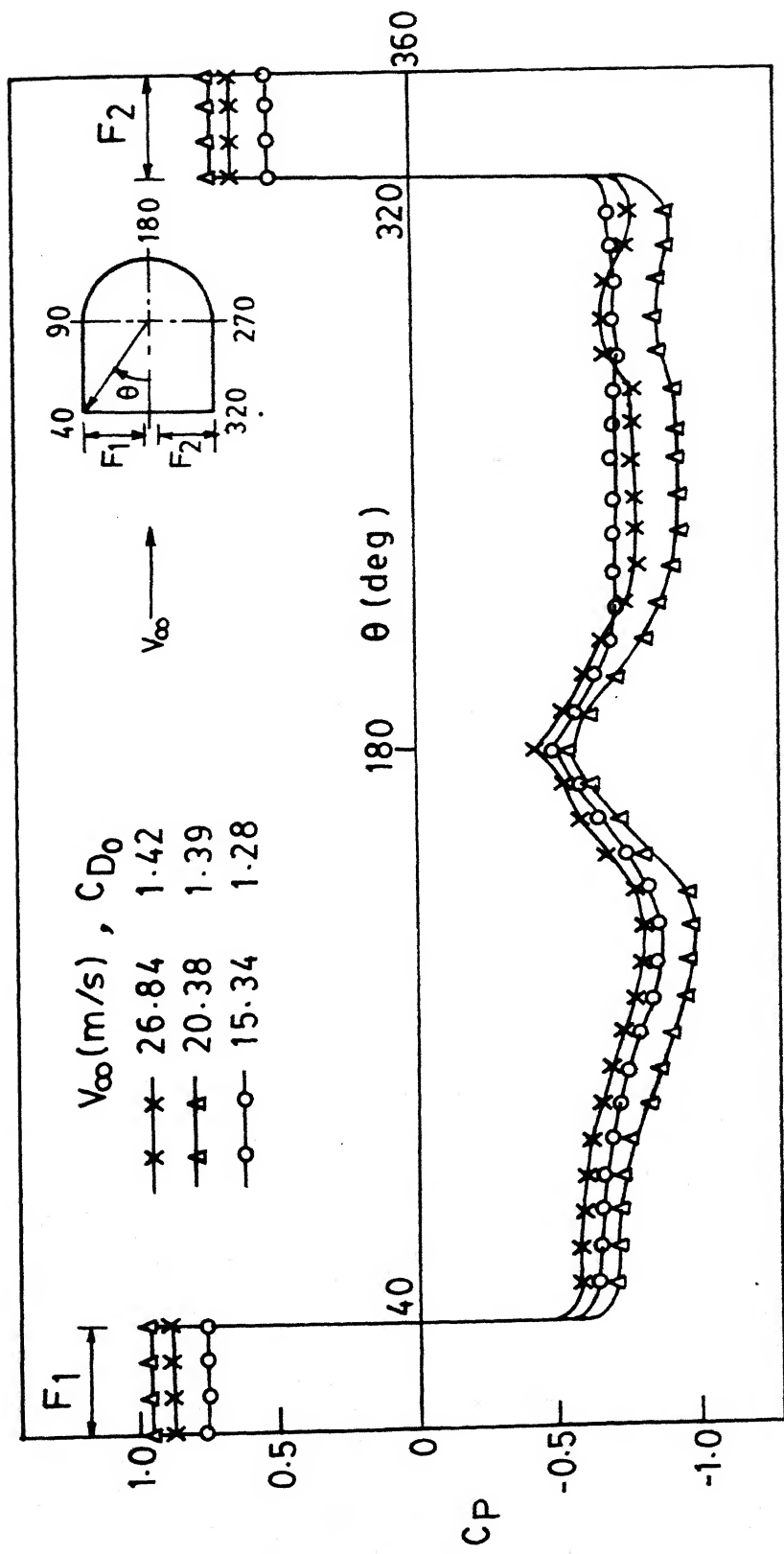


FIG. 8 Pressure distribution for basic model.

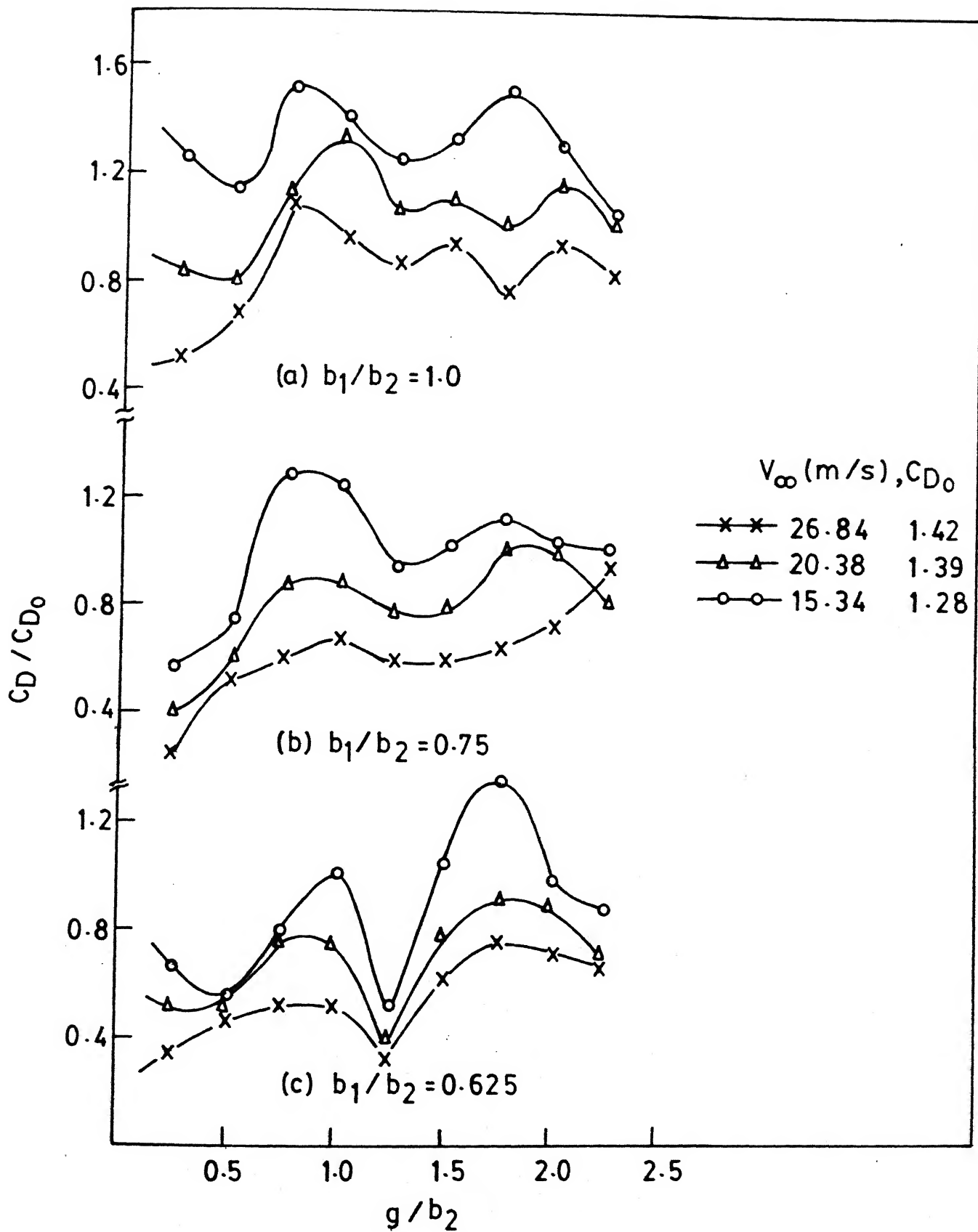


Fig. 9 Contd.

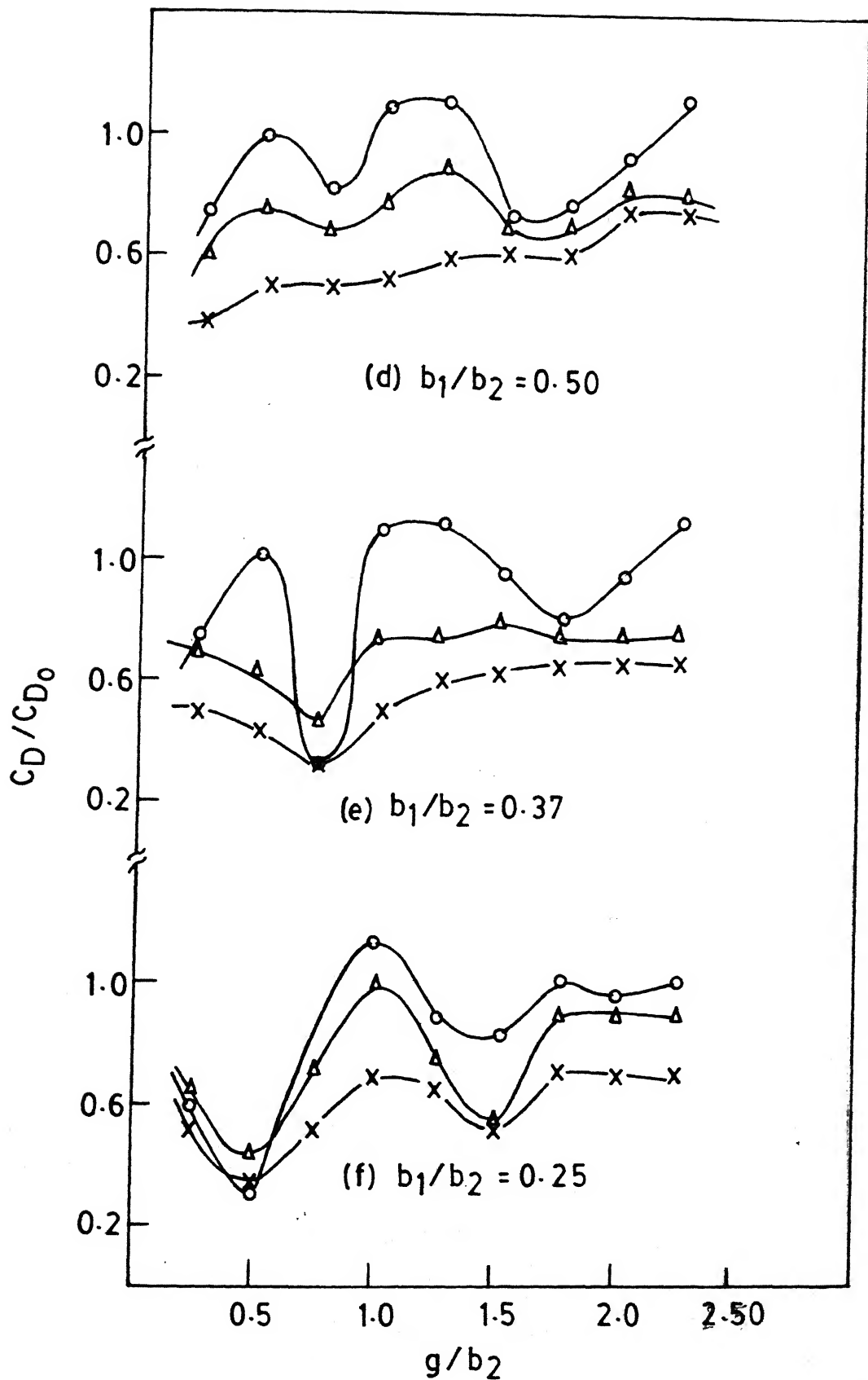


Fig. 9 Drag coefficient ratio vs. gap ratio for D-Shape front body, $Re = 1 \times 10^5 - 1.8 \times 10^5$.

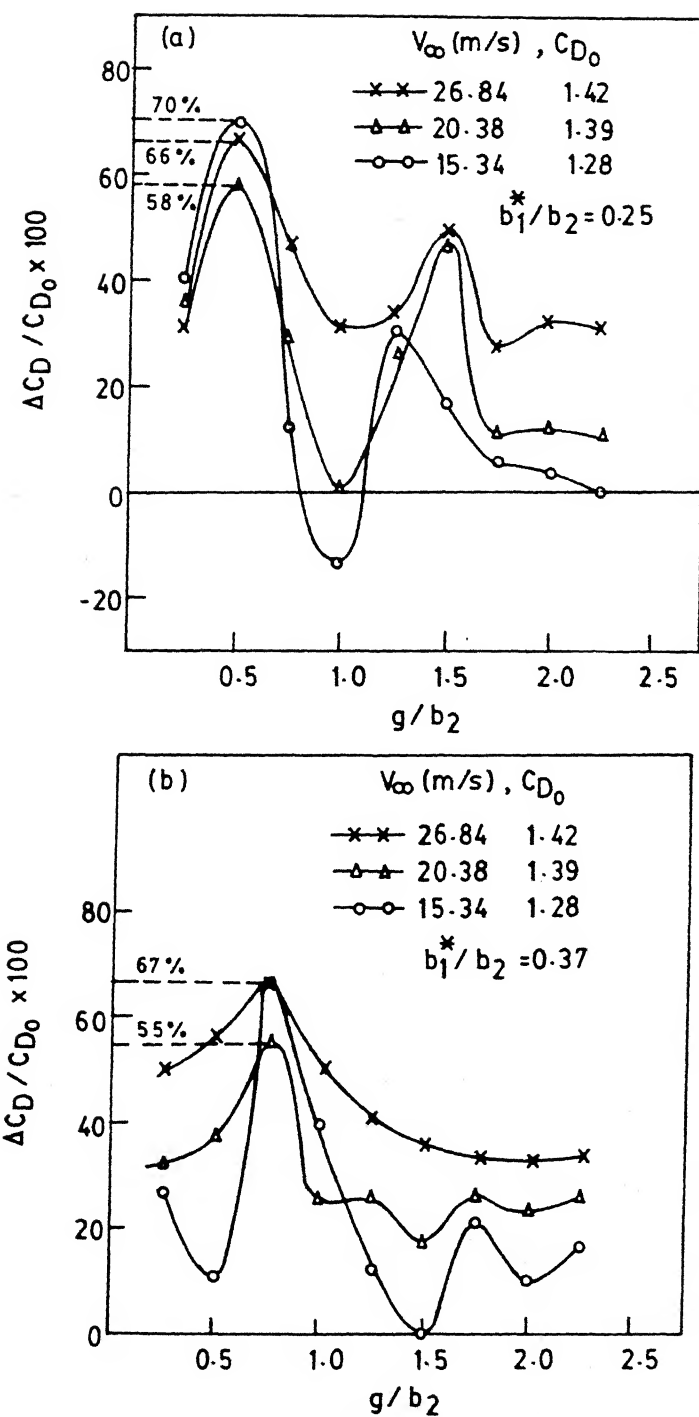


Fig. 10 Contd.

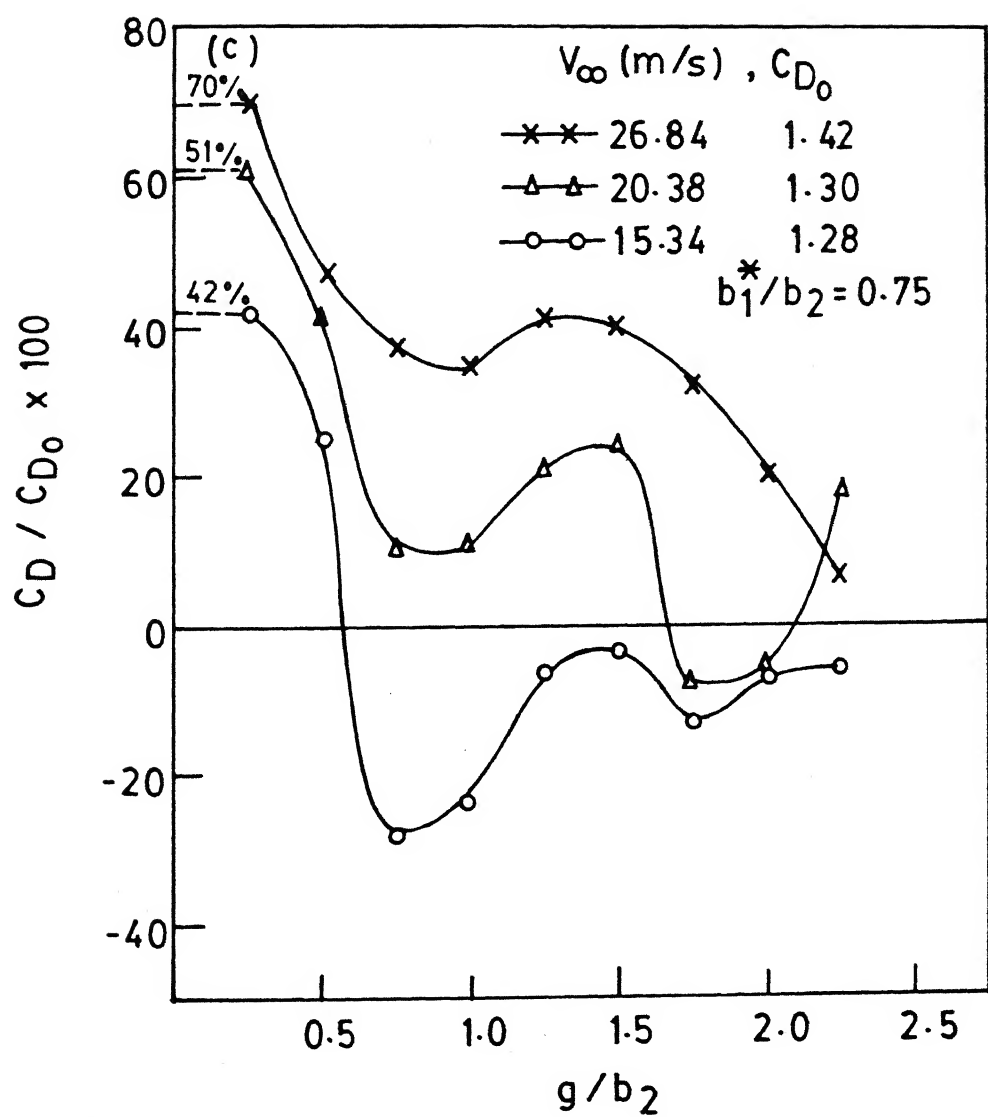
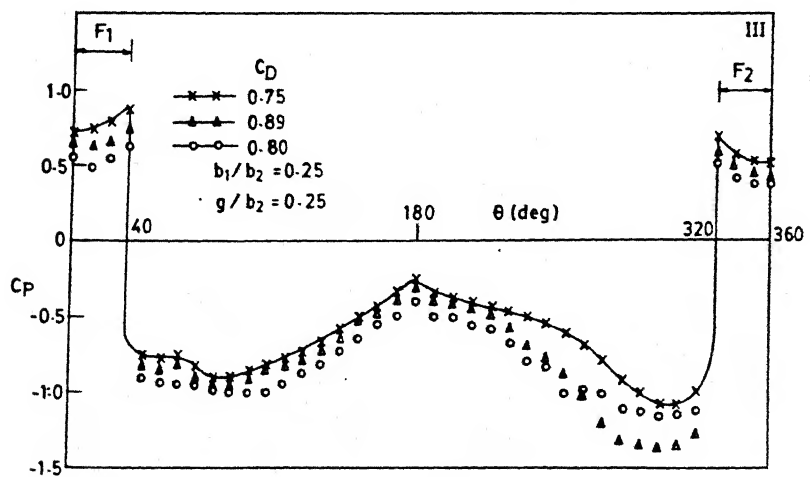
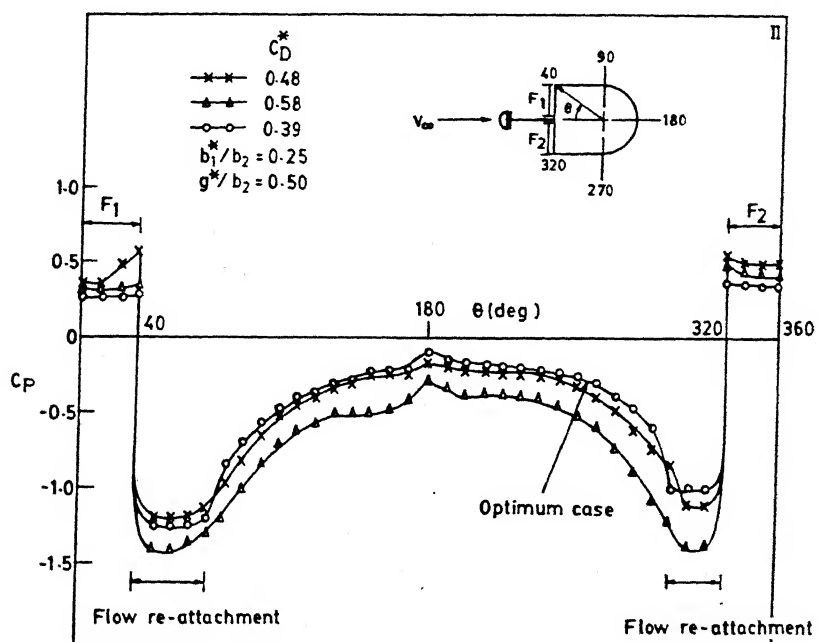
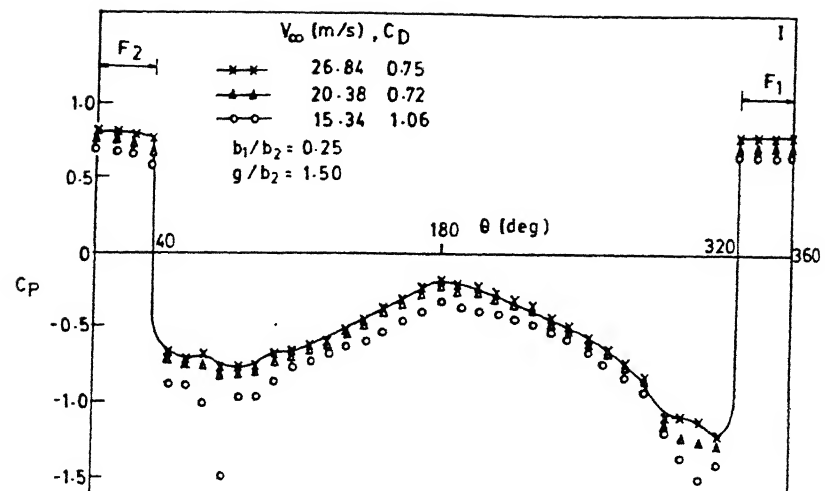
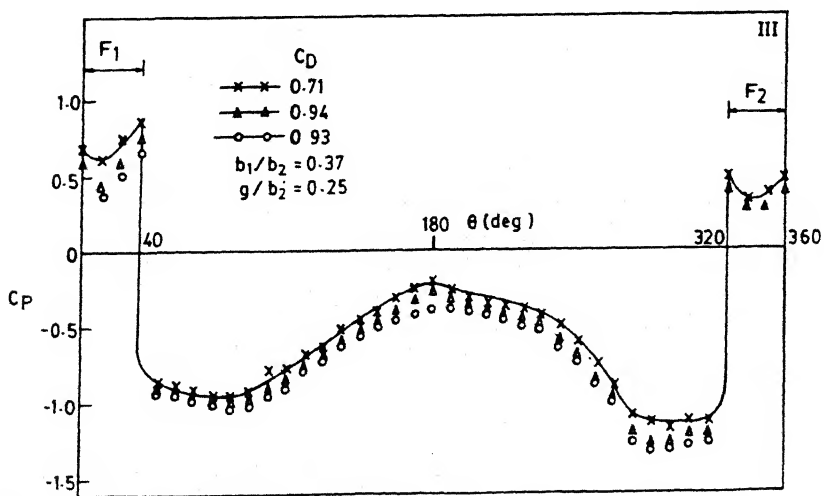
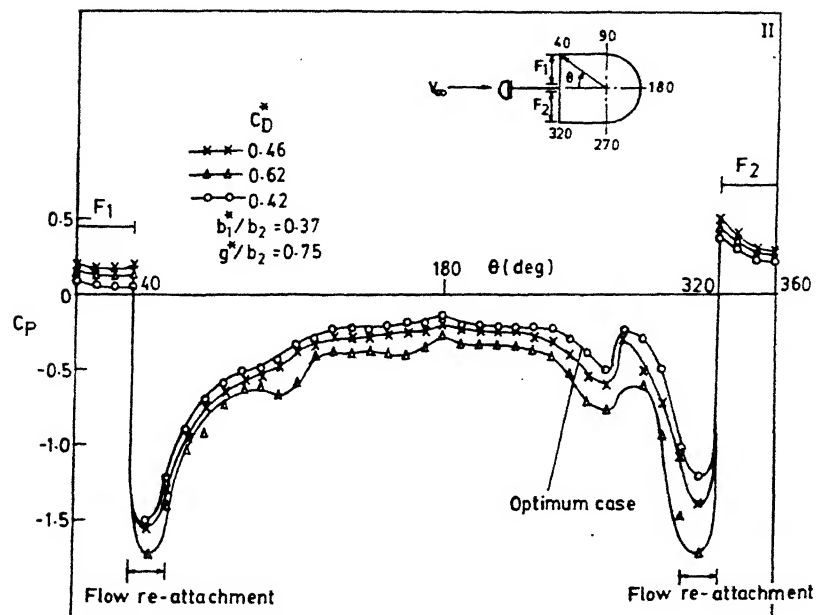
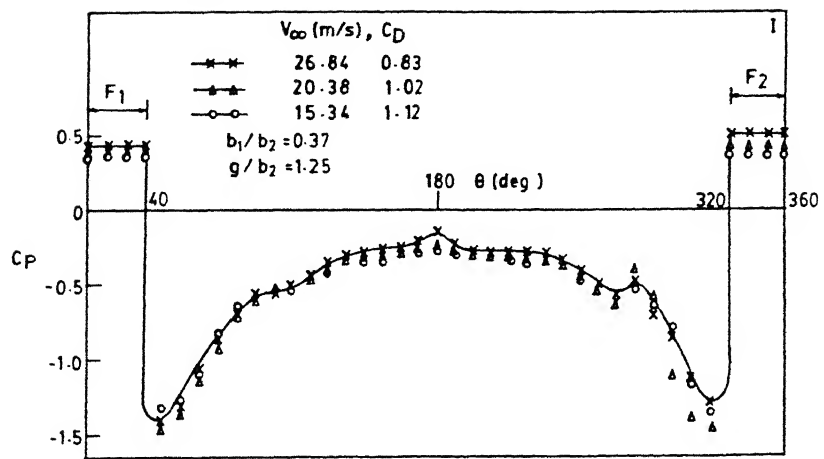


Fig. 10 Percentage drag reduction for D-Shape front body in optimum b_1 / b_2 ratio



Pressure distribution (Contd.)



Pressure distribution (Contd.)

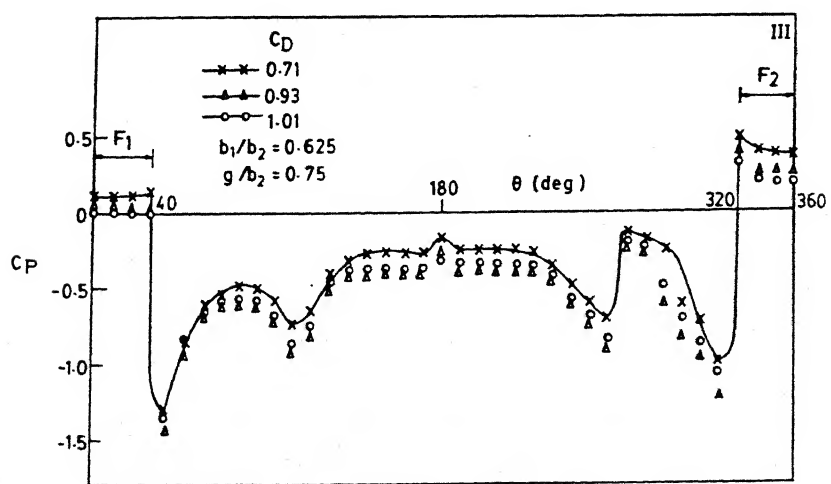
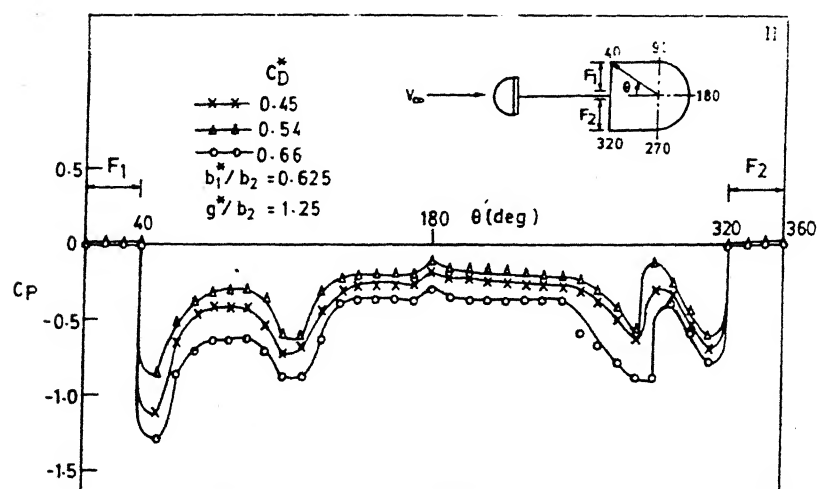
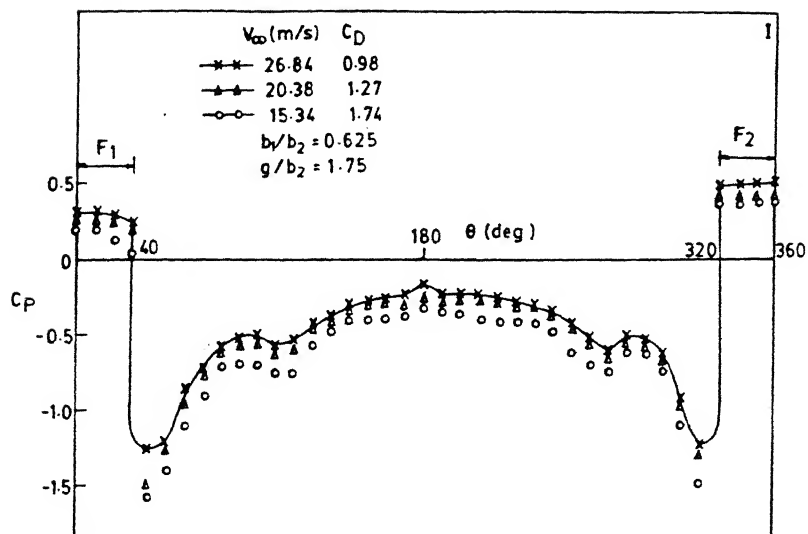


Fig.1.3 Pressure distribution on rear body surface with D-Shaped front body ;
* Optimum case .

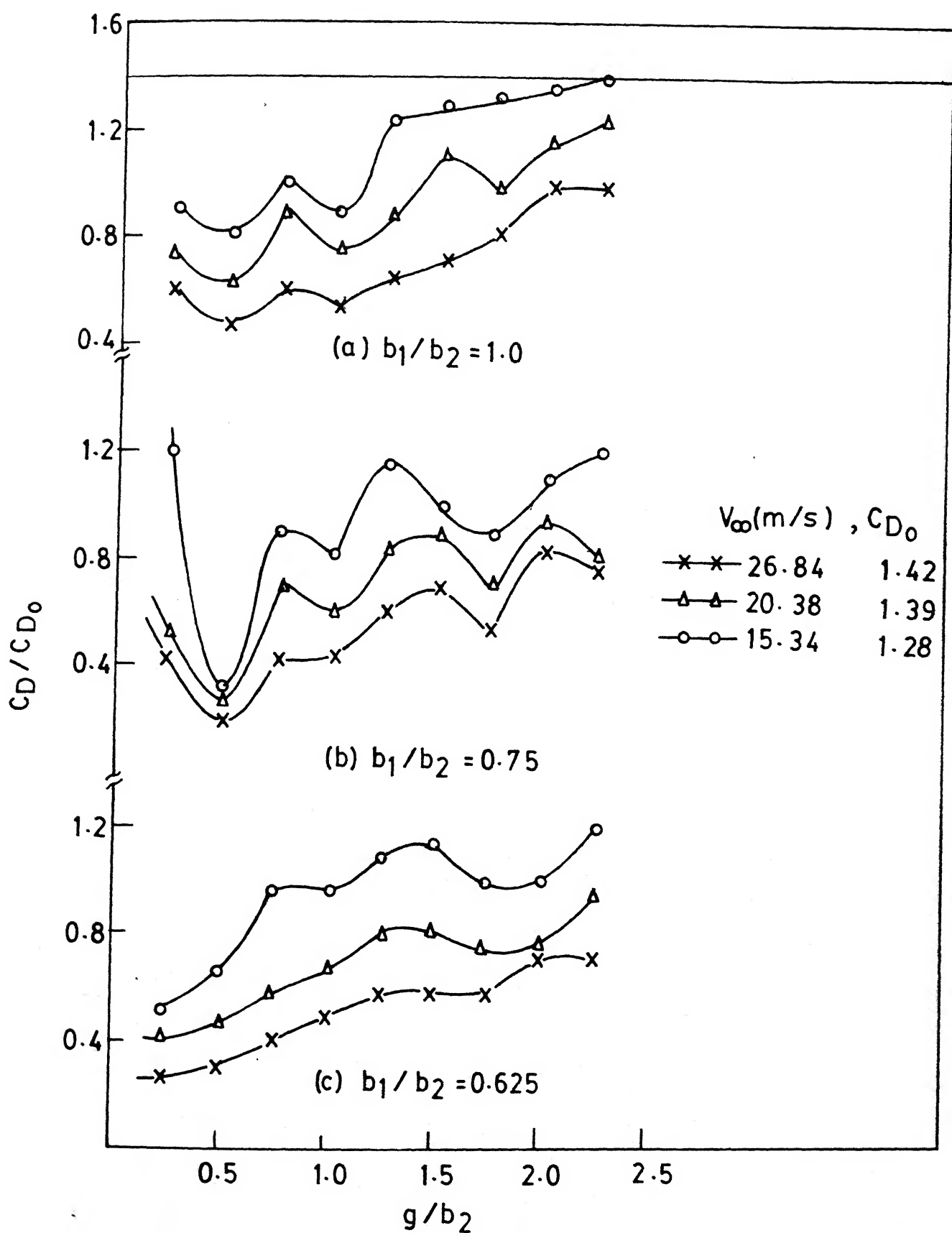


Fig.12 Contd.

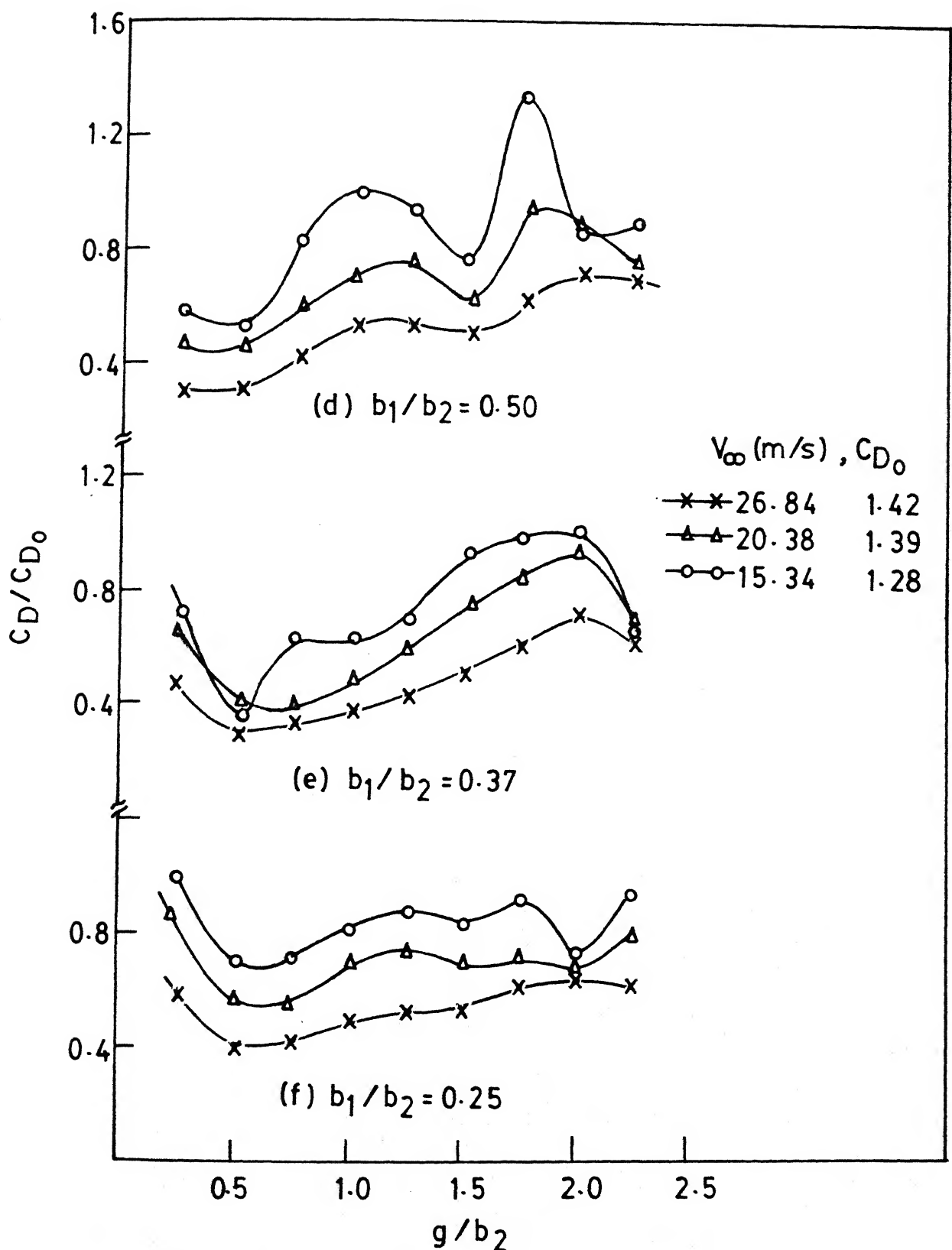


Fig. 12 Drag coefficient ratio vs. gap ratio for square-shape front body, $Re = 1 \times 10^5 - 1.8 \times 10^5$.

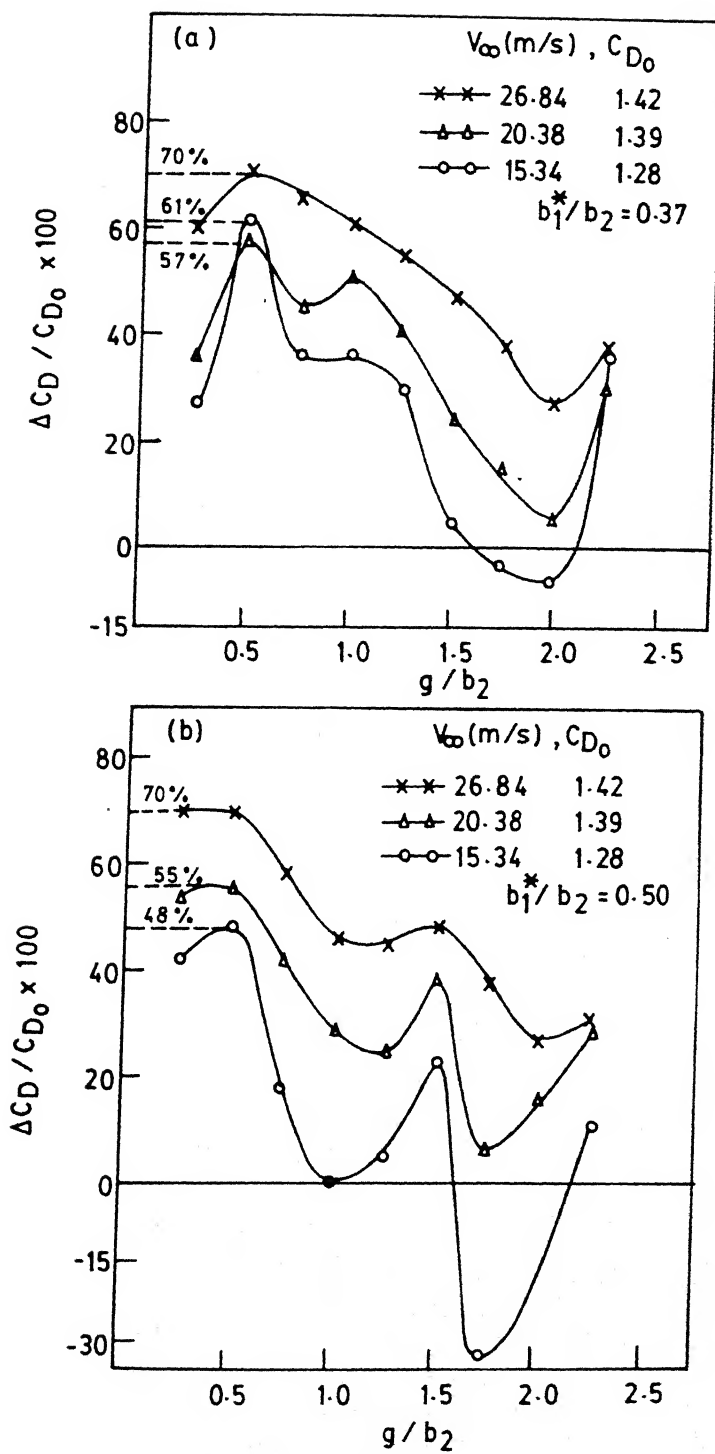


Fig. 13 Contd.

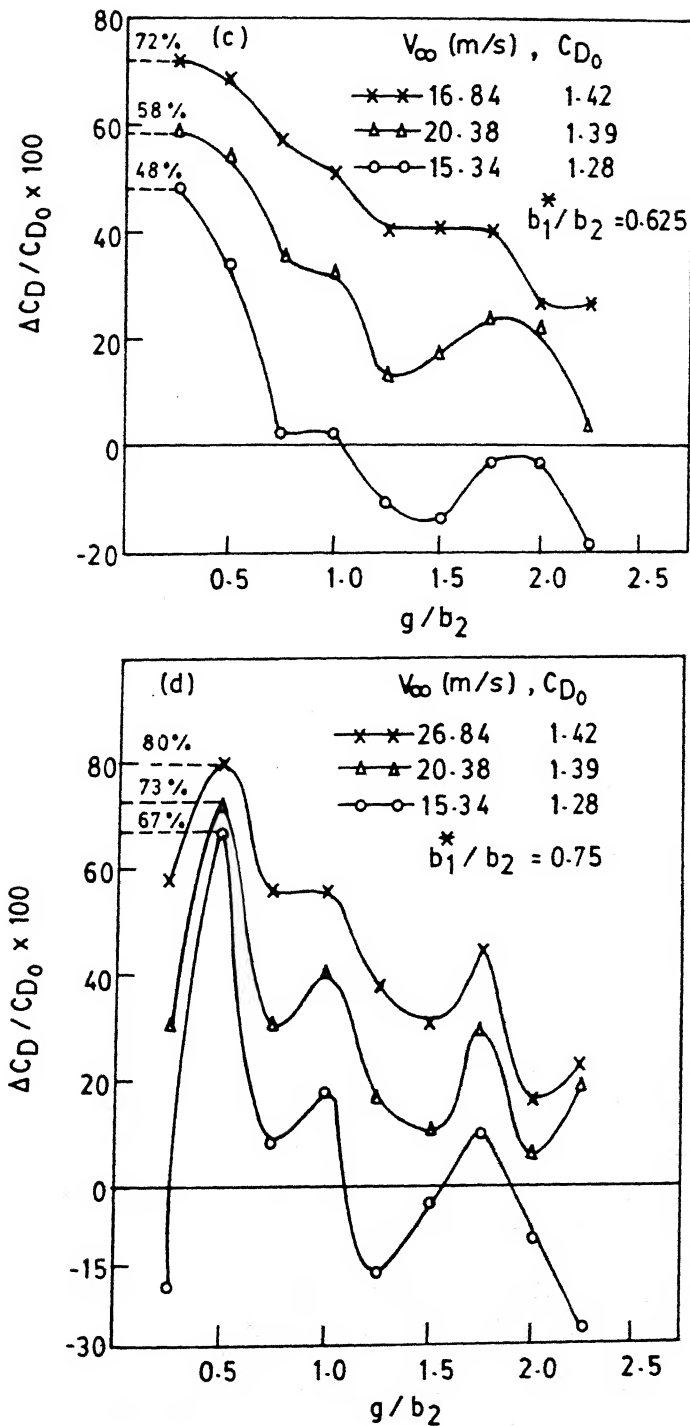
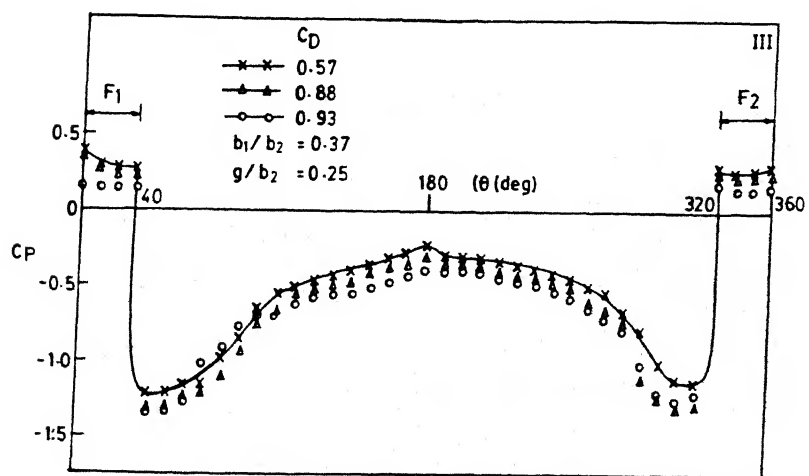
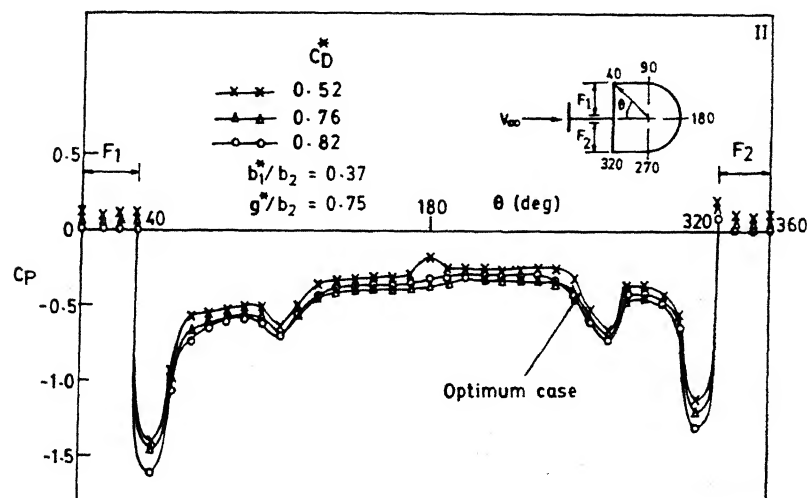
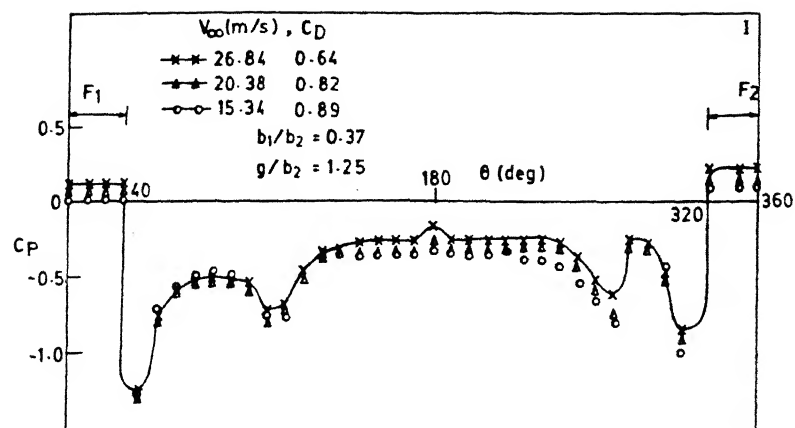
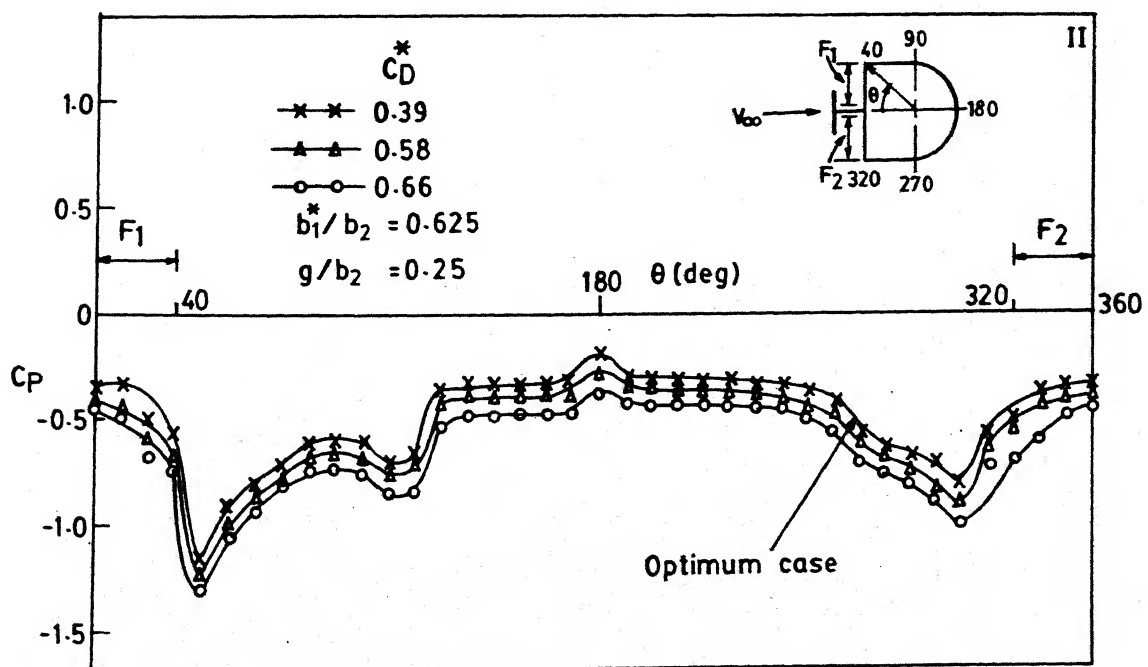
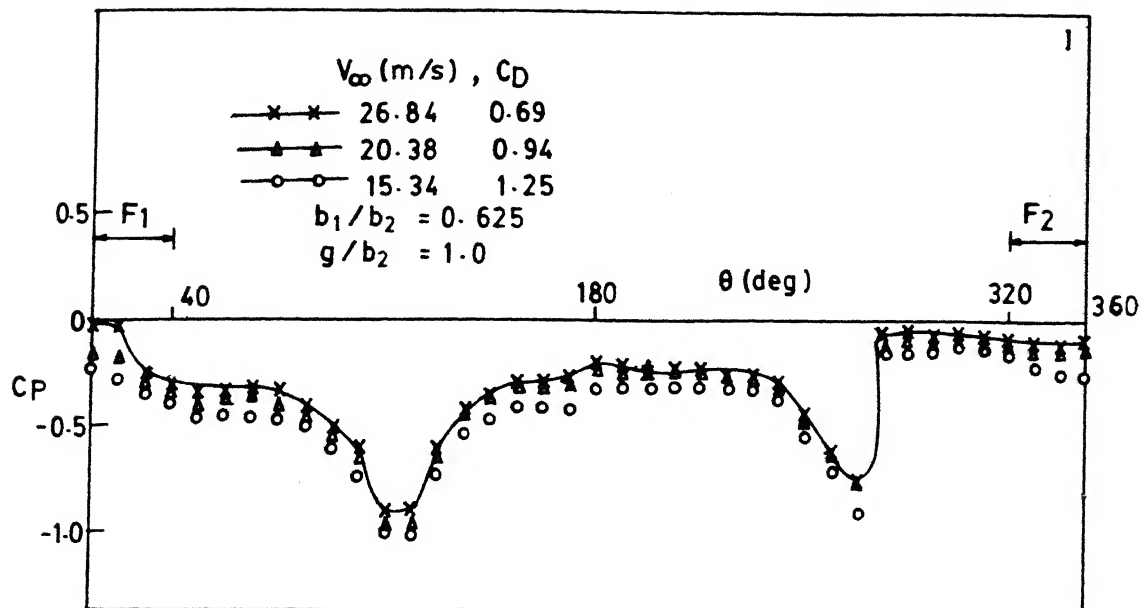


Fig. 13 Percentage drag reduction for Sq.-shape front body in optimum b_1 / b_2 ratio



Pressure distribution (Contd)



Pressure distribution (Contd.)

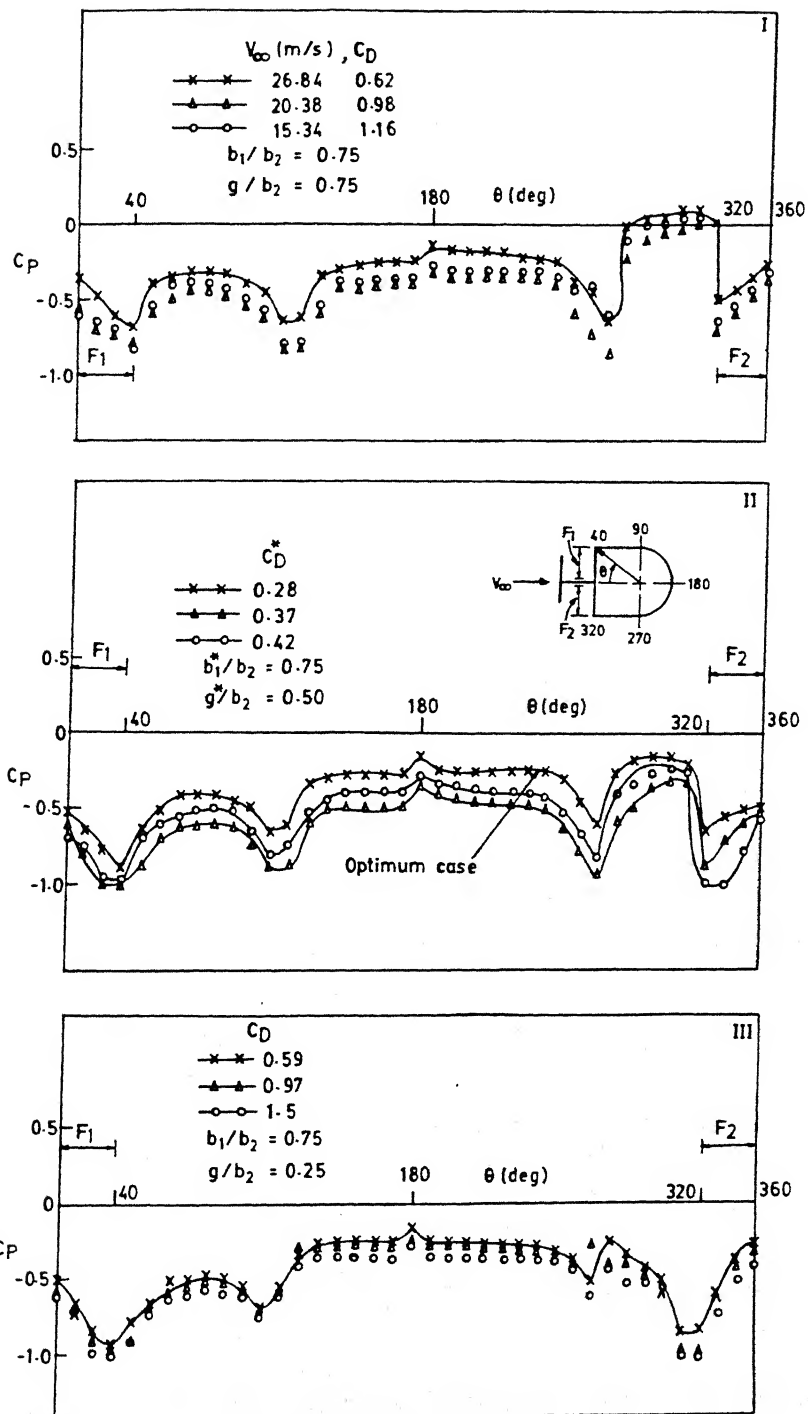


Fig. 14 Pressure distribution on rearbody with square-plate front body; * Optimum case.

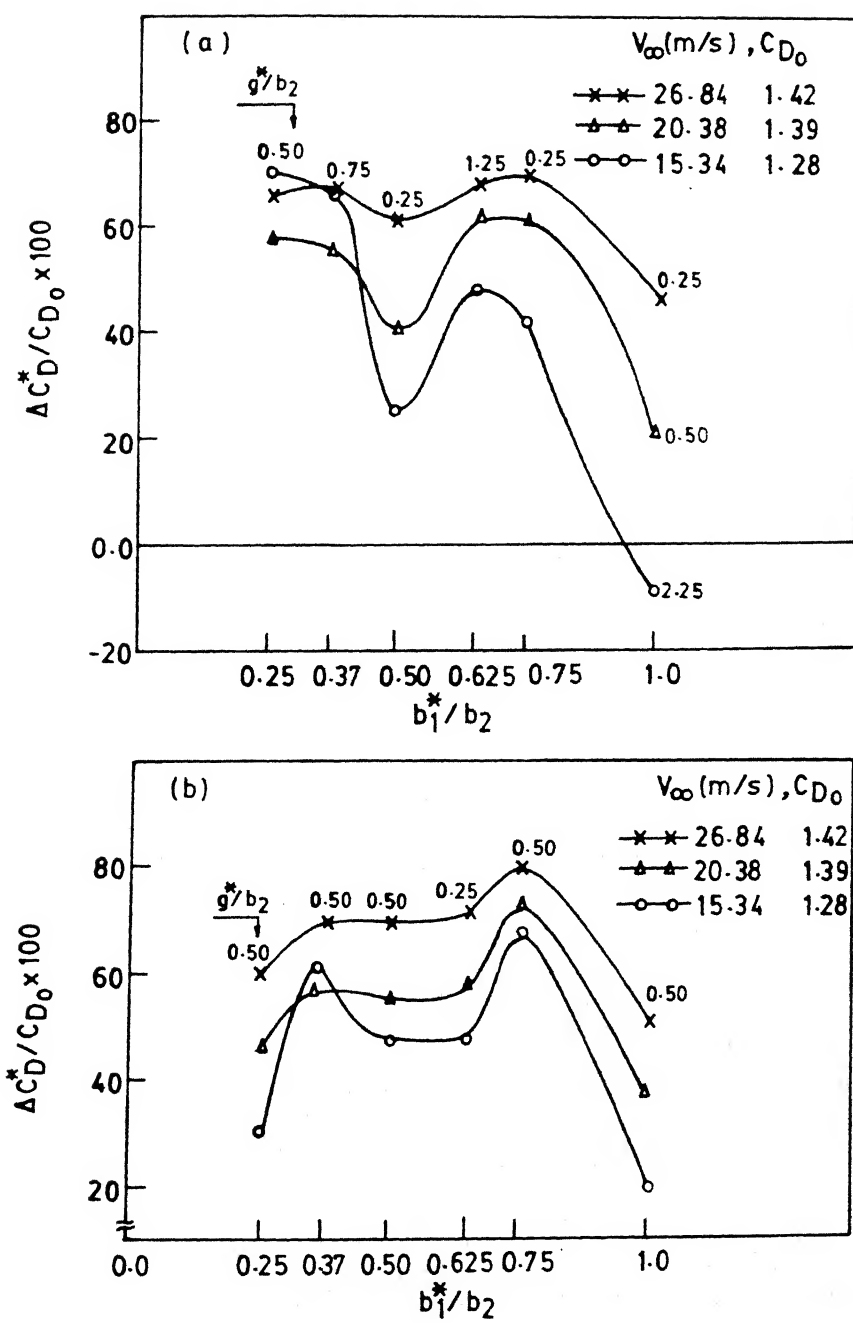


Fig.15 Maximum percentage drag reduction for each b_1/b_2 , the gap g^*/b_2 at which it occurs is shown beside each points;(a) D-shape (b) Sq. shape front body.

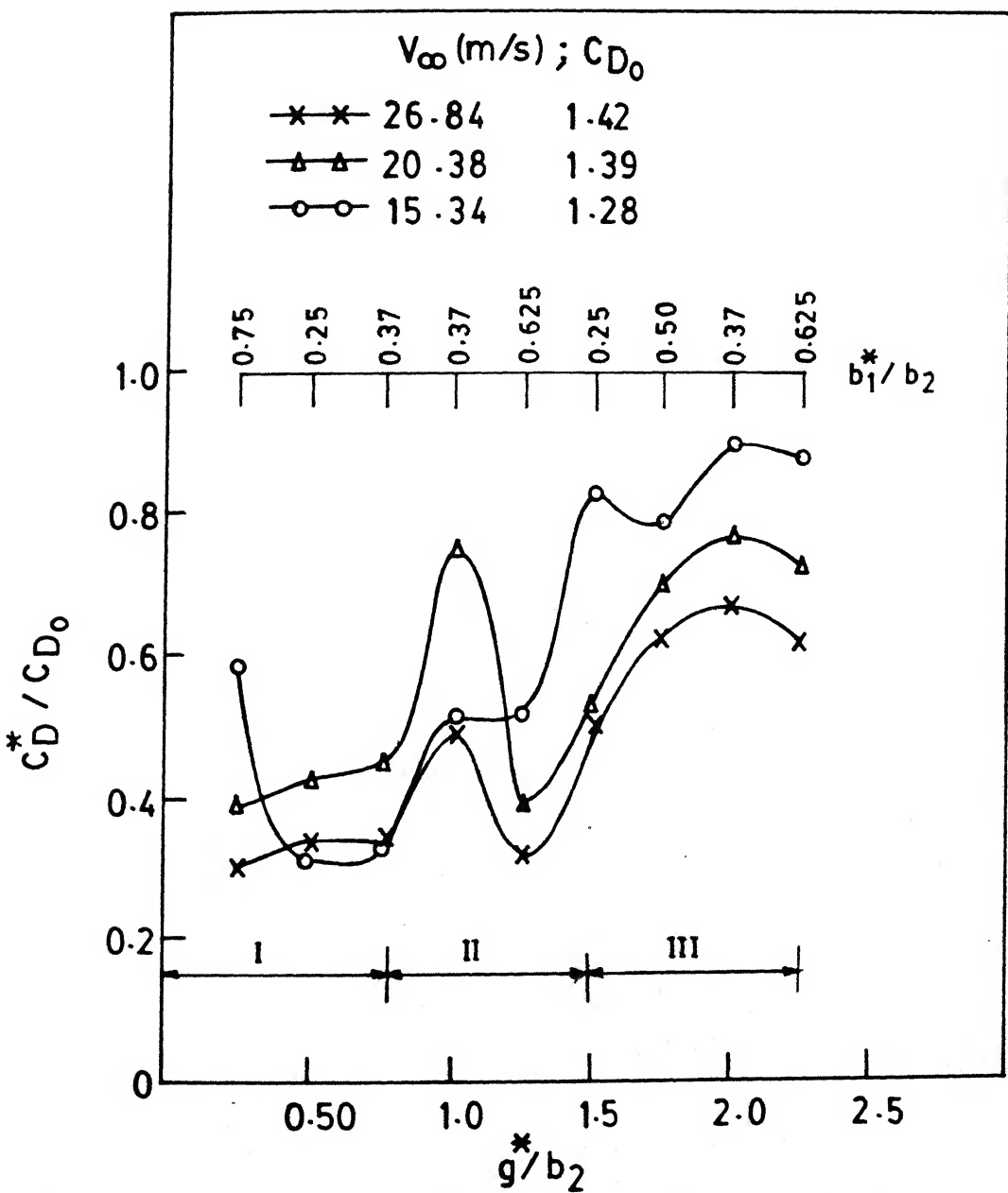


Fig.16 Minimum drag coefficient for each D-shape and the gap at which it occurs ; (I,II,III) refer to flow regimes .

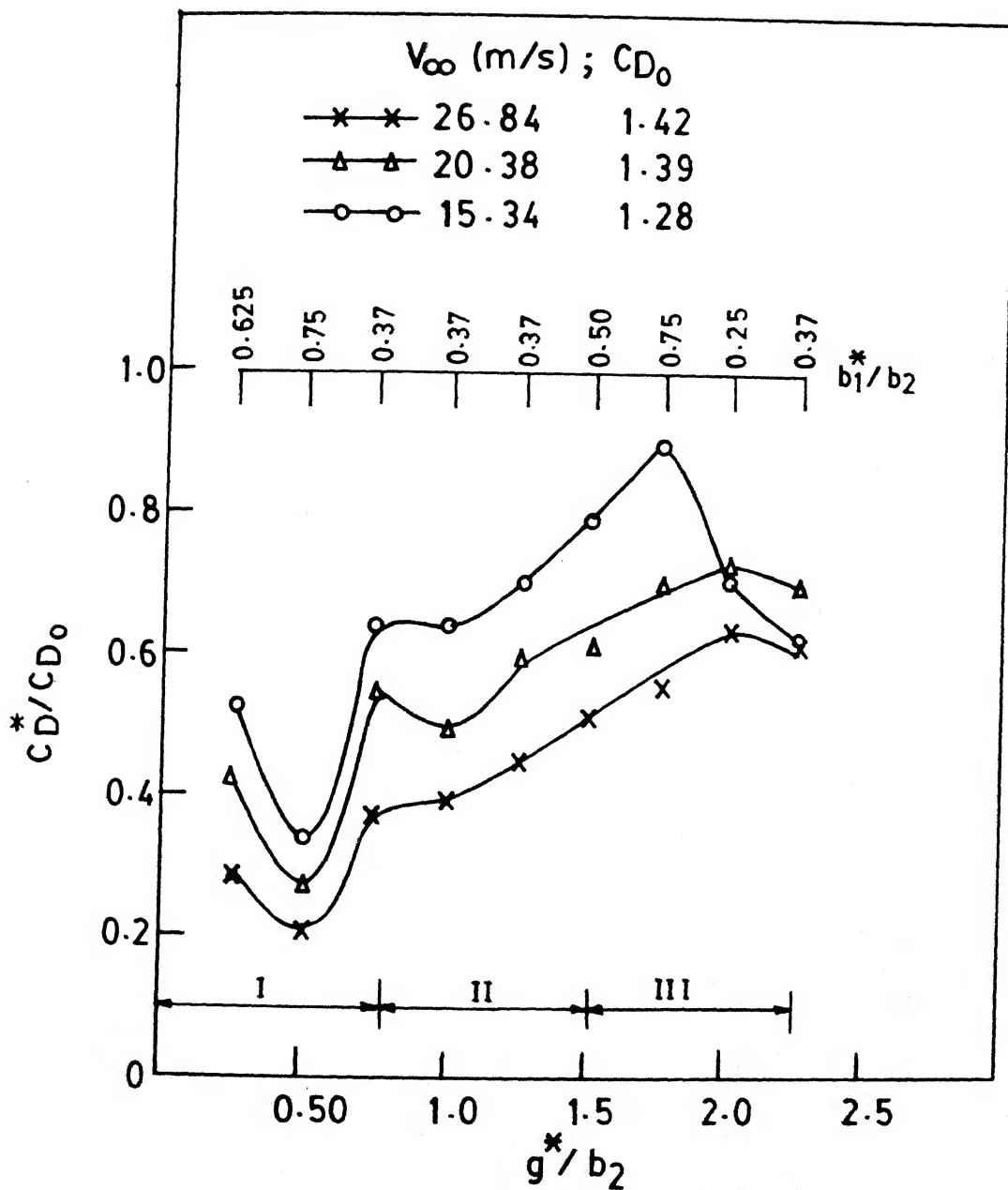


Fig. 17 Minimum drag coefficient for each square -shape and the gap at which it occurs; (I,II,III) refer to flow regimes.

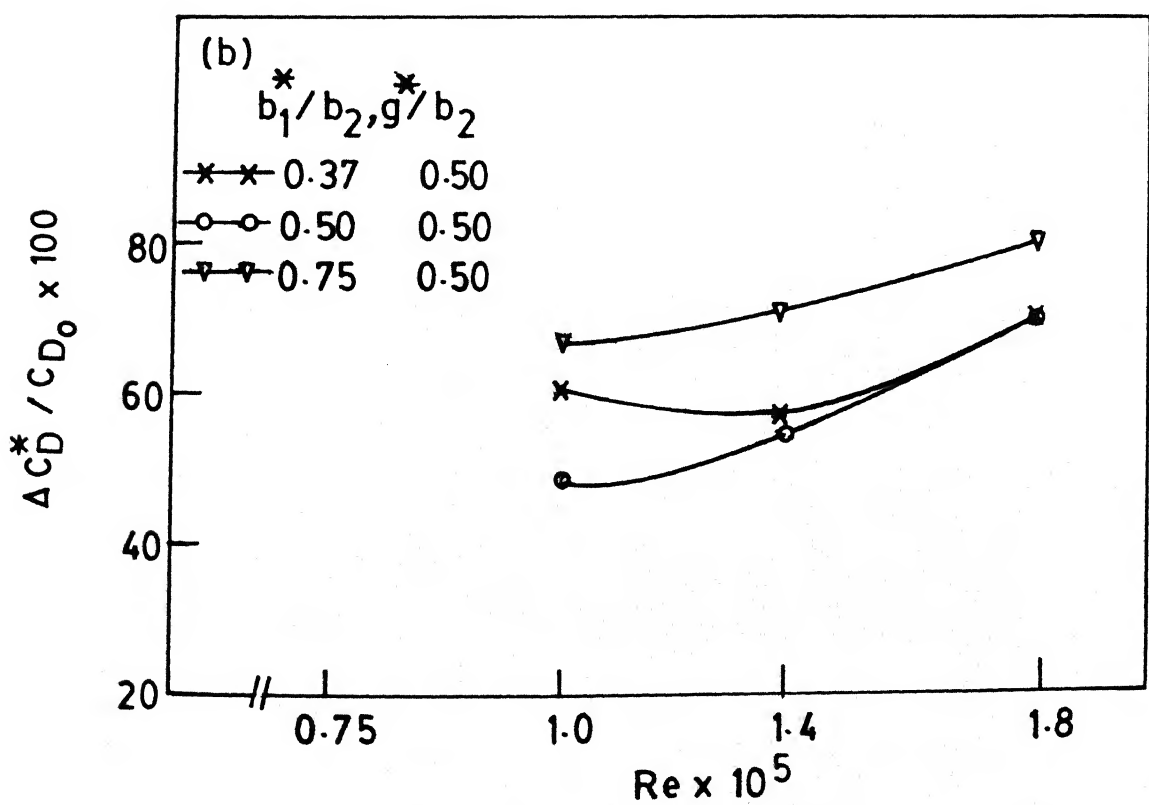
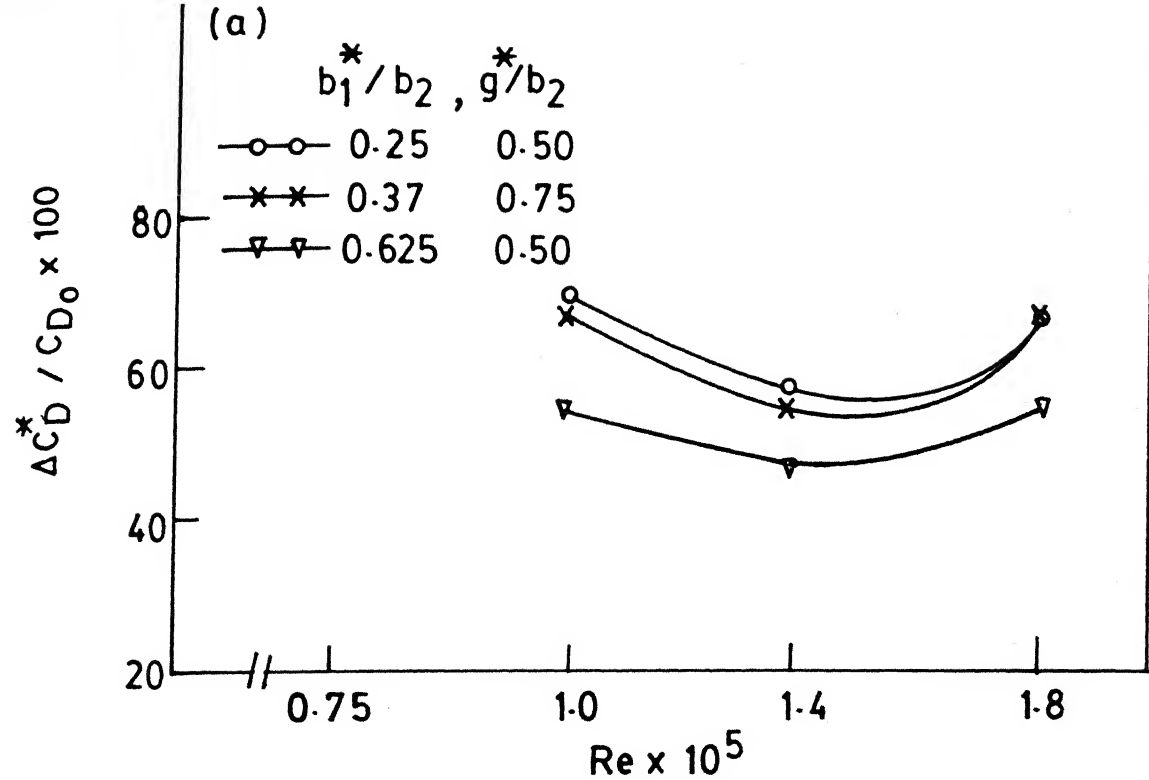
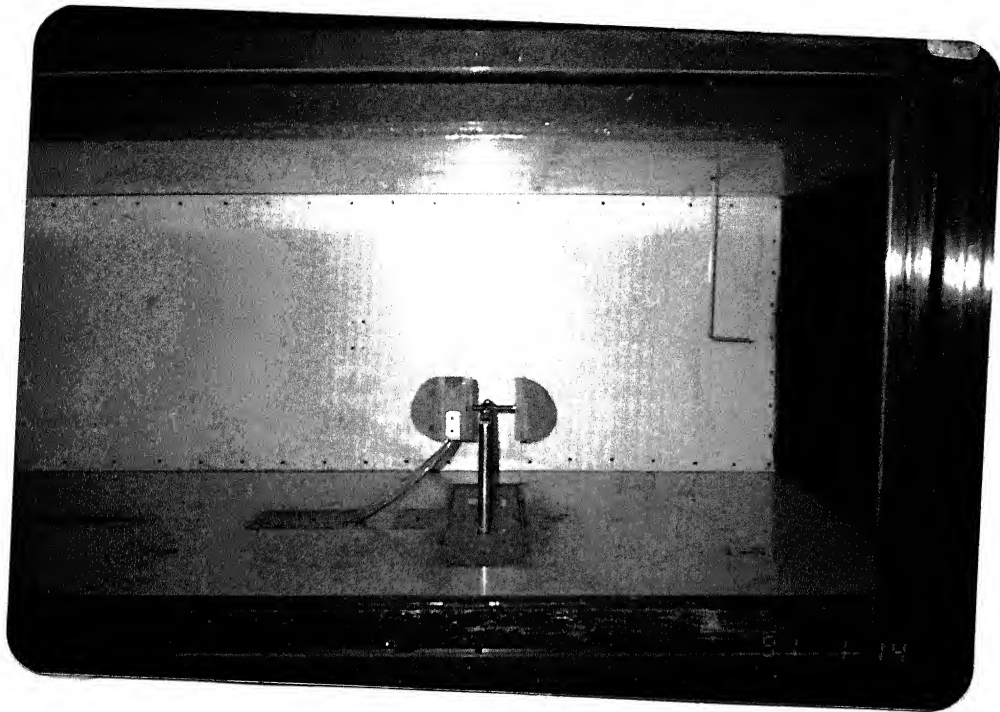
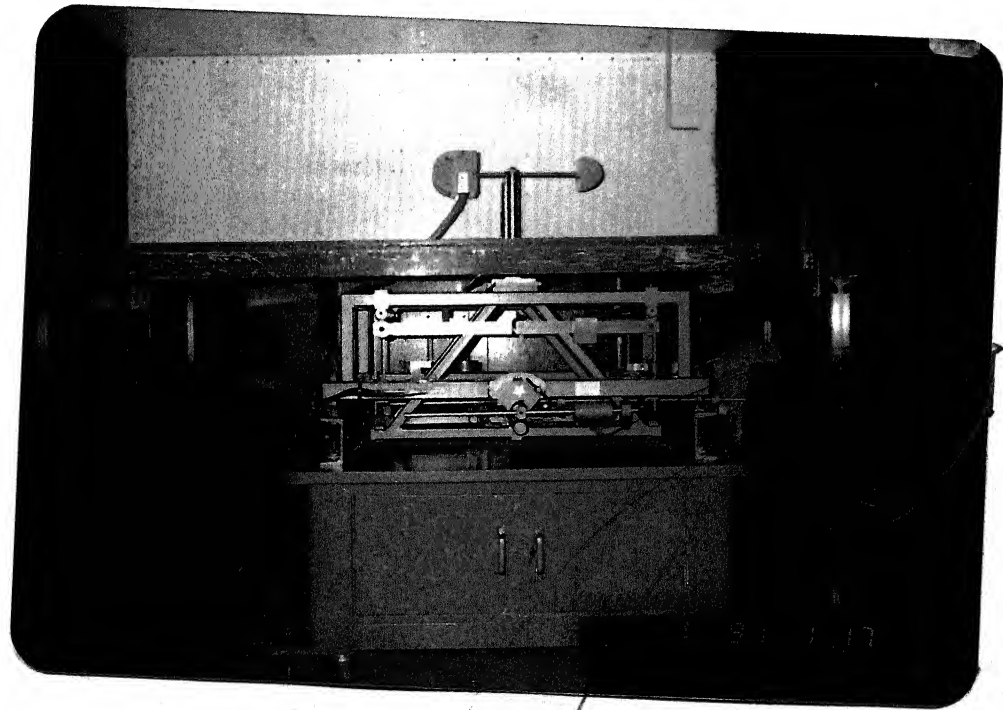


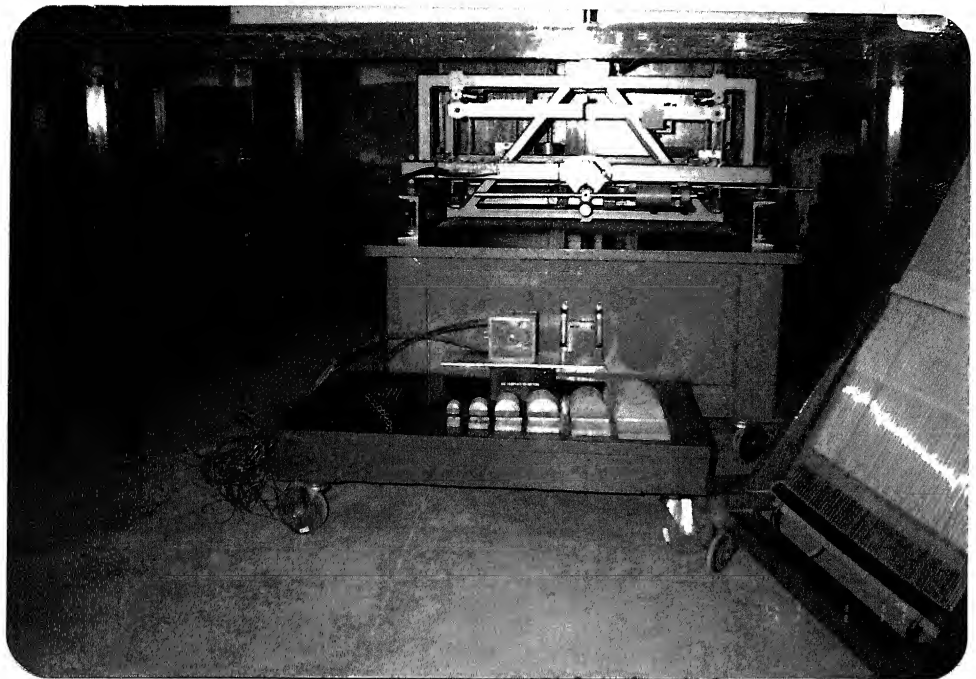
Fig. 1.8 Percentage drag reduction for optimum b_1/b_2 ratio variation with Re no. (a) D-Shape (b) Sq.-Shape front body



Photograph 1. A view of the model in the tunnel showing test-section and pitot-static tube.



Photograph 2. Experimental model with three-component balance.



Photograph 3. Experimental models,
multimanometer.



Photograph 4. Experimental three-component
digital display.

APPENDIX A

Tables Of Drag Coefficient And Percentage Of Drag Reduction Results

Drag calibration curve for three-component balance is represented in Fig. 19, measured Drag coefficient data for D-shape and square shape front body and the corresponding percentage drag reduction are represented in Tables (1,2,3 and 4), respectively.

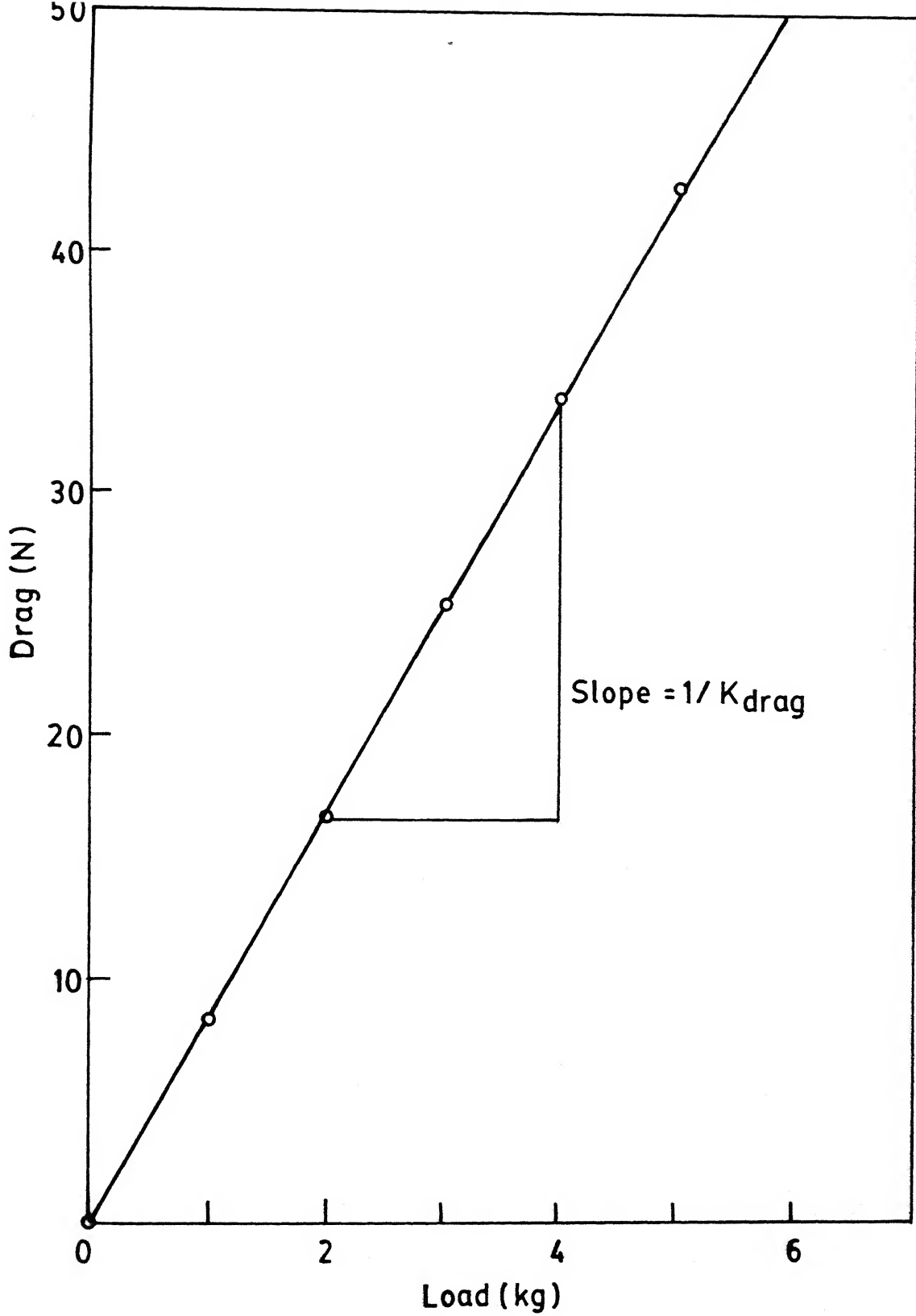


FIG. 19 CALIBRATION OF 3 COMPONENT BALANCE

Table 1
Drag Coefficient for rear body with D-shape frontbody

#	b_1/b_2	g/b_2	CD/CD ₀		
			$V_\infty = 26.84 \text{ m/s}$	$V_\infty = 20.38 \text{ m/s}$	$V_\infty = 15.34 \text{ m/s}$
1	1.0	2.25	0.82	1.06	1.08
		2.0	0.94	1.16	1.31
		1.75	0.76	1.02	1.50
		1.50	0.94	1.10	1.33
		1.25	0.87	1.05	1.25
		1.0	0.98	1.32	1.40
		0.75	1.2	1.13	1.52
		0.50	0.69	0.78	1.14
		0.25	0.53	0.82	1.26
2	0.75	2.25	0.94	0.81	1.06
		2.0	0.80	1.06	1.07
		1.75	0.68	1.08	1.13
		1.50	0.60	0.76	1.03
		1.25	0.59	0.78	0.94
		1.0	0.86	0.89	1.24
		0.75	0.63	0.89	1.28
		0.50	0.52	0.59	0.75
		0.25	0.30	0.39	0.58
3	0.625	2.25	0.82	0.70	0.88
		2.0	0.71	0.92	1.00
		1.75	0.69	0.92	1.36
		1.50	0.62	0.79	1.05
		1.25	0.32	0.39	0.52
		1.0	0.52	0.74	1.00
		0.75	0.50	0.67	0.79
		0.50	0.45	0.53	0.55
		0.25	0.34	0.51	0.66
4	0.50	2.25	0.75	0.81	1.13
		2.0	0.75	0.84	0.95
		1.75	0.62	0.70	0.79
		1.50	0.63	0.79	0.95
		1.25	0.60	0.89	1.13
		1.0	0.50	0.67	0.83
		0.75	0.51	0.77	1.02
		0.50	0.53	0.76	1.10
		0.25	0.39	0.59	0.75
5	0.37	2.25	0.66	0.74	0.83
		2.0	0.67	0.77	0.90
		1.75	0.66	0.74	1.09
		1.50	0.62	0.83	1.03
		1.25	0.59	0.74	0.88
		1.0	0.49	0.75	0.52
		0.75	0.33	0.45	0.33
		0.50	0.44	0.63	0.89
		0.25	0.50	0.68	0.73
6	0.25	2.25	0.69	0.90	1.02
		2.0	0.68	0.88	0.96
		1.75	0.73	0.90	1.00
		1.50	0.51	0.52	0.83
		1.25	0.66	0.76	0.70
		1.0	0.69	1.00	1.14
		0.75	0.53	0.71	0.88
		0.50	0.34	0.42	0.31
		0.25	0.53	0.64	0.63

$$C_{D0} = 1.42 \text{ at } V_\infty = 26.84 \text{ m/s}$$

$$C_{D0} = 1.39 \text{ at } V_\infty = 20.38 \text{ m/s}$$

$$C_{D0} = 1.28 \text{ at } V_\infty = 15.34 \text{ m/s}$$

Table 2
Drag Coefficient for rear body with square-shape frontbody

#	b_1/b_2	g/b_2	CD/CD ₀	CD/CD ₀	CD/CD ₀
			$V_\infty = 26.84 \text{ m/s}$	$V_\infty = 20.38 \text{ m/s}$	$V_\infty = 15.34 \text{ m/s}$
1	1.0	2.25	1.08	1.22	1.37
		2.0	1.07	1.16	1.35
		1.75	0.79	1.06	1.32
		1.50	0.77	1.13	1.30
		1.25	0.86	0.94	1.24
		1.0	0.54	0.75	0.89
		0.75	0.61	0.90	1.02
		0.50	0.49	0.62	0.81
		0.25	0.60	0.71	0.91
	
2	0.75	2.25	0.77	0.81	1.27
		2.0	0.84	0.95	1.10
		1.75	0.55	0.70	0.90
		1.50	0.69	0.90	1.03
		1.25	0.62	0.84	1.18
		1.0	0.44	0.59	0.82
		0.75	0.44	0.71	0.91
		0.50	0.20	0.27	0.33
		0.25	0.42	0.70	1.19
	
3	0.625	2.25	0.73	0.87	1.18
		2.0	0.73	0.78	1.03
		1.75	0.60	0.76	1.03
		1.50	0.59	0.83	1.14
		1.25	0.60	0.87	1.11
		1.0	0.49	0.68	0.98
		0.75	0.43	0.65	0.98
		0.50	0.31	0.46	0.66
		0.25	0.28	0.42	0.52
	
4	0.50	2.25	0.69	0.71	0.89
		2.0	0.73	0.84	0.85
		1.75	0.62	0.94	1.33
		1.50	0.51	0.81	0.77
		1.25	0.55	0.76	0.95
		1.0	0.54	0.71	1.0
		0.75	0.42	0.59	0.82
		0.50	0.31	0.45	0.52
		0.25	0.31	0.46	0.58
	
5	0.37	2.25	0.62	0.70	0.84
		2.0	0.73	0.95	1.06
		1.75	0.62	0.85	1.03
		1.50	0.53	0.76	0.95
		1.25	0.45	0.59	0.70
		1.0	0.39	0.49	0.64
		0.75	0.37	0.53	0.64
		0.50	0.31	0.43	0.39
		0.25	0.40	0.64	0.73
	
6	0.25	2.25	0.63	0.81	0.94
		2.0	0.64	0.74	0.70
		1.75	0.64	0.77	0.93
		1.50	0.55	0.70	0.85
		1.25	0.54	0.76	0.78
		1.0	0.49	0.69	0.82
		0.75	0.42	0.55	0.73
		0.50	0.40	0.54	0.70
		0.25	0.60	0.84	0.99
	

$C_{D0} = 1.42$ at $V_\infty = 26.84 \text{ m/s}$

$C_{D0} = 1.39$ at $V_\infty = 20.38 \text{ m/s}$

$C_{D0} = 1.28$ at $V_\infty = 15.34 \text{ m/s}$

Table 3
Percentage of Drag reduction for rear body with D-shape

b_1/b_2	g/b_2	$\Delta CD/CD \times 100$		$\Delta CD/CD \times 100$	$\Delta CD/CD \times 100$
		$V_\infty = 26.84 \text{ m/s}$	$V_\infty = 20.38 \text{ m/s}$		
1.0	2.25	18	- 8	- 8	- 8
	2.0	8	-16	-31	-31
	1.75	23	- 2	-50	-50
	1.50	8	-10	-33	-33
	1.25	13	- 5	-25	-25
	1.0	2	-32	-40	-40
	0.75	-16	-13	-52	-52
	0.50	30	22	-14	-14
	0.25	47	18	-26	-26
0.75	2.25	6	18	- 6	- 6
	2.0	20	-6	- 7	- 7
	1.75	32	-8	-13	-13
	1.50	40	24	- 3	- 3
	1.25	41	21	- 6	- 6
	1.0	34	11	-24	-24
	0.75	37	11	-28	-28
	0.50	47	41	25	25
	0.25	70	61	42	42
0.625	2.25	38	28	12	12
	2.0	29	8	0	0
	1.75	31	8	-36	-36
	1.50	38	21	- 5	- 5
	1.25	68	61	-48	-48
	1.0	48	26	0	0
	0.75	50	33	21	21
	0.50	55	47	45	45
	0.25	66	49	34	34
0.50	2.25	25	19	-13	-13
	2.0	25	16	5	5
	1.75	38	30	21	21
	1.50	37	21	5	5
	1.25	40	11	-13	-13
	1.0	47	22	-10	-10
	0.75	50	33	17	17
	0.50	49	23	-2	-2
	0.25	61	41	25	25
0.37	2.25	34	26	17	17
	2.0	33	23	10	10
	1.75	34	26	21	21
	1.50	38	17	1	1
	1.25	41	26	12	12
	1.0	51	25	48	48
	0.75	67	55	67	67
	0.50	56	37	11	11
	0.25	50	32	27	27
0.25	2.25	31	10	2	2
	2.0	32	12	4	4
	1.75	27	10	5	5
	1.50	49	48	17	17
	1.25	34	25	30	30
	1.0	31	0	-14	-14
	0.75	47	29	12	12
	0.50	66	58	70	70
	0.25	31	36	40	40

$C_{D0} = 1.42$ at $V_\infty = 26.84 \text{ m/s}$

$C_{D0} = 1.30$ at $V_\infty = 20.38 \text{ m/s}$

$C_{D0} = 1.28$ at $V_\infty = 15.34 \text{ m/s}$

Table 4
Percentage of Drag reduction for rear body with square-shape

b_1/b_2	g/b_2	$\Delta CD/CD_0 \times 100$	$\Delta CD/CD_0 \times 100$	$\Delta CD/CD_0 \times 100$
		$V_\infty = 26.84 \text{ m/s}$	$V_\infty = 20.38 \text{ m/s}$	$V_\infty = 15.34 \text{ m/s}$
1.0	2.25	-8	-22	-37
	2.0	-7	-16	-35
	1.75	21	-6	-32
	1.50	23	-13	-30
	1.25	34	6	-24
	1.0	45	25	11
	0.75	39	10	-2
	0.50	51	38	19
	0.25	40	29	9
0.75	2.25	23	19	-27
	2.0	16	5	-10
	1.75	45	30	10
	1.50	31	10	-3
	1.25	38	16	-16
	1.0	56	41	18
	0.75	56	29	8
	0.50	80	73	67
	0.25	58	30	-19
0.625	2.25	27	3	-19
	2.0	27	22	-3
	1.75	40	24	-3
	1.50	41	17	-14
	1.25	40	13	-11
	1.0	51	32	2
	0.75	57	35	2
	0.50	69	54	34
	0.25	72	58	48
0.50	2.25	31	29	11
	2.0	27	16	15
	1.75	38	6	-33
	1.50	49	39	23
	1.25	45	24	5
	1.0	46	29	0
	0.75	58	41	18
	0.50	70	55	48
	0.25	70	54	42
0.37	2.25	38	30	36
	2.0	27	5	-6
	1.75	38	15	-3
	1.50	47	24	5
	1.25	55	41	30
	1.0	61	51	36
	0.75	63	45	3
	0.50	70	57	61
	0.25	60	36	27
0.25	2.25	37	19	6
	2.0	36	26	30
	1.75	37	23	7
	1.50	45	30	15
	1.25	46	25	22
	1.0	51	31	18
	0.75	58	45	28
	0.50	60	46	30
	0.25	40	16	1

$C_{D0} = 1.42$ at $V_\infty = 26.84 \text{ m/s}$

$C_{D0} = 1.39$ at $V_\infty = 20.38 \text{ m/s}$

$C_{D0} = 1.28$ at $V_\infty = 15.34 \text{ m/s}$

APPENDIX B

Tabulation of Measured Data and Computed Pressure Distribution

Computer programme which is used to compute the freestream velocity and pressure coefficient is given here. Measured static pressure and computed pressure coefficient for rearbody alone, rearbody with D and square-shape frontbodies at various b_1/b_2 and g/b_2 for three different speeds are tabulated. The location of the static pressure taps in the midplane (AA) are indicated by ($\theta = 0 - 360^\circ$) as shown in Fig. 3.

```

C.....
C
C      THIS PROGRAM CALCULATES PRESSURE DISTRIBUTION AROUND THE BASIC
C      BODY IN TWO BODY TENDOM.
C
C.....I= RUN VELOCITY(THREE VELOCITY FOR EACH FRONT BODY MODELS)
C.....J= TAPS NUMBERS(FROM 1 TO 39)
C.....PSINF=FREE STREAM STATIC PRESSURE
C.....PTINF=FREE STREAM TOTAL PRESSURE
C.....PSL = LOCAL STATIC PRESSURE
C.....VINF = FREE STREAM VELOCITY (M/SEC)
C.....CP= LOCAL PRESSURE COEFFICIENT
C
C.....PROGRAM PROCESS_DATA
C
C.....VARIABLES & PARAMETER DECLERATIONS.....
C
      REAL PSL(6,39),PSREF(6),PSINF(6),PTINF(6)
      REAL CP(6,39),VINF(6)
      CHARACTER INFILE*20,OUTFILE*20,TITLE*80
      INTEGER FIN,FOUT
      PARAMETER (G=9.8,RHOA=1.225,RHOW=1000.0)
C
C.....GET THE INPUT FILE NAME.....
C
100   WRITE(*,9100) 'INPUT'
      READ(*,*,END=10000,ERR=100) INFILE
      FIN=20
      OPEN(UNIT=FIN,FILE=INFILE)
C
C.....GET THE OUTPUT FILE NAME.....
C
200   WRITE(*,9100) 'OUTPUT'
      READ(*,*,END=10001,ERR=100) OUTFILE
      FOUT=22
      OPEN(UNIT=FOUT,FILE=OUTFILE)
C
C.....READ DATA FROM THE INPUT FILE.....
C
      I=0
      J=0
      READ(FIN,*,END=300,ERR=999) TITLE
      DO I=1,6
        READ(FIN,*,END=300,ERR=999) PSREF(I),PSINF(I),PTINF(I)
        READ(FIN,*,END=300,ERR=999) (PSL(I,J),J=1,39)
      ENDDO
      GOTO 400
300   WRITE(*,*) 'ERROR : IN THE INPUT FILE AT (I,J) : (',I,J,)'
      GOTO 999
400   CONTINUE
C
C.....DO CALCULATIONS : PROCESS THE DATA.....
C
      COS30=COSD(30.0)
      DO I=1,6
        VINF(I)=SQRT(2*(PSINF(I)-PTINF(I))*COS30*0.01*G*RHOW/RHOA)
        DO J=1,39
          CP(I,J)=(PSL(I,J)-PSINF(I))/(PTINF(I)-PSINF(I))
          PSL(I,J)=(PSREF(I)-PSL(I,J))*COS30
        ENDDO
      ENDDO
C
C.....WRITE THE RESULTS IN THE OUTPUT FILE.....
C
      WRITE(FOUT,9200) TITLE
      WRITE(FOUT,9300) (VINF(I),I=1,6)

```

```
DO J=1,39
    WRITE(FDUT,9500) J,(PSL(I,J),CP(I,J),I=1,6)
ENDDO
WRITE(FDOUT,9700)

C
C.....JUMP FOR NORMAL END OF EXECUTION IN NO ERROR IN THE INPUT FILE..
C
    GOTO 1000
999  WRITE(*,9999)
1000  CLOSE(FDOUT)
1001  CLOSE(FIN)
C
C.....END OF EXECUTION . . . . . .
C
10000 STOP " NORMAL END OF EXECUTION."
C
C.....FORMAT STATEMENTS . . . . . .
C
9100  FORMAT(A6' FILE NAME ?')
9200  FORMAT(A20)
9300  FORMAT(114(''-
8      '1'4X'1'22X'D - SHAPE'22X'1'19X'SQUARE - SHAPE'20X'1'/
8      '1'4X'1'53(''-'1'53(''-'1'/
8      '1'4X'1'6(2XF7.4,X'(M/S)'2X'1')/
8      '1'4X'1'6(17(''-'1')/
8      '1'2X'6'X'1'6(3X'PS'3X'1'3X'CP'3X'1')/
8      '1'4X'1'6(X'CM.H20'X'1'8X'1')/
8      '1'4(''-'1'12(8(''-'1')/
8      )
9500  FORMAT('1'XI2X'1'12(XF6.3,X'1')
9700  FORMAT(114(''-'1')
9999  FORMAT('ERROR IN INPUT FILE FORMAT'/
8      'ENDING EXECUTION . . .')

C
C.....END OF THE PROGRAM LISTING . . . . . .
C
    END
C
C.....
```

Appendix B Table 2 Measured data and computed pressure distribution for $b_1/b_2=1.0$, $g/b_2=2.25$, $T_1=290$ K.

#	D - Shape						Square - Shape					
	26.8427 (m/s)		20.3885 (m/s)		15.3479 (m/s)		26.8427 (m/s)		20.3885 (m/s)		15.3479 (m/s)	
	Ps cm.H2O	Cp	Ps cm.H2O	Cp	Ps cm.H2O	Cp	Ps cm.H2O	Cp	Ps cm.H2O	Cp	Ps cm.H2O	Cp
1	-1.212	.365	-.866	.300	-.433	.294	-3.377	-.115	-2.978	-.167	-1.212	-.235
2	-1.472	.368	-.866	.300	-.433	.294	-3.264	-.077	-2.978	-.167	-1.212	-.235
3	-1.645	.269	-.1.039	.233	-.606	.176	-3.637	-.173	-2.165	-.200	-1.299	-.294
4	-1.705	.212	-1.212	.167	-.693	.118	-3.637	-.173	-2.511	-.373	-1.386	-.353
5	-7.101	.942	-4.936	-.1.267	-2.685	-.1.235	-4.070	-.269	-2.598	-.367	-1.472	-.412
6	-6.666	.846	-4.503	-.1.100	-2.511	-.1.118	-3.811	-.212	-2.338	-.267	-1.299	-.294
7	-5.456	.577	-2.811	-.823	-2.165	-.882	-3.637	-.173	-2.165	-.200	-1.299	-.294
8	-4.936	.462	-3.377	-.667	-1.905	-.766	-3.637	-.173	-2.165	-.200	-1.299	-.294
9	-4.330	.237	-3.031	-.533	-1.819	-.647	-3.637	-.173	-2.165	-.200	-1.299	-.294
10	-4.590	.395	-2.944	-.500	-1.732	-.588	-3.637	-.173	-2.165	-.200	-1.299	-.294
11	-4.244	.305	-3.031	-.533	-1.732	-.588	-3.811	-.212	-2.338	-.267	-1.299	-.294
12	-5.110	.500	-3.464	-.700	-1.905	-.706	-4.503	-.365	-2.771	-.433	-1.472	-.412
13	-5.110	.500	-3.464	-.700	-1.905	-.706	-4.677	-.404	-2.944	-.500	-1.645	-.529
14	-4.002	.365	-3.031	-.533	-1.732	-.588	-4.503	-.365	-2.771	-.433	-1.472	-.412
15	-4.076	.269	-2.771	-.433	-.559	-.471	-4.244	-.388	-2.685	-.460	-1.472	-.412
16	-3.897	.231	-2.685	-.400	-1.472	-.412	-4.070	-.269	-2.511	-.333	-1.386	-.353
17	-3.897	.231	-2.598	-.367	-1.472	-.412	-3.811	-.212	-2.338	-.267	-1.299	-.294
18	-2.338	.115	-2.338	-.267	-2.338	-1.000	-3.637	-.173	-2.252	-.233	-1.212	-.235
19	-3.811	.212	-2.511	-.333	-1.472	-.412	-3.637	-.173	-2.252	-.233	-1.212	-.235
20	-3.811	.212	-2.511	-.333	-1.299	-.294	-3.551	-.154	-2.165	-.200	-1.212	-.235
21	-3.204	.077	-2.165	-.200	-1.212	-.235	-3.204	-.077	-2.078	-.167	-1.212	-.235
22	-3.811	.212	-2.511	-.333	-1.299	-.294	-3.464	-.135	-2.165	-.200	-1.212	-.235
23	-3.811	.212	-2.511	-.333	-1.299	-.294	-3.551	-.154	-2.165	-.200	-1.212	-.235
24	-3.811	.212	-2.511	-.333	-1.299	-.294	-3.551	-.154	-2.165	-.200	-1.212	-.235
25	-3.811	.212	-2.598	-.367	-1.299	-.294	-3.637	-.173	-2.165	-.200	-1.212	-.235
26	-5.629	.615	-2.771	-.433	-1.472	-.412	-3.724	-.192	-2.338	-.267	-1.299	-.294
27	-4.244	.305	-2.858	-.467	-1.559	-.471	-4.070	-.269	-2.511	-.333	-1.472	-.412
28	-4.677	.464	-3.204	-.600	-1.732	-.588	-4.417	-.346	-2.771	-.433	-1.559	-.471
29	-4.936	.462	-3.377	-.667	-1.819	-.647	-4.417	-.346	-2.771	-.433	-1.472	-.412
30	-5.369	.558	-3.637	-.767	-1.905	-.706	-4.677	-.404	-2.944	-.500	-1.645	-.529
31	-3.637	.173	-2.771	-.433	-1.472	-.412	-3.637	-.173	-2.338	-.267	-1.472	-.412
32	-3.897	.231	-2.771	-.433	-1.472	-.412	-3.204	-.077	-2.338	-.267	-1.299	-.294
33	-0.076	.269	-3.031	-.533	-1.386	-.353	-3.204	-.077	-1.905	-.100	-0.866	0.000
34	-5.365	.556	-3.637	-.767	-1.905	-.706	-4.685	-.338	-1.645	-.000	-0.866	0.000
35	-6.666	.846	-4.503	-.1.100	-2.338	-.1.000	-2.685	-.038	-1.645	-.000	-0.866	0.000
36	-1.299	.346	.775	-.333	-.433	-.294	-2.944	-.019	-1.819	-.067	-1.039	-.118
37	-1.026	.404	.606	.400	.346	.353	-2.944	-.019	-1.819	-.067	-1.039	-.118
38	-1.026	.404	.606	.400	.346	.353	-2.944	-.019	-1.819	-.067	-1.039	-.118
39	-0.693	.491	.806	.400	.260	.412	-2.685	-.038	-1.732	-.033	-1.039	-.118

Appendix B Table 3 Measured data and compute pressure distribution for $b_1/b_2=0.75$, $g/b_2=2.25$, $T_1=290$ K.

#	D - Shape						Square - Shape					
	26.8427 (m/s)		20.3885 (m/s)		15.3479 (m/s)		26.8427 (m/s)		20.3885 (m/s)		15.3479 (m/s)	
	Ps cm.H2O	Cp	Ps cm.H2O	Cp	Ps cm.H2O	Cp	Ps cm.H2O	Cp	Ps cm.H2O	Cp	Ps cm.H2O	Cp
1	-.606	.500	-.433	.467	-.173	.471	-2.338	.115	-1.472	.067	-.779	.059
2	-.775	.462	-.433	.467	-.260	.412	-2.338	.115	-1.472	.067	-.866	.000
3	-1.039	.404	-.606	.400	-.346	.353	-2.511	.077	-1.645	.000	-.953	.059
4	-1.295	.346	-.779	.333	-.433	.294	-2.771	.019	-1.819	-.067	-1.039	-.118
5	-8.227	-1.192	-.511	-.1.333	-2.771	-.1.294	-5.976	-.692	-3.637	-.767	-2.338	-.1.000
6	-8.227	-1.192	-.511	-.1.333	-2.771	-.1.294	-4.936	-.462	-3.031	-.533	-1.905	-.706
7	-7.101	.942	-4.590	-.1.133	-2.598	-.1.176	-4.503	-.365	-2.771	-.433	-1.645	-.529
8	-6.666	.846	-4.070	-.933	-2.338	-.1.000	-4.417	-.346	-2.771	-.433	-1.645	-.529
9	-5.196	.519	-3.637	-.767	-1.992	-.765	-4.417	-.346	-2.771	-.433	-1.645	-.529
10	-5.196	.519	-3.377	-.667	-1.905	-.706	-4.417	-.346	-2.771	-.433	-1.645	-.529
11	-4.502	.305	-3.204	-.600	-1.819	-.647	-4.503	-.365	-3.031	-.533	-1.819	-.647
12	-5.110	.500	-3.204	-.600	-1.819	-.647	-5.629	-.615	-3.551	-.733	-1.992	.765
13	-4.536	.462	-3.031	-.533	-1.819	-.647	-5.802	-.654	-3.637	-.767	-1.992	.765
14	-4.503	.365	-2.685	-.467	-1.645	-.529	-5.110	-.500	-3.204	-.600	-1.905	.706
15	-4.244	.306	-2.685	-.400	-1.472	-.412	-4.503	-.365	-2.944	-.566	-1.819	.647
16	-4.076	.269	-2.511	-.333	-1.472	-.412	-4.070	-.269	-2.685	-.400	-1.645	-.529
17	-4.076	.269	-2.511	-.333	-1.472	-.412	-4.070	-.269	-2.685	-.400	-1.645	-.529
18	-4.070	.269	-2.511	-.333	-1.472	-.412	-4.070	-.269	-2.685	-.400	-1.645	-.529
19	-2.554	.250	-2.511	-.333	-1.472	-.412	-3.897	-.231	-2.511	-.333	-1.472	-.412
20	-3.897	.231	-2.638	-.667	-1.472	-.412	-3.724	-.231	-2.511	-.333	-1.472	-.412
21	-3.811	.212	-2.338	-.267	-1.472	-.412	-3.551	-.154	-2.338	-.267	-1.472	-.412
22	-3.897	.231	-2.511	-.333	-1.472	-.412	-3.724	-.192	-2.338	-.267	-1.472	-.412
23	-3.897	.231	-2.511	-.333	-1.472	-.412	-3.811	-.212	-2.338	-.267	-1.472	-.412
24	-3.847	.231	-2.511	-.333	-1.472	-.412	-3.811	-.212	-2.425	-.306	-1.472	-.412
25	-4.076	.269	-2.511	-.333	-1.472	-.412	-3.897	-.231	-2.425	-.306	-1.472	-.412
26	-4.157	.235	-2.771	-.433	-1.472	-.412	-3.897	-.231	-2.511	-.333	-1.472	-.412
27	-4.503	.305	-2.685	-.467	-1.645	-.529	-4.070	-.269	-2.598	-.367	-1.645	-.529
28	-4.936	.462	-3.204	-.600	-1.819	-.647	-4.763	-.423	-3.031	-.533	-1.819	-.647
29	-5.110	.500	-3.377	-.667	-1.905	-.706	-5.110	-.500	-3.291	-.633	-1.905	-.706
30	-5.365	.558	-3.551	-.723	-1.992	-.765	-5.629	-.615	-3.637	-.767	-2.078	.824
31	-5.369	.558	-3.204	-.600	-1.992	-.765	-4.070	-.269	-2.771	-.433	-1.732	.588
32	-5.365	.558	-3.551	-.723	-1.905	-.706	-3.637	-.173	-2.511	-.333	-1.386	.353
33	-5.605	.654	-3.724	-.800	-1.905	-.706	-3.204	-.077	-2.338	-.267	-1.039	-.118
34	-7.001	.942	-4.503	-.1.100	-6.685	-1.235	-3.637	-.173	-2.338	-.267	-0.866	0.000
35	-7.534	.1.029	-4.936	-.1.267	-2.771	-1.294	-4.070	-.269	-2.511	-.333	-1.039	-.118
36	-1.031	.404	-.433	.467	-.433	.294	-1.905	-.212	-1.039	.233	-.606	.176
37	-6.606	.500	-.260	.533	-.087	.529	-1.819	.231	-1.039	.233	-.606	.176
38	-6.606	.500	-.260	.533	-.087	.471	-2.165	.154	-1.299	.153	-.693	.118
39	-6.532	.491	-.433	.467	-.433	.294	-1.905	-.212	-1.039	.233	-.606	.176

Appendix B Table 6 Measured data and computed pressure distribution for $b_1/b_2=0.37$, $g/b_2=2.25$, $T_1=290$ K.

S	D - Shape				Square - Shape							
	26.8427 (m/s)		20.3085 (m/s)		15.3479 (m/s)		26.8427 (m/s)					
	P _s cm.H2O	C _p										
1	-662	.692	.433	.800	.260	.765	-.433	.538	-.173	.567	-.087	.529
2	-662	.692	.433	.800	.260	.765	-.433	.538	-.173	.567	-.087	.529
3	-662	.692	.433	.800	.260	.765	-.433	.538	-.173	.567	-.087	.529
4	-687	.615	.087	.667	.087	.647	-.696	.500	-.433	.467	-.260	.412
5	-7.015	-.923	-4.244	-1.000	-2.511	-1.118	-7.967	-1.135	-4.936	-1.267	-2.771	-1.294
6	-7.361	-.1000	-4.503	-1.180	-2.685	-1.235	-8.400	-1.231	-5.283	-1.400	-2.771	-1.294
7	-7.361	-.1000	-4.763	-1.200	-2.771	-1.294	-7.967	-1.135	-4.936	-1.267	-2.771	-1.294
8	-7.524	-.1038	-4.677	-1.167	-2.771	-1.294	-7.534	-1.038	-4.763	-1.200	-2.511	-1.118
9	-6.542	-.895	-4.244	-1.000	-2.425	-1.059	-6.668	-.846	-4.070	-1.933	-8.165	-.882
10	-6.145	-.731	-3.897	-.867	-2.165	-.884	-5.629	-.615	-3.724	-.800	-1.992	-.765
11	-5.582	-.536	-2.551	-.733	-1.992	-.765	-4.763	-.423	-3.464	-.700	-1.819	-.647
12	-4.526	-.428	-2.377	-.667	-1.905	-.766	-4.936	-.452	-3.291	-.633	-1.732	-.588
13	-4.592	-.395	-2.031	-.533	-1.819	-.647	-4.503	-.365	-3.118	-.567	-1.645	-.529
14	-4.502	-.395	-.656	-.467	-1.645	-.529	-4.503	-.365	-2.944	-.500	-1.645	-.529
15	-4.417	-.346	-.771	-.433	-.553	-.471	-4.330	-.327	-2.858	-.467	-1.559	-.471
16	-4.246	-.309	-.685	-.400	-.472	-.412	-4.157	-.288	-2.771	-.433	-1.472	-.412
17	-4.070	-.269	-.685	-.400	-.472	-.412	-4.157	-.288	-2.771	-.433	-1.472	-.412
18	-4.070	-.269	-.511	-.333	-.472	-.412	-4.070	-.269	-2.685	-.400	-1.472	-.412
19	-2.897	-.231	-.251	-.333	-.472	-.412	-3.984	-.250	-2.685	-.400	-1.472	-.412
20	-3.811	-.212	-.251	-.333	-.472	-.412	-3.897	-.231	-2.511	-.333	-1.386	-.353
21	-3.811	-.212	-.238	-.267	-.299	-.294	-3.724	-.192	-2.425	-.300	-1.386	-.353
22	-3.811	-.212	-.236	-.267	-.299	-.294	-3.984	-.250	-2.511	-.333	-1.386	-.353
23	-3.857	-.231	-.238	-.267	-.299	-.294	-3.984	-.250	-2.598	-.367	-1.386	-.353
24	-2.957	-.231	-.238	-.267	-.299	-.294	-3.984	-.250	-2.598	-.367	-1.472	-.412
25	-3.644	-.231	-.245	-.300	-.472	-.412	-3.984	-.250	-2.685	-.400	-1.472	-.412
26	-4.070	-.269	-.251	-.333	-.472	-.412	-4.070	-.269	-2.771	-.433	-1.472	-.412
27	-4.344	-.308	-.265	-.400	-.559	-.471	-4.417	-.346	-2.944	-.500	-1.559	-.471
28	-4.762	-.433	-.258	-.467	-.645	-.529	-4.936	-.462	-3.291	-.633	-1.732	-.588
29	-5.110	-.570	-.304	-.600	-.819	-.647	-5.196	-.519	-3.551	-.733	-1.905	-.706
30	-5.292	-.538	-.304	-.600	-.819	-.647	-5.369	-.558	-3.637	-.767	-1.905	-.706
31	-5.293	-.538	-.304	-.600	-.819	-.647	-5.196	-.519	-3.551	-.733	-1.992	-.765
32	-6.643	-.855	-.403	-.100	-2.425	-.1059	-6.755	-.865	-4.503	-.1100	-2.338	-.1000
33	-7.785	-.962	-.473	-.200	-2.771	-.294	-7.275	-.981	-5.369	-.1433	-2.511	-.1118
34	-9.967	-.125	-.196	-.1367	-2.858	-.1353	-8.054	-.1154	-5.802	-.1600	-3.031	-.1471
35	-7.567	-.135	-.196	-.1367	-2.858	-.1353	-8.054	-.1154	-5.802	-.1600	-2.771	-.1294
36	-8.07	-.654	-.173	.567	-.173	.471	-.173	.596	-.173	.567	.000	.588
37	-8.07	-.654	-.173	.567	-.173	.471	-.087	.615	-.087	.600	.000	.588
38	-0.57	-.615	-.173	.567	-.087	.529	-.087	.615	-.087	.600	.000	.588
39	-0.57	-.615	-.173	.567	-.087	.529	-.087	.615	-.087	.600	.000	.588

Appendix B Table 7. Measured data and computed pressure distribution for $b_1/b_2=0.25$, $g/b_2=2.25$, $T_1=290$ K.

S	D - Shape				Square - Shape							
	26.8427 (m/s)		20.3085 (m/s)		15.3479 (m/s)		26.8427 (m/s)					
	P _s cm.H2O	C _p										
1	-.775	.808	.606	.867	.260	.765	.520	.750	.260	.733	.173	.706
2	-.775	.806	.606	.867	.260	.765	.520	.750	.260	.733	.173	.706
3	-.775	.808	.606	.867	.260	.765	.520	.750	.260	.733	.173	.706
4	-.601	.729	.660	.733	.087	.647	.433	.731	.173	.700	.087	.647
5	-5.576	-.692	-.070	-.933	-.2165	-.882	-.7101	-.942	-.4070	-.933	-.2338	-.1000
6	-6.725	-.750	-.244	-.1000	-.252	-.941	-.7275	-.981	-.4244	-.1000	-.2485	-.1059
7	-6.321	-.769	-.433	-.033	-.2338	-.1000	-.7361	-.1000	-.4417	-.1067	-.2511	-.1118
8	-6.656	-.846	-.4503	-.1000	-.2338	-.1000	-.7534	-.1038	-.4417	-.1067	-.2511	-.1118
9	-6.656	-.846	-.244	-.1000	-.2352	-.941	-.7101	-.942	-.4070	-.933	-.2338	-.1000
10	-6.263	-.769	-.470	-.933	-.2165	-.882	-.6588	-.882	-.3637	-.767	-.1615	-.882
11	-5.543	-.596	-.274	-.800	-.1992	-.765	-.5716	-.635	-.3777	-.667	-.1905	-.706
12	-6.802	-.654	-.351	-.733	-.1819	-.647	-.5283	-.538	-.3031	-.533	-.1732	-.588
13	-5.265	-.558	-.377	-.667	-.1732	-.588	-.4850	-.448	-.2771	-.433	-.1645	-.529
14	-4.931	-.412	-.318	-.567	-.1645	-.529	-.4677	-.404	-.2685	-.400	-.1559	-.471
15	-4.590	-.305	-.031	-.533	-.1559	-.471	-.4503	-.365	-.2598	-.367	-.1472	-.412
16	-4.507	-.345	-.285	-.467	-.1472	-.412	-.4330	-.327	-.2598	-.367	-.1472	-.412
17	-4.331	-.327	-.271	-.433	-.1472	-.412	-.4244	-.308	-.2598	-.367	-.1472	-.412
18	-4.071	-.209	-.2598	-.367	-.1386	-.353	-.4070	-.269	-.2598	-.367	-.1386	-.353
19	-3.897	-.231	-.511	-.333	-.1386	-.353	-.3984	-.250	-.2598	-.367	-.1386	-.353
20	-3.511	-.212	-.245	-.300	-.1299	-.294	-.3811	-.212	-.2511	-.333	-.1299	-.294
21	-3.724	-.102	-.245	-.300	-.1299	-.294	-.3811	-.212	-.2511	-.333	-.1299	-.294
22	-3.811	-.212	-.511	-.333	-.1299	-.294	-.3897	-.231	-.2685	-.400	-.1299	-.294
23	-3.897	-.231	-.251	-.333	-.1299	-.294	-.3897	-.231	-.2685	-.400	-.1299	-.294
24	-3.954	-.501	-.211	-.333	-.1386	-.353	-.3984	-.250	-.2685	-.400	-.1299	-.294
25	-3.595	-.250	-.611	-.333	-.1386	-.353	-.3984	-.250	-.2771	-.433	-.1386	-.353
26	-4.070	-.209	-.258	-.400	-.1472	-.412	-.4070	-.269	-.2858	-.467	-.1472	-.412
27	-4.417	-.346	-.258	-.467	-.1559	-.471	-.4417	-.346	-.3031	-.533	-.1559	-.471
28	-4.762	-.423	-.304	-.600	-.1645	-.529	-.4936	-.462	-.3377	-.667	-.1645	-.588
29	-5.110	-.500	-.377	-.667	-.1732	-.588	-.5283	-.538	-.3551	-.733	-.1732	-.588
30	-5.282	-.528	-.346	-.700	-.1819	-.647	-.5283	-.538	-.3637	-.767	-.1819	-.647
31	-5.455	-.577	-.237	-.767	-.1905	-.706	-.5369	-.558	-.3897	-.867	-.1985	-.766
32	-7.015	-.973	-.473	-.200	-.2338	-.1000	-.7101	-.942	-.4936	-.1267	-.2425	-.1059
33	-7.534	-.102	-.510	-.333	-.2598	-.1176	-.7521	-.1058	-.5369	-.1433	-.2685	-.1235
34	-.126	-.695	-.543	-.1500	-.2944	-.1412	-.7967	-.1135	-.5369	-.1433	-.2771	-.1294
35	-7.621	-.108	-.569	-.1433	-.2771	-.1294	-.7967	-.1135	-.5369	-.1433	-.2771	-.1294
36	-7.104	-.106	-.667	-.087	-.647	-.087	-.615	-.1615	-.173	.567	-.087	.529
37	-0.57	-.615	-.087	.667	-.087	.647	-.087	.615	-.173	.567	-.087	.529
38	-0.57	-.615	-.087	.667	-.087	.647	-.087	.615	-.173	.567	-.087	.529
39	-0.57	-.615	-.087	.667	-.087	.647	-.087	.615	-.173	.567	-.087	.529

Appendix E Table 10 Measured data and computed pressure distribution for $b_1/b_2=0.625$, $g/b_2=2.0$, $T_1=290$ K

#	D - Shape				Square - Shape			
	26.8427 (m/s)		20.3885 (m/s)		15.3479 (m/s)		26.8427 (m/s)	
	Ps cm H2O	Cp	Ps cm H2O	Cp	Ps cm H2O	Cp	Ps cm H2O	Cp
1	-866	442	-520	.433	-.260	.412	-2.511	.077
2	-953	423	-520	.433	-.260	.412	-2.511	.077
3	-1.126	395	-693	.367	-.346	.353	-2.771	.819
4	-1.472	398	-953	.267	-.520	.235	-3.831	.038
5	-8.054	-1.154	-4.924	-1.267	-2.771	-1.894	-5.976	.692
6	-7.967	-1.135	-4.850	-1.233	-2.685	-1.235	-4.936	.462
7	-6.842	-865	-4.417	-1.067	-2.328	-1.000	-4.503	.365
8	-6.145	-721	-3.724	-0.866	-2.078	-.884	-4.417	.346
9	-5.365	-1.569	-3.291	-0.633	-1.819	-.647	-4.503	.365
10	-5.022	-481	-3.031	-0.533	-1.738	-.588	-4.677	.404
11	-4.763	-423	-2.958	-0.467	-1.645	-.529	-4.936	.462
12	-4.936	-462	-2.031	-0.533	-1.645	-.529	-6.149	.731
13	-7.763	-423	-2.944	-0.500	-1.645	-.529	-6.149	.731
14	-4.936	-462	-2.685	-.400	-1.472	-.412	-5.369	.558
15	-7.763	-423	-2.511	-0.333	-1.386	-.353	-4.677	.404
16	-4.417	-346	-2.425	-.300	-1.386	-.353	-4.157	.288
17	-4.070	-269	-2.338	-0.267	-1.386	-.353	-4.070	.269
18	-3.984	-250	-2.236	-0.267	-1.386	-.353	-3.984	.250
19	-3.984	-250	-2.236	-0.267	-1.386	-.353	-3.984	.250
20	-3.897	-221	-2.330	-0.267	-1.299	-.294	-3.897	.231
21	-3.897	-271	-2.255	-0.233	-1.299	-.294	-3.897	.212
22	-3.724	-192	-2.252	-0.233	-1.299	-.294	-3.811	.212
23	-3.724	-192	-2.330	-0.267	-1.386	-.353	-3.811	.212
24	-3.511	-212	-2.425	-.300	-1.386	-.353	-3.897	.231
25	-3.811	-212	-2.511	-0.333	-1.386	-.353	-3.897	.231
26	-3.697	-231	-2.598	-0.367	-1.472	-.412	-3.984	.250
27	-3.984	-250	-2.685	-0.400	-1.559	-.471	-4.070	.269
28	-4.070	-269	-3.031	-0.533	-1.645	-.529	-4.763	.423
29	-4.244	-308	-3.204	-.600	-1.819	-.647	-5.110	.500
30	-4.763	-423	-3.464	-.700	-1.905	-.706	-5.802	.654
31	-5.622	-481	-2.511	-0.333	-1.472	-.412	-3.464	.135
32	-5.283	-538	-3.031	-0.533	-1.732	-.588	-3.204	.077
33	-4.070	-869	-4.076	-0.933	-2.165	-.882	-3.204	.077
34	-4.936	-422	-4.763	-1.200	-2.598	-1.176	-3.464	.135
35	-6.062	-716	-5.283	-1.400	-2.858	-1.353	-4.070	.269
36	-7.275	-981	-433	-0.467	-.173	.471	-1.905	.212
37	-7.709	-1.07	-433	-0.467	-.173	.471	-1.992	.192
38	-6.606	500	-423	-0.467	-.173	.471	-1.905	.212
39	-5.820	519	-432	-0.467	-.173	.471	-1.039	.404

Appendix E Table 11 Measured data and computed pressure distribution for $b_1/b_2=0.50$, $g/b_2=2.0$, $T_1=290$ K

#	D - Shape				Square - Shape			
	26.8427 (m/s)		20.3885 (m/s)		15.3479 (m/s)		26.8427 (m/s)	
	Ps cm H2O	Cp	Ps cm H2O	Cp	Ps cm H2O	Cp	Ps cm H2O	Cp
1	-6.66	500	-346	.500	-.173	.471	-1.819	.831
2	-6.66	500	-346	.500	-.173	.471	-1.819	.831
3	-7.779	412	-346	.500	-.173	.471	-1.905	.812
4	-1.039	464	-.600	.400	-0.433	.294	-1.992	.192
5	-7.967	-1.135	-5.196	-1.367	-2.771	-1.894	-8.400	-1.231
6	-8.400	-1.221	-5.456	-1.467	-2.858	-1.353	-7.101	.942
7	-7.267	-1.125	-5.023	-1.300	-2.685	-1.235	-5.716	.635
8	-7.534	-1.026	-4.850	-1.233	-2.425	-1.059	-5.369	.558
9	-6.322	-759	-4.157	-0.967	-2.165	-0.882	-5.196	.519
10	-5.603	-654	-3.811	-0.833	-1.905	-.706	-5.110	.500
11	-5.262	-526	-3.551	-0.733	-1.819	-.647	-5.196	.519
12	-5.116	-500	-3.464	-0.700	-1.732	-.588	-5.976	.692
13	-4.926	-466	-3.377	-0.667	-1.645	-.529	-5.802	.654
14	-4.901	-385	-3.204	-0.600	-1.559	-.471	-4.936	.462
15	-4.503	-365	-2.031	-0.533	-1.472	-.412	-4.417	.346
16	-4.417	-346	-2.944	-0.500	-1.472	-.412	-4.244	.308
17	-4.323	-327	-2.658	-0.467	-1.472	-.412	-4.844	.308
18	-4.244	-308	-2.658	-0.467	-1.472	-.412	-4.157	.288
19	-4.157	-226	-2.658	-0.467	-1.472	-.412	-4.157	.288
20	-4.070	-269	-2.771	-0.433	-1.386	-.353	-4.070	.269
21	-4.070	-269	-2.771	-0.433	-1.386	-.353	-3.811	.212
22	-4.070	-259	-2.771	-0.433	-1.386	-.353	-3.964	.250
23	-4.070	-259	-2.771	-0.433	-1.386	-.353	-4.070	.269
24	-4.070	-259	-2.658	-0.467	-1.472	-.412	-4.070	.269
25	-4.070	-219	-2.658	-0.467	-1.472	-.412	-4.070	.269
26	-4.330	-327	-2.944	-0.500	-1.559	-.471	-4.070	.269
27	-4.503	-345	-3.116	-0.567	-1.645	-.529	-4.244	.308
28	-5.023	-451	-3.377	-0.667	-1.819	-.647	-4.763	.483
29	-5.683	-536	-3.464	-0.700	-1.905	-.706	-5.369	.558
30	-5.456	-577	-3.551	-0.733	-1.992	-.765	-4.936	.462
31	-5.345	-578	-3.637	-0.767	-1.992	-.765	-3.637	.173
32	-6.666	-846	-3.897	-.867	-2.338	-1.000	-3.897	.231
33	-7.534	-1.028	-4.503	-1.100	-2.771	-1.294	-4.417	.346
34	-7.794	-1.026	-5.196	-1.367	-2.944	-1.412	-5.110	.500
35	-8.227	-1.192	-5.283	-1.400	-3.031	-1.471	-7.534	-1.028
36	-4.33	538	-173	567	-.173	.471	-1.039	.404
37	-4.23	528	-173	567	-.173	.471	-1.039	.404
38	-4.23	528	-173	567	-.173	.471	-1.039	.404
39	-4.23	526	-173	567	-.173	.471	-1.039	.404

Appendix E Table 12 Measured data and computed pressure distribution for $b_1/b_2=0.37$, $g/b_2=2.0$, $T_1=290$ K

#	D - Shape						Square - Shape						
	26.8427 (m/s)		20.3885 (m/s)		15.3479 (m/s)		26.8427 (m/s)		20.3885 (m/s)		15.3479 (m/s)		
	Ps cm H2O	Cp	Ps cm H2O	Cp	Ps cm H2O	Cp	Ps cm H2O	Cp	Ps cm H2O	Cp	Ps cm H2O	Cp	
1	1.039	.815	.346	.767	.173	.706	-.953	.423	-.606	.400	-.346	.353	
2	1.029	.805	.346	.767	.173	.706	-.953	.423	-.606	.400	-.346	.353	
3	1.029	.805	.346	.767	.173	.706	-.953	.423	-.606	.400	-.346	.353	
4	1.693	.758	.260	.733	-.087	.529	-1.212	.365	-.779	.333	-.433	.254	
5	-6.755	-.865	-.450	-.100	-2.598	-1.176	-8.833	-1.387	-5.196	-1.367	-2.858	-1.353	
6	-7.015	-.923	-.476	-.763	-1.200	-2.605	-1.235	-8.660	-1.288	-4.936	-1.267	-2.685	-1.235
7	-6.845	-.855	-.450	-.850	-1.233	-2.771	-1.294	-7.621	-1.058	-4.417	-1.067	-2.425	-1.059
8	-7.534	-.100	-.450	-.233	-2.605	-1.235	-6.668	-.846	-3.897	-8.867	-8.165	-8.862	
9	-7.361	-.100	-.417	-.107	-2.425	-1.059	-5.802	-.654	-3.377	-6.667	-1.819	-6.47	
10	-7.015	.823	-.070	-.933	-2.252	-.941	-5.369	-.558	-3.204	-.600	-1.732	-5.588	
11	-6.235	.750	.237	.637	-.705	.706	-.519	-.331	-.533	-.1645	-.529		
12	-5.802	.654	.204	.600	-.189	.647	-.519	-.331	-.533	-.1645	-.529		
13	-5.369	.558	.031	.533	-.732	.588	-.4936	-.462	-.2944	-.500	-.1559	-.471	
14	-5.110	.500	.058	.467	-.1645	.529	-.4503	-.365	-.2685	-.490	-.1472	-.412	
15	-4.855	.442	.277	.433	-.1559	.471	-.4320	-.387	-.2598	-.367	-.1366	-.353	
16	-4.677	.404	.265	.400	-.1472	.412	-.4244	-.308	-.2511	-.333	-.1366	-.353	
17	-4.503	.365	.258	.367	-.1472	.412	-.4157	-.288	-.2511	-.333	-.1366	-.353	
18	-4.244	.309	.211	.333	-.1472	.412	-.4157	-.288	-.2425	-.300	-.1366	-.353	
19	-4.070	.249	.151	.333	-.1386	.353	-.3897	-.231	-.2338	-.267	-.1299	-.294	
20	-3.924	.230	.142	.326	-.1386	.353	-.3784	-.192	-.2522	-.233	-.1212	-.235	
21	-3.724	.192	.124	.300	-.1386	.353	-.3784	-.192	-.2522	-.233	-.1212	-.235	
22	-3.070	.269	.124	.300	-.1386	.353	-.3784	-.250	-.2338	-.267	-.1299	-.294	
23	-3.457	.298	.124	.300	-.1386	.353	-.3784	-.269	-.2338	-.267	-.1299	-.294	
24	-3.157	.217	.124	.300	-.1386	.353	-.3784	-.269	-.2338	-.267	-.1299	-.294	
25	-3.037	.226	.124	.300	-.1386	.353	-.3784	-.269	-.2338	-.267	-.1299	-.294	
26	-4.157	.346	.258	.367	-.1472	.412	-.4157	-.288	-.2511	-.333	-.1366	-.353	
27	-4.070	.309	.211	.333	-.1472	.412	-.4157	-.288	-.2511	-.333	-.1366	-.353	
28	-3.924	.230	.151	.333	-.1472	.412	-.4157	-.288	-.2425	-.300	-.1366	-.353	
29	-3.724	.192	.124	.300	-.1472	.412	-.4157	-.288	-.2425	-.300	-.1366	-.353	
30	-3.070	.269	.124	.300	-.1472	.412	-.4157	-.288	-.2338	-.267	-.1299	-.294	
31	-3.457	.298	.124	.300	-.1472	.412	-.4157	-.288	-.2338	-.267	-.1299	-.294	
32	-3.037	.226	.124	.300	-.1472	.412	-.4157	-.288	-.2338	-.267	-.1299	-.294	
33	-2.754	.1036	.476	.1200	-.2771	-.1294	-.4736	-.462	-.3637	-.767	-.1732	-.588	
34	-6.400	.1221	.563	.1400	-.3031	-.1294	-.6149	-.731	-.417	-.1067	-.1905	.706	
35	-8.314	.1218	.5196	.1367	-.2771	-.1294	-.8400	-.231	-.5629	-.1533	-.2685	-.1235	
36	-.087	.615	-.087	.600	-.000	.588	-.520	.519	-.433	.467	-.260	.412	
37	-.087	.615	-.087	.600	-.000	.588	-.520	.519	-.433	.467	-.260	.412	
38	-.097	.615	-.087	.600	-.000	.588	-.520	.519	-.433	.467	-.260	.412	
39	-.087	.615	-.087	.600	-.000	.588	-.520	.519	-.433	.467	-.260	.412	

Appendix E Table 13 Measured data and computed pressure distribution for $b_1/b_2=0.25$, $g/b_2=2.0$, $T_1=290$ K

#	D - Shape						Square - Shape					
	26.8427 (m/s)		20.3885 (m/s)		15.3479 (m/s)		26.8427 (m/s)		20.3885 (m/s)		15.3479 (m/s)	
	Ps cm H2O	Cp	Ps cm H2O	Cp	Ps cm H2O	Cp	Ps cm H2O	Cp	Ps cm H2O	Cp	Ps cm H2O	Cp
1	.953	.846	.520	.833	.260	.765	.260	.692	.173	.700	.000	.588
2	.952	.846	.520	.833	.260	.765	.260	.692	.173	.700	.000	.588
3	.953	.846	.520	.833	.260	.765	.260	.692	.173	.700	.000	.588
4	.606	.769	.067	.667	.087	.647	.260	.692	.173	.700	.000	.588
5	-6.235	-.750	-.4070	-.933	-2.252	-.941	-7.534	-.1038	-.4417	-.1067	-2.511	-.1118
6	-6.495	.808	-.157	.967	-.238	-.1000	-7.881	-.1115	-.4590	-.1133	-2.598	-.1176
7	-6.382	.769	.430	.033	-.238	-.1000	-7.967	-.1135	-.4763	-.1200	-2.685	-.1235
8	-7.015	.553	-.417	-.1067	-.238	-.1000	-7.881	-.1115	-.4590	-.1133	-2.598	-.1176
9	-6.845	.825	-.4244	-.000	-.2525	-.941	-7.101	-.942	-.4244	-.1000	-2.338	-.1000
10	-6.665	.846	-.4070	-.933	-.2165	-.882	-6.495	-.808	-.3897	-.867	-.2165	-.882
11	-6.062	.712	.272	.800	-.1992	.765	-5.629	-.615	-.3464	-.700	-.1905	-.706
12	-5.976	.692	.3551	.733	-.1819	.647	-5.283	-.538	-.3377	-.667	-.1732	-.588
13	-5.543	.596	.3204	.600	-.1732	.588	-4.850	-.442	-.3031	-.533	-.1732	-.588
14	-5.282	.538	.204	.600	-.1645	.529	-4.590	-.385	-.2771	-.433	-.1645	-.529
15	-4.936	.462	.2031	.533	-.1559	.471	-4.417	-.346	-.2685	-.400	-.1472	-.412
16	-4.850	.442	.2944	.500	-.1472	.412	-4.330	-.327	-.2685	-.400	-.1472	-.412
17	-4.503	.305	.2944	.500	-.1472	.412	-4.244	-.308	-.2685	-.400	-.1472	-.412
18	-4.244	.308	.2855	.467	-.1386	.352	-4.157	-.288	-.2598	-.367	-.1472	-.412
19	-4.070	.269	.2771	.433	-.1386	.353	-4.070	-.269	-.2598	-.367	-.1472	-.412
20	-3.984	.250	.2845	.400	-.1299	.294	-3.897	-.231	-.2425	-.300	-.1299	-.294
21	-3.811	.212	.2511	.333	-.1299	.294	-3.784	-.192	-.2528	-.233	-.1299	-.294
22	-4.157	.858	.2771	.433	-.1386	.353	-3.984	-.250	-.2598	-.367	-.1386	-.353
23	-4.244	.306	.2771	.433	-.1386	.353	-3.984	-.250	-.2598	-.367	-.1386	-.353
24	-4.244	.306	.2771	.433	-.1386	.353	-3.984	-.250	-.2598	-.367	-.1386	-.353
25	-4.330	.307	.2771	.433	-.1386	.353	-4.070	-.269	-.2598	-.367	-.1386	-.353
26	-4.417	.346	.2944	.500	-.1472	.412	-4.157	-.288	-.2771	-.433	-.1472	-.412
27	-4.677	.414	.204	.600	-.1645	.529	-4.503	-.365	-.3031	-.533	-.1559	-.471
28	-5.110	.500	.2551	.733	-.1732	.588	-5.023	-.481	-.3291	-.633	-.1732	-.588
29	-5.365	.568	.2724	.800	-.1819	.647	-5.196	-.519	-.3464	-.700	-.1819	-.647
30	-5.629	.615	.3111	.833	-.1905	.706	-5.456	-.577	-.3637	-.767	-.1819	-.647
31	-5.802	.654	.4070	.933	-.2252	.941	-5.629	-.615	-.3784	-.800	-.1992	-.765
32	-7.361	-.1000	.5110	.1333	-.2338	-.1000	-7.101	-.942	-.4763	-.1200	-.2338	-.1000
33	-7.534	-.036	.5369	.1433	-.2771	-.1294	-7.534	-.1038	-.5110	-.1333	-.2511	-.1118
34	-7.967	.125	.5802	.1600	-.2685	-.1235	-7.967	-.135	-.5456	-.1467	-.2658	-.1353
35	-8.054	.1154	.5716	.1567	-.2598	-.1176	-8.054	-.154	-.5369	-.1433	-.2771	-.1294
36	.260	.692	.260	.733	-.000	.588	.087	.654	.087	.667	.000	.588
37	.260	.692	.260	.733	-.000	.588	.087	.654	.087	.667	.000	.588
38	.260	.692	.087	.667	-.000	.588	.087	.654	.087	.667	.000	.588
39	.260	.692	.097	.667	-.000	.588	.087	.654	.087	.667	.000	.588

Appendix E Table 14 Measured data and computed pressure distribution for $b_1/b_2=1.0$, $g/b_2=1.75$, $T_1=290$ K.

#	D - Shape						Square - Shape					
	26.8427 (m/s)		20.3885 (m/s)		15.3479 (m/s)		26.8427 (m/s)		20.3885 (m/s)		15.3479 (m/s)	
	Ps cm H2O	Cp	Ps cm H2O	Cp	Ps cm H2O	Cp	Ps cm H2O	Cp	Ps cm H2O	Cp	Ps cm H2O	Cp
1	-2.511	.077	-1.559	.033	-.953	-.059	-4.330	-.387	-2.771	-.433	-1.645	-.529
2	-2.511	.077	-1.559	.033	-.953	-.059	-4.330	-.387	-2.771	-.433	-1.645	-.529
3	-2.771	.019	-1.819	-.067	-1.039	-.110	-4.936	-.462	-3.110	-.567	-1.732	-.588
4	-3.204	-.077	-2.076	-.167	-1.212	-.235	-4.850	-.442	-3.377	-.667	-1.813	-.647
5	-5.629	-.615	-3.204	-.600	-1.905	-.706	-4.503	-.365	-2.685	-.400	-1.472	-.412
6	-4.936	-.462	-2.771	-.433	-1.645	-.529	-3.897	-.231	-2.338	-.267	-1.386	-.353
7	-4.503	-.305	-2.685	-.400	-1.559	-.471	-3.637	-.173	-2.338	-.267	-1.299	-.294
8	-4.230	-.367	-2.511	-.333	-1.472	-.412	-3.551	-.154	-2.165	-.200	-1.212	-.235
9	-4.330	-.367	-2.425	-.300	-1.472	-.412	-3.551	-.154	-2.165	-.200	-1.126	-.176
10	-4.417	-.346	-2.598	-.367	-1.472	-.412	-3.637	-.173	-2.252	-.233	-1.299	-.294
11	-4.503	-.305	-2.685	-.400	-1.559	-.471	-3.724	-.192	-2.338	-.267	-1.299	-.294
12	-5.369	-.568	-3.204	-.600	-1.819	-.647	-4.503	-.365	-2.771	-.433	-1.472	-.412
13	-5.629	-.615	-3.291	-.633	-1.905	-.766	-4.763	-.423	-3.431	-.533	-1.559	-.471
14	-4.936	-.462	-2.031	-.533	-1.732	-.588	-4.503	-.365	-2.658	-.467	-1.559	-.471
15	-4.417	-.346	-2.685	-.400	-1.559	-.471	-4.417	-.346	-2.771	-.433	-1.472	-.412
16	-4.070	-.269	-2.425	-.300	-1.472	-.412	-3.984	-.250	-2.594	-.367	-1.386	-.353
17	-3.297	-.231	-2.338	-.267	-1.386	-.353	-3.724	-.192	-2.338	-.267	-1.386	-.353
18	-3.811	-.212	-2.338	-.267	-1.386	-.353	-3.637	-.173	-2.338	-.267	-1.299	-.294
19	-3.811	-.212	-2.338	-.267	-1.386	-.353	-3.551	-.154	-2.338	-.267	-1.299	-.294
20	-3.637	-.173	-2.252	-.233	-1.299	-.294	-3.464	-.135	-2.252	-.233	-1.212	-.235
21	-3.464	-.135	-2.078	-.167	-1.212	-.235	-3.204	-.077	-2.078	-.167	-1.126	-.176
22	-3.637	-.173	-2.252	-.233	-1.299	-.294	-3.377	-.115	-2.252	-.233	-1.212	-.176
23	-3.637	-.173	-2.252	-.233	-1.299	-.294	-3.464	-.135	-2.252	-.233	-1.212	-.176
24	-3.724	-.192	-2.252	-.233	-1.299	-.294	-3.464	-.135	-2.252	-.233	-1.212	-.235
25	-3.811	-.212	-2.338	-.267	-1.386	-.353	-3.551	-.154	-2.252	-.233	-1.212	-.235
26	-3.897	-.231	-2.425	-.300	-1.386	-.353	-3.637	-.173	-2.338	-.267	-1.299	-.294
27	-4.070	-.269	-2.598	-.367	-1.472	-.412	-3.984	-.250	-2.598	-.367	-1.386	-.353
28	-4.590	-.385	-2.685	-.467	-1.732	-.588	-4.244	-.308	-2.858	-.467	-1.472	-.412
29	-4.850	-.442	-2.031	-.533	-1.732	-.588	-4.070	-.269	-2.771	-.433	-1.472	-.412
30	-5.369	-.558	-3.204	-.600	-1.905	-.706	-4.503	-.365	-2.944	-.500	-1.472	-.412
31	-3.691	-.026	-2.078	-.167	-1.212	-.235	-2.858	-.000	-1.905	-.100	-1.039	-.118
32	-3.464	-.135	-2.165	-.200	-1.299	-.294	-2.685	-.038	-1.819	-.067	-1.039	-.118
33	-3.551	-.154	-2.252	-.233	-1.386	-.353	-2.511	-.077	-1.732	-.033	-1.039	-.118
34	-3.637	-.173	-2.338	-.267	-1.386	-.353	-2.685	-.038	-1.819	-.067	-1.039	-.118
35	-3.984	-.250	-2.598	-.367	-1.472	-.412	-3.204	-.077	-2.165	-.200	-1.039	-.118
36	-2.165	-.154	-1.472	-.067	-1.866	-.000	-4.417	-.346	-2.944	-.500	-1.472	-.412
37	-2.165	-.154	-1.472	-.067	-1.866	-.000	-4.070	-.269	-2.685	-.400	-1.472	-.412
38	-2.165	-.154	-1.472	-.067	-1.866	-.000	-4.070	-.269	-2.685	-.400	-1.472	-.412
39	-2.165	-.154	-1.779	-.333	-1.520	-.235	-2.511	-.077	-1.645	-.000	-1.039	-.000

Appendix E Table 15 Measured data and computed pressure distribution for $b_1/b_2=0.75$, $g/b_2=1.75$, $T_1=290$ K.

#	D - Shape						Square - Shape						
	26.8427 (m/s)		20.3885 (m/s)		15.3479 (m/s)		26.8427 (m/s)		20.3885 (m/s)		15.3479 (m/s)		
	Ps cm H2O	Cp	Ps cm H2O	Cp	Ps cm H2O	Cp	Ps cm H2O	Cp	Ps cm H2O	Cp	Ps cm H2O	Cp	
1	-1.905	.212	-1.212	.167	-.606	.176	-3.291	-.096	-1.992	-.133	-1.126	-.176	
2	-1.905	.212	-1.212	.167	-.693	.118	-3.291	-.096	-1.992	-.133	-1.126	-.176	
3	-2.076	.173	-1.299	.133	-.779	.059	-3.897	-.231	-2.252	-.233	-1.212	-.235	
4	-2.329	.115	-1.366	.100	-.866	.000	-4.503	-.365	-2.598	-.367	-1.478	-.412	
5	-8.400	-.123	-2.583	-.1400	-2.944	-.1412	-4.417	-.346	-2.598	-.367	-1.559	-.471	
6	-6.928	-.904	-1.417	-.1067	-1.067	-.2358	-1.000	-.4070	-.269	-2.425	-.300	-1.386	-.353
7	-5.629	-.615	-3.724	-.600	-2.078	-.824	-4.070	-.269	-2.425	-.300	-1.386	-.353	
8	-6.265	-.558	-2.377	-.667	-1.819	-.647	-4.070	-.269	-2.425	-.300	-1.386	-.353	
9	-6.110	.500	-3.204	-.600	-1.732	-.588	-4.157	-.288	-2.511	-.333	-1.386	-.353	
10	-6.027	.491	-3.204	-.600	-1.732	-.588	-4.330	-.327	-2.511	-.333	-1.472	-.412	
11	-5.110	.500	-3.204	-.600	-1.732	-.588	-4.590	-.385	-2.771	-.433	-1.559	-.471	
12	-5.206	.654	-3.811	-.833	-1.992	-.765	-5.716	-.635	-3.291	-.633	-1.819	-.647	
13	-5.716	.635	-3.724	-.800	-1.992	-.765	-5.889	-.673	-3.464	-.700	-1.905	-.706	
14	-4.036	.462	-3.204	-.600	-1.732	-.588	-5.369	-.558	-3.118	-.567	-1.732	-.588	
15	-4.417	.346	-2.658	-.467	-1.559	-.471	-4.936	-.462	-2.858	-.467	-1.645	-.529	
16	-4.157	.258	-2.685	-.400	-1.472	-.412	-4.070	-.269	-2.425	-.367	-1.472	-.412	
17	-4.157	.258	-2.685	-.400	-1.472	-.412	-3.984	-.250	-2.338	-.267	-1.386	-.353	
18	-4.070	.269	-2.685	-.400	-1.472	-.412	-3.984	-.250	-2.338	-.267	-1.386	-.353	
19	-4.070	.269	-2.685	-.400	-1.472	-.412	-3.897	-.231	-2.252	-.233	-1.299	-.294	
20	-3.924	.250	-2.598	-.367	-1.386	-.353	-3.897	-.231	-2.252	-.233	-1.299	-.294	
21	-3.637	-.173	-2.338	-.267	-1.299	-.294	-3.637	-.173	-2.165	-.200	-1.299	-.294	
22	-3.984	-.250	-2.511	-.333	-1.386	-.353	-3.724	-.192	-2.252	-.233	-1.212	-.235	
23	-3.064	-.250	-2.511	-.333	-1.386	-.353	-3.811	-.212	-2.252	-.233	-1.212	-.235	
24	-3.984	-.250	-2.511	-.333	-1.386	-.353	-3.897	-.231	-2.252	-.233	-1.212	-.235	
25	-4.670	.249	-2.598	-.467	-1.559	-.471	-4.070	-.269	-2.425	-.367	-1.472	-.412	
26	-4.070	.219	-2.685	-.400	-1.472	-.412	-3.897	-.231	-2.252	-.233	-1.299	-.294	
27	-4.230	.327	-2.656	-.467	-1.559	-.471	-4.070	-.269	-2.425	-.367	-1.386	-.353	
28	-4.936	-.462	-3.204	-.600	-1.732	-.588	-4.763	-.423	-3.724	-.433	-1.559	-.471	
29	-5.369	-.558	-3.377	-.667	-1.819	-.647	-5.023	-.481	-3.118	-.167	-1.559	-.471	
30	-5.716	-.625	-3.724	-.800	-1.992	-.765	-5.629	-.615	-3.291	-.633	-1.819	-.647	
31	-3.724	-.192	-2.338	-.267	-1.299	-.294	-3.204	-.077	-1.992	-.133	-1.039	-.118	
32	-3.557	-.221	-2.338	-.267	-1.472	-.412	-2.944	-.019	-1.732	-.033	-1.953	-.059	
33	-4.244	.306	-2.425	-.300	-1.905	-.706	-2.771	-.019	-1.559	-.033	-1.866	-.000	
34	-5.282	-.528	-3.377	-.667	-2.511	-1.118	-2.598	-.058	-1.472	-.067	-1.779	-.059	
35	-7.101	-.942	-.677	-.167	-.433	-.294	-2.511	-.077	-1.472	-.067	-1.779	-.059	
36	-1.212	-.345	-.779	-.333	-.433	-.294	-2.685	-.038	-1.472	-.067	-1.779	-.059	
37	-1.212	-.345	-.779	-.333	-.433	-.294	-2.858	-.000	-1.472	-.067	-1.779	-.059	
38	-1.212	-.345	-.779	-.333	-.433	-.294	-2.771	-.019	-1.472	-.067	-1.779	-.059	
39	-1.212	-.345	-.779	-.333	-.433	-.294	-2.511	-.077	-1.472	-.067	-1.779	-.059	

Appendix E Table 16 Measured data and computed pressure distribution for $b_1/b_2=0.625$, $g/b_2=1.75$, $T_1=290$ K.

S	D - Shape				Square - Shape			
	26.8427 (m/s)		20.3885 (m/s)		15.3479 (m/s)		26.8427 (m/s)	
	Ps cm.H2O	Cp cm.H2O	Ps cm.H2O	Cp cm.H2O	Ps cm.H2O	Cp cm.H2O	Ps cm.H2O	Cp cm.H2O
1	-1.380	.327	-.666	.300	-.520	.235	-2.944	-.019
2	-1.380	.327	-.666	.300	-.520	.235	-2.944	-.019
3	-1.732	.250	-1.035	.233	-.606	.176	-3.377	-.115
4	-2.070	.173	-1.120	.205	-.779	.059	-3.637	-.173
5	-6.660	-1.248	-5.629	-1.533	-3.204	-1.584	-5.369	-5.556
6	-7.967	-1.135	-4.936	-1.267	-2.944	-1.412	-4.503	-3.855
7	-6.658	-1.846	-4.157	-1.967	-2.511	-1.116	-4.503	-3.365
8	-6.062	.712	-3.637	.767	-2.165	-.882	-4.596	-3.385
9	-5.265	.558	-3.204	.600	-1.905	-.786	-4.850	-4.442
10	-5.190	.519	-3.116	.567	-1.905	-.786	-4.936	-4.462
11	-5.110	.500	-3.116	.567	-1.905	-.786	-6.235	-5.759
12	-5.456	.577	-2.377	.667	-1.992	-.765	-6.235	-5.984
13	-5.283	.526	-2.204	.600	-1.992	-.745	-5.543	-5.596
14	-4.590	.355	-2.771	.433	-1.732	.588	-4.850	-4.442
15	-4.330	.327	-2.598	.367	-1.559	.471	-4.330	-3.327
16	-4.157	.286	-2.511	.333	-1.472	.412	-4.157	-2.888
17	-4.157	.258	-2.425	.300	-1.472	.412	-4.070	-2.669
18	-4.157	.286	-2.425	.300	-1.472	.412	-4.070	-2.771
19	-4.070	.269	-2.425	.300	-1.472	.412	-3.984	-2.550
20	-3.984	.250	-2.336	.267	-1.386	.353	-3.637	-1.173
21	-3.637	.173	-2.252	.233	-1.386	.353	-3.697	-2.311
22	-3.984	.250	-2.336	.267	-1.386	.353	-3.984	-2.550
23	-3.984	.220	-2.338	.267	-1.472	.412	-3.984	-2.425
24	-4.070	.269	-2.338	.267	-1.472	.412	-3.984	-2.550
25	-4.070	.269	-2.338	.267	-1.472	.412	-3.984	-2.511
26	-4.070	.269	-2.425	.300	-1.472	.412	-4.070	-2.669
27	-4.330	.327	-2.598	.367	-1.559	.471	-4.763	-4.223
28	-4.936	.462	-3.031	.533	-1.819	.647	-5.283	-3.031
29	-5.283	.538	-3.118	.567	-1.905	.706	-5.889	-6.731
30	-5.625	.615	-3.291	.633	-1.992	.765	-3.291	-0.96
31	-4.157	.268	-2.511	.333	-1.559	.471	-3.204	-0.777
32	-4.677	.404	-2.685	.400	-1.732	.588	-3.204	-0.777
33	-5.606	.654	-3.291	.633	-1.905	.706	-3.291	-0.96
34	-7.015	.963	-4.070	.933	-2.511	-1.118	-3.204	-0.777
35	-8.227	-1.142	-4.936	-1.267	-3.031	-1.471	-3.204	-0.777
36	-6.06	.500	-5.20	.433	-2.60	.412	-3.204	-0.777
37	-6.06	.500	-5.20	.433	-2.60	.412	-3.291	-0.956
38	-6.06	.500	-5.20	.433	-2.60	.412	-2.338	-0.115
39	-1.433	.526	-1.73	.567	-1.73	.471	-2.338	-.115

Appendix E Table 17 Measured data and computed pressure distribution for $b_1/b_2=0.50$, $g/b_2=1.75$, $T_1=290$ K.

S	D - Shape				Square - Shape			
	26.8427 (m/s)		20.3885 (m/s)		15.3479 (m/s)		26.8427 (m/s)	
	Ps cm.H2O	Cp cm.H2O	Ps cm.H2O	Cp cm.H2O	Ps cm.H2O	Cp cm.H2O	Ps cm.H2O	Cp cm.H2O
1	-.866	.442	-.520	.433	-.433	.294	-2.338	.115
2	-.866	.442	-.520	.433	-.433	.294	-2.338	.115
3	-1.039	.404	-.606	.400	-.433	.294	-2.771	.019
4	-1.472	.308	-.866	.300	-.520	.235	-2.944	-.019
5	-8.660	-1.288	-5.283	-1.400	-3.031	-1.471	-7.188	-.962
6	-8.833	-1.327	-5.369	-1.433	-3.031	-1.471	-5.543	-.596
7	-7.967	-1.135	-4.763	-1.200	-2.771	-1.294	-4.936	-.462
8	-7.101	-1.942	-4.157	-1.967	-2.338	-1.000	-4.650	-.442
9	-5.976	.692	-3.637	.767	-2.076	-.824	-4.850	-.442
10	-5.542	.596	-3.464	.700	-1.905	.706	-4.936	-.462
11	-5.110	.500	-3.204	.600	-1.819	.647	-5.110	-.500
12	-5.110	.500	-3.204	.600	-1.819	.647	-5.110	-.500
13	-4.936	.462	-3.118	.567	-1.732	.588	-5.802	-.654
14	-4.503	.305	-2.858	.467	-1.645	.529	-5.023	-.481
15	-4.330	.327	-2.771	.433	-1.559	.471	-4.503	-.365
16	-4.244	.308	-2.685	.400	-1.472	.412	-4.157	-.288
17	-4.244	.308	-2.685	.400	-1.472	.412	-4.070	-.269
18	-4.157	.258	-2.685	.400	-1.472	.412	-4.070	-.269
19	-4.070	.269	-2.598	.367	-1.472	.412	-4.070	-.269
20	-3.897	.231	-2.511	.333	-1.386	.353	-4.070	-.269
21	-3.637	.173	-2.338	.287	-1.299	.294	-3.724	-.192
22	-3.984	.270	-2.511	.333	-1.386	.353	-3.897	-.231
23	-3.984	.250	-2.511	.333	-1.386	.353	-3.984	-.250
24	-3.984	.250	-2.596	.367	-1.386	.353	-3.984	-.250
25	-4.070	.269	-2.596	.367	-1.559	.471	-3.984	-.250
26	-4.157	.288	-2.685	.400	-1.732	.588	-4.070	-.269
27	-4.503	.305	-2.858	.467	-1.819	.647	-4.070	-.269
28	-4.936	.462	-3.204	.600	-1.905	.706	-4.677	-.404
29	-5.190	.519	-3.291	.633	-1.645	.529	-5.196	-.519
30	-5.283	.526	-3.377	.667	-1.905	.706	-5.802	-.654
31	-4.503	.305	-3.118	.567	-1.645	.529	-3.377	-.115
32	-5.869	.673	-3.637	.767	-1.992	.765	-3.464	-.135
33	-6.405	.786	-4.230	-1.033	-2.338	-1.000	-3.724	-.192
34	-7.709	-1.077	-5.110	-1.333	-2.771	-1.294	-4.070	-.269
35	-8.400	-1.231	-5.369	-1.433	-2.944	-1.412	-4.936	-.462
36	-6.600	.500	-4.33	.467	-1.173	.471	-1.472	.308
37	-6.600	.500	-4.33	.467	-1.173	.471	-1.645	.269
38	-6.600	.500	-4.33	.467	-1.173	.471	-1.905	.212
39	-1.73	.596	-1.433	.467	-0.887	.529	-1.039	.323

Appendix E Table 10. Measured data and computed pressure distribution for $b_1/b_2=0.37$, $g/b_2=1.75$, $T_1=290$ K.

#	D - Shape				Square - Shape			
	26.8427 (m/s)		20.3885 (m/s)		15.3479 (m/s)		26.8427 (m/s)	
	Ps cm H2O	Cp cm H2O	Ps cm H2O	Cp cm H2O	Ps cm H2O	Cp cm H2O	Ps cm H2O	Cp cm H2O
1	775	.868	173	.700	.087	.647	-1.472	.300
2	775	.868	173	.700	.087	.647	-1.472	.300
3	693	.788	.087	.667	.000	.588	-1.645	.269
4	423	.731	-.260	.533	-.173	.471	-1.985	.212
5	-7.101	-.942	-4.417	-1.067	-2.685	-1.235	-9.266	-1.423
6	-7.534	-1.038	-4.677	-1.167	-2.771	-1.294	-8.490	-1.231
7	-7.275	-0.921	-4.763	-1.200	-2.771	-1.294	-6.668	-0.846
8	-7.967	-1.135	-4.503	-1.100	-2.685	-1.235	-6.235	-0.750
9	-7.351	-1.050	-3.897	-1.867	-2.338	-1.000	-5.716	-0.635
10	-7.101	-0.942	-3.555	-1.733	-2.165	-.882	-5.369	-0.558
11	-6.062	-0.712	-3.118	-1.567	-1.905	-.706	-5.369	-0.558
12	-5.826	-0.654	-2.771	-1.433	-1.819	-.647	-5.002	-0.558
13	-5.365	-0.558	-2.685	-1.400	-1.645	-.529	-5.369	-0.558
14	-5.110	-0.500	-2.511	-1.333	-1.559	-.471	-4.763	-0.423
15	-4.650	-0.442	-2.338	-1.267	-1.472	-.412	-4.503	-0.365
16	-4.783	-0.423	-2.338	-1.267	-1.472	-.412	-4.417	-0.346
17	-4.592	-0.395	-2.338	-1.267	-1.472	-.412	-4.330	-0.327
18	-4.417	-0.346	-2.338	-1.267	-1.472	-.412	-4.330	-0.327
19	-4.244	-0.308	-2.338	-1.267	-1.472	-.412	-4.330	-0.327
20	-4.070	-0.265	-2.165	-1.200	-1.386	-.353	-4.070	-0.269
21	-3.911	-0.218	-2.165	-1.200	-1.299	-.294	-3.811	-0.212
22	-4.070	-0.269	-2.165	-1.200	-1.299	-.294	-4.070	-0.269
23	-4.157	-0.258	-2.165	-1.200	-1.386	-.353	-4.070	-0.269
24	-4.157	-0.258	-2.165	-1.200	-1.386	-.353	-4.070	-0.269
25	-4.157	-0.258	-2.165	-1.200	-1.386	-.353	-4.157	-0.288
26	-4.503	-0.365	-2.252	-1.333	-1.386	-.353	-4.244	-0.308
27	-4.590	-0.395	-2.338	-1.467	-1.472	-.412	-4.503	-0.365
28	-5.022	-0.481	-0.598	-0.367	-1.645	-.529	-4.936	-0.462
29	-5.365	-0.588	-2.771	-1.433	-1.732	-.588	-5.543	-0.596
30	-5.456	-0.577	-2.852	-1.467	-1.732	-.588	-5.802	-0.654
31	-5.715	-0.635	-2.944	-1.500	-1.905	-.706	-4.070	-0.269
32	-7.442	-1.013	-3.724	-0.800	-2.165	-.882	-4.503	-0.365
33	-7.524	-1.028	-3.984	-0.900	-2.338	-1.000	-5.369	-0.558
34	-8.141	-1.173	-4.503	-1.100	-2.771	-1.294	-6.842	-0.885
35	-8.314	-1.212	-4.417	-1.067	-2.685	-1.235	-8.400	-1.231
36	-1.173	.596	-.087	.600	.087	.647	-1.039	.404
37	-1.172	.596	-.087	.600	.087	.647	-1.039	.404
38	-1.173	.596	-.087	.600	.087	.647	-1.039	.404
39	-1.172	.596	0.000	.633	.087	.647	-1.039	.404

Appendix E Table 11. Measured data and computed pressure distribution for $b_1/b_2=0.25$, $g/b_2=1.75$, $T_1=290$ K.

#	D - Shape				Square - Shape			
	26.8427 (m/s)		20.3885 (m/s)		15.3479 (m/s)		26.8427 (m/s)	
	Ps cm H2O	Cp cm H2O	Ps cm H2O	Cp cm H2O	Ps cm H2O	Cp cm H2O	Ps cm H2O	Cp cm H2O
1	693	.768	.860	.733	.860	.765	.000	.635
2	692	.768	.260	.733	.260	.765	.000	.635
3	432	.731	.260	.733	.087	.647	.000	.635
4	-0.087	615	-.087	.600	-.087	.529	-.173	.596
5	-6.227	-7.811	-8.833	-2.165	-8.82	-7.794	-1.096	-4.677
6	-6.668	-8.846	-3.897	-0.867	-2.252	-3.41	-8.141	-1.173
7	-6.688	-8.846	-4.070	-0.933	-2.338	-1.000	-7.967	-1.135
8	-7.101	-9.42	-4.157	-0.967	-2.338	-1.000	-7.794	-1.096
9	-6.842	-8.895	-4.070	-0.933	-2.338	-1.000	-7.101	-9.42
10	-6.582	-8.877	-3.897	-0.867	-2.252	-0.941	-6.409	-7.788
11	-5.976	-6.92	-3.724	-0.800	-2.072	-0.824	-5.629	-3.464
12	-5.976	-6.92	-3.551	-0.733	-1.905	-0.706	-5.196	-3.118
13	-5.716	-6.35	-3.464	-0.700	-1.819	-0.647	-4.850	-4.442
14	-5.456	-5.77	-3.204	-0.600	-1.732	-0.568	-4.677	-4.04
15	-5.195	-5.19	-3.118	-0.567	-1.645	-0.529	-4.563	-3.365
16	-4.925	-4.42	-3.031	-0.533	-1.559	-0.471	-4.330	-3.027
17	-4.590	-3.865	-2.771	-0.433	-1.472	-0.412	-4.244	-3.00
18	-4.330	-3.27	-2.598	-0.367	-1.472	-0.412	-4.070	-2.265
19	-4.070	-2.80	-2.425	-0.300	-1.386	-.353	-3.984	-2.250
20	-4.070	-2.80	-2.425	-0.300	-1.299	-.294	-3.897	-2.231
21	-3.997	-2.221	-2.338	-0.267	-1.299	-.294	-3.637	-1.73
22	-4.157	-2.88	-2.511	-0.333	-1.386	-.353	-3.984	-2.250
23	-4.244	-3.02	-2.598	-0.367	-1.386	-.353	-3.984	-2.230
24	-4.244	-3.02	-2.685	-0.400	-1.472	-0.412	-3.984	-2.230
25	-4.244	-3.08	-2.685	-0.400	-1.472	-0.412	-4.070	-2.230
26	-4.417	-2.746	-2.771	-0.433	-1.472	-0.412	-4.157	-2.288
27	-4.677	-1.404	-2.652	-0.467	-1.559	-.471	-4.503	-3.365
28	-4.936	-1.402	-3.031	-0.533	-1.645	-.529	-4.936	-4.462
29	-5.456	-5.77	-3.291	-0.633	-1.619	-.647	-5.283	-5.367
30	-5.629	-6.15	-3.464	-0.700	-1.619	-.647	-5.456	-5.577
31	-6.835	-7.50	-3.637	-0.767	-1.992	-.765	-5.802	-3.654
32	-7.681	-1.058	-4.763	-1.200	-2.511	-1.118	-7.534	-1.038
33	-7.821	-1.115	-5.023	-1.300	-2.685	-1.235	-7.708	-1.077
34	-7.967	-1.125	-5.283	-1.400	-2.658	-1.353	-7.967	-1.135
35	-8.054	-1.154	-5.110	-1.333	-2.771	-1.294	-8.141	-1.173
36	-6.06	500	-433	467	-.087	.529	0.000	.635
37	-345	500	-.087	600	-.087	.529	0.000	.635
38	-345	500	-.087	600	-.087	.529	0.000	.635
39	346	712	260	733	0.087	.647	0.000	.635

Appendix E Table 20 Measured data and computed pressure distribution for $b_1/b_2=1.0$, $g/b_2=1.50$, $T_1=290$ K

#	D - Shape				Square - Shape			
	26.8427 (m/s)		20.3885 (m/s)		26.8427 (m/s)		20.3885 (m/s)	
	Ps cm H2O	Cp	Ps cm H2O	Cp	Ps cm H2O	Cp	Ps cm H2O	Cp
1	-2.771	.019	-1.819	-.067	-1.039	-.118	-5.196	-.519
2	-2.511	.077	-1.619	-.067	-1.039	-.118	-4.936	-.462
3	-2.771	.019	-1.992	-.133	-1.126	-.176	-5.349	-.558
4	-2.944	-.019	-2.165	-.200	-1.212	-.235	-5.802	-.654
5	-5.976	-.692	-3.204	-.600	-1.732	-.508	-4.936	-.462
6	-4.936	.462	-3.771	-.433	-1.472	-.412	-4.330	-.327
7	-4.503	.345	-2.685	-.400	-1.472	-.412	-4.070	-.269
8	-4.503	.365	-2.595	-.367	-1.472	-.412	-3.724	-.192
9	-4.503	.365	-2.598	-.367	-1.472	-.412	-3.637	-.173
10	-4.677	.404	-2.771	-.433	-1.472	-.412	-3.724	-.192
11	-4.850	.442	-2.859	-.467	-1.559	-.471	-3.811	-.212
12	-5.976	.652	-3.551	-.733	-1.819	-.647	-4.503	-.365
13	-6.065	.712	-3.637	-.767	-1.905	-.706	-4.936	-.462
14	-5.365	.558	-3.204	-.600	-1.732	-.588	-4.563	-.365
15	-4.936	.462	-2.944	-.500	-1.645	-.529	-4.417	-.346
16	-4.417	.346	-2.771	-.433	-1.472	-.412	-4.070	-.269
17	-4.157	.298	-2.685	-.400	-1.472	-.412	-3.897	-.231
18	-4.070	.269	-2.598	-.367	-1.472	-.412	-3.724	-.192
19	-4.070	.269	-2.598	-.367	-1.472	-.412	-3.724	-.192
20	-3.984	.250	-2.598	-.367	-1.366	-.353	-3.551	-.154
21	-3.637	.173	-2.336	-.267	-1.299	-.294	-3.264	-.077
22	-3.611	.212	-2.511	-.333	-1.386	-.353	-3.464	-.135
23	-3.611	.212	-2.511	-.333	-1.386	-.353	-3.464	-.135
24	-3.611	.212	-2.598	-.367	-1.386	-.353	-3.464	-.135
25	-3.611	.212	-2.598	-.367	-1.386	-.353	-3.551	-.154
26	-3.897	.231	-2.685	-.400	-1.472	-.412	-3.637	-.173
27	-4.070	.269	-2.858	-.467	-1.559	-.471	-4.070	-.269
28	-4.936	.462	-3.377	-.667	-1.819	-.647	-4.503	-.365
29	-5.365	.558	-3.551	.733	-1.819	-.647	-4.070	-.269
30	-6.149	.731	-2.984	.900	-1.992	.765	-4.477	-.404
31	-3.031	.038	-2.076	-.167	-1.126	-.176	-2.598	.058
32	-3.031	.038	-1.992	-.133	-1.039	-.118	-2.598	.058
33	-2.944	.019	-2.076	-.167	-1.039	-.086	-1.905	-.100
34	-2.338	.115	-2.165	-.200	-1.212	-.235	-2.858	-.000
35	-4.244	.308	-2.252	-.233	-1.212	-.235	-3.551	-.154
36	-1.039	.404	-2.815	-.067	-1.039	-.118	-4.936	-.462
37	-1.645	.269	-2.515	-.067	-1.039	-.118	-4.936	-.462
38	-1.905	.212	-2.515	-.067	-1.039	-.118	-4.936	-.462
39	-1.039	.424	-2.029	-.233	-1.606	-.176	-3.264	-.077

Appendix E Table 21 Measured data and computed pressure distribution for $b_1/b_2=0.75$, $g/b_2=1.50$, $T_1=290$ K.

#	D - Shape				Square - Shape			
	26.8427 (m/s)		20.3885 (m/s)		26.8427 (m/s)		20.3885 (m/s)	
	Ps cm H2O	Cp	Ps cm H2O	Cp	Ps cm H2O	Cp	Ps cm H2O	Cp
1	-2.511	.077	-1.472	.067	-.866	.800	-3.464	-.135
2	-2.511	.077	-1.472	.067	-.866	.000	-3.464	-.135
3	-2.585	.028	-1.645	.000	-.953	-.059	-4.330	-.327
4	-2.585	.040	-1.905	-.100	-1.039	-.118	-4.590	-.385
5	-7.361	-1.000	-4.844	-1.000	-2.338	-1.000	-4.244	-.308
6	-5.007	-.654	-2.377	-.667	-1.819	-.647	-4.070	-.269
7	-4.936	-.462	-2.031	-.533	-1.645	-.529	-4.157	-.288
8	-4.936	-.462	-2.056	-.467	-1.645	-.529	-4.244	-.308
9	-4.850	-.442	-2.771	-.433	-1.559	-.471	-4.417	-.346
10	-4.850	-.442	-2.858	-.467	-1.559	-.471	-4.677	-.404
11	-4.936	-.462	-3.031	-.533	-1.645	-.529	-5.023	-.481
12	-5.976	-.672	-2.464	-.700	-1.905	-.706	-6.328	-.769
13	-5.602	-.654	-2.464	-.700	-1.905	-.706	-6.582	-.827
14	-4.936	-.462	-3.031	-.533	-1.645	-.529	-5.802	-.654
15	-4.417	.346	-2.771	-.433	-1.472	-.412	-5.023	-.481
16	-4.070	.259	-2.425	-.300	-1.386	-.353	-4.590	-.385
17	-4.070	.259	-2.425	-.300	-1.386	-.353	-4.417	-.346
18	-2.984	.250	-2.336	-.267	-1.386	-.353	-4.244	-.308
19	-2.984	.250	-2.336	-.267	-1.386	-.353	-4.070	-.269
20	-3.597	.821	-2.252	-.233	-1.386	-.353	-4.070	-.269
21	-3.551	.154	-2.076	-.167	-1.218	-.235	-3.811	-.212
22	-3.611	.212	-2.252	-.233	-1.299	-.294	-3.984	-.250
23	-3.697	.821	-2.052	-.233	-1.299	-.294	-3.984	-.250
24	-2.697	.231	-2.252	-.233	-1.299	-.294	-3.984	-.250
25	-3.897	.231	-2.339	-.267	-1.299	-.294	-3.984	-.250
26	-3.897	.231	-2.339	-.267	-1.299	-.294	-4.070	-.269
27	-4.070	.269	-2.511	-.333	-1.386	-.353	-4.330	-.327
28	-4.677	.404	-2.858	-.467	-1.559	-.471	-5.196	-.519
29	-5.192	.519	-3.031	-.533	-1.645	-.529	-5.363	-.558
30	-5.602	.654	-3.377	-.667	-1.905	-.706	-6.062	-.712
31	-3.291	.076	-1.619	-.067	-1.126	-.176	-3.031	-.038
32	-3.291	.096	-1.819	-.067	-1.039	-.118	-2.944	-.019
33	-3.691	.096	-1.732	-.033	-1.126	-.176	-2.858	-.000
34	-3.697	.221	-2.339	-.267	-1.212	-.235	-2.598	-.058
35	-4.936	.418	-2.858	-.467	-1.645	-.529	-2.525	-.135
36	-1.472	.308	-2.295	-.133	-.606	.176	-3.204	-.077
37	-1.645	.210	-2.295	-.133	-.606	.176	-3.204	-.077
38	-1.732	.210	-1.126	.200	-.606	.176	-3.204	-.077
39	-1.472	.308	-1.952	.267	-.520	.235	-2.858	-.135

Appendix E Table E2 Measured data and computed pressure distribution for $b_1/b_2=0.625$, $g/b_2=1.50$, $T=290$ K.

#	D - Shape						Square - Shape					
	26.8427 (m/s)		20.3885 (m/s)		15.3479 (m/s)		26.8427 (m/s)		20.3885 (m/s)		15.3479 (m/s)	
	Ps cm H2O	Cp cm H2O	Ps cm H2O	Cp cm H2O	Ps cm H2O	Cp cm H2O	Ps cm H2O	Cp cm H2O	Ps cm H2O	Cp cm H2O	Ps cm H2O	Cp cm H2O
1	-1.905	212	-1.126	200	-606	176	-2.771	.819	-1.985	-.100	-1.039	-.118
2	-1.905	212	-1.126	200	-606	176	-2.771	.819	-1.985	-.100	-1.039	-.118
3	-2.076	173	-1.299	133	-779	.059	-3.291	-.096	-2.078	-.167	-1.126	-.176
4	-2.165	154	-1.472	.067	-.866	.000	-3.464	-.135	-2.165	-.200	-1.126	-.176
5	-8.655	-1.252	-5.110	-1.323	-2.944	-1.412	-4.677	-.464	-8.771	-.433	-1.645	-.529
6	-7.185	-902	-4.070	-933	-2.338	-1.900	-4.157	-.288	-2.598	-.367	-1.386	-.353
7	-5.802	-654	-3.551	-733	-1.992	-1.765	-4.157	-.288	-2.511	-.333	-1.386	-.353
8	-5.365	-558	-3.204	-600	-1.905	-1.706	-4.244	-.308	-2.511	-.333	-1.386	-.353
9	-5.110	-500	-2.944	-500	-1.732	-.588	-4.417	-.346	-2.685	-.400	-1.386	-.353
10	-5.110	-500	-2.944	-500	-1.732	-.588	-4.677	-.464	-2.858	-.467	-1.559	-.471
11	-5.110	-500	-2.944	-500	-1.732	-.588	-4.883	-.481	-3.118	-.567	-1.645	-.529
12	-5.202	-654	-3.377	-667	-1.905	-1.766	-5.499	-.788	-3.897	-.867	-2.978	-.864
13	-5.365	-558	-3.891	-633	-1.905	-1.766	-6.409	-.788	-3.897	-.867	-2.978	-.824
14	-4.677	-404	-2.771	-433	-1.559	-.471	-5.369	-.558	-3.377	-.667	-1.819	-.647
15	-4.244	-308	-2.511	-333	-1.472	-.412	-4.677	-.404	-3.031	-.533	-1.645	-.529
16	-4.070	-269	-2.338	-267	-1.472	-.412	-4.244	-.308	-2.685	-.400	-1.472	-.412
17	-4.070	-269	-2.338	-267	-1.472	-.412	-4.070	-.269	-2.511	-.333	-1.472	-.412
18	-4.070	-269	-2.338	-267	-1.472	-.412	-4.070	-.269	-2.511	-.333	-1.472	-.412
19	-4.070	-269	-2.338	-267	-1.472	-.412	-3.984	-.250	-2.511	-.333	-1.472	-.412
20	-3.897	-231	-2.330	-267	-1.386	-.353	-3.637	-.173	-2.485	-.300	-1.386	-.353
21	-3.637	-173	-2.256	-233	-1.299	-.294	-3.811	-.212	-2.253	-.233	-1.212	-.235
22	-3.897	-221	-2.252	-233	-1.386	-.353	-3.811	-.212	-2.338	-.267	-1.299	-.294
23	-3.897	-231	-2.330	-267	-1.386	-.353	-3.811	-.212	-2.338	-.267	-1.299	-.294
24	-3.897	-231	-2.330	-267	-1.386	-.353	-3.811	-.212	-2.338	-.267	-1.299	-.294
25	-3.897	-231	-2.330	-267	-1.386	-.353	-3.897	-.231	-2.338	-.267	-1.386	-.353
26	-3.984	-256	-2.330	-267	-1.386	-.353	-3.894	-.250	-2.338	-.267	-1.386	-.353
27	-4.070	-269	-2.425	-300	-1.472	-.412	-4.070	-.269	-2.598	-.367	-1.386	-.353
28	-4.763	-423	-2.258	-467	-1.732	-.588	-4.936	-.462	-3.118	-.567	-1.732	-.588
29	-5.110	-500	-3.031	-533	-1.819	-.647	-5.283	-.538	-3.291	-.633	-1.819	-.647
30	-5.716	-376	-3.377	-667	-1.812	-.235	-5.889	-.673	-3.724	-.800	-2.978	-.824
31	-3.464	-135	-1.992	-133	-1.812	-.235	-3.031	-.038	-1.905	-.100	-1.126	-.176
32	-3.637	-173	-2.076	-167	-1.386	-.353	-3.031	-.038	-1.819	-.067	-1.866	-.000
33	-3.897	-221	-2.165	-200	-1.645	-.529	-2.858	-.000	-1.819	-.067	-1.866	-.000
34	-5.023	-461	-2.771	-423	-1.732	-.588	-2.858	-.000	-1.819	-.067	-1.039	-.118
35	-7.101	-942	-4.244	-1.000	-2.338	-1.000	-2.685	-.038	-1.819	-.067	-1.953	-.059
36	-1.212	365	-779	333	-520	.235	-2.598	-.058	-1.645	-.000	-1.866	-.000
37	-1.212	365	-779	333	-520	.235	-2.598	-.058	-1.645	-.000	-1.866	-.000
38	-1.212	365	-779	333	-520	.235	-2.598	-.058	-1.645	-.000	-1.866	-.000
39	-1.035	464	-606	400	-433	.294	-1.645	.269	-1.039	.233	-1.606	.176

Appendix E Table E3 Measured data and computed pressure distribution for $b_1/b_2=0.50$, $g/b_2=1.50$, $T=290$ K.

#	D - Shape						Square - Shape					
	26.8427 (m/s)		20.3885 (m/s)		15.3479 (m/s)		26.8427 (m/s)		20.3885 (m/s)		15.3479 (m/s)	
	Ps cm H2O	Cp cm H2O	Ps cm H2O	Cp cm H2O	Ps cm H2O	Cp cm H2O	Ps cm H2O	Cp cm H2O	Ps cm H2O	Cp cm H2O	Ps cm H2O	Cp cm H2O
1	-1.216	365	-.693	.367	-.433	.294	-2.598	.058	-1.472	.067	-.779	.059
2	-1.216	365	-.692	.367	-.433	.294	-2.598	.058	-1.559	.033	-.779	.059
3	-1.386	367	-.779	333	-.433	.294	-3.031	-.038	-1.645	.000	-.866	.000
4	-1.645	269	-.666	300	-.520	.235	-3.031	-.038	-1.819	-.067	-.953	-.059
5	-8.747	-1.308	-.5369	-1.433	-2.771	-1.294	-7.101	-.942	-4.070	-.333	-2.452	-.941
6	-8.400	-1.231	-.4936	-1.267	-2.598	-1.176	-5.369	-.558	-3.031	-.533	-1.819	-.647
7	-6.926	-904	-.4503	-1.100	-1.118	-.529	-7.101	-.942	-4.070	-.333	-2.452	-.529
8	-6.235	-760	-.3724	-.800	-1.905	-.706	-4.936	-.462	-2.598	-.467	-1.645	-.471
9	-5.626	-615	-.3777	-.667	-1.732	-.588	-4.936	-.462	-2.771	-.433	-1.559	-.471
10	-5.196	-519	-.3204	-.600	-1.645	-.529	-5.110	-.500	-2.858	-.467	-1.645	-.529
11	-5.110	-500	-.2931	-.533	-1.559	-.471	-5.454	-.577	-3.116	-.567	-1.819	-.647
12	-5.196	-519	-.3118	-.567	-1.645	-.529	-6.666	-.846	-3.724	-.600	-2.165	-.882
13	-4.936	-466	-.3031	-.533	-1.559	-.471	-6.495	-.808	-3.784	-.600	-2.165	-.882
14	-4.502	-365	-.2771	-.433	-1.472	-.412	-5.369	-.558	-3.831	-.533	-1.819	-.647
15	-4.244	-308	-.2598	-.367	-1.299	-.294	-4.590	-.385	-2.771	-.433	-1.645	-.529
16	-4.157	-258	-.2511	-.333	-1.299	-.294	-4.330	-.327	-2.511	-.333	-1.472	-.412
17	-4.070	-269	-.2511	-.333	-1.299	-.294	-4.330	-.327	-2.425	-.300	-1.472	-.412
18	-4.070	-269	-.2511	-.333	-1.299	-.294	-4.244	-.308	-2.425	-.300	-1.472	-.412
19	-3.984	-250	-.2511	-.333	-1.299	-.294	-4.244	-.308	-2.425	-.300	-1.472	-.412
20	-3.897	-231	-.2338	-267	-1.299	-.294	-4.070	-.269	-2.425	-.300	-1.472	-.412
21	-3.551	-154	-.2556	-233	-1.212	-.235	-3.897	-.231	-2.252	-.233	-2.978	-.824
22	-3.597	-231	-.2338	-267	-1.299	-.294	-3.984	-.250	-2.338	-.267	-1.386	-.353
23	-3.897	-231	-.2338	-267	-1.299	-.294	-3.984	-.250	-2.338	-.267	-1.386	-.353
24	-3.984	-250	-.2485	-.300	-1.299	-.294	-4.070	-.269	-2.338	-.267	-1.386	-.353
25	-3.894	-250	-.2425	-.300	-1.299	-.294	-4.070	-.269	-2.338	-.267	-1.386	-.353
26	-4.070	-269	-.2511	-.333	-1.299	-.294	-4.070	-.269	-2.338	-.267	-1.386	-.353
27	-4.244	-308	-.2685	-.400	-1.366	-.353	-4.244	-.308	-2.598	-.367	-1.386	-.353
28	-4.336	-462	-.2118	-.567	-1.559	-.471	-4.936	-.462	-2.944	-.560	-1.645	-.529
29	-5.110	-500	-.2921	-.633	-1.645	-.529	-5.456	-.577	-3.291	-.633	-1.905	-.766
30	-5.456	-577	-.2464	-.700	-1.732	-.508	-6.235	-.750	-3.724	-.800	-2.165	-.882
31	-4.070	-269	-.2338	-.667	-1.299	-.294	-3.291	-.096	-1.992	-.133	-1.212	-.235
32	-4.590	-345	-.2771	-.433	-1.366	-.353	-3.291	-.096	-1.992	-.133	-1.212	-.235
33	-5.803	-654	-.2321	-.633	-1.732	-.588	-3.291	-.096	-1.992	-.133	-1.212	-.235
34	-7.361	-1.000	-.4503	-.100	-2.165	-.082	-3.724	-.192	-2.338	-.267	-1.299	-.294
35	-8.400	1.231	-.5369	-.1433	-2.685	-.1235	-4.677	-.404	-2.771	-.433	-1.559	-.471
36	-6.606	500	-.520	-.433	-.173	-.471	-1.905	.212	-1.299	.133	-1.779	.059
37	-6.004	500	-.520	-.433	-.173	-.471	-2.165	.154	-1.299	.133	-1.779	.059
38	-6.93	461	-.520	-.433	-.173	-.471	-2.165	.154	-1.299	.133	-1.779	.059
39	-6.006	500	-.500	-.433	-.167	-.467	.260	.765	-.1472	.308	-.666	.235

Appendix E Table 24 Measured data and computed pressure distribution for $b_1/b_2=0.37$, $g/b_2=1.50$, $T=290$ K

#	D - Shape				Square - Shape			
	26.8427 (m/s)		20.3885 (m/s)		15.3479 (m/s)		26.8427 (m/s)	
	Ps cm H2O	Cp	Ps cm H2O	Cp	Ps cm H2O	Cp	Ps cm H2O	Cp
1	-172	506	-173	.567	-.087	.529	-1.998	.192
2	-172	596	-173	.567	-.087	.529	-1.998	.192
3	-520	519	-660	.533	-.087	.529	-1.998	.192
4	-600	500	-433	.467	-1.173	.471	-2.165	.154
5	-8.314	-1.212	-5.369	-1.433	-2.685	-1.235	-8.928	-1.346
6	-8.400	-1.221	-5.456	-1.467	-2.685	-1.235	-7.181	-.942
7	-7.567	-1.135	-5.110	-1.333	-2.598	-1.176	-5.716	-.625
8	-7.524	-1.038	-4.936	-1.267	-2.425	-1.059	-5.369	-.558
9	-6.666	-846	-5.196	-1.367	-2.165	-.882	-5.283	-.464
10	-5.976	-692	-3.897	-.867	-1.965	-.766	-5.196	-.519
11	-5.369	-552	-3.464	-.760	-1.645	-.529	-3.699	-.690
12	-5.112	-500	-3.291	-.633	-1.559	-.471	-3.862	-.712
13	-4.763	-423	-3.204	-.600	-1.559	-.471	-5.808	-.654
14	-4.502	-305	-7.944	-.500	-1.472	-.412	-4.936	-.462
15	-4.330	-327	-2.771	-.433	-1.472	-.412	-4.563	-.365
16	-4.330	-327	-2.771	-.433	-1.366	-.353	-4.244	-.308
17	-4.244	-308	-2.771	-.433	-1.306	-.353	-4.244	-.308
18	-4.070	-269	-2.771	-.433	-1.386	-.353	-4.244	-.308
19	-3.988	-250	-2.665	-.400	-1.388	-.353	-4.244	-.308
20	-3.897	-231	-2.598	-.367	-1.386	-.353	-4.070	-.269
21	-2.724	-192	-2.252	-2.233	-1.126	-.176	-3.784	-.192
22	-2.984	-250	-2.685	-.400	-1.299	-.294	-3.984	-.250
23	-2.984	-250	-2.685	-.400	-1.299	-.294	-3.984	-.250
24	-2.984	-250	-2.771	-.433	-1.299	-.294	-3.984	-.250
25	-2.984	-250	-2.771	-.433	-1.299	-.294	-3.984	-.250
26	-4.070	-249	-2.858	-.467	-1.386	-.353	-4.244	-.308
27	-4.417	-346	-3.031	-.533	-1.472	-.412	-4.070	-.269
28	-4.536	-462	-3.377	-.667	-1.559	-.471	-4.677	-.404
29	-5.195	-519	-3.637	-.767	-1.645	-.529	-5.369	-.558
30	-5.456	-577	-3.291	-.633	-1.732	-.588	-5.808	-.654
31	-5.456	-577	-4.503	-1.100	-1.819	-.647	-3.637	-.338
32	-6.928	-904	-5.110	-1.333	-1.992	-.765	-3.784	-.192
33	-7.675	-981	-5.802	-1.600	-2.258	-.941	-3.877	-.231
34	-7.967	-1.125	-5.976	-1.667	-2.685	-.1235	-4.936	-.462
35	-8.400	-1.231	-5.976	-1.667	-2.685	-.1235	-7.101	-.942
36	-1.173	596	-1.173	567	-1.173	471	-1.186	385
37	-1.172	596	-1.173	567	-1.173	471	-1.472	308
38	-4.233	578	-1.173	567	-1.173	471	-1.472	308
39	-1.173	596	-1.173	567	-1.173	471	-1.039	404

Appendix E Table 25 Measured data and computed pressure distribution for $b_1/b_2=0.25$, $g/b_2=1.50$, $T=290$ K

#	D - Shape				Square - Shape			
	26.8427 (m/s)		20.3885 (m/s)		15.3479 (m/s)		26.8427 (m/s)	
	Ps cm H2O	Cp	Ps cm H2O	Cp	Ps cm H2O	Cp	Ps cm H2O	Cp
1	.953	846	.433	800	.173	.706	-.580	.519
2	.953	846	.433	800	.173	.706	-.580	.519
3	779	806	260	.733	.260	.765	-.580	.519
4	606	769	.087	.667	.000	.588	-.606	.500
5	-5.802	-654	-3.464	-700	-2.165	-.882	-8.660	-1.288
6	-5.976	-692	-3.551	-733	-2.165	-.882	-9.980	-1.346
7	-5.802	-654	-3.637	-767	-2.338	-.1000	-8.400	-1.231
8	-6.825	-750	-3.724	-800	-3.118	-.159	-7.967	-1.135
9	-6.325	-769	-3.637	-767	-2.258	-.941	-6.842	-.685
10	-2.235	-750	-2.637	-767	-2.252	-.941	-6.235	-.750
11	-5.802	-654	-2.464	-700	-2.076	-.824	-5.543	-.596
12	-5.802	-654	-3.291	-633	-1.992	-.765	-5.369	-.558
13	-5.716	-635	-3.118	-567	-1.905	-.706	-5.023	-.481
14	-5.369	-598	-2.944	-500	-1.819	-.647	-4.850	-.442
15	-5.023	-491	-2.771	-433	-1.732	-.588	-4.590	-.385
16	-4.930	-462	-2.685	-400	-1.732	-.588	-4.503	-.365
17	-4.503	-365	-2.556	-367	-1.645	-.529	-4.417	-.346
18	-4.244	-316	-2.338	-267	-1.472	-.412	-4.244	-.308
19	-4.070	-269	-2.336	-267	-1.472	-.412	-4.157	-.288
20	-4.070	-269	-2.338	-267	-1.386	-.353	-4.070	-.269
21	-3.984	-250	-2.852	-233	-1.386	-.353	-3.811	-.212
22	-4.244	-300	-2.425	-300	-1.472	-.412	-4.070	-.269
23	-4.244	-348	-2.425	-300	-1.472	-.412	-4.070	-.269
24	-4.244	-348	-2.425	-300	-1.472	-.412	-4.070	-.269
25	-4.417	-346	-2.511	-333	-1.472	-.412	-4.157	-.288
26	-4.590	-355	-2.596	-367	-1.553	-.471	-4.330	-.327
27	-4.536	-462	-2.858	-467	-1.645	-.529	-4.590	-.385
28	-5.369	-558	-3.204	-600	-1.819	-.647	-5.110	-.500
29	-5.715	-625	-3.291	-633	-1.992	-.765	-5.456	-.577
30	-5.802	-654	-3.464	-700	-1.992	-.765	-5.629	-.615
31	-6.565	-827	-3.724	-800	-2.165	-.882	-5.543	-.596
32	-7.967	-1.135	-4.590	-1.133	-2.511	-1.116	-6.928	-.904
33	-7.534	-1.038	-4.536	-1.267	-2.771	-1.294	-7.534	-1.038
34	-8.054	-1.154	-5.110	-1.333	-3.118	-1.529	-8.400	-1.231
35	-8.400	-1.231	-5.110	-1.333	-3.031	-1.471	-8.833	-1.327
36	-6.693	758	260	733	.173	.706	-.260	.577
37	-6.693	768	260	733	.173	.706	-.260	.577
38	-6.693	758	260	733	.173	.706	-.260	.577
39	-6.693	759	693	900	.433	.882	-.260	.577

Appendix E Table 26 Measured data and computed pressure distribution for $b_1/b_2=1.0$, $g/b_2=1.25$, $T_1=290$ K.

#	D - Shape								Square - Shape									
	26.8427 (m/s)		20.3885 (m/s)		15.3479 (m/s)		26.8427 (m/s)		20.3885 (m/s)		15.3479 (m/s)		26.8427 (m/s)		20.3885 (m/s)		15.3479 (m/s)	
	Ps cm H2O	Cp	Ps cm H2O	Cp	Ps cm H2O	Cp	Ps cm H2O	Cp	Ps cm H2O	Cp	Ps cm H2O	Cp						
1	-2.771	.019	-1.905	-.100	-1.126	-.176	-5.802	-.654	-3.377	-.667	-1.992	-.745						
2	-2.335	.115	-1.905	-.100	-1.126	-.176	-5.369	-.556	-3.377	-.667	-1.992	-.765						
3	-2.771	.019	-1.905	-.100	-1.126	-.176	-5.802	-.654	-3.551	-.733	-2.078	-.824						
4	-2.855	.060	-1.992	-.133	-1.212	-.235	-5.976	-.692	-3.811	-.833	-2.145	-.882						
5	-5.802	-.654	-3.031	-.533	-1.472	-.412	-5.369	-.556	-3.118	-.567	-1.905	-.766						
6	-4.503	-.365	-1.771	-.433	-1.299	-.294	-4.503	-.365	-2.685	-.400	-1.645	-.529						
7	-4.330	-.327	-1.771	-.433	-1.299	-.294	-4.070	-.269	-2.425	-.300	-1.472	-.412						
8	-4.330	-.327	-1.771	-.433	-1.299	-.294	-3.897	-.231	-2.252	-.233	-1.386	-.353						
9	-4.503	-.365	-7.858	-.467	-1.386	-.353	-3.637	-.173	-2.165	-.200	-1.299	-.294						
10	-4.677	-.404	-2.291	-.633	-1.386	-.353	-3.637	-.173	-2.165	-.200	-1.299	-.294						
11	-4.936	-.402	-1.070	-.933	-1.472	-.412	-3.724	-.192	-2.165	-.200	-1.386	-.353						
12	-6.495	-.808	-1.070	-.933	-1.559	-.471	-4.244	-.306	-2.334	-.267	-1.478	-.412						
13	-6.495	-.810	-1.070	-.933	-1.905	-.766	-4.590	-.385	-2.598	-.367	-1.559	-.471						
14	-5.365	-.558	-2.637	-.767	-1.992	-.766	-4.244	-.306	-2.511	-.333	-1.472	-.412						
15	-4.595	-.385	-2.637	-.767	-1.819	-.647	-4.244	-.306	-2.511	-.333	-1.472	-.412						
16	-4.157	-.288	-2.118	-.567	-1.472	-.412	-4.070	-.269	-2.338	-.267	-1.472	-.412						
17	-4.070	-.219	-2.771	-.433	-1.386	-.353	-3.724	-.192	-2.252	-.233	-1.386	-.353						
18	-3.984	-.250	-2.685	-.400	-1.386	-.353	-3.637	-.173	-2.252	-.233	-1.299	-.294						
19	-3.984	-.250	-2.685	-.400	-1.386	-.353	-3.551	-.154	-2.252	-.233	-1.299	-.294						
20	-3.897	-.231	-2.598	-.367	-1.386	-.353	-3.464	-.135	-2.165	-.200	-1.218	-.235						
21	-3.551	-.154	-2.338	-.267	-1.386	-.353	-3.118	-.095	-1.905	-.100	-1.126	-.176						
22	-3.811	-.212	-2.425	-.300	-1.212	-.235	-3.291	-.096	-1.992	-.133	-1.212	-.235						
23	-3.811	-.212	-2.425	-.300	-1.299	-.294	-3.377	-.115	-1.992	-.133	-1.212	-.235						
24	-3.811	-.212	-2.511	-.333	-1.299	-.294	-3.377	-.115	-2.078	-.167	-1.299	-.294						
25	-3.897	-.231	-2.511	-.333	-1.386	-.353	-3.377	-.115	-2.252	-.233	-1.299	-.294						
26	-3.897	-.231	-2.598	-.367	-1.386	-.353	-3.637	-.173	-2.330	-.267	-1.386	-.353						
27	-4.070	-.219	-2.771	-.433	-1.386	-.353	-3.897	-.231	-2.511	-.333	-1.472	-.412						
28	-4.650	-.442	-2.377	-.667	-1.472	-.412	-4.070	-.269	-2.425	-.300	-1.472	-.412						
29	-5.269	-.568	-2.637	-.767	-1.819	-.647	-4.311	-.212	-2.771	-.433	-1.472	-.412						
30	-6.235	-.750	-4.070	-.933	-1.819	-.647	-4.244	-.306	-1.819	-.067	-1.559	-.471						
31	-2.955	-.000	-.078	-.167	-1.905	-.706	-2.858	-.000	-1.819	-.067	-1.039	-.118						
32	-2.771	-.019	-2.165	-.800	-1.039	-.118	-2.858	-.000	-1.992	-.133	-1.126	-.176						
33	-2.771	-.019	-2.165	-.800	-1.053	-.118	-2.858	-.000	-2.252	-.233	-1.212	-.235						
34	-3.204	-.077	-2.652	-.823	-1.953	-.059	-3.377	-.115	-2.858	-.467	-1.299	-.294						
35	-4.936	-.462	-2.338	-.267	-1.039	-.118	-4.244	-.308	-4.070	-.933	-1.645	-.529						
36	-6.606	-.606	-1.645	-.000	-1.039	-.118	-5.976	-.692	-3.984	-.900	-2.252	-.941						
37	-1.472	-.308	-1.645	-.000	-1.039	-.118	-5.802	-.654	-3.097	-.867	-2.165	-.882						
38	-1.965	-.212	-1.645	-.000	-1.039	-.118	-5.716	-.635	-2.771	-.433	-2.165	-.882						
39	-1.035	-.404	-1.039	-.823	-1.039	-.118	-3.724	-.192	-2.598	-.367	-1.472	-.412						

Appendix E Table 27 Measured data and computed pressure distribution for $b_1/b_2=0.75$, $g/b_2=1.25$, $T_1=290$ K.

#	D - Shape								Square - Shape									
	26.8427 (m/s)		20.3885 (m/s)		15.3479 (m/s)		26.8427 (m/s)		20.3885 (m/s)		15.3479 (m/s)		26.8427 (m/s)		20.3885 (m/s)		15.3479 (m/s)	
	Ps cm H2O	Cp	Ps cm H2O	Cp	Ps cm H2O	Cp	Ps cm H2O	Cp	Ps cm H2O	Cp	Ps cm H2O	Cp						
1	-2.511	.077	-1.645	.000	-.866	.000	-3.637	-.173	-2.334	-.267	-1.212	-.235						
2	-2.511	.077	-1.645	.000	-.866	.000	-3.637	-.173	-2.334	-.267	-1.212	-.235						
3	-2.685	.028	-1.819	-.067	-.953	-.059	-4.417	-.346	-2.685	-.400	-1.299	-.294						
4	-2.771	.019	-1.905	-.100	-1.039	-.118	-4.936	-.442	-2.771	-.433	-1.386	-.353						
5	-7.771	-.942	-4.070	-.933	-2.078	-.824	-3.637	-.173	-2.334	-.267	-1.299	-.294						
6	-5.365	-.558	-2.204	-.600	-1.645	-.529	-3.637	-.173	-2.334	-.267	-1.299	-.294						
7	-4.850	-.448	-3.031	-.533	-1.559	-.471	-3.724	-.192	-2.334	-.267	-1.299	-.294						
8	-4.850	-.442	-3.031	-.533	-1.472	-.412	-3.897	-.231	-2.338	-.267	-1.299	-.294						
9	-4.850	-.442	-3.031	-.533	-1.472	-.412	-4.070	-.269	-2.425	-.300	-1.386	-.353						
10	-5.110	-.500	-2.204	-.600	-1.645	-.529	-4.503	-.365	-2.771	-.433	-1.478	-.412						
11	-5.365	-.558	-3.377	-.667	-1.645	-.529	-4.936	-.462	-2.944	-.500	-1.645	-.529						
12	-6.666	-.846	-4.070	-.933	-2.078	-.824	-4.235	-.570	-3.897	-.867	-1.992	-.765						
13	-6.495	-.808	-3.984	-.908	-2.078	-.824	-4.495	-.600	-3.984	-.900	-2.165	-.882						
14	-5.365	-.558	-3.464	-.701	-1.732	-.568	-5.716	-.635	-3.464	-.700	-1.905	-.706						
15	-4.502	-.365	-2.944	-.500	-1.472	-.412	-4.936	-.626	-3.204	-.600	-1.645	-.529						
16	-4.226	-.367	-2.771	-.433	-1.472	-.412	-4.244	-.308	-2.685	-.400	-1.472	-.412						
17	-4.244	-.368	-2.771	-.433	-1.386	-.353	-4.070	-.269	-2.685	-.400	-1.472	-.412						
18	-4.157	-.288	-2.771	-.433	-1.386	-.353	-4.070	-.269	-2.598	-.367	-1.472	-.412						
19	-4.157	-.288	-2.771	-.433	-1.386	-.353	-4.070	-.269	-2.598	-.367	-1.472	-.412						
20	-4.070	-.269	-2.685	-.400	-1.386	-.353	-3.984	-.250	-2.511	-.333	-1.386	-.353						
21	-3.637	-.173	-2.332	-.267	-1.812	-.235	-3.637	-.173	-2.338	-.267	-1.212	-.235						
22	-3.984	-.250	-2.511	-.333	-1.299	-.294	-3.811	-.212	-2.511	-.333	-1.299	-.294						
23	-3.984	-.250	-2.511	-.333	-1.899	-.294	-3.897	-.231	-2.511	-.333	-1.299	-.294						
24	-3.984	-.250	-2.598	-.367	-1.899	-.294	-3.897	-.231	-2.511	-.333	-1.386	-.353						
25	-3.984	-.250	-2.685	-.400	-1.899	-.353	-3.897	-.231	-2.511	-.333	-1.386	-.353						
26	-3.984																	

Appendix E Table 28 Measured data and computed pressure distribution for $b1/b2=0.625$, $g/b2=1.25$, $T1=290$ K.

D - Shape						Square - Shape											
26.8427 (m/s)			20.3885 (m/s)			15.3479 (m/s)			26.8427 (m/s)			20.3885 (m/s)			15.3479 (m/s)		
#	Ps cm.H2O	Cp	Ps cm.H2O	Cp	Ps cm.H2O	Cp	Ps cm.H2O	Cp	Ps cm.H2O	Cp	Ps cm.H2O	Cp	Ps cm.H2O	Cp			
1	-6.235	115	-1.212	.167	-.779	.059	-2.944	.019	-1.905	-.100	-1.839	-.118					
2	-6.235	115	-1.212	.167	-.866	.000	-2.944	.019	-1.905	-.100	-1.839	-.118					
3	-6.593	058	-1.295	.133	-.953	-.059	-3.377	-.115	-2.878	-.167	-1.126	-.176					
4	-6.771	019	-1.386	.100	-.953	-.059	-3.551	-.154	-2.252	-.233	-1.126	-.176					
5	-7.651	-1.115	-1.397	-.867	-2.771	-1.294	-4.157	-.286	-2.771	-.433	-1.472	-.412					
6	-5.803	654	-3.031	.533	-2.078	-.024	-3.984	-.250	-2.598	-.367	-1.386	-.353					
7	-4.930	-4.462	-2.685	-.400	-1.905	-.706	-4.070	-.269	-2.511	-.333	-1.386	-.353					
8	-4.930	-4.462	-2.511	-.333	-1.819	-.647	-4.070	-.269	-2.598	-.367	-1.472	-.412					
9	-4.930	-4.462	-2.425	-.300	-1.819	-.647	-4.244	-.308	-2.771	-.433	-1.472	-.412					
10	-4.930	-4.462	-2.425	-.300	-1.819	-.647	-4.590	-.305	-2.944	-.500	-1.645	-.529					
11	-5.195	515	-2.598	-.367	-1.905	-.706	-5.023	-.481	-2.338	-.267	-1.019	-.647					
12	-6.145	731	-3.204	-.600	-2.165	-.882	-6.409	-.788	-4.076	-.933	-2.165	-.882					
13	-5.603	654	-3.204	-.600	-2.165	-.882	-6.409	-.788	-4.076	-.933	-2.252	-.941					
14	-4.763	423	-2.511	-.333	-1.819	-.647	-5.369	-.558	-3.637	-.767	-1.905	-.706					
15	-4.157	258	-2.252	-.233	-1.559	-.471	-4.677	-.404	-3.264	-.600	-1.645	-.529					
16	-3.924	-250	-2.165	-.200	-1.472	-.412	-4.070	-.269	-2.771	-.433	-1.472	-.412					
17	-3.924	-250	-2.165	-.200	-1.472	-.412	-4.070	-.269	-2.771	-.433	-1.472	-.412					
18	-3.924	-250	-2.165	-.200	-1.472	-.412	-3.984	-.250	-2.685	-.400	-1.386	-.353					
19	-3.594	-250	-2.165	-.200	-1.472	-.412	-3.984	-.250	-2.598	-.367	-1.386	-.353					
20	-3.811	-212	-2.078	-.167	-1.472	-.412	-3.897	-.231	-2.511	-.333	-1.299	-.294					
21	-3.551	-154	-1.905	-.100	-1.299	-.294	-3.551	-.154	-2.338	-.267	-1.299	-.294					
22	-3.724	152	-2.078	-.167	-1.472	-.412	-3.811	-.212	-2.425	-.300	-1.299	-.294					
23	-3.724	152	-2.078	-.167	-1.472	-.412	-3.811	-.212	-2.425	-.300	-1.299	-.294					
24	-3.611	-212	-2.078	-.167	-1.472	-.412	-3.897	-.231	-2.511	-.333	-1.299	-.294					
25	-3.857	-231	-2.165	-.200	-1.472	-.412	-3.897	-.231	-2.598	-.367	-1.299	-.294					
26	-2.897	-231	-2.165	-.200	-1.472	-.412	-3.884	-.250	-2.685	-.400	-1.386	-.353					
27	-3.564	-250	-2.252	-.233	-1.472	-.412	-4.070	-.269	-3.204	-.600	-1.386	-.353					
28	-4.503	365	-2.252	-.233	-1.732	-.588	-4.850	-.442	-3.464	-.790	-1.645	-.529					
29	-4.536	462	-2.511	-.333	-1.819	-.647	-5.369	-.558	-3.697	-.867	-1.819	-.647					
30	-5.625	615	-2.771	-.433	-1.992	-.765	-6.062	-.712	-2.078	-.167	-1.998	-.765					
31	-3.291	567	-3.118	-.567	-2.165	-.882	-3.118	-.056	-1.992	-.133	-2.078	-.024					
32	-3.377	115	-1.905	-.100	-2.165	-.882	-2.944	-.019	-1.992	-.133	-1.039	-.118					
33	-3.627	-173	-2.944	-.500	-1.386	-.353	-2.944	-.019	-1.992	-.133	-1.953	-.059					
34	-4.070	269	-2.338	-.267	-1.472	-.412	-2.944	-.019	-1.905	-.100	-1.953	-.059					
35	-5.805	654	-3.204	-.600	-1.905	-.706	-2.858	-.000	-1.905	-.100	-1.953	-.059					
36	-1.905	212	-1.039	.233	-.693	-.118	-2.771	-.019	-1.905	-.100	-1.953	-.059					
37	-1.905	212	-1.039	.233	-.693	-.118	-2.858	-.000	-1.905	-.100	-1.953	-.059					
38	-1.905	212	-1.039	.233	-.693	-.118	-2.858	-.000	-1.905	-.100	-1.953	-.059					
39	-1.472	308	-775	.333	-.693	-.118	-1.905	-.212	-1.299	-.133	-1.606	-.176					

Appendix E Table 29 Measured data and computed pressure distribution for $b1/b2=0.50$, $g/b2=1.25$, $T1=290$ K.

D - Shape						Square - Shape											
26.8427 (m/s)			20.3885 (m/s)			15.3479 (m/s)			26.8427 (m/s)			20.3885 (m/s)			15.3479 (m/s)		
#	Ps cm.H2O	Cp	Ps cm.H2O	Cp	Ps cm.H2O	Cp	Ps cm.H2O	Cp	Ps cm.H2O	Cp	Ps cm.H2O	Cp	Ps cm.H2O	Cp			
1	-6.245	229	-1.039	.233	-.606	.176	-2.511	.077	-1.472	.067	-1.866	.000					
2	-1.645	.859	-1.039	.233	-.606	.176	-2.598	.058	-1.645	.000	-1.866	.000					
3	-1.732	250	-1.186	.200	-.606	.176	-2.944	-.019	-1.819	-.067	-1.953	-.059					
4	-1.819	221	-1.126	.200	-.693	.118	-2.944	-.019	-1.819	-.067	-1.939	-.118					
5	-9.352	-1.422	-6.666	-1.700	-2.858	-.1353	-5.976	-.692	-3.637	-.767	-1.905	-.706					
6	-7.167	-1.125	-4.936	-1.267	-2.333	-.1000	-4.763	-.423	-2.944	-.500	-1.472	-.412					
7	-6.409	-7.8	-1.070	-.933	-1.992	-.765	-4.677	-.404	-2.771	-.433	-1.472	-.412					
8	-5.802	564	-3.677	-.767	-1.732	-.588	-4.590	-.385	-2.771	-.433	-1.472	-.412					
9	-5.365	558	-2.377	-.667	-1.645	-.529	-4.763	-.423	-2.858	-.467	-1.472	-.412					
10	-4.282	528	-3.291	-.633	-1.645	-.529	-4.936	-.462	-2.944	-.500	-1.559	-.471					
11	-3.365	558	-3.377	-.667	-1.645	-.529	-5.369	-.558	-3.291	-.633	-1.645	-.529					
12	-5.976	692	-3.627	-.767	-1.819	-.647	-6.668	-.846	-3.984	-.900	-1.992	-.765					
13	-5.547	596	-3.551	-.733	-1.819	-.647	-6.235	-.750	-3.984	-.900	-1.992	-.765					
14	-4.763	423	-2.856	-.467	-1.472	-.412	-5.196	-.519	-3.204	-.600	-1.645	-.529					
15	-4.117	346	-2.771	-.433	-1.386	-.353	-4.417	-.346	-2.771	-.433	-1.472	-.412					
16	-4.330	327	-2.685	-.400	-1.386	-.353	-4.244	-.308	-2.598	-.367	-1.386	-.353					
17	-4.244	308	-2.771	-.433	-1.386	-.353	-4.157	-.289	-2.598	-.367	-1.386	-.353					
18	-4.157	258	-2.771	-.433	-1.386	-.353	-4.157	-.289	-2.511	-.333	-1.386	-.353					
19	-4.157	258	-2.771	-.433	-1.386	-.353	-4.157	-.289	-2.511	-.333	-1.299	-.294					
20	-4.070	269	-2.685	-.400	-1.386	-.353	-4.070	-.269	-2.338	-.267	-1.299	-.294					
21	-3.627	-173	-2.338	-.267	-1.818	-.235	-3.811	-.212	-2.338	-.267	-1.299	-.294					
22	-3.984	250	-2.685	-.400	-1.386	-.353	-3.897	-.231	-2.425	-.300	-1.299	-.294					
23	-3.984	250	-2.685	-.400	-1.386	-.353	-3.897	-.231	-2.425	-.300	-1.299	-.294					
24	-4.070	259	-2.595	-.367	-1.818	-.235	-3.777	-.115	-2.078	-.167	-1.126	-.176					
25	-4.070	259	-2.595	-.367	-1.818	-.235	-3.777	-.115	-2.078	-.167	-1.126	-.176					
26	-4.070	269	-2.656	-.467	-1.386	-.353	-3.984	-.250	-2.425	-.300	-1.299	-.294					
27	-4.330	327	-2.944	-.500	-1.386	-.353	-4.070	-.269	-2.511	-.333	-1.386	-.353					
28	-4.936	-422	-3.377	-.667	-1.645	-.529	-4.763	-.423	-2.944	-.500	-1.472	-.412					
29	-5.368	558	-2.637	-.767	-1.732	-.588	-5.369	-.558	-3.204	-.600	-1.645	-.529					
30	-5.802	654	-4.070	-.933	-1.819	-.647	-6.149	-.731	-3.637	-.767	-1.905	-.706					
31	-4.070	269	-2.595	-.367	-1.818	-.235	-3.777	-.115	-2.078	-.167	-1.126	-.176					
32	-4.563	345															

Appendix E Table 30 Measured data and computed pressure distribution for $b_1/b_2=0.37$, $g/b_2=1.25$, $T_1=290$ K.

#	D - Shape				Square - Shape							
	26.8427 (m/s)		20.3885 (m/s)		15.3479 (m/s)		26.8427 (m/s)		20.3885 (m/s)		15.3479 (m/s)	
	Ps cm.H2O	Cp	Ps cm.H2O	Cp	Ps cm.H2O	Cp	Ps cm.H2O	Cp	Ps cm.H2O	Cp	Ps cm.H2O	Cp
1	-.866	.442	-.606	.400	-.260	.412	-.252	.135	-.1366	.100	-.693	.118
2	-.866	.442	-.606	.400	-.260	.412	-.238	.115	-.1472	.067	-.779	.059
3	-.952	.423	-.605	.400	-.260	.412	-.2685	.038	-.1472	.067	-.866	.000
4	-.1.039	.404	-.606	.400	-.346	.353	-.2685	.038	-.1.559	.033	-.953	.059
5	-.926	-.1.423	-.5.369	-.1.433	-.2.771	-.1.294	-.2.574	-.1.269	-.5.110	-.1.333	-.2.771	-.1.254
6	-.820	-.1.346	-.5.196	-.1.367	-.2.771	-.1.294	-.2.235	-.750	-.3.637	-.767	-.1.905	-.706
7	-.7.706	-.1.077	-.4.596	-.1.133	-.2.425	-.1.059	-.5.283	-.5.283	-.3.204	-.600	-.1.645	-.529
8	-.6.665	-.846	-.4.070	-.9.933	-.2.076	-.824	-.5.196	-.5.19	-.3.118	-.567	-.1.559	-.471
9	-.5.869	-.673	-.2.464	-.7.700	-.1.819	-.647	-.5.110	-.5.00	-.3.031	-.533	-.1.559	-.471
10	-.5.365	-.556	-.2.204	-.6.000	-.1.732	-.588	-.5.196	-.5.19	-.3.031	-.533	-.1.559	-.471
11	-.5.196	-.519	-.2.031	-.5.533	-.1.645	-.529	-.5.196	-.5.19	-.3.031	-.533	-.1.559	-.471
12	-.5.263	-.538	-.2.031	-.5.533	-.1.645	-.529	-.2.235	-.750	-.3.204	-.600	-.1.645	-.529
13	-.4.936	-.462	-.2.944	-.5.500	-.1.559	-.471	-.5.976	-.6.92	-.3.351	-.733	-.1.819	-.647
14	-.4.503	-.365	-.2.598	-.3.67	-.1.472	-.418	-.4.850	-.4.442	-.2.771	-.433	-.1.472	-.412
15	-.4.244	-.306	-.2.511	-.3.333	-.1.386	-.353	-.4.330	-.3.287	-.2.598	-.367	-.1.386	-.353
16	-.4.244	-.306	-.2.425	-.3.000	-.1.386	-.353	-.4.244	-.3.208	-.2.511	-.333	-.1.299	-.294
17	-.4.244	-.306	-.2.425	-.3.000	-.1.386	-.353	-.4.157	-.2.288	-.2.511	-.333	-.1.299	-.294
18	-.4.152	-.258	-.2.338	-.2.867	-.1.386	-.353	-.4.157	-.2.288	-.2.511	-.333	-.1.299	-.294
19	-.4.070	-.269	-.2.326	-.2.867	-.1.299	-.294	-.4.157	-.2.288	-.2.511	-.333	-.1.299	-.294
20	-.3.984	-.250	-.2.252	-.2.833	-.1.299	-.294	-.4.070	-.2.269	-.2.338	-.267	-.1.299	-.294
21	-.3.637	-.173	-.2.252	-.2.833	-.1.212	-.235	-.3.637	-.1.173	-.2.252	-.233	-.1.212	-.235
22	-.3.984	-.250	-.2.252	-.2.833	-.1.299	-.294	-.3.984	-.2.250	-.2.338	-.267	-.1.299	-.294
23	-.4.070	-.269	-.2.252	-.2.833	-.1.299	-.294	-.3.984	-.2.250	-.2.338	-.267	-.1.299	-.294
24	-.4.070	-.269	-.2.338	-.2.867	-.1.299	-.294	-.3.984	-.2.250	-.2.338	-.267	-.1.299	-.294
25	-.4.070	-.269	-.2.338	-.2.867	-.1.299	-.294	-.3.984	-.2.250	-.2.338	-.267	-.1.299	-.294
26	-.4.157	-.258	-.2.338	-.2.867	-.1.299	-.294	-.3.984	-.2.250	-.2.338	-.267	-.1.299	-.294
27	-.4.17	-.246	-.2.511	-.3.333	-.1.386	-.353	-.4.070	-.2.269	-.2.511	-.333	-.1.386	-.353
28	-.4.935	-.462	-.2.771	-.4.433	-.1.645	-.529	-.4.590	-.3.385	-.2.858	-.467	-.1.472	-.412
29	-.5.369	-.506	-.2.031	-.5.533	-.1.645	-.529	-.5.196	-.5.19	-.3.204	-.600	-.1.645	-.529
30	-.5.543	-.596	-.2.118	-.5.567	-.1.732	-.588	-.5.802	-.6.654	-.3.637	-.767	-.1.905	-.706
31	-.4.230	-.462	-.2.685	-.4.400	-.1.645	-.529	-.3.637	-.1.733	-.2.338	-.267	-.1.472	-.412
32	-.5.976	-.652	-.2.118	-.5.567	-.1.819	-.647	-.3.724	-.1.92	-.2.425	-.300	-.1.472	-.412
33	-.6.668	-.846	-.4.590	-.1.133	-.1.992	-.765	-.3.697	-.2.31	-.2.511	-.333	-.1.472	-.412
34	-.7.967	-.1.135	-.5.369	-.1.433	-.2.511	-.1.118	-.4.590	-.3.365	-.2.858	-.467	-.1.472	-.412
35	-.8.832	-.1.327	-.5.802	-.1.600	-.2.658	-.1.353	-.6.668	-.8.846	-.4.070	-.933	-.2.338	-.1.000
36	-.6.693	-.461	-.520	-.433	-.260	-.412	-.1.905	-.2.12	-.1.212	-.167	-.606	-.176
37	-.6.693	-.461	-.520	-.433	-.260	-.412	-.1.905	-.2.12	-.1.212	-.167	-.606	-.176
38	-.6.693	-.461	-.520	-.433	-.260	-.412	-.1.905	-.2.12	-.1.212	-.167	-.606	-.176
39	-.520	-.519	-.433	-.467	-.1.73	-.471	-.1.299	-.346	-.1.039	-.233	-.520	-.235

Appendix E Table 31 Measured data and computed pressure distribution for $b_1/b_2=0.25$, $g/b_2=1.25$, $T_1=290$ K.

#	D - Shape				Square - Shape							
	26.8427 (m/s)		20.3885 (m/s)		15.3479 (m/s)		26.8427 (m/s)		20.3885 (m/s)		15.3479 (m/s)	
	Ps cm.H2O	Cp	Ps cm.H2O	Cp	Ps cm.H2O	Cp	Ps cm.H2O	Cp	Ps cm.H2O	Cp	Ps cm.H2O	Cp
1	-.866	.827	-.346	.767	.087	.647	-.1.478	.308	-.866	.300	-.520	.235
2	-.866	.827	-.346	.767	.087	.647	-.1.478	.308	-.866	.300	-.520	.235
3	-.866	.827	-.346	.767	.000	.633	-.1.73	.471	-.1.732	.250	-.1.039	.260
4	-.606	.769	-.000	.633	-.173	.471	-.1.732	.250	-.1.519	-.5.802	-.1.600	-.3.377
5	-.6.665	-.846	-.4.070	-.9.933	-.2.511	-.1.118	-.9.699	-.1.519	-.5.802	-.1.600	-.2.598	-.1.176
6	-.7.015	-.923	-.4.330	-.1.033	-.8.598	-.1.176	-.8.833	-.1.327	-.5.283	-.1.400	-.3.031	-.1.471
7	-.6.755	-.845	-.5.03	-.1.100	-.2.771	-.1.294	-.7.101	-.9.492	-.4.593	-.1.100	-.2.598	-.1.176
8	-.7.361	-.1.000	-.4.590	-.1.133	-.2.598	-.1.176	-.6.668	-.8.46	-.3.897	-.8.667	-.2.652	-.941
9	-.7.361	-.1.000	-.4.17	-.1.067	-.2.338	-.1.000	-.5.802	-.6.554	-.3.551	-.7.33	-.1.905	-.706
10	-.7.101	-.942	-.4.244	-.1.000	-.2.852	-.941	-.5.369	-.5.558	-.3.291	-.6.33	-.1.905	-.706
11	-.6.409	-.768	-.3.697	-.847	-.2.165	-.882	-.5.283	-.5.38	-.3.294	-.6.00	-.1.819	-.647
12	-.6.409	-.768	-.3.637	-.767	-.1.905	.706	-.5.196	-.5.19	-.3.294	-.6.00	-.1.819	-.647
13	-.6.062	-.712	-.3.377	-.667	-.1.819	.647	-.4.936	-.4.66	-.3.118	-.567	-.1.732	-.588
14	-.5.802	-.654	-.3.204	-.600	-.1.732	.588	-.4.503	-.3.365	-.2.771	-.433	-.1.645	-.529
15	-.5.369	-.506	-.3.118	-.567	-.1.645	.529	-.4.244	-.3.306	-.2.605	-.400	-.1.472	-.412
16	-.5.110	-.500	-.3.031	-.533	-.1.559	.471	-.4.157	-.2.288	-.2.598	-.367	-.1.472	-.412
17	-.4.850	-.442	-.2.858	-.467	-.1.472	.412	-.4.157	-.2.288	-.2.598	-.367	-.1.472	-.412
18	-.4.330	-.327	-.2.598	-.367	-.1.472	.412	-.4.070	-.2.269	-.2.598	-.367	-.1.472	-.412
19	-.4.244	-.308	-.2.511	-.333	-.1.386	.353	-.3.997	-.2.231	-.2.338	-.267	-.1.386	-.353
20	-.4.070	-.249	-.2.425	-.360	-.1.299	.294	-.3.637	-.1.173	-.2.338	-.267	-.1.299	-.294
21	-.4.070	-.249	-.2.425	-.360	-.1.299	.294	-.3.637	-.1.173	-.2.338	-.267	-.1.299	-.294
22	-.4.330	-.327	-.2.605	-.400	-.1.386	.353	-.3.984	-.2.250	-.2.425	-.300	-.1.386	-.353
23	-.4.417	-.346	-.2.665	-.400	-.1.386	.353	-.3.984	-.2.250	-.2.425	-.300	-.1.386	-.353
24	-.4.417	-.346	-.2.685	-.400	-.1.386	.353	-.3.984	-.2.250	-.2.511	-.333	-.1.386	-.353
25	-.4.677	-.404	-.2.771	-.433	-.1.472	.412	-.4.367	-.2.288	-.2.598	-.367	-.1.472	-.412
26	-.4.450	-.442	-.2.858	-.467	-.1.472	.412	-.4.070	-.2.269	-.2.598	-.367	-.1.472	-.412
27	-.4.450	-.442	-.2.858	-.467	-.1.472	.412	-.4.070	-.2.269	-.2.598	-.367	-.1.472	-.412
28	-.4.936	-.462	-.3.031	-.533	-.1.559	.471	-.4.157	-.2.288	-.2.685	-.400	-.1.472	-.412
29	-.5.362	-.558	-.3.291	-.633	-.1.732	.588	-.4.850	-.4.442	-.2.944	-.500	-.1.645	-.529
30	-.5.002	-.654	-.3.551	-.733	-.1.819	.647	-.5.196	-.5.19	-.3.204	-.600	-.1.819	-.647
31	-.6.235	-.750	-.3.897	-.867	-.1.905	.706	-.5.543	-.5.596	-.3.377	-.667	-.1.905	-.706
32	-.7.101	-.942	-.4.157	-.967	-.2.165	.882	-.4.936	-.4.250	-.2.771	-.433	-.1.905	-.706
33	-.8.833	-.1.327	-.5.369	-.1.433	-.2.771	-.1.294	-.5.369	-.5.358	-.3.464	-.766	-.1.902	-.765
34	-.8.574	-.1.269	-.5.456	-.1.467	-.2.658	-.1.353	-.6.235	-.7.534	-.4.007	-.1.365	-.5.629	-.1.235
35	-.8.574	-.1.269	-.5.467	-.1.400	-.2.771	-.1.294	-.6.007	-.7.534	-.4.007	-.1.365	-.5.629	-.1.235
36	-.8.574	-.1.269	-.5.456	-.1.467	-.2.658	-.1.353	-.6.007	-.7.534	-.4.007	-.1.365	-.5.629	-.1.235
37	-.7.779	-.808	-.433	-.800	-.1.73	.706	-.6.006	-.5.600	-.2.600	-.433	-.1.73	-.471
38	-.7.779	-.808</td										

Appendix B Table 32 Measured data and computed pressure distribution for $b1/b2=1.0$, $g/b2=1.0$, $T=290$ K.

0	D - Shape				Square - Shape			
	26.8427 (m/s)		20.3885 (m/s)		26.8427 (m/s)		20.3885 (m/s)	
	Ps cm.H2O	Cp	Ps cm.H2O	Cp	Ps cm.H2O	Cp	Ps cm.H2O	Cp
1	-2.338	.115	-1.992	-.133	-1.386	-.353	-6.409	-.788
2	-2.165	.154	-1.819	-.067	-1.126	-.176	-6.062	-.712
3	-1.992	.198	-1.819	-.067	-1.126	-.176	-6.149	-.731
4	-1.645	.269	-1.819	-.067	-1.212	-.235	-6.149	-.731
5	-1.101	.942	-3.118	-.567	-1.386	-.353	-6.062	-.712
6	-5.365	.568	-2.511	-.333	-1.386	-.353	-5.456	-.577
7	-4.590	.385	-2.511	-.333	-1.386	-.353	-4.936	-.462
8	-4.502	.365	-2.598	-.367	-1.386	-.353	-4.503	-.365
9	-4.677	.404	-2.777	-.433	-1.472	-.412	-4.970	-.269
10	-5.110	.500	-2.037	-.537	-1.645	-.529	-3.897	-.231
11	-5.625	.615	-3.377	-.667	-1.819	-.647	-3.897	-.231
12	-7.101	.942	-4.244	-.1000	-2.165	-.082	-4.157	-.288
13	-7.101	.942	-4.244	-.1000	-2.165	-.082	-4.330	-.327
14	-5.802	.654	-3.464	-.700	-1.905	-.706	-4.157	-.288
15	-4.936	.462	-2.858	-.467	-1.645	-.529	-4.070	-.269
16	-4.503	.365	-2.685	-.400	-1.472	-.412	-3.897	-.231
17	-4.417	.346	-2.598	-.367	-1.472	-.412	-3.631	-.173
18	-4.330	.327	-2.598	-.367	-1.472	-.412	-3.551	-.154
19	-4.244	.308	-2.598	-.367	-1.472	-.412	-3.551	-.154
20	-4.157	.288	-2.511	-.333	-1.386	-.353	-3.464	-.135
21	-3.897	.231	-2.338	-.267	-1.299	-.294	-3.204	-.077
22	-4.070	.265	-2.425	-.300	-1.386	-.353	-3.291	-.096
23	-4.070	.265	-2.511	-.333	-1.386	-.353	-3.291	-.096
24	-4.157	.288	-2.511	-.333	-1.386	-.353	-3.291	-.096
25	-4.244	.308	-2.511	-.333	-1.386	-.353	-3.377	-.115
26	-4.590	.365	-2.598	-.367	-1.386	-.353	-3.637	-.173
27	-5.369	.558	-2.771	-.433	-1.559	-.471	-3.897	-.231
28	-5.802	.654	-3.291	-.633	-1.619	-.647	-4.070	-.269
29	-6.668	.846	-3.551	-.733	-1.905	-.796	-3.984	-.250
30	-3.204	.077	-4.070	-.933	-2.165	-.882	-4.070	-.269
31	-3.204	.077	-1.905	-.100	-1.039	-.118	-2.204	-.077
32	-3.204	.077	-1.905	-.100	-1.039	-.118	-2.204	-.077
33	-4.244	.308	-1.905	-.100	-1.039	-.118	-3.551	-.154
34	-5.802	.654	-1.905	-.100	-1.039	-.118	-3.984	-.250
35	-5.802	.654	-2.338	-.267	-1.039	-.118	-4.936	-.462
36	-6.606	.500	-1.039	.233	-.866	.000	-6.668	-.846
37	-1.299	.346	-1.299	.133	-.866	.000	-6.235	-.750
38	-1.472	.308	-1.472	.067	-.866	.000	-6.235	-.750
39	-1.905	.212	-1.559	.033	-.953	-.059	-6.235	-.750

Appendix B Table 33 Measured data and computed pressure distribution for $b1/b2=0.75$, $g/b2=1.0$, $T=290$ K.

0	D - Shape				Square - Shape			
	26.8427 (m/s)		20.3885 (m/s)		26.8427 (m/s)		20.3885 (m/s)	
	Ps cm.H2O	Cp	Ps cm.H2O	Cp	Ps cm.H2O	Cp	Ps cm.H2O	Cp
1	-2.338	.115	-1.645	.000	-1.039	-.118	-4.503	-.365
2	-2.338	.115	-1.645	.000	-1.039	-.118	-4.244	-.308
3	-2.338	.115	-1.645	.000	-1.039	-.118	-4.936	-.462
4	-2.165	.154	-1.645	.000	-1.039	-.118	-5.369	-.550
5	-7.967	.135	-4.244	-.1000	-2.338	-.1000	-4.070	-.269
6	-6.235	.750	-3.204	-.600	-1.732	-.588	-4.070	-.269
7	-5.369	.558	-2.944	-.500	-1.645	-.529	-4.157	-.288
8	-4.936	.462	-2.858	-.467	-1.559	-.471	-4.244	-.308
9	-4.936	.462	-2.858	-.467	-1.559	-.471	-4.503	-.345
10	-5.283	.528	-3.204	-.600	-1.645	-.529	-4.850	-.442
11	-5.802	.654	-3.551	-.733	-1.819	-.647	-5.369	-.558
12	-7.101	.942	-4.244	-.1000	-2.165	-.882	-6.495	-.808
13	-6.668	.846	-4.070	-.933	-2.165	-.882	-6.495	-.808
14	-5.369	.500	-3.204	-.600	-1.645	-.529	-5.369	-.558
15	-4.503	.365	-2.771	-.433	-1.472	-.412	-4.763	-.423
16	-4.330	.327	-2.598	-.367	-1.386	-.353	-4.417	-.346
17	-4.244	.308	-2.511	-.333	-1.386	-.353	-4.244	-.308
18	-4.244	.308	-2.511	-.333	-1.386	-.353	-4.070	-.269
19	-4.244	.308	-2.511	-.333	-1.386	-.353	-4.070	-.269
20	-4.070	.269	-2.338	-.267	-1.299	-.294	-3.984	-.250
21	-3.811	.212	-2.852	-.233	-1.212	-.235	-3.784	-.192
22	-3.984	.250	-3.338	-.267	-1.299	-.294	-3.811	-.212
23	-4.070	.269	-3.336	-.267	-1.299	-.294	-3.811	-.212
24	-4.070	.269	-3.336	-.267	-1.299	-.294	-3.811	-.212
25	-4.070	.269	-3.336	-.267	-1.299	-.294	-3.784	-.192
26	-4.070	.269	-3.336	-.267	-1.299	-.294	-3.984	-.250
27	-4.417	.346	-2.598	-.367	-1.299	-.294	-3.984	-.250
28	-4.936	.462	-3.031	-.533	-1.559	-.471	-4.503	-.365
29	-5.629	.615	-3.377	-.667	-1.732	-.588	-4.936	-.462
30	-6.235	.750	-3.811	-.833	-1.992	-.765	-5.543	-.596
31	-3.204	.077	-1.905	-.100	-1.039	-.118	-2.605	-.038
32	-3.637	.173	-1.905	-.100	-1.039	-.118	-2.338	-.115
33	-4.503	.365	-2.165	-.200	-1.039	-.118	-2.338	-.067
34	-5.802	.654	-2.771	-.433	-1.299	-.294	-2.511	-.077
35	-7.101	.942	-3.637	-.767	-1.732	-.588	-4.858	-.467
36	-1.173	.596	-1.039	.233	-.606	.176	-2.425	-.300
37	-1.039	.404	-1.039	.233	-.606	.176	-2.425	-.300
38	-1.472	.308	-1.039	.233	-.606	.176	-2.425	-.300
39	-1.732	.250	-1.039	.233	-.606	.176	-2.425	-.300

Appendix B Table 34 Measured data and computed pressure distribution for $b_1/b_2=0.625$, $g/b_2=1.0$, $T=290$ K.

S	D - Shape								Square - Shape								26.8427 (m/s)			
	26.8427 (m/s)				20.3885 (m/s)				15.3479 (m/s)				26.8427 (m/s)				20.3885 (m/s)			
	Ps cm.H2O	Cp cm.H2O	Ps cm.H2O	Cp cm.H2O	Ps cm.H2O	Cp cm.H2O	Ps cm.H2O	Cp cm.H2O	Ps cm.H2O	Cp cm.H2O	Ps cm.H2O	Cp cm.H2O	Ps cm.H2O	Cp cm.H2O	Ps cm.H2O	Cp cm.H2O	Ps cm.H2O	Cp cm.H2O	Ps cm.H2O	Cp cm.H2O
1	-2.595	.058	-1.559	.033	-1.953	-.059	-3.291	-.056	-2.978	-.167	-1.812	-.235								
2	-2.595	.058	-1.645	.000	-1.953	-.059	-3.291	-.056	-2.978	-.167	-1.895	-.294								
3	-2.771	.019	-1.732	-.033	-1.039	-.116	-4.070	-.269	-2.338	-.267	-1.386	-.353								
4	-2.771	.019	-1.819	-.067	-1.039	-.116	-4.070	-.269	-2.338	-.267	-1.386	-.353								
5	-5.976	-1.192	-4.503	-1.100	-2.511	-1.118	-4.244	-.398	-2.338	-.300	-1.476	-.412								
6	-5.976	-6.02	-3.377	-.667	-1.819	-.647	-4.330	-.327	-2.598	-.367	-1.476	-.412								
7	-5.110	-5.00	-3.031	-.533	-1.732	-.508	-4.417	-.346	-2.598	-.367	-1.476	-.412								
8	-5.110	-5.00	-2.944	-.500	-1.645	-.529	-4.503	-.365	-2.685	-.486	-1.476	-.412								
9	-5.110	-5.00	-2.944	-.500	-1.645	-.529	-4.763	-.423	-2.771	-.433	-1.559	-.471								
10	-5.369	-.558	-.031	-.533	-1.645	-.529	-5.110	-.500	-3.031	-.533	-1.732	-.588								
11	-5.808	-.654	-3.291	-.633	-1.732	-.568	-5.629	-.615	-3.264	-.686	-1.905	-.706								
12	-6.668	-.846	-3.984	-.900	-1.992	-.765	-6.928	-.904	-4.070	-.933	-2.338	-1.000								
13	-6.625	-.750	-3.811	-.833	-1.992	-.765	-6.842	-.885	-4.070	-.933	-2.338	-1.000								
14	-5.110	-.500	-2.944	-.500	-1.645	-.529	-5.629	-.615	-3.264	-.686	-1.905	-.706								
15	-4.503	-.365	-2.771	-.433	-1.472	-.412	-4.763	-.423	-2.771	-.433	-1.645	-.529								
16	-4.330	-.327	-2.598	-.367	-1.386	-.353	-4.417	-.346	-2.511	-.333	-1.559	-.471								
17	-4.244	-.308	-2.511	-.333	-1.386	-.353	-4.330	-.327	-2.511	-.333	-1.472	-.412								
18	-4.244	-.308	-2.511	-.333	-1.386	-.353	-4.244	-.308	-2.511	-.333	-1.472	-.412								
19	-4.244	-.308	-2.511	-.333	-1.386	-.353	-4.157	-.288	-2.511	-.333	-1.472	-.412								
20	-4.070	-.269	-2.425	-.300	-1.899	-.294	-4.070	-.269	-2.338	-.267	-1.386	-.353								
21	-3.724	-.192	-2.338	-.267	-1.299	-.294	-3.724	-.192	-2.252	-.233	-1.386	-.353								
22	-3.984	-.250	-2.338	-.267	-1.299	-.294	-3.897	-.231	-2.252	-.233	-1.386	-.353								
23	-3.984	-.250	-2.338	-.267	-1.299	-.294	-3.897	-.231	-2.252	-.233	-1.386	-.353								
24	-4.070	-.269	-2.338	-.267	-1.299	-.294	-3.897	-.231	-2.252	-.233	-1.386	-.353								
25	-4.070	-.269	-2.338	-.267	-1.299	-.294	-3.984	-.250	-2.338	-.267	-1.386	-.353								
26	-4.070	-.269	-2.338	-.267	-1.299	-.294	-3.984	-.250	-2.338	-.267	-1.386	-.353								
27	-4.157	-.266	-2.511	-.333	-1.386	-.353	-4.070	-.266	-2.425	-.300	-1.472	-.412								
28	-4.157	-.266	-2.511	-.333	-1.386	-.353	-4.157	-.266	-2.425	-.300	-1.472	-.412								
29	-5.369	-.588	-3.204	-.600	-1.645	-.529	-5.369	-.558	-3.204	-.600	-1.905	-.706								
30	-6.149	-.731	-3.637	-.767	-1.905	-.706	-6.235	-.750	-3.724	-.806	-2.165	-.882								
31	-3.377	-.115	-2.076	-.167	-1.039	-.118	-3.118	-.058	-1.905	-.100	-1.039	-.118								
32	-3.637	-.173	-2.165	-.200	-1.039	-.118	-3.118	-.058	-1.819	-.067	-1.039	-.118								
33	-3.984	-.250	-2.252	-.233	-1.039	-.118	-3.031	-.038	-1.732	-.033	-1.953	-.059								
34	-4.936	-.422	-2.771	-.433	-1.472	-.412	-3.118	-.058	-1.905	-.100	-1.039	-.118								
35	-6.842	-.895	-3.897	-.867	-1.905	-.706	-3.118	-.058	-1.732	-.033	-1.039	-.118								
36	-6.605	-.605	-3.291	-.400	-1.606	-.176	-3.204	-.077	-1.905	-.100	-1.039	-.118								
37	-1.472	-.308	-1.299	-.133	-.606	-.176	-3.031	-.038	-1.905	-.100	-1.039	-.118								
38	-1.472	-.312	-1.299	-.133	-.606	-.176	-2.771	.019	-1.645	.000	-1.953	-.059								
39	-1.472	-.312	-1.299	-.133	-.606	-.176	-2.338	.115	-1.472	.067	-1.779	-.059								

Appendix B Table 35 Measured data and computed pressure distribution for $b_1/b_2=0.50$, $g/b_2=1.0$, $T=290$ K.

S	D - Shape								Square - Shape								26.8427 (m/s)			
	26.8427 (m/s)				20.3885 (m/s)				15.3479 (m/s)				26.8427 (m/s)				20.3885 (m/s)			
	Ps cm.H2O	Cp cm.H2O	Ps cm.H2O	Cp cm.H2O	Ps cm.H2O	Cp cm.H2O	Ps cm.H2O	Cp cm.H2O	Ps cm.H2O	Cp cm.H2O	Ps cm.H2O	Cp cm.H2O	Ps cm.H2O	Cp cm.H2O	Ps cm.H2O	Cp cm.H2O	Ps cm.H2O	Cp cm.H2O	Ps cm.H2O	Cp cm.H2O
1	-2.165	.154	-1.472	.067	-1.866	.000	-2.944	-.019	-1.732	-.033	-1.039	-.118								
2	-2.252	.135	-1.472	.067	-.866	.000	-2.944	-.019	-1.965	-.100	-1.126	-.176								
3	-2.336	.115	-1.472	.067	-.866	.000	-3.551	-.154	-1.992	-.133	-1.126	-.176								
4	-2.338	.115	-1.472	.067	-.866	.000	-3.551	-.154	-2.078	-.167	-1.126	-.176								
5	-9.266	-.143	-.862	-.160	-3.118	-.152	-6.409	-.766	-3.097	-.867	-2.165	-.882								
6	-7.101	-.942	-4.244	-.100	-2.338	-.100	-5.110	-.560	-3.264	-.600	-1.732	-.588								
7	-5.718	-.635	-3.637	-.767	-1.905	-.706	-4.936	-.462	-3.118	-.567	-1.645	-.529								
8	-5.369	-.558	-3.377	-.667	-1.819	-.647	-4.936	-.462	-3.031	-.533	-1.645	-.529								
9	-5.196	-.519	-3.204	-.600	-1.732	-.588	-5.023	-.481	-3.118	-.567	-1.645	-.529								
10	-5.196	-.519	-3.277	-.667	-1.732	-.588	-5.196	-.519	-3.204	-.600	-1.732	-.588								
11	-5.543	-.596	-3.551	-.733	-1.619	-.647	-5.716	-.635	-3.551	-.733	-1.905	-.766								
12	-6.235	-.750	-3.984	-.900	-2.078	-.824	-6.755	-.665	-4.070	-.933	-2.165	-.882								
13	-6.602	-.654	-3.697	-.667	-1.905	-.535	-6.695	-.566	-3.264	-.600	-1.732	-.588								
14	-4.590	-.385	-3.118	-.567	-1.645	-.529	-5.110	-.500	-3.264	-.600	-1.732	-.588								
15	-4.244	-.308	-2.771	-.433	-1.472	-.412	-4.503	-.365	-2.771	-.433	-1.472	-.412								
16	-4.157	-.266	-2.771	-.433	-1.472	-.412	-4.244	-.308	-2.685	-.400	-1.386	-.353								
17	-4.157	-.266	-2.771	-.433	-1.472	-.412	-4.244	-.308	-2.685	-.400	-1.386	-.353								
18	-4.157	-.266	-2.771	-.433	-1.472	-.412	-4.244	-.308	-2.685	-.400	-1.386	-.353								
19	-4.157	-.266	-2.771	-.433	-1.472	-.412	-4.244	-.308	-2.685	-.400	-1.386	-.353				</				

Appendix B Table 36 Measured data and computed pressure distribution
for $b_1/b_2=0.37$, $g/b_2=1.0$, $T_1=290$ K.

S	D - Shape						Square - Shape					
	26.8427 (m/s)		20.3885 (m/s)		15.3479 (m/s)		26.8427 (m/s)		20.3885 (m/s)		15.3479 (m/s)	
	Ps cm. H2O	Cp	Ps cm. H2O	Cp	Ps cm. H2O	Cp	Ps cm. H2O	Cp	Ps cm. H2O	Cp	Ps cm. H2O	Cp
1	-1.645	.269	-1.039	.233	-.666	.176	-2.336	.115	-1.472	.067	-.866	.060
2	-1.732	.250	-1.039	.233	-.666	.176	-2.511	.077	-1.732	-.033	-.866	.060
3	-1.732	.250	-1.039	.233	-.666	.176	-2.771	.019	-1.732	-.033	-.953	-.059
4	-1.732	.250	-1.039	.233	-.666	.176	-2.771	.019	-1.732	-.033	-.953	-.059
5	-9.613	-1.500	-2.235	-1.767	-3.464	-1.765	-8.633	-1.327	-5.369	-1.433	-2.858	-1.353
6	-8.929	-1.346	-5.369	-1.423	-2.944	-1.412	-6.235	-1.750	-3.811	-1.833	-2.678	-1.353
7	-7.446	-0.19	-4.503	-1.100	-2.338	-1.000	-5.363	-1.558	-3.464	-1.700	-1.819	-1.647
8	-6.665	-1.846	-4.070	-1.933	-2.078	-1.824	-5.196	-1.519	-3.264	-1.600	-1.732	-1.588
9	-5.802	-1.654	-3.637	-1.767	-1.905	-1.706	-5.110	-1.500	-3.118	-1.567	-1.645	-1.529
10	-5.543	-5.56	-3.551	-1.733	-1.905	-1.706	-5.196	-1.519	-3.204	-1.600	-1.732	-1.588
11	-5.665	-615	-3.551	-1.733	-1.905	-1.706	-5.543	-1.596	-3.464	-1.700	-1.819	-1.647
12	-5.802	-654	-3.637	-1.767	-1.992	-1.765	-6.322	-1.769	-3.811	-1.833	-2.078	-1.824
13	-5.365	-578	-2.551	-1.733	-1.905	-1.706	-5.802	-1.654	-3.637	-1.767	-1.905	-1.706
14	-4.850	-442	-3.118	-1.567	-1.645	-1.529	-4.677	-1.404	-2.058	-1.467	-1.559	-1.471
15	-4.503	-365	-2.858	-1.467	-1.559	-1.471	-4.244	-1.308	-2.485	-1.400	-1.472	-1.412
16	-4.503	-365	-2.858	-1.467	-1.559	-1.471	-4.157	-1.288	-2.598	-1.367	-1.472	-1.412
17	-4.417	-346	-2.858	-1.467	-1.559	-1.471	-4.157	-1.288	-2.598	-1.367	-1.472	-1.412
18	-4.417	-346	-2.858	-1.467	-1.559	-1.471	-4.157	-1.288	-2.598	-1.367	-1.472	-1.412
19	-4.417	-346	-2.858	-1.467	-1.559	-1.471	-4.157	-1.288	-2.598	-1.367	-1.472	-1.412
20	-4.157	-238	-2.685	-1.400	-1.478	-1.412	-4.070	-1.269	-2.511	-1.333	-1.386	-1.353
21	-3.811	-212	-2.511	-1.333	-1.386	-1.353	-3.637	-1.213	-2.338	-1.267	-1.299	-1.294
22	-4.070	-269	-2.485	-1.400	-1.472	-1.412	-3.984	-1.250	-2.425	-1.300	-1.366	-1.353
23	-4.070	-269	-2.771	-1.433	-1.472	-1.412	-3.984	-1.250	-2.425	-1.300	-1.366	-1.353
24	-4.157	-288	-2.771	-1.433	-1.472	-1.412	-3.984	-1.250	-2.511	-1.333	-1.386	-1.353
25	-4.244	-368	-2.771	-1.433	-1.472	-1.412	-3.984	-1.250	-2.511	-1.333	-1.386	-1.353
26	-4.330	-387	-2.771	-1.433	-1.472	-1.412	-3.984	-1.250	-2.511	-1.333	-1.386	-1.353
27	-5.503	-365	-2.944	-1.500	-1.559	-1.471	-4.070	-1.269	-2.511	-1.333	-1.386	-1.353
28	-5.110	-500	-3.377	-1.667	-1.732	-1.598	-4.503	-1.365	-2.944	-1.500	-1.559	-1.471
29	-5.542	-596	-3.637	-1.767	-1.905	-1.706	-5.110	-1.500	-3.291	-1.633	-1.732	-1.588
30	-5.802	-654	-3.811	-1.833	-2.078	-1.824	-5.802	-1.654	-3.811	-1.833	-1.905	-1.706
31	-4.070	-269	-2.685	-1.400	-1.472	-1.412	-3.291	-1.096	-2.165	-1.200	-1.186	-1.176
32	-5.369	-556	-3.204	-1.600	-1.472	-1.412	-3.551	-1.154	-2.252	-1.233	-1.126	-1.176
33	-6.062	-712	-4.157	-1.967	-1.905	-1.706	-3.811	-1.212	-2.511	-1.333	-1.212	-1.235
34	-7.534	-1.038	-5.110	-1.333	-2.425	-1.059	-4.590	-1.385	-3.118	-1.567	-1.472	-1.412
35	-9.266	-1483	-6145	-1.733	-3.031	-1.471	-6.842	-1.865	-4.677	-1.167	-2.252	-1.941
36	-1.606	.510	-.606	.400	-.520	.235	.308	-.1039	.233	-.606	.176	
37	-1.035	404	-.606	.400	-.520	.235	-.1905	.212	-.1386	.100	-.606	.176
38	-1.299	346	-.953	.267	-.580	.235	-.1905	.212	-.1386	.100	-.606	.176
39	-1.299	346	-.953	.267	-.580	.235	-.1645	.269	-.1386	.100	-.606	.176

Appendix B Table 37 Measured data and computed pressure distribution
for $b_1/b_2=0.25$, $g/b_2=1.0$, $T_1=290$ K.

S	D - Shape						Square - Shape					
	26.8427 (m/s)		20.3885 (m/s)		15.3479 (m/s)		26.8427 (m/s)		20.3885 (m/s)		20.3885 (m/s)	
	Ps cm. H2O	Cp	Ps cm. H2O	Cp	Ps cm. H2O	Cp	Ps cm. H2O	Cp	Ps cm. H2O	Cp	Ps cm. H2O	Cp
1	.775	.808	.260	.733	-.087	.529	-1.645	.269	-1.039	.233	-.606	.400
2	.775	.808	.260	.733	-.087	.529	-1.905	.212	-1.039	.233	-.779	.333
3	.692	.758	.260	.733	-.087	.529	-1.905	.212	-1.039	.233	-.779	.333
4	.520	.750	.260	.733	-.087	.529	-1.905	*****	-1.615	.576	-1.667	-1.811
5	-7.101	-942	-4.070	-1.933	-8.771	-1.294	-1.294	-8.833	-1.327	-4.936	-1.267	-3.204
6	-7.275	-951	-4.244	-1.903	-8.771	-1.294	-1.294	-7.015	-1.923	-4.070	-1.933	-2.685
7	-7.015	-923	-4.330	-1.033	-2.771	-1.294	-1.294	-3.291	-1.096	-2.165	-1.200	-1.186
8	-7.621	-1058	-4.503	-1.100	-2.685	-1.235	-1.235	-6.235	-1.750	-3.637	-1.767	-2.338
9	-7.361	-1060	-4.417	-1.067	-2.338	-1.000	-5.802	-1.654	-3.204	-1.690	-2.165	-2.000
10	-7.101	-946	-4.230	-1.033	-2.852	-1.941	-1.941	-5.588	-1.558	-3.118	-1.567	-2.165
11	-6.409	-758	-4.070	-1.933	-1.992	-1.765	-1.765	-5.802	-1.654	-3.204	-1.690	-2.252
12	-6.235	-750	-3.811	-1.833	-1.819	-1.647	-1.647	-5.369	-1.558	-3.031	-1.533	-2.165
13	-5.716	-625	-2.551	-1.733	-1.645	-1.529	-1.529	-3.27	-1.271	-1.433	-1.819	-1.667
14	-5.369	-558	-3.377	-1.667	-1.559	-1.471	-1.471	-4.330	-1.346	-2.511	-1.333	-1.732
15	-4.936	-468	-3.204	-1.600	-1.478	-1.412	-1.412	-4.417	-1.346	-2.511	-1.333	-1.732
16	-4.850	-442	-3.031	-1.533	-1.478	-1.412	-1.412	-4.330	-1.327	-2.511	-1.333	-1.732
17	-4.677	-404	-2.944	-1.500	-1.472	-1.412	-1.412	-4.330	-1.327	-2.511	-1.333	-1.732
18	-4.417	-346	-2.858	-1.467	-1.386	-1.353	-1.353	-4.244	-1.308	-2.511	-1.333	-1.645
19	-4.157	-258	-2.771	-1.433	-1.386	-1.353	-1.353	-4.244	-1.267	-2.338	-1.267	-1.472
20	-4.070	-269	-2.685	-1.400	-1.299	-1.294	-1.294	-4.070	-1.269	-2.338	-1.267	-1.472
21	-3.724	-192	-2.511	-1.333	-1.299	-1.294	-1.294	-3.724	-1.192	-2.522	-1.233	-1.366
22	-4.157	-288	-2.685	-1.400	-1.299	-1.294	-1.294	-4.070	-1.269	-2.338	-1.267	-1.386
23	-4.157	-288	-2.771	-1.433	-1.299	-1.294	-1.294	-4.070	-1.269	-2.338	-1.267	-1.386
24	-4.157	-288	-2.771	-1.433	-1.299	-1.294	-1.294	-4.070	-1.269	-2.338	-1.267	-1.386
25	-6.244	-306	-2.858	-1.467	-1.299	-1.294	-1.294	-4.070	-1.269	-2.338	-1.267	-1.386
26	-4.503	-315	-2.944	-1.500	-1.386	-1.353	-1.353	-4.070	-1.269	-2.338	-1.267	-1.472
27	-4.677	-404	-3.118	-1.567	-1.478	-1.412	-1.412	-4.244	-1.308	-2.511	-1.333	-1.472
28	-5.196	-519	-3.464	-1.700	-1.559	-1.471	-1.471	-4.936	-1.462	-3.771	-1.433	-1.472
29	-5.629	-615	-3.637	-1.767	-1.645	-1.589	-1.589	-5.369	-1.558	-7.361	-2.266	-1.559
30	-6.235	-750	-3.924	-1.900	-1.732	-1.588	-1.588	-5.802	-1.654	-3.291	-1.633	-1.732
31	-6.668	-846	-4.157	-1.967	-1.819	-1.647	-1.647	-3.984	-1.250	-2.338	-1.267	-1.212
32	-8.141	-1.173	-5.500	-1.473	-2.852	-1.941	-1.941	-4.677	-1.404	-2.518	-1.367	-1.212
33	-8.141	-1.173	-5.543	-1.500	-2.338	-1.000	-1.000	-5.369	-1.558	-3.204	-1.600	-1.472
34	-8.141	-1.173	-5.716	-1.567	-2.511	-1.118	-1.118	-7.534	-1.038	-4.330	-1.033	-2.165
35	-8.141	-1.173	-5.543	-1.500	-2.598	-1.176	-1.176	-9.266	-1.463	-5.802	-1.600	-2.685
36	.606	.769	.260	.733	.000	.588	-.1386	.387	-.666	.400	-.520	.433
37	.693	.758	.260	.733	.000	.588	-.1386	.387	-.666	.400	-.520	.433
38	.606	.769	.260	.733	.000	.588	-.1386	.387	-.666	.400	-.520	.433
39	.606	.769	.260	.733	.000	.588	-.1386	.387	-.666	.400	-.520	.433

Appendix B Table 38 Measured data and computed pressure distribution for $b_1/b_2=1.0$, $g/bz=0.75$, $T_1=290$ K.

S	D - Shape				Square - Shape			
	26.8427 (m/s)		20.3885 (m/s)		26.8427 (m/s)		20.3885 (m/s)	
	Ps cm.H2O	Cp	Ps cm.H2O	Cp	Ps cm.H2O	Cp	Ps cm.H2O	Cp
1	-2.771	0.19	-2.204	-0.600	-1.819	-0.647	-6.928	-0.904
2	-2.239	0.15	-2.771	-0.473	-1.819	-0.647	-6.409	-0.788
3	-2.335	0.15	-2.858	-0.467	-1.819	-0.647	-6.495	-0.804
4	-1.472	0.308	-2.858	-0.467	-1.819	-0.647	-6.926	-0.904
5	-7.361	-1.000	-3.464	-0.700	-1.805	-0.706	-6.755	-0.865
6	-4.503	-0.365	-3.031	-0.533	-1.732	-0.568	-6.499	-0.788
7	-4.590	-0.385	-2.944	-0.500	-1.645	-0.529	-5.283	-0.538
8	-4.763	-0.423	-2.944	-0.500	-1.472	-0.412	-5.369	-0.556
9	-5.023	-0.481	-2.031	-0.533	-1.472	-0.412	-4.936	-0.462
10	-5.456	-0.577	-2.204	-0.600	-1.472	-0.412	-4.590	-0.505
11	-6.235	-0.750	-3.464	-0.700	-1.645	-0.569	-4.244	-0.308
12	-7.567	-1.125	-4.070	-0.933	-1.819	-0.647	-4.244	-0.308
13	-7.881	-1.115	-2.964	-0.900	-1.819	-0.647	-4.244	-0.308
14	-6.235	-0.750	-3.204	-0.600	-1.645	-0.569	-4.076	-0.269
15	-5.283	-0.528	-2.858	-0.467	-1.386	-0.353	-4.076	-0.269
16	-4.936	-0.462	-2.686	-0.400	-1.386	-0.353	-3.984	-0.250
17	-4.850	-0.446	-2.686	-0.400	-1.386	-0.353	-3.897	-0.231
18	-4.763	-0.423	-2.686	-0.400	-1.386	-0.353	-3.811	-0.212
19	-4.677	-0.404	-2.686	-0.400	-1.386	-0.353	-3.637	-0.173
20	-4.590	-0.365	-2.598	-0.367	-1.299	-0.294	-3.637	-0.173
21	-4.444	-0.308	-2.338	-0.267	-1.212	-0.235	-3.291	-0.096
22	-4.503	-0.365	-2.511	-0.333	-1.212	-0.235	-3.551	-0.154
23	-4.502	-0.365	-2.511	-0.333	-1.212	-0.235	-3.551	-0.154
24	-4.590	-0.365	-2.511	-0.333	-1.212	-0.235	-3.551	-0.154
25	-4.590	-0.365	-2.511	-0.333	-1.212	-0.235	-3.637	-0.173
26	-4.763	-0.423	-2.686	-0.400	-1.212	-0.235	-3.724	-0.192
27	-5.110	-0.500	-2.686	-0.467	-1.559	-0.471	-3.976	-0.212
28	-5.976	-0.692	-3.291	-0.633	-1.645	-0.569	-4.076	-0.269
29	-6.666	-0.846	-3.637	-0.767	-1.732	-0.588	-3.984	-0.250
30	-7.534	-1.036	-4.070	-0.933	-1.039	-0.118	-4.244	-0.308
31	-3.204	-0.077	-1.819	-0.067	-0.866	-0.000	-3.637	-0.173
32	-3.204	-0.077	-1.645	0.000	-0.693	-0.118	-4.070	-0.269
33	-3.204	-0.077	-1.472	-0.067	-1.039	-0.118	-4.330	-0.327
34	-3.637	-1.173	-1.819	-0.067	-1.039	-0.118	-4.936	-0.462
35	-6.668	-0.846	-1.732	-0.033	-2.12	-0.235	-5.802	-0.654
36	-1.172	0.596	-2.252	-0.233	-1.386	-0.353	-7.101	-0.942
37	-1.472	0.308	-2.252	-0.233	-1.386	-0.353	-6.668	-0.845
38	-1.723	0.250	-2.252	-0.233	-1.386	-0.353	-6.755	-0.865
39	-2.765	0.154	-2.252	-0.233	-1.386	-0.353	-6.322	-0.769

Appendix B Table 39 Measured data and computed pressure distribution for $b_1/b_2=0.75$, $g/bz=0.75$, $T_1=290$ K.

S	D - Shape				Square - Shape			
	26.8427 (m/s)		20.3885 (m/s)		26.8427 (m/s)		20.3885 (m/s)	
	Ps cm.H2O	Cp	Ps cm.H2O	Cp	Ps cm.H2O	Cp	Ps cm.H2O	Cp
1	-3.204	-0.077	-1.905	-0.100	-1.212	-0.235	-4.677	-0.404
2	-2.771	0.19	-1.905	-0.100	-1.212	-0.235	-5.023	-0.481
3	-2.771	0.19	-1.905	-0.100	-1.212	-0.235	-5.629	-0.615
4	-3.204	-0.077	-1.905	-0.100	-0.892	0.194	-5.976	-0.692
5	-7.534	-1.036	-4.070	-0.933	-2.338	-1.000	-6.477	-0.404
6	-5.603	-0.654	-3.204	-0.600	-1.819	-0.647	-4.593	-0.365
7	-5.369	-0.558	-3.031	-0.533	-1.732	-0.588	-4.417	-0.346
8	-5.196	-0.519	-2.544	-0.500	-1.732	-0.588	-4.417	-0.346
9	-5.110	-0.500	-2.944	-0.500	-1.732	-0.588	-4.503	-0.365
10	-5.196	-0.519	-3.204	-0.600	-1.819	-0.647	-4.677	-0.404
11	-5.625	-0.615	-3.377	-0.667	-1.998	-0.765	-4.936	-0.462
12	-6.666	-0.846	-4.070	-0.933	-2.425	-1.059	-5.802	-0.654
13	-6.235	-0.750	-3.657	-0.867	-2.338	-1.000	-5.689	-0.615
14	-4.936	-0.462	-3.116	-0.567	-1.905	-0.706	-4.503	-0.365
15	-4.417	-0.346	-2.771	-0.433	-1.645	-0.529	-4.244	-0.308
16	-4.330	-0.337	-2.598	-0.367	-1.559	-0.471	-4.157	-0.288
17	-4.344	-0.316	-2.596	-0.367	-1.559	-0.471	-4.070	-0.269
18	-4.244	-0.308	-2.596	-0.367	-1.559	-0.471	-4.070	-0.269
19	-4.244	-0.308	-2.596	-0.367	-1.559	-0.471	-4.070	-0.269
20	-4.070	-0.269	-2.511	-0.333	-1.472	-0.412	-3.984	-0.250
21	-3.637	-1.173	-2.252	-0.233	-1.386	-0.353	-3.551	-0.154
22	-4.070	-0.269	-2.425	-0.300	-1.472	-0.412	-3.724	-0.192
23	-4.070	-0.269	-2.425	-0.300	-1.472	-0.412	-3.764	-0.192
24	-4.070	-0.219	-2.425	-0.300	-1.472	-0.412	-3.724	-0.192
25	-4.070	-0.269	-2.511	-0.333	-1.472	-0.412	-3.811	-0.212
26	-4.157	-0.268	-2.511	-0.333	-1.472	-0.412	-3.811	-0.212
27	-4.417	-0.346	-2.598	-0.367	-1.559	-0.471	-3.984	-0.250
28	-5.023	-0.451	-2.944	-0.500	-1.732	-0.588	-4.763	-0.423
29	-5.802	-0.654	-3.464	-0.700	-1.992	-0.765	-5.110	-0.500
30	-6.562	-0.837	-3.984	-0.900	-2.338	-1.000	-5.602	-0.654
31	-2.656	0.0	-1.819	-0.067	-1.216	-0.176	-2.058	0.000
32	-3.204	-0.077	-1.905	-0.100	-1.212	-0.235	-2.771	0.019
33	-4.763	-0.453	-2.338	-0.267	-1.299	-0.294	-2.685	-0.038
34	-6.666	-0.846	-3.204	-0.600	-1.732	-0.588	-2.338	-0.115
35	-7.534	-1.038	-4.070	-0.933	-2.338	-1.000	-2.338	-0.115
36	-3.660	0.692	-1.666	-0.400	-0.953	-0.059	-5.110	-0.500
37	-1.035	0.404	-1.212	-0.167	-0.953	-0.059	-4.763	-0.423
38	-3.204	0.306	-1.212	-0.167	-0.953	-0.059	-4.417	-0.346
39	-1.471	0.308	-1.212	-0.167	-0.953	-0.059	-3.811	-0.212

Appendix B Table 40 Measured data and computed pressure distribution
for $b_1/b_2=0.625$, $g/b_2=0.75$, $T_1=290$ K.

#	D - Shape								Square - Shape								D - Shape							
	26.8427 (m/s)				20.3885 (m/s)				15.3479 (m/s)				26.8427 (m/s)				20.3885 (m/s)				15.3479 (m/s)			
	Ps	Cp	Ps	Cp	Ps	Cp	Ps	Cp	Ps	Cp	Ps	Cp	Ps	Cp	Ps	Cp	Ps	Cp	Ps	Cp	Ps	Cp		
1	-2.338	115	-1.732	-.033	-1.039	-.118	-3.984	-.250	-2.425	-.300	-1.386	-.353												
2	-2.328	115	-1.732	-.033	-1.039	-.118	-4.970	-.269	-2.685	-.400	-1.472	-.412												
3	-8.338	115	-1.819	-.067	-1.039	-.118	-4.677	-.404	-2.944	-.500	-1.645	-.529												
4	-1.905	212	-1.732	-.033	-1.039	-.118	-4.936	-.462	-3.031	-.533	-1.732	-.586												
5	-8.833	-1.327	-5.369	-1.433	-2.771	-1.294	-4.936	-.462	-3.031	-.533	-1.732	-.586												
6	-6.666	-846	-4.070	-9.933	-2.078	-.824	-4.763	-.423	-2.944	-.500	-1.645	-.529												
7	-5.625	-615	-3.464	-7.700	-1.819	-.647	-4.763	-.423	-2.944	-.500	-1.559	-.471												
8	-5.365	-558	-3.204	-6.600	-1.732	-.588	-4.763	-.423	-2.944	-.500	-1.559	-.471												
9	-5.023	-451	-3.204	-6.600	-1.732	-.588	-4.936	-.462	-3.031	-.533	-1.559	-.471												
10	-5.195	-519	-2.291	-4.633	-1.732	-.588	-5.110	-.500	-3.118	-.567	-1.732	-.588												
11	-5.543	-596	-3.551	-7.733	-1.985	-.706	-5.456	-.577	-3.377	-.667	-1.732	-.588												
12	-6.409	-788	-4.070	-9.933	-2.165	-.882	-6.495	-.808	-3.897	-.867	-1.992	-.765												
13	-5.802	-654	-3.811	-8.833	-1.992	-.765	-5.376	-.692	-3.637	-.767	-1.905	-.706												
14	-4.677	-404	-3.031	-5.533	-1.559	-.471	-4.763	-.423	-2.944	-.500	-1.559	-.471												
15	-4.244	-308	-2.771	-4.333	-1.472	-.412	-4.417	-.346	-2.771	-.433	-1.472	-.412												
16	-4.070	-269	-2.771	-4.333	-1.472	-.412	-4.244	-.308	-2.685	-.400	-1.472	-.412												
17	-4.070	-269	-2.771	-4.333	-1.472	-.412	-4.244	-.308	-2.685	-.400	-1.472	-.412												
18	-4.070	-269	-2.771	-4.333	-1.472	-.412	-4.244	-.308	-2.685	-.400	-1.472	-.412												
19	-4.070	-269	-2.771	-4.333	-1.472	-.412	-4.244	-.308	-2.685	-.400	-1.472	-.412												
20	-3.984	-250	-2.685	-4.000	-1.386	-.353	-3.897	-.231	-2.425	-.300	-1.386	-.353												
21	-3.984	-250	-2.685	-4.000	-1.386	-.353	-3.897	-.231	-2.425	-.300	-1.386	-.353												
22	-4.070	-269	-2.771	-4.333	-1.472	-.412	-4.244	-.308	-2.685	-.400	-1.472	-.412												
23	-3.984	-250	-2.685	-4.000	-1.386	-.353	-3.897	-.231	-2.425	-.300	-1.386	-.353												
24	-6.666	-846	-4.070	-9.933	-2.078	-.824	-3.264	-.077	-1.992	-.100	-1.126	-.118												
25	-3.551	-154	-2.327	-4.233	-1.294	-.706	-4.590	-.385	-2.898	-.400	-1.472	-.412												
26	-6.629	-615	-2.637	-4.767	-1.819	-.647	-5.369	-.558	-3.377	-.667	-1.905	-.105												
27	-6.062	-712	-4.070	-9.933	-2.078	-.824	-6.062	-.712	-3.897	-.867	-2.165	-.882												
28	-5.944	-500	-3.464	-7.700	-1.819	-.647	-5.944	-.558	-3.377	-.667	-1.905	-.105												
29	-5.766	-596	-3.204	-6.600	-1.732	-.588	-5.766	-.558	-3.377	-.667	-1.905	-.105												
30	-5.766	-596	-3.204	-6.600	-1.732	-.588	-5.766	-.558	-3.377	-.667	-1.905	-.105												
31	-5.766	-596	-3.204	-6.600	-1.732	-.588	-5.766	-.558	-3.377	-.667	-1.905	-.105												
32	-5.766	-596	-3.204	-6.600	-1.732	-.588	-5.766	-.558	-3.377	-.667	-1.905	-.105												
33	-5.802	-654	-3.204	-6.600	-1.732	-.588	-5.802	-.558	-3.377	-.667	-1.905	-.105												
34	-6.666	-846	-4.070	-9.933	-2.078	-.824	-3.264	-.077	-1.992	-.100	-1.126	-.118												
35	-7.534	-1036	-4.936	-1.267	-2.338	-1.000	-8.944	-.019	-1.905	-.100	-1.039	-.118												
36	-6.260	-692	-1.173	567	-1.173	471	-3.984	-.250	-2.511	-.333	-1.472	-.412												
37	-1.039	404	-1.039	233	-520	235	-3.984	-.250	-2.511	-.333	-1.472	-.412												
38	-1.476	306	-1.039	233	-520	235	-3.984	-.250	-2.511	-.333	-1.472	-.412												
39	-1.472	306	-1.039	233	-520	235	-3.984	-.250	-2.511	-.333	-1.472	-.412												

Appendix B Table 41 Measured data and computed pressure distribution
for $b_1/b_2=0.50$, $g/b_2=0.75$, $T_1=290$ K.

#	D - Shape								Square - Shape								D - Shape							
	26.8427 (m/s)				20.3885 (m/s)				15.3479 (m/s)				26.8427 (m/s)				20.3885 (m/s)				15.3479 (m/s)			
	Ps	Cp	Ps	Cp	Ps	Cp	Ps	Cp	Ps	Cp	Ps	Cp	Ps	Cp	Ps	Cp	Ps	Cp	Ps	Cp	Ps	Cp		
1	-2.338	115	-1.472	.067	-.866	.000	-3.031	-.038	-1.905	-.100	-1.039	-.118												
2	-2.511	.077	-1.559	.033	-.866	.000	-3.377	-.115	-1.992	-.133	-1.645	-.176												
3	-2.592	.058	-1.732	-.033	-.953	-.059	-3.637	-.173	-2.165	-.200	-1.212	-.235												
4	-2.598	.058	-1.732	-.033	-.953	-.059	-3.637	-.173	-2.165	-.200	-1.212	-.235												
5	-2.440	-1.462	-5.976	-1.667	-3.204	-1.588	-4.677	-.588	-3.264	-.600	-2.165	-.647												
6	-7.534	-1.038	-4.503	-1.100	-2.338	-1.000	-5.369	-.706	-4.049	-.788	-2.685	-.867												
7	-5.976	-692	-2.984	-9.00	-1.992	-.765	-5.110	-.500	-3.204	-.600	-1.645	-.529												
8	-5.716	-635	-3.551	-7.733	-1.819	-.647	-5.110	-.500	-3.118	-.567	-1.645	-.529												
9	-5.369	-558	-3.377	-6.667	-1.732	-.588	-5.110	-.500	-3.118	-.567	-1.645	-.529												
10	-5.882	-578	-3.377	-6.667	-1.732	-.588	-5.283	-.615	-3.464	-.700	-1.819	-.647												
11	-5.456	-577	-3.464	-7.700	-1.819	-.647	-5.456	-.706	-3.464	-.788	-2.070	-.933												
12	-5.976	-692	-3.724	-8.800	-1.905	-.706	-5.802	-.654	-3.637	-.767	-2.165	-.705												
13	-5.369	-558	-3.551	-7.733	-1.819	-.647	-5.802	-.385	-2.858	-.467	-1.472	-.412												
14	-4.503	-365	-3.811	-8.833	-1.472	-.412	-4.590	-.385	-2.858	-.400	-1.386	-.353												
15	-4.244	-308	-3.551	-7.733	-1.386	-.353	-4.330	-.327	-2.685	-.367	-1.386	-.353												
16	-4.244	-308	-3.551	-7.733	-1.386	-.353	-4.244	-.308	-2.598	-.367	-1.386	-.353												
17	-4.244	-308	-3.551	-7.733	-1.386	-.353	-4.244	-.308	-2.598	-.367	-1.386	-.353												
18	-4.244	-308	-3.551	-7.733	-1.386	-.353	-4.244																	

Appendix B Table 42 Measured data and computed pressure distribution for $b_1/b_2=0.37$, $g/b_2=0.75$, $T=290$ K.

S	D - Shape						Square - Shape					
	26.8427 (m/s)		20.3885 (m/s)		15.3479 (m/s)		26.8427 (m/s)		20.3885 (m/s)		15.3479 (m/s)	
	Ps cm H2O	Cp	Ps cm H2O	Cp	Ps cm H2O	Cp	Ps cm H2O	Cp	Ps cm H2O	Cp	Ps cm H2O	Cp
1	-1.965	212	-1.039	233	-.693	.118	-2.338	.115	-1.472	.067	-.779	.059
2	-2.076	173	-1.266	100	-.775	.059	-2.771	.019	-1.732	-.033	-.866	.000
3	-2.076	173	-1.366	100	-.779	.059	-2.944	-.019	-1.819	-.067	-.866	.000
4	-1.905	212	-1.126	200	-.779	.059	-2.685	.038	-1.819	-.067	-.866	.000
5	-9.673	-1.556	-6.235	1	-1.767	-3.204	-1.588	-9.866	-1.423	-5.369	-1.433	-3.294
6	-8.574	-1.265	-5.365	1	-1.433	-2.685	-1.235	-7.015	-1.923	-4.070	-1.933	-2.252
7	-7.101	-1.942	-4.503	1	-1.100	-2.252	-.941	-5.543	-.596	-3.551	-1.733	-1.905
8	-6.235	-750	-4.076	1	-1.933	-1.905	-.706	-5.543	-.596	-3.204	-.600	-1.732
9	-5.602	-654	-3.464	1	-1.700	-1.819	-.647	-5.456	-.577	-3.031	-.533	-1.645
10	-5.365	-556	-3.277	1	-1.667	-1.645	-.529	-5.456	-.577	-3.031	-.533	-1.732
11	-5.365	-556	-3.291	1	-1.633	-1.645	-.529	-5.543	-.596	-3.118	-.547	-1.732
12	-5.365	-556	-3.464	1	-1.600	-1.645	-.529	-5.976	-.692	-3.377	-.667	-1.905
13	-4.930	-412	-3.204	1	-1.600	-1.559	-.471	-5.456	-.577	-3.118	-.547	-1.732
14	-4.417	-346	-1.771	1	-1.433	-1.386	-.353	-4.503	-.365	-2.511	-.333	-1.472
15	-4.244	-308	-2.685	1	-1.400	-1.299	-.294	-4.417	-.346	-2.425	-.300	-1.386
16	-4.157	-288	-2.685	1	-1.299	-1.299	-.294	-4.330	-.327	-2.425	-.300	-1.386
17	-4.157	-288	-2.685	1	-1.299	-1.299	-.294	-4.330	-.327	-2.425	-.300	-1.386
18	-4.157	-288	-2.685	1	-1.299	-1.299	-.294	-4.330	-.327	-2.425	-.300	-1.386
19	-4.070	-269	-2.598	1	-1.295	-1.295	-.294	-4.244	-.308	-2.425	-.300	-1.386
20	-3.597	-231	-2.511	1	-1.333	-1.212	-.235	-4.070	-.269	-2.338	-.267	-1.295
21	-3.637	-173	-2.252	1	-1.233	-1.212	-.235	-3.551	-.154	-2.252	-.233	-1.212
22	-3.584	-250	-2.511	1	-1.333	-1.212	-.235	-4.670	-.269	-2.252	-.233	-1.295
23	-3.584	-250	-2.511	1	-1.333	-1.212	-.235	-4.670	-.269	-2.252	-.233	-1.295
24	-3.584	-250	-2.511	1	-1.333	-1.212	-.235	-4.670	-.269	-2.252	-.233	-1.295
25	-3.584	-250	-2.511	1	-1.333	-1.212	-.235	-4.670	-.269	-2.252	-.233	-1.295
26	-4.070	-269	-2.598	1	-1.367	-1.212	-.235	-4.070	-.269	-2.252	-.233	-1.295
27	-4.330	-327	-2.771	1	-1.433	-1.212	-.235	-4.157	-.288	-2.338	-.267	-1.386
28	-4.530	-468	-3.118	1	-1.567	-1.386	-.353	-4.590	-.365	-2.598	-.367	-1.472
29	-5.365	-558	-3.464	1	-1.700	-1.472	-.412	-5.196	-.519	-2.944	-.500	-1.645
30	-5.625	-615	-3.637	1	-1.767	-1.645	-.529	-5.869	-.673	-3.377	-.667	-1.905
31	-4.157	-298	-2.338	1	-1.267	-1.267	-.176	-3.551	-.154	-2.078	-.167	-1.386
32	-5.365	-556	-3.204	1	-1.600	-1.295	-.294	-3.724	-.192	-2.078	-.167	-1.386
33	-6.063	-712	-4.070	1	-1.933	-1.645	-.529	-4.157	-.268	-2.425	-.300	-1.386
34	-7.534	-1.036	-4.936	1	-1.267	-2.338	-1.000	-5.196	-.519	-2.944	-.500	-1.645
35	-6.633	-137	-5.602	1	-1.600	-2.511	-1.118	-7.967	-.135	-4.503	-.100	-2.771
36	-1.173	596	-173	1	-1.567	-1.73	-.471	-1.905	.212	-1.039	.233	-.606
37	-1.039	404	-606	1	-1.400	-1.294	-2.338	-.115	-1.472	-.067	-1.779	.059
38	-1.472	306	-1.039	1	-1.233	-1.294	-2.338	-.115	-1.472	-.067	-1.779	.059
39	-1.472	306	-1.039	1	-1.233	-1.294	-1.965	-.212	-1.126	.200	-.693	118

Appendix B Table 43 Measured data and computed pressure distribution for $b_1/b_2=0.25$, $g/b_2=0.75$, $T=290$ K.

S	D - Shape						Square - Shape					
	26.8427 (m/s)		20.3885 (m/s)		15.3479 (m/s)		26.8427 (m/s)		20.3885 (m/s)		15.3479 (m/s)	
	Ps cm H2O	Cp	Ps cm H2O	Cp	Ps cm H2O	Cp	Ps cm H2O	Cp	Ps cm H2O	Cp	Ps cm H2O	Cp
1	-1.775	462	-1.039	233	-.606	.176	-1.732	.250	-1.039	.233	-.606	.176
2	-7.775	462	-1.039	233	-.606	.176	-2.252	.135	-1.299	.133	-.693	.118
3	-520	519	-553	.267	-.606	.176	-2.338	.115	-1.366	.100	-.779	.059
4	-266	692	-866	.300	-.522	.235	-2.338	.115	-1.366	.100	-.606	.176
5	-6.635	-1.317	-5.716	1	-1.567	-3.204	-.1586	-9.699	-1.519	-5.802	-1.600	-2.771
6	-6.633	-1.327	-5.369	1	-1.433	-3.031	-.1471	-6.833	-1.327	-4.936	-1.267	-2.338
7	-8.400	-1.231	-4.936	1	-1.267	-2.771	-.1294	-7.361	-1.000	-4.157	-.967	-2.078
8	-7.967	-1.135	-4.330	1	-1.033	-2.511	-.1118	-6.582	-.827	-3.637	-.767	-1.905
9	-7.101	-942	-3.811	1	-1.633	-2.165	-.866	-6.73	-.673	-3.204	-.600	-1.732
10	-6.409	-766	-3.551	1	-1.733	-1.992	-.765	-5.456	-.577	-3.031	-.533	-1.645
11	-5.716	-625	-3.204	1	-1.600	-1.819	-.647	-5.369	-.558	-3.031	-.533	-1.559
12	-5.369	-558	-3.118	1	-1.567	-1.732	-.586	-5.369	-.558	-3.031	-.533	-1.645
13	-4.533	-462	-2.944	1	-1.500	-1.732	-.586	-4.936	-.462	-2.771	-.433	-1.472
14	-4.763	-433	-6.771	1	-1.433	-1.645	-.529	-4.503	-.346	-2.598	-.367	-1.472
15	-4.596	-365	-2.685	1	-1.400	-1.559	-.471	-4.330	-.327	-2.425	-.300	-1.366
16	-4.503	-365	-2.685	1	-1.400	-1.559	-.471	-4.330	-.327	-2.425	-.300	-1.366
17	-4.417	-346	-2.598	1	-1.367	-1.559	-.471	-4.244	-.308	-2.425	-.300	-1.366
18	-4.330	-327	-2.598	1	-1.333	-1.472	-.412	-4.157	-.288	-2.338	-.267	-1.366
19	-4.072	-269	-2.511	1	-1.333	-1.472	-.412	-4.070	-.249	-2.522	-.233	-1.299
20	-4.070	-269	-2.338	1	-1.267	-1.366	-.353	-4.070	-.249	-2.522	-.233	-1.299
21	-3.637	-173	-2.252	1	-1.333	-1.366	-.353	-3.637	-.173	-2.522	-.233	-1.366
22	-4.070	-269	-2.425	1	-1.300	-1.384	-.353	-3.984	-.250	-2.338	-.267	-1.366
23	-2.69	-269	-2.511	1	-1.333	-1.472	-.412	-3.984	-.250	-2.338	-.267	-1.366
24	-4.070	-269	-2.511	1	-1.333	-1.472	-.412	-3.984	-.250	-2.338	-.267	-1.366
25	-4.070	-269	-2.685	1	-1.400	-1.472	-.412	-3.984	-.250	-2.338	-.267	-1.366
26	-4.244	-316	-2.511	1	-1.333	-1.472	-.412	-4.070	-.249	-2.338	-.267	-1.472
27	-4.503	-365	-2.685	1	-1.400	-1.472	-.412	-4.070	-.249	-2.338	-.267	-1.472
28	-4.622	-462	-2.944	1	-1.500	-1.645	-.529	-4.503	-.346	-2.685	-.400	-1.645
29	-5.365	-558	-2.204	1	-1.600	-1.819	-.647	-5.023	-.481	-2.344	-.500	-1.819
30	-5.543	-596	-3.291	1	-1.633	-1.905	-.706	-5.456	-.577	-3.244	-.600	-1.905
31	-5.603	-654	-3.204	1	-1.600	-2.252	-.941	-4.070	-.269	-2.338	-.267	-1.559
32	-7.521	-1.036	-3.697	1	-1.867	-1.902	-.765	-4.763	-.483	-2.771	-.433	-1.645
33	-7.567	-1.135	-4.844	1	-1.000	-2.338	-.1000	-5.802	-.654	-3.377	-.667	-2.165
34	-8.661	-1.268	-5.023	1	-1.300	-2.771	-.1000	-5.802	-.654	-3.377	-.667	-2.165
35	-6.833	-1.317	-5.625	1	-1.533	-3.204	-.1588	-9.866	-.1423	-5.456	-.1467	-3.551
36	-2.69	652	-173	1	567	-2.60	-.412	-1.039	-.404	-2.344	-.400	-.606
37	-1.172	596	-606	1	400	-1.520	-.235	-1.645	-.269	-2.338	-.300	-.606
38	-5.821	519	-666	1	300	-1.520	-.235	-1.645	-.269	-2.338	-.300	-.606
39	-5.585	519	-606	1	400	-.520	-.235	-1.472	-.308	-2.779	-.333	-.353

Appendix E Table 44 Measured data and computed pressure distribution for $b_1/b_2=1.0$, $g/b_2=0.50$, $T=290$ K.

#	D - Shape						Square - Shape					
	26.8427 (m/s)		20.3885 (m/s)		15.3479 (m/s)		26.8427 (m/s)		20.3885 (m/s)		15.3479 (m/s)	
	Ps cm.H2O	Cp	Ps cm.H2O	Cp	Ps cm.H2O	Cp	Ps cm.H2O	Cp	Ps cm.H2O	Cp	Ps cm.H2O	Cp
1	-4.503	-365	-3.031	-533	-1.559	-471	-7.101	-942	-4.070	-933	-2.338	-1.000
2	-4.070	-269	-3.031	-533	-1.645	-529	-7.101	-942	-4.070	-933	-2.338	-1.000
3	-5.116	-1.000	-3.204	-600	-1.645	-529	-6.928	-994	-4.070	-933	-2.338	-1.000
4	-6.235	-750	-3.377	-667	-1.819	-647	-7.101	-942	-4.070	-933	-2.338	-1.000
5	-4.070	-269	-2.771	-433	-1.819	-647	-7.361	-1.000	-4.070	-933	-2.338	-1.000
6	-4.244	-308	-2.685	-400	-1.645	-529	-7.101	-942	-4.070	-933	-2.338	-1.000
7	-4.503	-305	-2.596	-367	-1.472	-412	-6.235	-750	-3.637	-767	-2.165	-0.882
8	-4.677	-404	-2.596	-367	-1.386	-353	-6.235	-750	-3.551	-733	-1.905	-0.706
9	-4.936	-402	-2.685	-400	-1.386	-353	-5.456	-577	-3.031	-533	-1.819	-0.647
10	-5.369	-558	-2.856	-467	-1.386	-353	-4.936	-462	-2.856	-467	-1.645	-0.529
11	-5.802	-654	-3.116	-567	-1.472	-412	-4.503	-345	-2.598	-367	-1.472	-0.412
12	-7.534	-1.038	-3.637	-767	-1.645	-529	-4.244	-308	-2.338	-267	-1.386	-0.353
13	-7.361	-1.000	-3.551	-733	-1.645	-529	-4.070	-269	-2.338	-267	-1.386	-0.353
14	-5.629	-615	-2.771	-433	-1.386	-353	-3.984	-250	-2.338	-267	-1.386	-0.353
15	-4.677	-404	-2.596	-367	-1.299	-294	-3.897	-231	-2.165	-200	-1.299	-0.294
16	-4.417	-346	-2.425	-300	-1.212	-235	-3.811	-212	-2.165	-200	-1.299	-0.294
17	-4.244	-308	-2.425	-300	-1.212	-235	-3.724	-192	-2.165	-200	-1.299	-0.294
18	-4.244	-308	-2.425	-300	-1.212	-235	-3.637	-173	-2.165	-200	-1.299	-0.294
19	-4.244	-308	-2.425	-300	-1.212	-235	-3.551	-154	-2.078	-167	-1.212	-0.235
20	-4.157	-288	-3.336	-267	-1.126	-176	-3.464	-135	-1.992	-133	-1.212	-0.235
21	-3.811	-212	-2.251	-233	-1.126	-176	-3.118	-058	-1.992	-133	-1.126	-0.176
22	-4.070	-269	-2.236	-267	-1.126	-176	-3.464	-135	-1.992	-133	-1.126	-0.176
23	-4.070	-269	-2.336	-267	-1.126	-176	-3.551	-154	-2.078	-167	-1.212	-0.176
24	-4.070	-269	-2.336	-267	-1.126	-176	-3.551	-154	-2.078	-167	-1.212	-0.176
25	-4.070	-269	-2.336	-267	-1.126	-176	-3.637	-173	-2.165	-200	-1.299	-0.294
26	-4.157	-288	-2.425	-300	-1.212	-235	-3.811	-212	-2.252	-233	-1.212	-0.235
27	-5.590	-355	-2.595	-367	-1.299	-294	-3.984	-250	-2.338	-267	-1.386	-0.353
28	-5.543	-595	-3.204	-600	-1.472	-412	-4.070	-269	-2.338	-267	-1.386	-0.353
29	-6.235	-750	-3.377	-667	-1.559	-471	-4.330	-327	-2.425	-300	-1.386	-0.353
30	-7.101	-942	-3.724	-800	-1.645	-529	-4.850	-442	-2.771	-433	-1.472	-0.412
31	-8.944	-619	-1.905	-100	-1.186	-176	-4.936	-462	-2.598	-367	-1.472	-0.412
32	-8.944	-619	-1.732	-033	-0.953	-059	-5.369	-558	-2.944	-500	-1.472	-0.412
33	-8.655	-600	-1.905	-100	-0.953	-059	-5.543	-596	-3.204	-600	-1.559	-0.471
34	-3.112	-058	-1.905	-100	-1.039	-118	-6.235	-750	-3.724	-800	-2.165	-0.882
35	-2.598	-658	-3.204	-600	-1.039	-118	-6.842	-885	-3.984	-900	-2.165	-0.882
36	-4.244	-308	-2.945	-500	-1.472	-412	-7.101	-942	-4.070	-933	-2.252	-0.941
37	-4.070	-219	-2.771	-433	-1.559	-471	-6.668	-846	-4.070	-933	-2.252	-0.941
38	-3.112	-058	-2.771	-433	-1.472	-412	-7.101	-942	-4.070	-933	-2.252	-0.941
39	-2.855	-658	-2.771	-433	-1.472	-412	-6.668	-846	-4.070	-933	-2.252	-0.941

Appendix E Table 45 Measured data and computed pressure distribution for $b_1/b_2=0.75$, $g/b_2=0.50$, $T=290$ K.

#	D - Shape						Square - Shape					
	26.8427 (m/s)		20.3885 (m/s)		15.3479 (m/s)		26.8427 (m/s)		20.3885 (m/s)		15.3479 (m/s)	
	Ps cm.H2O	Cp	Ps cm.H2O	Cp	Ps cm.H2O	Cp	Ps cm.H2O	Cp	Ps cm.H2O	Cp	Ps cm.H2O	Cp
1	-3.984	-250	-2.338	-267	-1.299	-294	-5.196	-519	-3.204	-606	-1.905	-766
2	-3.984	-250	-2.338	-267	-1.299	-294	-5.802	-654	-3.897	-867	-2.078	-824
3	-4.503	-345	-2.771	-433	-1.559	-471	-6.409	-786	-4.503	-1.100	-2.338	-1.000
4	-5.369	-558	-3.204	-600	-1.905	-706	-6.928	-984	-4.677	-1.167	-2.338	-1.000
5	-7.534	-1.038	-3.637	-767	-1.992	-765	-5.802	-654	-3.984	-900	-1.905	-706
6	-5.976	-652	-3.204	-600	-1.819	-647	-5.110	-500	-3.464	-700	-1.819	-647
7	-5.196	-519	-3.116	-567	-1.732	-588	-4.763	-423	-3.377	-667	-1.732	-588
8	-5.365	-558	-3.231	-533	-1.645	-529	-4.677	-494	-3.204	-600	-1.645	-588
9	-5.365	-558	-2.944	-500	-1.645	-529	-4.677	-494	-3.204	-600	-1.645	-588
10	-5.365	-558	-3.031	-533	-1.645	-529	-4.850	-442	-3.377	-667	-1.732	-588
11	-5.802	-654	-3.591	-633	-1.732	-588	-5.023	-481	-3.551	-733	-1.819	-647
12	-6.582	-887	-3.724	-800	-1.992	-765	-5.802	-654	-4.070	-933	-2.078	-824
13	-5.802	-654	-3.464	-700	-1.905	-706	-5.716	-635	-3.984	-900	-1.992	-765
14	-4.936	-462	-2.858	-467	-1.559	-471	-4.503	-365	-3.204	-600	-1.732	-588
15	-4.503	-365	-2.685	-400	-1.472	-412	-4.244	-308	-3.031	-533	-1.559	-471
16	-4.503	-365	-2.595	-367	-1.472	-412	-4.070	-269	-2.944	-500	-1.472	-412
17	-4.503	-365	-2.596	-367	-1.472	-412	-4.070	-269	-2.944	-500	-1.472	-412
18	-4.502	-365	-2.598	-367	-1.472	-412	-4.070	-269	-2.944	-500	-1.472	-412
19	-4.503	-365	-2.598	-367	-1.472	-412	-4.070	-269	-2.944	-500	-1.472	-412
20	-4.417	-346	-2.511	-333	-1.386	-353	-3.984	-250	-2.858	-467	-1.386	-353
21	-4.070	-269	-2.338	-367	-1.386	-353	-3.551	-154	-2.598	-367	-1.299	-353
22	-4.503	-365	-2.598	-367	-1.386	-353	-3.811	-212	-2.771	-433	-1.386	-353
23	-4.503	-365	-2.598	-367	-1.386	-353	-3.811	-212	-2.858	-467	-1.386	-353
24	-4.503	-365	-2.598	-367	-1.386	-353	-3.811	-212	-2.858	-467	-1.472	-412
25	-4.590	-365	-2.685	-400	-1.386	-353	-3.811	-212	-2.858	-467	-1.472	-412
26	-4.677	-404	-2.771	-433	-1.472	-412	-3.811	-212	-2.858	-467	-1.472	-412
27	-4.936	-462	-2.771	-433	-1.472	-412	-3.897	-231	-2.944	-500	-1.559	-471
28	-5.629	-615	-3.204	-600	-1.645	-529	-4.503	-365	-3.464	-700	-1.732	-588
29	-6.495	-808	-2.637	-767	-1.992	-765	-4.936	-462	-3.724	-800	-1.819	-647
30	-7.101	-942	-4.070	-933	-2.165	-882	-5.629	-615	-4.157	-967	-2.078	-824
31	-5.283	-538	-1.505	-100	-1.472	-412	-3.984	-250	-3.204	-600	-1.472	-412
32	-5.283	-538	-1.905	-100	-1.559	-471	-3.984	-250	-2.944	-500	-1.472	-412
33	-4.936	-462	-2.338	-267	-1.645	-529	-3.551	-154	-2.858	-467	-1.299	-294
34	-7.534	-1.038	-2.637	-767	-1.992	-765	-3.551	-154	-1.905	-100	-1.266	-176
35	-7.967	-1.135	-4.503	-1.100	-2.338	-1.000	-3.551	-154	-1.905	-100	-1.266	-176
36	-6.695	-652	-1.173	-567	-1.173	-471	-5.976	-692	-3.984	-900	-2.338	-1.000
37	-1.035	-404	-1.039	-233	-0.606	-176	-5.369	-558	-3.551	-733	-2.338	-1.000
38	-1.212	-365	-1.039	-233	-0.606	-176	-5.196	-519	-3.204	-600	-2.078	-824
39	-1.555	-278	-1.039	-233	-0.606	-176	-4.936	-462	-2.771	-433	-1.645	-529

Appendix B Table 46 Measured data and computed pressure distribution for $b_1/b_2=0.625$, $g/b_2=0.50$, $T_1=290$ K.

#	D - Shape				Square - Shape			
	26.8427 (m/s)		20.3885 (m/s)		15.3479 (m/s)		26.8427 (m/s)	
	Ps cm.H2O	Cp	Ps cm.H2O	Cp	Ps cm.H2O	Cp	Ps cm.H2O	Cp
1	-3.204	-0.077	-1.905	-1.100	-1.039	-1.118	-4.503	-3.365
2	-3.204	-0.077	-2.078	-1.167	-1.212	-1.235	-5.196	-3.110
3	-4.070	-0.269	-2.511	-1.333	-1.472	-1.412	-5.629	-6.15
4	-4.502	-3.5	-2.771	-1.433	-1.732	-1.588	-5.976	-6.92
5	-6.400	-1.231	-5.369	-1.433	-2.771	-1.294	-6.862	-5.882
6	-6.235	-750	-4.070	-933	-2.165	-6.882	-6.554	-3.264
7	-5.625	-615	-2.637	-767	-1.905	-7.706	-5.196	-3.118
8	-5.192	-519	-3.377	-667	-1.819	-6.647	-5.283	-3.031
9	-4.936	-462	-3.204	-600	-1.732	-5.886	-5.283	-3.031
10	-4.936	-462	-3.204	-600	-1.732	-5.886	-5.369	-3.110
11	-5.365	-558	-3.377	-667	-1.732	-5.886	-5.456	-3.204
12	-5.456	-577	-3.637	-767	-1.905	-7.06	-5.976	-6.92
13	-4.936	-462	-3.377	-667	-1.732	-5.886	-5.369	-3.264
14	-4.329	-327	-2.771	-433	-1.472	-4.412	-4.503	-3.65
15	-4.070	-269	-2.685	-400	-1.386	-3.53	-4.330	-2.586
16	-4.070	-269	-2.685	-400	-1.386	-3.53	-4.244	-3.08
17	-4.070	-269	-2.685	-400	-1.386	-3.53	-4.244	-3.08
18	-4.070	-269	-2.685	-400	-1.386	-3.53	-4.244	-3.08
19	-4.070	-269	-2.685	-400	-1.386	-3.53	-4.244	-3.08
20	-3.964	-250	-2.596	-367	-1.299	-2.94	-4.157	-2.688
21	-3.724	-152	-3.511	-333	-1.212	-2.35	-3.637	-1.73
22	-4.157	-258	-2.598	-367	-1.299	-2.94	-3.984	-2.250
23	-4.157	-258	-2.598	-367	-1.299	-2.94	-3.984	-2.250
24	-4.157	-258	-2.598	-367	-1.299	-2.94	-3.984	-2.250
25	-4.157	-258	-2.598	-367	-1.299	-2.94	-3.984	-2.250
26	-4.329	-317	-2.685	-400	-1.386	-3.53	-4.244	-3.08
27	-4.590	-355	-2.771	-433	-1.472	-4.412	-4.070	-2.688
28	-5.369	-558	-3.204	-600	-1.732	-5.886	-5.365	-3.271
29	-5.802	-654	-3.637	-767	-1.905	-7.967	-5.196	-3.204
30	-6.235	-750	-3.984	-900	-1.905	-7.06	-5.976	-6.92
31	-4.070	-269	-3.464	-700	-1.559	-4.71	-4.330	-2.327
32	-4.763	-463	-3.897	-867	-1.472	-4.412	-4.330	-2.327
33	-6.066	-712	-4.157	-967	-1.472	-4.412	-4.244	-3.08
34	-7.534	-1.038	-5.022	-1.300	-1.905	-7.706	-4.330	-2.327
35	-8.287	-1.192	-5.365	-1.433	-2.338	-1.000	-4.330	-2.327
36	-6.693	-768	-6.606	-400	-1.606	-1.76	-4.677	-4.464
37	-6.606	-500	-1.299	-133	-1.606	-1.76	-4.244	-3.08
38	-1.039	404	-1.299	-133	-1.606	-1.76	-3.377	-1.115
39	-1.039	404	-1.299	-133	-1.606	-1.76	-3.204	-1.133

Appendix B Table 47. Measured data and computed pressure distribution for $b_1/b_2=0.50$, $g/b_2=0.50$, $T_1=290$ K.

#	D - Shape				Square - Shape			
	26.8427 (m/s)		20.3885 (m/s)		15.3479 (m/s)		26.8427 (m/s)	
	Ps cm.H2O	Cp	Ps cm.H2O	Cp	Ps cm.H2O	Cp	Ps cm.H2O	Cp
1	-2.771	019	-1.732	-0.333	-0.779	.059	-3.110	-0.058
2	-2.771	019	-1.732	-0.333	-0.953	-0.059	-3.637	-1.173
3	-3.031	-036	-1.905	-1.100	-1.039	-1.118	-4.070	-2.269
4	-2.944	-019	-619	-0.67	-1.039	-1.118	-4.070	-2.269
5	*****	-1.712	-6.405	-1.833	-3.204	-1.588	-7.967	-1.135
6	-8.400	-1.231	-4.936	-1.267	-2.511	-1.118	-6.235	-1.750
7	-6.668	-846	-4.070	-933	-2.078	-0.824	-5.369	-1.558
8	-6.235	-750	-3.637	-767	-1.819	-0.647	-5.369	-1.558
9	-5.456	-577	-3.291	-633	-1.645	-0.529	-5.196	-1.377
10	-5.369	-558	-3.204	-600	-1.645	-0.529	-5.196	-1.377
11	-5.369	-568	-3.291	-633	-1.645	-0.529	-5.283	-1.377
12	-5.456	-577	-3.377	-667	-1.645	-0.529	-5.489	-1.377
13	-4.936	-462	-3.031	-533	-1.472	-0.412	-4.336	-1.462
14	-4.503	-315	-2.771	-433	-1.386	-0.353	-4.330	-1.387
15	-4.157	-226	-2.598	-367	-1.299	-0.294	-4.244	-1.308
16	-4.157	-226	-2.598	-367	-1.299	-0.294	-4.244	-1.308
17	-4.157	-226	-2.598	-367	-1.299	-0.294	-4.244	-1.308
18	-4.157	-226	-2.598	-367	-1.299	-0.294	-4.244	-1.308
19	-4.157	-226	-2.598	-367	-1.299	-0.294	-4.244	-1.308
20	-0.070	-269	-511	-333	-1.299	-0.294	-4.070	-2.269
21	-3.611	-226	-511	-333	-1.299	-0.294	-3.637	-1.173
22	-4.157	-226	-511	-333	-1.299	-0.294	-3.984	-2.250
23	-4.157	-226	-511	-333	-1.299	-0.294	-3.984	-2.250
24	-4.157	-226	-511	-333	-1.299	-0.294	-3.984	-2.250
25	-4.157	-226	-511	-333	-1.299	-0.294	-3.984	-2.250
26	-4.503	-315	-2.685	-400	-1.299	-0.294	-3.984	-2.511
27	-4.936	-462	-2.944	-500	-1.386	-0.353	-4.070	-2.511
28	-5.692	-654	-3.464	-700	-1.645	-0.529	-4.503	-3.45
29	-5.802	-654	-3.637	-767	-1.732	-0.588	-5.023	-4.481
30	-5.602	-654	-3.551	-733	-1.819	-0.647	-5.802	-5.654
31	-6.235	-750	-3.637	-767	-1.905	-0.706	-6.238	-6.115
32	-6.668	-846	-4.503	-1.100	-2.076	-0.824	-8.511	-0.077
33	-7.534	-1.038	-4.936	-1.267	-2.165	-0.882	-8.511	-0.077
34	-8.400	-1.231	-5.369	-1.433	-2.425	-1.059	-2.598	-2.771
35	-8.833	-1.317	-5.229	-1.533	-2.771	-1.294	-2.771	-0.019
36	-2.66	692	-693	900	-600	176	-5.802	-6.654
37	-1.172	596	-606	400	-606	176	-3.464	-1.35
38	-1.039	404	-606	400	-606	176	-3.204	-0.077
39	-1.039	404	-606	400	-606	176	-3.204	-0.067

Appendix B Table 45 Measured data and computed pressure distribution
for $b1/b2=0.37$, $g/b2=0.50$, $T1=290$ K.

S	D - Shape						Square - Shape					
	26.6427 (m/s)		20.3885 (m/s)		15.3479 (m/s)		26.6427 (m/s)		20.3885 (m/s)		15.3479 (m/s)	
	Ps cm H2O	Cp cm H2O	Ps cm H2O	Cp cm H2O	Ps cm H2O	Cp cm H2O	Ps cm H2O	Cp cm H2O	Ps cm H2O	Cp cm H2O	Ps cm H2O	Cp cm H2O
1	-1.819	.831	-1.212	.167	-.666	.176	-2.252	.135	-1.472	.067	-.866	.000
2	-2.252	.135	-1.472	.067	-.779	.059	-2.598	.050	-1.645	.066	-1.953	-.059
3	-2.252	.125	-1.472	.067	-.779	.059	-2.858	.000	-1.819	.067	-1.033	-.118
4	-1.905	.212	-1.039	.233	-.466	.176	-2.771	.019	-1.819	.067	-1.039	-.118
5	-9.440	-1.462	-5.602	-1.600	-3.204	-1.588	-9.699	-1.519	-6.235	-1.767	-3.464	-1.765
6	-8.747	-1.308	-5.365	-1.433	-2.771	-1.294	-7.794	-1.036	-4.850	-1.823	-2.685	-1.235
7	-7.534	-1.038	-4.677	-1.167	-2.511	-1.118	-6.328	-0.769	-4.157	-0.967	-2.338	-1.000
8	-6.922	-0.964	-4.070	-0.933	-2.252	-0.941	-6.062	-0.712	-3.724	-0.800	-2.074	-0.824
9	-6.235	-0.750	-3.637	-0.767	-1.905	-0.706	-5.456	-0.577	-3.464	-0.700	-1.905	-0.706
10	-5.543	-0.556	-3.272	-0.667	-1.819	-0.647	-5.369	-0.558	-3.291	-0.633	-1.819	-0.647
11	-5.365	-0.588	-3.264	-0.600	-1.732	-0.588	-5.196	-0.519	-3.264	-0.600	-1.819	-0.647
12	-4.936	-0.462	-3.031	-0.533	-1.645	-0.529	-5.110	-0.500	-3.110	-0.567	-1.732	-0.588
13	-4.677	-0.404	-2.944	-0.500	-1.472	-0.412	-4.763	-0.423	-2.944	-0.500	-1.645	-0.529
14	-4.503	-0.305	-2.771	-0.433	-1.472	-0.412	-4.417	-0.346	-2.771	-0.433	-1.472	-0.412
15	-4.244	-0.308	-2.685	-0.400	-1.386	-0.353	-4.336	-0.327	-2.685	-0.400	-1.472	-0.412
16	-4.244	-0.306	-2.685	-0.400	-1.386	-0.353	-4.336	-0.327	-2.685	-0.400	-1.472	-0.412
17	-4.244	-0.308	-2.685	-0.400	-1.386	-0.353	-4.336	-0.327	-2.685	-0.400	-1.472	-0.412
18	-4.244	-0.308	-2.685	-0.400	-1.386	-0.353	-4.244	-0.308	-2.685	-0.400	-1.472	-0.412
19	-4.076	-0.269	-2.596	-0.367	-1.386	-0.353	-4.076	-0.269	-2.685	-0.400	-1.472	-0.412
20	-2.252	1.35	-2.511	-1.333	-1.299	-0.294	-3.984	-0.250	-2.511	-0.333	-2.252	0.941
21	-3.637	-1.173	-2.425	-1.301	-1.299	-0.294	-3.637	-0.173	-2.338	-0.267	-1.386	-0.353
22	-4.070	-0.219	-2.511	-1.333	-1.299	-0.294	-4.070	-0.269	-2.511	-0.333	-1.386	-0.353
23	-4.070	-0.269	-2.511	-1.333	-1.299	-0.294	-4.070	-0.269	-2.511	-0.333	-1.386	-0.353
24	-4.070	-0.269	-2.511	-1.333	-1.299	-0.294	-4.070	-0.269	-2.511	-0.333	-1.386	-0.353
25	-4.070	-0.269	-2.511	-1.333	-1.299	-0.294	-4.070	-0.269	-2.511	-0.333	-1.386	-0.353
26	-4.070	-0.269	-2.511	-1.333	-1.299	-0.294	-4.070	-0.269	-2.511	-0.333	-1.386	-0.353
27	-4.330	-0.327	-2.771	-1.433	-1.472	-0.412	-4.070	-0.269	-2.511	-0.333	-1.386	-0.353
28	-4.536	-0.412	-3.204	-1.600	-1.732	-0.588	-4.503	-0.345	-2.858	-0.467	-1.472	-0.412
29	-5.365	-0.588	-3.464	-1.701	-1.905	-0.706	-4.936	-0.462	-3.204	-0.600	-1.645	-0.529
30	-5.543	-0.596	-3.464	-1.701	-2.078	-0.824	-5.369	-0.558	-3.637	-0.767	-1.905	-0.706
31	-6.062	-0.712	-3.637	-1.767	-2.252	-0.941	-5.403	-0.626	-4.157	-1.533	-2.060	-1.508
32	-6.668	-0.070	-0.933	-2.338	-1.000	-4.936	-0.462	-3.031	-0.533	-1.472	-0.412	
33	-7.101	-0.942	-0.936	-1.267	-2.771	-1.294	-5.802	-0.654	-3.464	-0.700	-1.645	-0.529
34	-8.227	-1.192	-5.369	-1.433	-3.118	-1.529	-5.269	-0.558	-4.070	-0.933	-2.338	-1.000
35	-8.633	-1.327	-5.602	-1.600	-3.204	-1.588	-9.266	-1.423	-5.802	-1.600	-3.204	-1.588
36	-6.60	0.692	-1.173	0.567	-3.204	-1.588	-2.252	0.135	-1.472	0.067	-1.953	-0.059
37	-1.472	0.308	-1.039	0.233	-3.204	-1.588	-2.338	0.115	-1.472	0.067	-1.953	-0.059
38	-1.472	0.308	-1.039	0.233	-3.204	-1.588	-2.338	0.115	-1.472	0.067	-1.953	-0.059
39	-1.472	0.308	-1.039	0.233	-3.204	-1.588	-1.472	0.308	-1.039	0.233	-1.666	0.176

Appendix B Table 45 Measured data and computed pressure distribution
for $b1/b2=0.25$, $g/b2=0.50$, $T1=290$ K.

S	D - Shape						Square - Shape					
	26.6427 (m/s)		20.3885 (m/s)		15.3479 (m/s)		26.6427 (m/s)		20.3885 (m/s)		15.3479 (m/s)	
	Ps cm H2O	Cp cm H2O	Ps cm H2O	Cp cm H2O	Ps cm H2O	Cp cm H2O	Ps cm H2O	Cp cm H2O	Ps cm H2O	Cp cm H2O	Ps cm H2O	Cp cm H2O
1	-1.035	.404	-.606	.400	-.520	.235	-1.039	.404	-.866	.300	-.606	.176
2	-1.295	.346	-.666	.300	-.520	.235	-1.645	.669	-.039	.233	-.606	.176
3	-6.06	.500	-.775	.333	-.520	.235	-1.732	.250	-1.126	.800	-.606	.176
4	-1.173	.596	-.606	.400	-.346	.353	-1.472	.308	-1.039	.233	-.606	.176
5	-7.967	-1.135	-5.365	-1.433	-2.598	-1.176	-9.093	-1.305	-5.802	-1.600	-3.204	-1.508
6	-7.967	-1.135	-5.369	-1.433	-2.598	-1.176	-8.747	-1.308	-5.629	-1.533	-3.118	-1.529
7	-7.534	-1.036	-5.023	-1.300	-2.425	-1.059	-7.967	-1.135	-5.116	-1.333	-2.858	-1.471
8	-7.534	-1.036	-5.023	-1.300	-2.336	-1.000	-7.440	-1.019	-4.763	-1.200	-2.685	-1.235
9	-7.101	.542	-0.763	-1.200	-2.165	-0.882	-6.668	-0.846	-4.157	-0.967	-2.338	-1.000
10	-6.668	-0.846	-2.330	-1.033	-1.905	-0.706	-5.689	-0.673	-3.097	-0.867	-2.165	-0.882
11	-5.606	-0.654	-3.897	-0.667	-1.732	-0.588	-5.369	-0.558	-3.551	-0.733	-1.992	-0.765
12	-5.196	-0.519	-3.551	-0.733	-1.645	-0.529	-5.023	-0.481	-3.204	-0.600	-1.905	-0.706
13	-4.936	-0.462	-3.291	-0.633	-1.559	-0.471	-4.763	-0.423	-3.118	-0.567	-1.819	-0.647
14	-4.763	-0.423	-3.204	-0.600	-1.472	-0.412	-4.590	-0.385	-3.031	-0.533	-1.732	-0.588
15	-4.503	-0.365	-3.031	-0.533	-1.386	-0.353	-4.417	-0.346	-2.858	-0.467	-1.645	-0.529
16	-4.417	-0.346	-3.031	-0.533	-1.386	-0.353	-4.417	-0.346	-2.858	-0.467	-1.645	-0.529
17	-4.244	-0.306	-3.031	-0.533	-1.366	-0.353	-4.330	-0.307	-2.685	-0.467	-1.472	-0.412
18	-4.070	-0.269	-2.944	-0.500	-1.386	-0.353	-4.070	-0.269	-2.771	-0.433	-1.645	-0.529
19	-3.584	-0.250	-2.771	-0.433	-1.212	-0.235	-3.897	-0.231	-2.598	-0.367	-1.472	-0.412
20	-3.697	-0.231	-2.665	-0.400	-1.212	-0.235	-3.637	-0.173	-2.425	-0.300	-1.472	-0.412
21	-3.551	-0.154	-2.511	-0.333	-1.186	-0.176	-3.235	-0.184	-2.598	-0.347	-1.559	-0.471
22	-3.597	-0.231	-2.665	-0.400	-1.212	-0.235	-3.235	-0.184	-2.598	-0.347	-1.559	-0.471
23	-3.897	-0.231	-2.665	-0.400	-1.212	-0.235	-4.070	-0.269	-2.685	-0.400	-1.559	-0.471
24	-3.984	-0.250	-2.665	-0.400	-1.212	-0.235	-4.070	-0.269	-2.685	-0.400	-1.559	-0.471
25	-3.984	-0.250	-2.771	-0.433	-1.212	-0.235	-4.070	-0.269	-2.685	-0.400	-1.559	-0.471
26	-4.070	-0.269	-2.771	-0.433	-1.212	-0.235	-4.070	-0.269	-2.685	-0.400	-1.559	-0.471
27	-4.244	-0.306	-2.944	-0.500	-1.299	-0.294	-4.157	-0.288	-2.771	-0.433	-1.645	-0.529
28	-4.590	-0.385	-3.116	-0.567	-1.386	-0.353	-4.593	-0.365	-3.031	-0.533	-2.732	-0.588
29	-5.110	-0.500	-3.464	-0.700	-1.472	-0.412	-5.023	-0.481	-3.377	-0.667	-1.905	-0.706
30	-5.369	-0.558	-3.551	-0.733	-1.472	-0.412	-5.196	-0.519	-3.464	-0.700	-1.992	-0.765
31	-5.543	-0.556	-3.897	-0.645	-1.645	-0.529	-5.369	-0.558	-3.637	-0.767	-2.165	-0.882
32	-6.666	-0.646	-4.503	-1.100	-1.905	-0.706	-6.235	-0.750	-4.244	-1.000	-2.338	-1.000
33	-6.665	-0.646	-4.536	-1.267	-2.336	-0.000	-6.668	-0.846	-4.763	-1.200	-2.685	-1.235
34	-7.867	-1.135	-5.369	-1.433	-2.511	-1.118	-9.180	-1.100	-4.404	-1.235	-2.637	-1.182
35	-7.567	-1.135	-5.369	-1.433	-2.511	-1.118	-9.180	-1.100	-4.404	-1.235	-2.637	-1.182
36	-1.73	0.566	-1.173	0.567	-1.173	0.471	-1.953	0.423	-0.606	0.400	-0.606	0.176
37	-0.606	0.500	-0.606	0.400	-0.260	0.412	-1.472	0.308	-0.666	0.300	-0.606	0.176</

Appendix B Table 50 Measured data and computed pressure distribution
for $b_1/b_2=1.0$, $g/b_2=0.25$, $T_1=290$ K.

No	D - Shape						Square - Shape					
	26.8427 (m/s)		20.3885 (m/s)		15.3479 (m/s)		26.8427 (m/s)		20.3885 (m/s)		15.3479 (m/s)	
	Ps cm.H2O	Cp	Ps cm.H2O	Cp	Ps cm.H2O	Cp	Ps cm.H2O	Cp	Ps cm.H2O	Cp	Ps cm.H2O	Cp
1	-5.802	-654	-3.637	-767	-2.076	-624	-6.928	-984	-4.417	-1.967	-2.425	-1.059
2	-5.369	-586	-3.637	-767	-2.076	-624	-6.668	-846	-4.417	-1.967	-2.425	-1.059
3	-5.543	-596	-3.637	-767	-2.165	-682	-6.928	-984	-4.417	-1.967	-2.425	-1.059
4	-5.802	-654	-3.637	-767	-2.165	-682	-7.015	-983	-4.417	-1.967	-2.425	-1.059
5	-5.116	-500	-3.204	-600	-1.819	-647	-7.015	-983	-4.417	-1.967	-2.425	-1.059
6	-4.763	-423	-2.944	-500	-1.655	-589	-7.015	-983	-4.503	-1.100	-2.425	-1.059
7	-4.677	-404	-2.856	-467	-1.472	-412	-6.928	-904	-4.503	-1.100	-2.425	-1.059
8	-4.677	-404	-2.771	-433	-1.472	-412	-6.928	-904	-4.417	-1.967	-2.425	-1.059
9	-4.650	-442	-2.856	-467	-1.472	-412	-6.668	-846	-4.076	-0.933	-2.338	-1.000
10	-5.283	-536	-3.031	-533	-1.645	-529	-6.322	-769	-3.897	-0.867	-2.338	-1.000
11	-5.802	-654	-3.291	-633	-1.732	-588	-5.889	-673	-3.637	-0.767	-2.165	-0.882
12	-7.101	-942	-3.897	-867	-1.905	-766	-5.543	-596	-3.377	-0.667	-1.992	-0.765
13	-6.666	-846	-3.637	-767	-1.819	-647	-5.023	-481	-3.551	-0.733	-1.819	-0.647
14	-4.763	-423	-2.771	-433	-1.472	-412	-4.050	-442	-2.858	-0.467	-1.732	-0.588
15	-4.070	-269	-2.511	-333	-1.299	-294	-4.503	-365	-2.771	-0.433	-1.559	-0.471
16	-4.070	-269	-2.511	-333	-1.299	-294	-4.330	-327	-2.685	-0.480	-1.559	-0.471
17	-4.070	-269	-2.511	-333	-1.299	-294	-4.076	-269	-2.511	-0.333	-1.472	-0.412
18	-4.070	-269	-2.511	-333	-1.299	-294	-3.984	-250	-2.338	-0.267	-1.472	-0.412
19	-4.070	-269	-2.511	-333	-1.299	-294	-3.811	-212	-2.338	-0.267	-1.386	-0.353
20	-3.984	-250	-2.425	-300	-1.212	-235	-3.637	-173	-2.052	-0.233	-1.386	-0.353
21	-3.637	-173	-2.336	-267	-1.212	-235	-3.464	-135	-2.165	-0.200	-1.386	-0.353
22	-3.897	-231	-2.336	-267	-1.212	-235	-3.311	-212	-2.252	-0.233	-1.386	-0.353
23	-3.897	-231	-2.336	-267	-1.212	-235	-3.087	-231	-2.070	-0.233	-1.472	-0.412
24	-3.897	-231	-2.336	-267	-1.212	-235	-2.984	-250	-2.070	-0.233	-1.472	-0.412
25	-3.897	-231	-2.336	-267	-1.212	-235	-2.811	-212	-2.338	-0.267	-1.386	-0.353
26	-3.897	-231	-2.425	-300	-1.212	-235	-2.444	-308	-4.330	-1.023	-1.559	-0.471
27	-3.984	-250	-2.596	-367	-1.299	-294	-4.330	-327	-4.417	-1.067	-1.645	-0.529
28	-4.503	-365	-3.031	-533	-1.472	-412	-4.590	-385	-4.590	-1.123	-1.732	-0.588
29	-5.369	-586	-3.377	-667	-1.559	-471	-4.936	-462	-4.763	-1.200	-1.819	-0.647
30	-6.235	-750	-3.897	-867	-1.732	-588	-5.802	-654	-5.283	-1.490	-2.165	-0.882
31	-4.070	-269	-2.771	-433	-1.212	-235	-5.976	-692	-5.456	-1.467	-2.165	-0.882
32	-4.070	-269	-2.425	-300	-1.039	-118	-6.495	-808	-5.543	-1.500	-2.165	-0.882
33	-3.984	-250	-2.425	-300	-1.039	-118	-6.582	-827	-5.629	-1.533	-2.338	-1.000
34	-3.204	-0.77	-2.511	-333	-1.039	-118	-7.101	-942	-6.062	-1.700	-2.511	-1.118
35	-3.204	-0.77	-2.511	-333	-1.212	-235	-7.101	-942	-6.062	-1.700	-2.511	-1.118
36	-5.802	-654	-4.070	-933	-1.905	-706	-7.101	-942	-6.062	-1.700	-2.511	-1.118
37	-5.625	-615	-3.637	-767	-1.905	-706	-6.928	-904	-6.062	-1.700	-2.511	-1.118
38	-4.936	-462	-3.637	-767	-1.905	-706	-6.928	-904	-6.062	-1.700	-2.511	-1.118
39	-3.637	-173	-2.771	-433	-1.905	-706	-6.928	-904	-6.062	-1.700	-2.511	-1.118

Appendix B Table 51 Measured data and computed pressure distribution
for $b_1/b_2=0.75$, $g/b_2=0.25$, $T_1=290$ K.

No	D - Shape						Square - Shape					
	26.8427 (m/s)		20.3885 (m/s)		15.3479 (m/s)		26.8427 (m/s)		20.3885 (m/s)		15.3479 (m/s)	
	Ps cm.H2O	Cp	Ps cm.H2O	Cp	Ps cm.H2O	Cp	Ps cm.H2O	Cp	Ps cm.H2O	Cp	Ps cm.H2O	Cp
1	-2.511	077	-2.336	-267	-1.299	-294	-5.196	-519	-3.284	-6.600	-1.732	-0.588
2	-4.417	-346	-2.511	-333	-1.386	-353	-5.802	-654	-3.637	-7.677	-1.992	-0.765
3	-5.369	-558	-2.944	-500	-1.472	-412	-6.668	-846	-4.076	-933	-2.338	-1.000
4	-4.503	-365	-3.031	-533	-1.559	-471	-7.101	-942	-4.157	-967	-2.338	-1.000
5	****	-1.712	-5.602	-1.600	-2.771	-1.299	-6.235	-750	-3.724	-800	-2.165	-0.882
6	-7.446	-1.019	-5.637	-767	-1.905	-706	-5.802	-654	-3.377	-667	-1.905	-0.706
7	-5.802	-654	-3.204	-600	-1.732	-588	-5.110	-580	-3.204	-600	-1.819	-0.647
8	-5.369	-558	-3.116	-567	-1.645	-529	-5.110	-500	-3.118	-567	-1.732	-0.588
9	-5.369	-558	-3.116	-567	-1.645	-529	-5.023	-481	-2.944	-500	-1.645	-0.529
10	-5.716	-635	-3.291	-633	-1.645	-589	-5.196	-519	-2.944	-500	-1.732	-0.588
11	-5.976	-692	-3.637	-767	-1.819	-647	-5.369	-558	-3.118	-567	-1.732	-0.588
12	-7.881	-1115	-4.330	-1.033	-2.165	-882	-5.976	-692	-3.464	-700	-1.905	-0.706
13	-7.534	-038	-3.984	-900	-1.905	-706	-5.369	-558	-3.118	-567	-1.732	-0.588
14	-5.369	-558	-2.656	-467	-1.472	-412	-4.330	-387	-2.425	-300	-1.472	-0.412
15	-4.936	-442	-2.685	-400	-1.386	-353	-4.076	-269	-2.338	-267	-1.386	-0.353
16	-4.677	-404	-2.685	-400	-1.386	-353	-4.076	-269	-2.338	-267	-1.386	-0.353
17	-4.590	-365	-2.625	-400	-1.386	-353	-4.076	-269	-2.338	-267	-1.386	-0.353
18	-4.503	-365	-2.685	-400	-1.386	-353	-4.076	-269	-2.338	-267	-1.386	-0.353
19	-4.417	-346	-2.685	-400	-1.386	-353	-4.076	-269	-2.338	-267	-1.386	-0.353
20	-4.244	-308	-2.596	-367	-1.386	-353	-3.984	-250	-2.525	-233	-1.386	-0.353
21	-3.984	-250	-2.336	-267	-1.386	-353	-3.637	-173	-2.252	-233	-1.299	-0.294
22	-4.070	-269	-2.425	-300	-1.299	-294	-3.984	-250	-2.338	-267	-1.299	-0.294
23	-4.070	-269	-2.425	-300	-1.299	-294	-3.984	-250	-2.338	-267	-1.299	-0.294
24	-4.070	-269	-2.425	-300	-1.299	-294	-4.076	-269	-2.338	-267	-1.299	-0.294
25	-4.070	-269	-2.425	-300	-1.299	-294	-4.076	-269	-2.338	-267	-1.299	-0.294
26	-4.070	-269	-2.425	-300	-1.299	-294	-4.076	-269	-2.338	-267	-1.299	-0.294
27	-4.157	-288	-2.425	-300	-1.299	-294	-4.076	-269	-2.338	-267	-1.299	-0.294
28	-4.503	-365	-2.856	-467	-1.732	-588	-4.590	-385	-2.771	-433	-1.559	-0.471
29	-4.850	-442	-2.856	-467	-1.732	-588	-4.590	-385	-2.771	-433	-1.559	-0.471
30	-5.543	-596	-3.637	-600	-1.472	-412	-5.283	-538	-3.338	-667	-1.732	-0.588
31	-4.070	-269	-2.771	-433	-1.472	-412	-4.870	-269	-2.771	-433	-1.645	-0.529
32	-4.244	-308	-2.944	-500	-1.472	-412	-4.244	-308	-2.771	-433	-1.645	-0.529
33	-4.503	-365	-3.031	-533	-1.559	-471	-4.330	-327	-2.511	-333	-1.559	-0.471
34	-4.936	-462	-3.204	-600	-1.559	-471	-4.593	-365	-2.771	-433	-1.645	-0.529
35	-6.409	-788	-3.637	-767	-2.165	-882	-5.110	-580	-3.204	-600	-1.819	-0.647
36	-4.070	-269	-2.425	-300	-1.299	-294	-6.668	-846	-4.330	-1.033	-2.338	-1.000
37	-4.070	-269	-2.425	-300	-1.299	-294	-6.668	-846	-4.330	-1.033	-2.338	-1.000
38	-4.070	-269	-2.425	-300	-1.299	-294	-5.629	-615	-3.377	-667	-1.905	-0.706
39	-3.804	-077	-1.905	-100	-1.299	-294	-4.503	-365	-2.771	-433	-1.472	-0.412

Appendix B Table 52 Measured data and computed pressure distribution for $b_1/b_2=0.625$, $g/b_2=0.25$, $T_1=290$ K.

b	D - Shape						Square - Shape					
	26.8427 (m/s)		20.3885 (m/s)		15.3479 (m/s)		26.8427 (m/s)		20.3885 (m/s)		15.3479 (m/s)	
	Ps cm.H2O	Cp	Ps cm.H2O	Cp	Ps cm.H2O	Cp	Ps cm.H2O	Cp	Ps cm.H2O	Cp	Ps cm.H2O	Cp
1	-779	462	-779	333	-606	.176	-4.590	.385	-2.338	.267	-1.472	.412
2	-3.204	077	-2.165	-200	-1.126	-.176	-4.503	.345	-2.771	.423	-1.472	.412
3	-3.204	077	-2.165	-200	-1.212	-.235	-5.116	.500	-3.204	.600	-1.645	.529
4	-173	556	-606	400	-606	.176	-5.369	.558	-3.377	.667	-1.819	.647
5	-8.833	-1.327	-5.369	-1.433	-3.021	-1.471	-8.141	-1.173	-4.936	-1.267	-2.771	-1.294
6	-9.166	-1.404	-5.456	-1.467	-3.031	-1.471	-9.928	-0.984	-4.244	-1.000	-2.338	-1.000
7	-8.247	-1.308	-5.283	-1.400	-2.858	-1.353	-6.668	-.846	-3.897	-.867	-2.165	-.862
8	-7.967	-1.135	-4.763	-1.206	-2.596	-1.174	-6.668	-.846	-3.551	-7.733	-1.992	-7.65
9	-6.666	-846	-4.070	-933	-2.165	-.882	-5.629	.615	-3.377	.667	-1.905	.706
10	-5.802	-654	-3.551	-733	-1.905	-.706	-5.629	.615	-3.377	.667	-1.905	.706
11	-5.629	-615	-3.464	-700	-1.905	-.706	-5.629	.615	-3.464	-700	-1.905	.706
12	-6.235	-750	-3.724	-800	-2.078	-.024	-6.495	.808	-3.637	.767	-1.995	.765
13	-6.145	-731	-3.637	-767	-1.992	-.765	-5.882	.545	-3.551	-7.733	-1.905	-7.66
14	-5.196	-519	-3.116	-567	-1.819	-.647	-4.677	.494	-2.771	.433	-1.645	.529
15	-4.677	-404	-2.656	-467	-1.559	-.471	-4.503	.365	-2.605	.400	-1.559	.471
16	-4.503	-365	-2.771	-433	-1.472	-.412	-4.503	.365	-2.605	.400	-1.559	.471
17	-4.503	-365	-2.665	-400	-1.472	-.412	-4.503	.365	-2.605	.400	-1.559	.471
18	-4.417	-346	-2.665	-400	-1.472	-.412	-4.503	.365	-2.605	.400	-1.559	.471
19	-4.417	-346	-2.665	-400	-1.472	-.412	-4.503	.365	-2.605	.400	-1.559	.471
20	-4.244	-306	-2.665	-400	-1.472	-.412	-4.330	.327	-2.592	.367	-1.472	.412
21	-3.984	-250	-2.336	-267	-1.386	-.353	-4.070	.269	-2.338	.267	-1.386	.353
22	-4.076	-269	-2.511	-333	-1.386	-.353	-4.157	.288	-2.425	.300	-1.472	.412
23	-4.076	-265	-2.511	-333	-1.386	-.353	-4.244	.308	-2.425	.300	-1.472	.412
24	-4.076	-269	-2.596	-367	-1.386	-.353	-4.244	.308	-2.511	.333	-1.472	.412
25	-4.076	-269	-2.598	-367	-1.386	-.353	-4.244	.308	-2.598	.367	-1.472	.412
26	-4.076	-269	-2.596	-367	-1.386	-.353	-4.244	.308	-2.598	.367	-1.472	.412
27	-4.076	-265	-2.685	-400	-1.386	-.353	-4.244	.308	-2.598	.367	-1.472	.412
28	-4.076	-265	-2.685	-400	-1.386	-.353	-4.244	.308	-2.598	.367	-1.472	.412
29	-4.177	-346	-2.771	-433	-1.472	-.412	-4.503	.365	-2.605	.400	-1.559	.471
30	-4.762	-423	-2.944	-500	-1.472	-.412	-4.850	.442	-2.855	.467	-1.645	.529
31	-5.365	-566	-3.377	-667	-1.472	-.412	-5.543	.596	-3.204	.600	-1.905	.706
32	-5.542	-556	-3.204	-600	-1.472	-.412	-5.629	.615	-3.031	.533	-1.386	.353
33	-5.625	-615	-3.291	-633	-1.472	-.412	-5.716	.635	-3.118	.567	-1.386	.353
34	-5.576	-692	-3.857	-867	-1.905	-.706	-5.716	.635	-3.204	.600	-1.619	.647
35	-6.314	-1.212	-5.110	-1.333	-2.771	-1.294	-5.976	.692	-3.637	.767	-2.165	.882
36	-3.204	-077	-2.165	-200	-1.039	-.118	-5.369	.558	-3.204	.600	-1.905	.706
37	-3.504	-077	-2.165	-200	-1.039	-.118	-5.110	.500	-2.944	.500	-1.732	.588
38	-3.204	-077	-2.165	-200	-1.039	-.118	-4.417	.346	-2.685	.400	-1.472	.412
39	-2.335	115	-1.645	000	-606	-.176	-3.637	-.173	-2.338	-.267	-1.299	-.294

Appendix B Table 53 Measured data and computed pressure distribution for $b_1/b_2=0.50$, $g/b_2=0.25$, $T_1=290$ K.

b	D - Shape						Square - Shape					
	26.8427 (m/s)		20.3885 (m/s)		15.3479 (m/s)		26.8427 (m/s)		20.3885 (m/s)		15.3479 (m/s)	
	Ps cm.H2O	Cp	Ps cm.H2O	Cp	Ps cm.H2O	Cp	Ps cm.H2O	Cp	Ps cm.H2O	Cp	Ps cm.H2O	Cp
1	-546	.556	-433	.467	-.433	.294	-2.338	.115	-1.472	.067	-1.866	.000
2	-1.905	212	-1.386	100	-0.779	.059	-2.685	.036	-1.645	.000	-1.953	-.059
3	-6.608	.500	-606	.400	-606	.176	-2.850	-.006	-1.819	-.067	-1.039	-.118
4	-1.559	921	.866	967	.346	.024	-3.204	-.077	-1.992	-.133	-1.126	-.176
5	-7.794	-1.056	-4.850	-1.233	-2.598	-1.176	-9.699	-1.519	-5.976	-1.667	-3.464	-1.765
6	-7.967	-1.125	-5.023	-1.300	-2.685	-1.235	-8.400	-1.231	-4.936	-1.267	-2.771	-1.294
7	-8.054	-1.154	-5.196	-1.367	-2.685	-1.235	-6.668	-.846	-4.330	-1.033	-2.425	-1.059
8	-8.227	-1.192	-5.369	-1.433	-2.685	-1.235	-6.495	-.808	-3.897	-.867	-2.252	-.941
9	-7.524	-1.038	-4.936	-1.267	-2.598	-1.176	-5.889	-.673	-3.551	-.733	-1.992	-.765
10	-6.666	-846	-4.503	-1.100	-2.338	-1.000	-5.456	-.577	-3.377	-.667	-1.905	.706
11	-5.602	-624	-3.857	-867	-1.992	-.765	-5.283	-.538	-2.804	-.600	-1.732	.588
12	-5.369	-558	-3.464	-700	-1.819	-.647	-4.936	-.462	-3.031	-.533	-1.732	.588
13	-4.936	-402	-3.204	-600	-1.905	-.706	-4.590	-.385	-2.858	-.467	-1.645	.529
14	-4.590	-385	-3.031	-533	-1.559	-.471	-4.503	-.365	-2.771	-.433	-1.559	.471
15	-4.417	-346	-2.658	-467	-1.472	-.412	-4.330	-.327	-2.685	-.400	-1.559	.471
16	-4.330	-327	-2.771	-433	-1.472	-.412	-4.330	-.327	-2.771	-.433	-1.559	.471
17	-4.244	-308	-2.771	-433	-1.472	-.412	-4.330	-.327	-2.771	-.433	-1.559	.471
18	-4.157	-288	-2.771	-433	-1.472	-.412	-4.330	-.327	-2.685	-.400	-1.472	.412
19	-4.076	-249	-2.771	-433	-1.386	-.353	-4.244	-.308	-2.685	-.400	-1.472	.412
20	-3.984	-250	-2.596	-367	-1.299	-.294	-4.070	-.269	-2.511	-.333	-1.386	.353
21	-3.637	-173	-2.511	-323	-1.299	-.294	-3.897	-.231	-2.425	-.300	-1.299	.294
22	-3.697	-231	-2.511	-333	-1.299	-.294	-4.070	-.269	-2.511	-.333	-1.472	.412
23	-3.897	-231	-2.596	-367	-1.299	-.294	-4.070	-.269	-2.511	-.333	-1.472	.412
24	-3.984	-250	-2.598	-367	-1.299	-.294	-4.070	-.269	-2.598	-.367	-1.472	.412
25	-3.986	-250	-2.685	-400	-1.386	-.353	-4.070	-.269	-2.598	-.367	-1.472	.412
26	-3.984	-250	-2.685	-400	-1.386	-.353	-4.070	-.269	-2.598	-.367	-1.472	.412
27	-4.076	-269	-2.771	-433	-1.386	-.353	-4.157	-.268	-2.598	-.367	-1.472	.412
28	-4.503	-365	-3.031	-533	-1.472	-.412	-4.244	-.308	-2.771	-.433	-1.472	.412
29	-4.650	-42	-3.204	-600	-1.559	-.471	-4.677	-.404	-2.944	-.500	-1.645	.529
30	-5.110	-500	-3.291	-633	-1.645	-.529	-5.110	-.500	-3.204	-.600	-1.619	.647
31	-5.192	-519	-3.377	-667	-1.645	-.529	-5.192	-.500	-3.204	-.600	-1.732	.588
32	-6.235	-750	-4.070	-933	-1.905	-.706	-5.369	-.558	-3.464	-.700	-1.819	.647
33	-6.409	-728	-4.503	-1.100	-2.076	-.824	-5.543	-.596	-3.551	-.733	-1.819	.647
34	-7.534	-1.038	-5.369	-1.433	-2.511	-1.118	-6.668	-.846	-4.330	-1.033	-2.511	-1.118
35	-7.967	-1.135	-5.629	-1.533	-2.771	-1.294	-8.400	-.841	-5.369	-1.433	-3.031	-1.471
36	-1.905	218	-1.039	233	-606	176	1.204	-.077	-2.165	-.200	-1.039	-.118
37	-2.336	115	-1.472	067	-693	118	-3.031	-.038	-1.905	-.100	-1.039	-.118
38	-1.905	212	-1.299	133	-606	176	-2.510	-.058	-1.819	-.067	-1.953	-.059
39	-1.905	212	-1.039	233	-520	235	-2.338	-.115	-1.472	-.067	-1.779	-.059

Appendix B Table 54 Measured data and computed pressure distribution for $b_1/b_2=0.37$, $g/b_2=0.25$, $T_1=290$ K

B	D - Shape						Square - Shape					
	26.8427 (m/s)		20.3885 (m/s)		15.3479 (m/s)		26.8427 (m/s)		20.3885 (m/s)		15.3479 (m/s)	
	Pb cm.H2O	Cp	Pb cm.H2O	Cp	Pb cm.H2O	Cp	Pb cm.H2O	Cp	Pb cm.H2O	Cp	Pb cm.H2O	Cp
1	-.260	.492	-.067	.600	-.173	.471	-.1039	.404	-.779	.333	-.606	.176
2	-.066	.442	-.606	.400	-.346	.353	-.1472	.308	-.866	.300	-.606	.176
3	.520	.750	.067	.667	.000	.588	-.1645	.269	-.039	.233	-.606	.176
4	1.732	1.019	.666	.967	.346	.824	-.1645	.269	-.039	.233	-.606	.176
5	-.6.668	-.846	-.3724	-.800	-.2076	-.824	-.8.400	-.1.231	-.5.110	-.1.333	-.2.771	-.1.294
6	-.6.755	-.815	-.3.611	-.833	-.2.165	-.882	-.8.400	-.1.231	-.5.110	-.1.333	-.2.685	-.1.235
7	-.6.842	-.815	-.3.564	-.900	-.2.165	-.882	-.8.141	-.1.173	-.4.936	-.1.267	-.2.598	-.1.176
8	-.7.161	-.942	-.4.157	-.967	-.2.852	-.941	-.7.967	-.1.135	-.4.763	-.1.200	-.2.511	-.1.118
9	-.7.101	-.942	-.4.330	-.1.033	-.2.338	-.1.000	-.7.101	-.1.042	-.4.503	-.1.100	-.2.338	-.1.000
10	-.7.015	-.923	-.4.070	-.933	-.2.338	-.1.000	-.6.668	-.0.846	-.4.970	-.0.933	-.2.165	-.0.882
11	-.6.405	-.758	-.4.070	-.933	-.2.252	-.941	-.5.802	-.0.654	-.3.637	-.0.767	-.1.992	-.0.765
12	-.6.405	-.758	-.3.857	-.667	-.2.165	-.882	-.5.369	-.0.558	-.3.377	-.0.667	-.1.819	-.0.647
13	-.5.685	-.673	-.3.637	-.767	-.1.992	-.765	-.5.196	-.0.519	-.3.110	-.0.567	-.1.645	-.0.529
14	-.5.625	-.615	-.3.464	-.700	-.1.905	-.706	-.5.023	-.0.481	-.3.118	-.0.567	-.1.645	-.0.529
15	-.5.196	-.519	-.3.204	-.600	-.1.732	-.588	-.4.850	-.0.442	-.3.031	-.0.533	-.1.559	-.0.471
16	-.4.936	-.468	-.3.116	-.567	-.1.645	-.529	-.4.650	-.0.442	-.3.031	-.0.533	-.1.559	-.0.471
17	-.4.763	-.423	-.2.858	-.467	-.1.559	-.471	-.4.477	-.0.404	-.3.031	-.0.533	-.1.472	-.0.412
18	-.4.503	-.365	-.2.771	-.433	-.1.472	-.412	-.4.417	-.0.346	-.2.771	-.0.433	-.1.472	-.0.412
19	-.4.244	-.306	-.2.598	-.367	-.1.386	-.353	-.4.244	-.0.308	-.2.685	-.0.400	-.1.386	-.0.353
20	-.4.070	-.269	-.2.511	-.333	-.1.299	-.294	-.4.070	-.0.269	-.2.511	-.0.333	-.1.299	-.0.294
21	-.3.984	-.250	-.2.338	-.267	-.1.299	-.294	-.3.897	-.0.231	-.2.425	-.0.300	-.1.299	-.0.294
22	-.4.244	-.318	-.2.511	-.333	-.1.366	-.353	-.4.244	-.0.308	-.2.598	-.0.367	-.1.366	-.0.353
23	-.4.244	-.306	-.2.598	-.367	-.1.366	-.353	-.4.244	-.0.308	-.2.598	-.0.367	-.1.366	-.0.353
24	-.4.330	-.327	-.2.685	-.400	-.1.366	-.353	-.4.330	-.0.327	-.2.685	-.0.400	-.1.366	-.0.353
25	-.4.503	-.365	-.2.771	-.433	-.1.386	-.353	-.4.330	-.0.327	-.2.685	-.0.400	-.1.366	-.0.353
26	-.4.590	-.365	-.2.771	-.433	-.1.472	-.412	-.4.417	-.0.346	-.2.771	-.0.433	-.1.366	-.0.353
27	-.4.936	-.402	-.2.658	-.467	-.1.472	-.412	-.4.503	-.0.365	-.2.858	-.0.467	-.1.366	-.0.353
28	-.5.196	-.519	-.3.204	-.600	-.1.732	-.588	-.4.763	-.0.423	-.2.944	-.0.500	-.1.559	-.0.471
29	-.5.629	-.615	-.3.464	-.700	-.1.905	-.706	-.5.283	-.0.536	-.3.284	-.0.600	-.1.732	-.0.588
30	-.6.235	-.750	-.3.724	-.800	-.1.905	-.706	-.5.369	-.0.558	-.3.377	-.0.667	-.1.819	-.0.647
31	-.6.926	-.904	-.4.070	-.933	-.2.076	-.824	-.5.889	-.0.673	-.4.876	-.0.933	-.1.992	-.0.765
32	-.7.567	-.1.135	-.4.536	-.1.267	-.2.425	-.1.059	-.7.534	-.1.038	-.4.503	-.1.100	-.2.252	-.0.941
33	-.7.567	-.1.135	-.5.023	-.1.300	-.2.511	-.1.118	-.7.967	-.1.135	-.4.936	-.1.267	-.2.336	-.1.000
34	-.8.054	-.1.154	-.5.369	-.1.433	-.2.771	-.1.294	-.8.141	-.1.173	-.5.369	-.1.433	-.2.771	-.1.294
35	-.8.141	-.1.173	-.5.369	-.1.433	-.2.771	-.1.294	-.8.141	-.1.173	-.5.369	-.1.433	-.2.771	-.1.294
36	-.606	5.01	-.606	400	-.346	353	-.1.645	.269	-.1.039	.233	-.606	.176
37	-.1.386	327	-.779	.333	-.346	.353	-.1.645	.269	-.1.039	.233	-.606	.176
38	-.1.295	346	-.866	.300	-.346	.353	-.1.645	.269	-.1.039	.233	-.606	.176
39	-.666	.442	-.606	.400	-.260	.412	-.1.386	.327	-.8.666	.300	-.606	.176

Appendix B Table 55 Measured data and computed pressure distribution for $b_1/b_2=0.25$, $q/b_2=0.25$, $T_1=290$ K.

D - Shape				Square - Shape								
#	26.8427 (m/s)		20.3885 (m/s)		15.3479 (m/s)		22.9465 (m/s)		20.3885 (m/s)		15.3479 (m/s)	
	Ps cm.H2O	Cp	Ps cm.H2O	Cp	Ps cm.H2O	Cp	Ps cm.H2O	Cp	Ps cm.H2O	Cp	Ps cm.H2O	Cp
1	-260	.692	.067	.667	-.067	.529	-.067	.474	-.173	.567	-.173	.471
2	-.067	6.15	-.173	567	-.173	.471	-.433	.368	-.433	.467	-.173	.471
3	779	.698	260	733	.260	.765	-.173	.447	-.346	.500	-.173	.471
4	1.299	923	.693	.900	.860	.765	.693	.711	.269	.733	.800	.588
5	-6.235	-.750	-3.551	-.733	-2.165	-.882	-6.409	-1.447	-4.876	-9.933	-2.252	-.941
6	-6.322	-.769	-3.637	-.767	-2.852	-.941	-6.495	-1.474	-4.876	-9.933	-2.252	-.941
7	-6.235	-.750	-3.724	-.800	-2.252	-.941	-6.666	-1.526	-4.876	-9.933	-2.252	-.941
8	-6.842	-.885	-3.811	-.833	-2.256	-.941	-7.015	-1.638	-4.244	-1.000	-2.252	-.941
9	-7.015	-.923	-3.897	-.867	-2.852	-.941	-7.015	-1.638	-4.244	-1.000	-2.252	-.941
10	-7.015	-.923	-3.984	-.900	-2.338	-1.000	-7.015	-1.638	-4.244	-1.000	-2.252	-.941
11	-6.669	-.846	-3.984	-.900	-2.338	-1.000	-6.582	-1.500	-4.244	-1.000	-2.252	-.941
12	-6.665	-.846	-3.897	-.867	-2.338	-1.000	-6.495	-1.474	-4.876	-9.933	-2.165	-.882
13	-6.409	-.788	-3.637	-.767	-2.852	-.941	-6.235	-1.395	-3.984	-.900	-2.078	.824
14	-6.235	-.750	-3.551	-.733	-2.165	-.882	-6.062	-1.342	-3.897	-.867	-1.992	-.765
15	-5.803	-.654	-3.204	-.600	-2.078	-.824	-5.802	-1.263	-3.637	-.767	-1.995	.706
16	-5.543	-.596	-3.118	-.567	-1.905	-.706	-5.629	-1.211	-3.551	-.733	-1.819	.647
17	-4.936	-.462	-2.944	-.500	-1.819	-.647	-5.110	-1.052	-3.204	-.600	-1.732	.588
18	-4.850	-.442	-2.771	-.433	-1.645	-.529	-4.936	-1.000	-3.031	-.533	-1.645	.529
19	-4.330	-.327	-2.598	-.367	-1.559	-.471	-4.503	-.868	-2.058	-.467	-1.559	.471
20	-4.244	-.308	-2.511	-.333	-1.472	-.412	-4.417	-.842	-2.771	-.433	-1.472	.412
21	-4.070	-.269	-2.425	-.300	-1.472	-.412	-4.157	-.763	-2.685	-.400	-1.472	.412
22	-4.563	-.365	-2.771	-.433	-1.559	-.471	-4.503	-.868	-2.944	-.500	-1.559	.471
23	-4.590	-.385	-2.771	-.433	-1.645	-.529	-4.936	-.900	-3.031	-.533	-1.559	.471
24	-4.590	-.385	-2.771	-.433	-1.645	-.529	-4.936	-.900	-3.031	-.533	-1.559	.471
25	-4.590	-.395	-2.944	-.500	-1.645	-.529	-4.936	-.900	-3.031	-.533	-1.645	.529
26	-4.677	-.404	-3.204	-.600	-1.732	-.588	-4.936	-.900	-3.204	-.600	-1.732	.588
27	-4.650	-.442	-3.464	-.700	-1.819	-.647	-5.023	-.822	-3.291	-.633	-1.732	.588
28	-5.369	-.558	-3.724	-.800	-1.992	-.765	-5.369	-.732	-3.637	-.767	-1.819	.447
29	-5.602	-.654	-4.157	-.967	-2.165	-.882	-5.802	-.626	-3.811	-.833	-1.995	.706
30	-6.662	-.646	-4.330	-.933	-2.338	-.900	-6.666	-.582	-4.330	-.633	-2.165	.682
31	-7.101	-.942	-4.936	-1.267	-2.338	-.900	-6.842	-.575	-4.503	-1.100	-2.252	-.941
32	-7.524	-1.038	-5.023	-1.300	-2.338	-.900	-7.361	-.573	-4.763	-1.200	-2.252	-.941
33	-7.534	-1.038	-5.196	-1.367	-2.338	-.900	-7.361	-.573	-4.936	-1.267	-2.338	-.1000
34	-7.967	-1.135	-5.456	-1.467	-2.338	-.900	-7.361	-.573	-4.936	-1.267	-2.338	-.1000
35	-7.967	-1.135	-5.369	-1.433	-2.338	-.900	-7.361	-.573	-4.936	-1.267	-2.338	-.1000
36	-6.662	642	260	733	.260	.765	-.173	.447	-.173	.567	.800	.588
37	-2.600	577	-.173	567	-.173	.471	-.520	.342	-.433	.467	-.173	.471
38	-5.821	519	-.173	567	-.173	.471	-.520	.342	-.433	.467	-.173	.471
39	-2.600	577	-.173	567	-.087	.529	-.433	.368	-.173	.567	-.087	.529

113535

Th

629-13234 Date Slip

So 94 This book is to be returned on the date last stamped.

AE-1992-m-sow-Exp